Deschutes Estuary Feasibility Study

Hydrodynamics and Sediment Transport Modeling

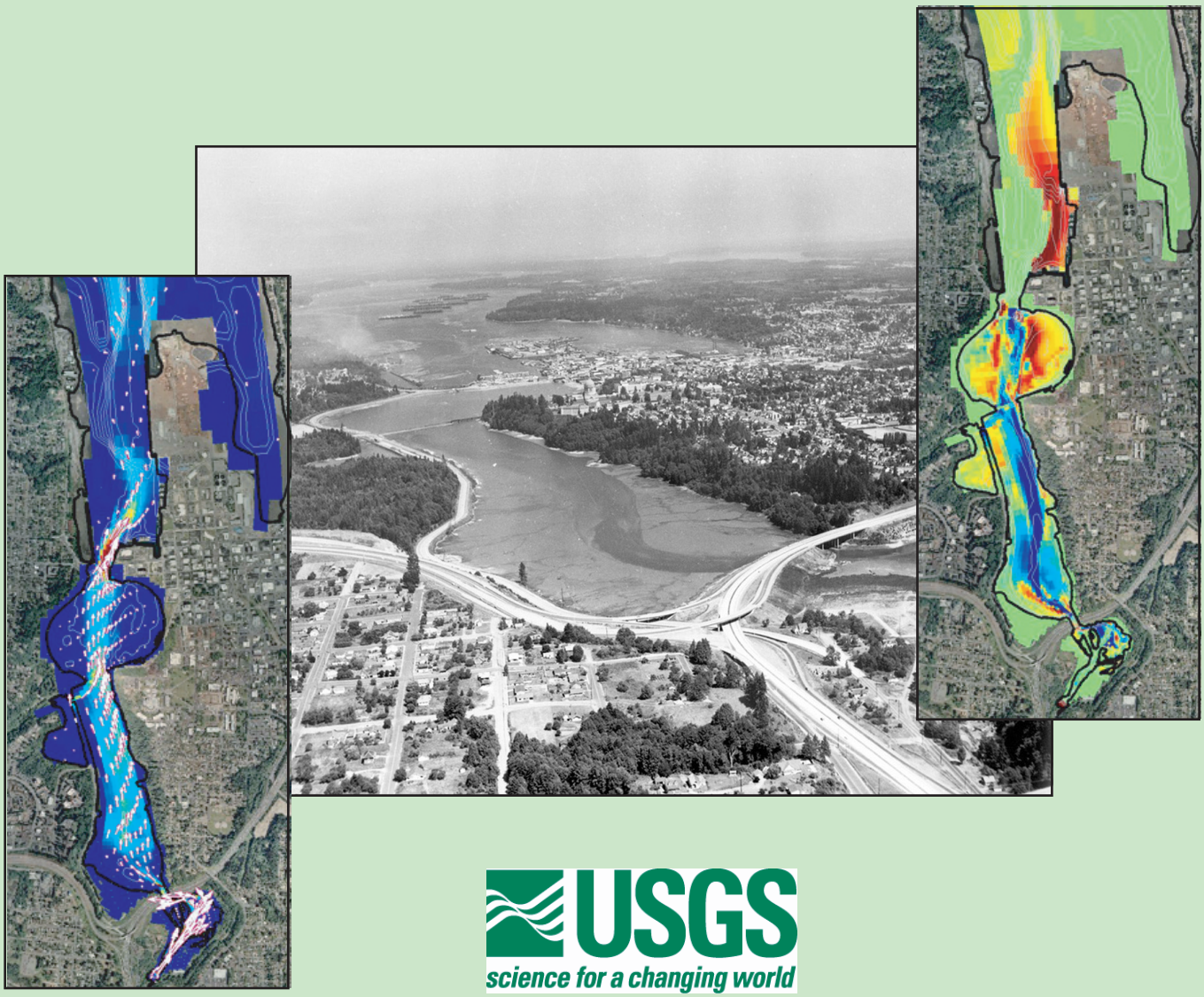

USGS
science for a changing world

Douglas A. George, Guy Gelfenbaum, Giles Lesser and Andrew W. Stevens

October 2006

Open File Report 2006-1318

USGS
science for a changing world

Deschutes Estuary Feasibility Study:

Hydrodynamics and Sediment Transport Modeling

By Douglas A. George[1], Guy Gelfenbaum[1], Giles Lesser[2] and Andrew W. Stevens[1]

[1]U.S. Geological Survey, 345 Middlefield Rd. MS 999, Menlo Park, California, 94025

[2]WL/Delft Hydraulics, 345 Middlefield Rd. MS 999, Menlo Park, California, 94025

Open File Report 2006-1318

U.S. Department of the Interior
U.S. Geological Survey

Table of Contents

Acknowledgements

This work was part of a large collaborative process with many people involved and we would like to acknowledge in particular the DEFS Project Manager Curtis Tanner, Steven Morrison, Nathaniel Jones, Bob Barnard, Perry Lund, Ralph Garono, and Susan Tonkin for many interesting and thoughtful discussions.

We thank Jodi Eshleman, Larry Kessel, George Kaminsky, Etienne Kingsley, Laura Bauleke, Blythe Mackey, and Bob Barnard for helping with the bathymetry and sediment data collection in the field. Carlin Dare helped with the sediment grain size analysis in the laboratory. Scott Carte provided the aerial photography of Capitol Lake and Budd Inlet.

We are grateful for the many comments and suggestions from technical reviewers of an earlier draft of this report. In particular, we would like to thank the CLAMP Technical Work Group, Edwin Elias, and Jingping Xu for their constructive reviews. We would especially like to thank Bert Jagers for many late night discussions about modeling multiple sediment grain sizes and variable MORFACs.

Funding for this work came primarily through a grant from the Salmon Recovery Funding Board (SRFB). Additional funds were supplied by the Washington Department of General Administration, Puget Sound Action Team, Port of Olympia, and the U.S. Geological Survey Coastal and Marine Geology Program.

List of Figures

List of Tables

Conversion Table

U.S. Customary to Metric

Multiply	By	To Obtain
feet (ft)	0.3048	meters (m)
yard (yd)	0.9144	meters (m)
miles (mi U.S. statute)	1.60935	kilometers (km)
square feet (ft^2)	0.092903	square meters (m^2)
acres (ac)	4047	square meters (m^2)
cubic feet (ft^3)	0.028317	cubic meters (m^3)
cubic feet per second (cfs)	0.028317	cubic meters per second (cms)
cubic yards (yd^3)	0.76456	cubic meters (m^3)
tons (2000 pounds)	907.185	kilograms (kg)

Multiply	By	To Obtain
meters (m)	3.281	feet (ft)
meters (m)	1.094	yard (yd)
kilometers (km)	0.6214	miles (mi U.S. statute)
square meters (m^2)	10.76	square feet (ft^2)
square meters (m^2)	$2.47x10^{-4}$	acres (ac)
cubic meters (m^3)	35.31	cubic feet (ft^3)
cubic meters per second (cms)	35.31	cubic feet per second (cfs)
cubic meters (m^3)	1.308	cubic yards (yd^3)
kilograms (kg)	$1.102x10^{-3}$	tons (2000 pounds)

Executive Summary

Continual sediment accumulation in Capitol Lake since the damming of the Deschutes River in 1951 has altered the initial morphology of the basin. As part of the Deschutes River Estuary Feasibility Study (DEFS), the United States Geological Survey (USGS) was tasked to model how tidal and storm processes will influence the river, lake and lower Budd Inlet should estuary restoration occur. Understanding these mechanisms will assist in developing a scientifically-sound assessment on the feasibility of restoring the estuary.

The goals of the DEFS are as follows.

- Increase understanding of the estuary alternative to the same level as managing the lake environment.
- Determine the potential to create a viable, self sustaining estuary at Capitol Lake, given all the existing physical constraints and the urban setting.
- Create a net-benefit matrix which will allow a fair evaluation of overall benefits and costs of various alternative scenarios.
- Provide the completed study to the CLAMP Steering Committee so that a recommendation about a long-term aquatic environment of the basin can be made.

The hydrodynamic and sediment transport modeling task developed a number of different model simulations using a process-based morphological model, Delft3D, to help address these goals. Modeling results provide a qualitative assessment of estuarine behavior both prior to dam construction and after various post-dam removal scenarios. Quantitative data from the model is used in the companion biological assessment and engineering design components of the overall study.

Overall, the modeling study found that after dam removal, tidal and estuarine processes are immediately restored, with marine water from Budd Inlet carried into North and Middle Basin on each rising tide and mud flats being exposed with each falling tide. Within the first year after dam removal, tidal processes, along with the occasional river floods, act to modify the estuary bed by redistributing sediment through erosion and deposition. The morphological response of the bed is rapid during the first couple of years, then slows as a dynamic equilibrium is reached within three to five years. By ten years after dam removal, the overall hydrodynamic and morphologic behavior of the estuary is similar to the pre-dam estuary, with the exception of South Basin, which has been permanently modified by human activities.

In addition to a qualitative assessment of estuarine behavior, process-based modeling provides the ability address specific questions to help to inform decision-making. Considering that predicting future conditions of a complex estuarine environment is wrought with uncertainties, quantitative results in this report are often expressed in terms of ranges of possible outcomes. Some important questions and the associated findings are as follows:

Question 1 –

What range of velocities is expected in a restored estuary under different restoration scenarios for average and extreme hydrologic events?

Four restoration scenario designs were examined under several hydrodynamic conditions. In general, the velocities among the restored scenarios are similar for average hydrologic events. During periods of slack tides and low river flows, current speeds are below 0.2 m/s in most of the estuary for each scenario. During periods of maximum ebb or flood tide and high river discharge, velocities exceeding 1.5 m/s are common at major constriction points (under the I-5 bridge, through the BNSF railroad trestle and exiting the estuary). Current velocities at the constriction points increase substantially during extreme hydrologic events, such as the 2- and 100-year floods. For the largest of the simulated extreme events, a 100-year flood with a large tide, speeds reach approximately 5 m/s. Localized differences are observed among the restoration scenario designs that are related to the details of a particular scenario. For example, maximum velocities through the trestle region decrease by approximately 40% when the trestle is widened. A small decrease in maximum velocity is seen under the Deschutes Parkway bridge when the opening to Percival Cove is doubled. Velocities through the entrance to Budd Inlet are not significantly affected when the eastern half of North Basin is converted to a freshwater impoundment.

Question 2 –

What are the percent inundation times under different restoration scenarios for average and extreme hydrologic events?

The average annual percent inundation times do not widely vary among the four restoration scenario designs. The main channel, North Basin and part of Middle Basin remain underwater at least 80% of the year while elevations above 2 m (MSL) get submerged less than 50% of the time. During extreme hydrologic events, portions of public spaces such as Tumwater Historical Park and Marathon Park may become submerged when a high tide combines with large river discharges.

Question 3 –

What are the expected ranges for salinity under different restoration scenarios and conditions (average annual and low-flow conditions)?

The near-bed salinity does not widely vary among the four restoration scenario designs. Average annual near-bed salinity ranges from 0 ppt at the river mouth to approximately 20 ppt in North Basin. During the dry season, North Basin salinities increase to above 20 ppt. Percival Cove is saltier than Middle Basin, possibly due to the limited influx of freshwater into the cove from Middle Basin and the absence of Percival Creek in the model. Expanding the connection between Middle Basin and Percival Cove does not appear to dramatically change the near-bed salinity distribution in the cove.

Question 4 –

Will there be an effect on sediment in Capitol Lake and near the city of Olympia if the tide gates are altered? What should be expected?

Sediment accumulated in Capitol Lake is mobilized in all restoration scenario designs and redistributed within a restored estuary as well as exported to Budd Inlet. A range of results are analyzed because of uncertainty in the erodibility of the bed. However, more variation in sediment transport is produced by uncertainties in the mud erodibility than by the individual restoration scenarios. More detail is provided below.

Question 4.a –

How much will the channels and mudflats erode or accumulate sediment and during what time frames (months to years) in a restored Deschutes Estuary?

The range for erosion and deposition does not change significantly with respect to the various restoration scenarios. Depending on the erodibility, the main channel of a restored estuary will erode up to 2 m after three years, with most of the change occurring in the first year. A channel in South and Middle Basins is preferentially eroded while deposition occurs in portions of North Basin and Percival Cove. Deposition does not exceed 2 m within the estuary and occurs primarily on the tidal flats. The estuary morphology will continue to evolve after a dynamic equilibrium is achieved approximately three to five years after dam removal, though at a slower rate. After ten years, the restored estuary morphology is similar to the predam estuary.

Question 4.b –

How much sediment will likely accumulate within Budd Inlet and where?

The marina and port region effectively traps most of the sediment that gets exported from the estuary with little difference among the various restoration scenarios. Depending on mud erodibility, approximately 125,000 – 280,000 m^3 of sediment should be expected to deposit in the region after three years. Slightly more (170,000 – 360,000 m^3) accumulates in the marina and port when the eastern half of North Basin is retained as a freshwater impoundment.

Question 5 –

How will the sediment grain size of the estuary evolve through time under different restoration scenarios?

Bed sediment grain sizes evolve consistently among the restoration scenarios to produce sandier channels and muddier flanks. During the initial response of a restored estuary, silt and clay are predominantly mobilized. Each successive year shows a coarsening of the channels and increased mud fractions on the flanks. However, as with the previous

sediment transport and morphological observations, a range in model results comes from the uncertainty in the mud erodibility parameters.

Future Considerations

Model results for salinity in Budd Inlet compare favorably to data from a previous field investigation. Unfortunately, additional model verification for this study was not possible. Several sensitivity analyses increase confidence in model performance but limitations in model design, sediment transport theory, and field data to initialize the model introduce some uncertainty in model predictions. Restrictions on resources and data will always be present but three specific topics warrant additional consideration: 1) determining the erodibility of the bed, 2) gathering sediment grain size information in deficient regions, and, 3) developing a modern sediment rating curve for the Deschutes River. Each of these would have a noticeable impact on reducing the uncertainty in the results. New queries can also be made of the functioning restored Deschutes Estuary model as management priorities change and additional investigations are desired.

CHAPTER 1

Introduction

History of Capitol Lake

The creation of Capitol Lake from the Deschutes Estuary in southern Puget Sound was the realization of a 1911 proposal for a freshwater reflecting pool below the Washington State Capitol campus in Olympia (Wilder and White, 1911). Construction of the earthen dam, 25-m wide tide gate with concrete spillways and the Deschutes Parkway was completed in 1951. A causeway over the tide gates extended 5th Avenue to the west and consequently, the structure become known as either the 5th Avenue Bridge and Dam or 5th Avenue Dam (Figure 1.1). The modern assembly consists of two radial gates to regulate lake level and a fish ladder (Figure 1.2).

The modern lake is separated into four distinct basins that are connected (Figure 1.1). The Burlington Northern Santa Fe railroad trestle, which existed before the dam, divides North and Middle Basin. Construction of the Deschutes Parkway cleaved Percival Cove from Middle Basin. Completion of the Interstate-5 (I-5) overpass bridge in 1957 split South Basin from Middle Basin. Other projects reduced the area of the lake but have not altered the hydrodynamics as severely as these constrictions.

The lake lies on a north-south axis with the Deschutes River entering from the south via Tumwater Falls, a municipal marina directly north of the dam and the Port of Olympia north of the marina. Several public spaces are contained within the original estuary boundaries – Marathon Park and Heritage Park in North Basin, the Capitol Lake Interpretative Center and Heritage Park wetland mitigation site in Middle Basin, and Tumwater Historical Park in South Basin (Figure 1.3). South Basin also has three vegetated islands; the other basins are open water.

The bathymetry and shape of the historic Deschutes Estuary in 1949 and modern Capitol Lake in 2004 are different (Figure 1.4). The wide tidal channel in the estuary has been replaced by less defined channels and submerged banks. The bathymetric difference

between the predam estuary and modern lake shows the most radical changes have occurred in South and Middle Basins with bed level elevation increases of more than 2 m (Figure 1.5). The depth of the tidal channel in North Basin also shows a large decrease of 2 – 3 m. Immediately south of the dam, depths have increased by more than 3 m, creating a hole lakeside of the structure. The average decrease in depth since 1949 translates to a 60% volume reduction due to filling and sedimentation within the modern lake boundary. All four basins have changed but not by uniform amounts (Table 1.1). The primary cause of the reduced depth and volume since construction of the dam is sediment accumulation.

Table 1.1. Depth and volume changes, 1949 – 2004

	average depth change (m)	volume change (m^3)	volume change (%)
Capitol Lake	1.1	13.1×10^5	60
North Basin	0.8	3.2×10^5	42
Middle Basin	1.1	6.7×10^5	69
South Basin	2.5	2.6×10^5	97
Percival Cove	0.6	0.6×10^5	62

As early as the 1970s, accumulation of sediment in the lake from the Deschutes River was identified as a problem to the long-term health of Capitol Lake. A flurry of studies between 1974 and 1977 led to dredging South and Middle Basins and creation of a sediment trap north of the I-5 bridges in 1979. A second dredging effort occurred in 1986 but removed only 25% of the 1979 amount. No dredging has been performed recently because of concern that seeds from noxious weeds (milfoil and Purple Loosestrife) would be present in dredge spoils. Inexpensive disposal options in Budd Inlet have been eliminated because of the risk of biological contamination. While Washington General Administration is acting on an eradication program, sediment continues to accumulate in the lake.

A second option for dredge spoils is upland disposal. Several additional steps, including review for the Endangered Species Act, potential for centrifugal dewatering of sediment and transport of material from the basin, raise the cost (CLAMP Plan 2003 – 2013). Estimates to remove sediment at the same rate as annual accumulation are $1.2 million; a more extensive removal of all 1.3 million m^3 of sediment deposited since formation of the lake would cost $40 million (CLAMP Plan 2003 – 2013). The desire to maintain an open water aquatic environment instead of a freshwater marsh as a centerpiece of Olympia prompted action. A long-term sediment management strategy was ordered under the Capitol Lake Adaptive Management Plan (CLAMP) Objective 13. The Deschutes Estuary Feasibility Study emerged from this directive.

The Deschutes Estuary Feasibility Study

The primary objective of the Deschutes Estuary Feasibility Study (DEFS) is to evaluate the possibility of a restored estuary as an alternative to the management actions necessary to maintain Capitol Lake. The specific goals of the project are listed in Box 1.1.

Box 1.1. Specific goals of the Deschutes Estuary Feasibility Study

- Increase understanding of the estuary alternative to the same level as managing the lake environment.
- Determine the potential to create a viable, self sustaining estuary at Capitol Lake, given all the existing physical constraints and the urban setting.
- Create a net-benefit matrix which will allow a fair evaluation of overall benefits and costs of various alternative scenarios.
- Provide the completed study to the CLAMP Steering Committee so that a recommendation about a long-term aquatic environment of the basin can be made.

Three overarching concepts define a 'successful' estuary restoration: 1) reconnect the Deschutes River with Budd Inlet, 2) establish a viable Deschutes River estuary, and 3) protect the civic and recreational values of the basin (CLAMP Technical Work Group, 2006). The CLAMP managers designed the study to address community concerns with equal emphasis to those of a scientific nature. As such, the study is composed of four parts with different groups executing a singular task (Figure 1.6). The first study is to model the hydrodynamics and sediment transport of a restored estuary under different restoration scenarios. Concurrently, a study was undertaken to assess the biological response for the restoration scenarios (Garono, et al., 2006). The third study is investigating the engineering design and cost estimate analysis for the different scenarios. The final study will perform analysis of the net benefits of restoring the estuary with interaction from community groups. Together, the four studies will present an interdisciplinary approach to evaluating estuary restoration.

DEFS Hydrodynamic and Sediment Transport Modeling

The United States Geological Survey (USGS) was tasked with the hydrodynamic and sediment transport modeling for the DEFS. Together with the CLAMP Technical Advisory Committee, the USGS developed questions to be answered by numerical modeling. Several questions were posed to address specific issues regarding the restored estuary as well as to provide information to the other three segments of the study (Box 1.2). This report describes the results for the Hydrodynamic and Sediment Transport modeling component of the study.

Box 1.2. Hydrodynamic and Sediment Transport Modeling Task Questions

1. What range of velocities is expected in a restored estuary under different restoration scenarios for average and extreme hydrologic events?

2. What are the percent inundation times under different restoration scenarios for average and extreme hydrologic events?

3. What are the expected ranges for salinity under different restoration scenarios and conditions (average annual and low-flow conditions)?

4. Will there be an effect on sediment in Capitol Lake and near the city of Olympia if the tide gates are altered? What should be expected?

    a. How much will the channels and mudflats erode or accumulate sediment and during what time frames (months to years) in a restored Deschutes Estuary?

    b. How much sediment will likely accumulate within Budd Inlet and where?

5. How will the sediment grain size of the estuary evolve through time under different restoration scenarios?

For the reference estuary and biological response portion of the feasibility study, the hydrodynamic and sediment transport model provides salinity regimes, inundation frequencies and sediment grain size distributions. Model output will be combined with field observations of flora and fauna from nearby 'reference estuaries' to estimate the communities that may colonize a restored estuary (Garono, et al., 2006). The model also yields velocity fields, circulation patterns and morphological change that will be used by engineers to analyze threats to existing infrastructure around the lake. The model results will assist in forming a physical description of the restored estuary, which will include exposure of mudflats.

The USGS enacted a multi-point modeling plan to answer the questions in Box 1.2 and provide information for the other related studies. The first modeling objective is to examine the predam environment and establish baseline information about hydrodynamics and sediment transport. The second objective is to investigate the anthropogenic effect on sediment dispersion in the lake. The third and most important modeling objective is to conduct hydrodynamic, sediment transport and morphologic analyses on the proposed restoration scenarios.

Standard investigation topics fall under the broad headings of hydrodynamics, sediment transport and morphological change. For hydrodynamics these include flow fields, stratification, salinity regimes and inundation frequencies. The hydrodynamic portion of the study incorporates both average and extreme hydrologic events. Within the sediment transport and morphological change categories are erosion, transport and deposition of

sand and mud fractions, interactions between sand and mud, timescales of change and geological controls on future morphology.

Different model simulations were assembled to address these three objectives (Table 1.2). The predam estuary, lake and Budd Inlet models were designed based on field information. The four restoration scenario alternatives were developed by the DEFS Technical Committee (Figure 1.7).

Table 1.2. Description of simulations used in the hydrodynamic and sediment transport modeling component of the study

Simulation	Description	Modeling goal
Predam Estuary	1949 bathymetry and shoreline for Deschutes Estuary, 150 m opening to Budd Inlet	Baseline data for historic environment
Initial lake	1949 bathymetry and 1957 shoreline of Capitol Lake	Sediment dispersion in initial lake
Modern lake	2004 bathymetry and shoreline of Capitol Lake	Sediment dispersion in modern lake
Restoration Scenario A	2004 bathymetry and shoreline of Capitol Lake, 150 m opening to Budd Inlet	Restoration scenario
Restoration Scenario B	2004 bathymetry and shoreline of Capitol Lake, 150 m opening to Budd Inlet and 150 m connection between North and Middle Basins	Restoration scenario
Restoration Scenario C	2004 bathymetry and shoreline of Capitol Lake, 150 m opening to Budd Inlet and 60 m opening between Middle Basin and Percival Cove	Restoration scenario
Restoration Scenario D	2004 bathymetry and shoreline of Capitol Lake, 150 m opening to Budd Inlet and North Basin split along a north-south axis	Restoration scenario

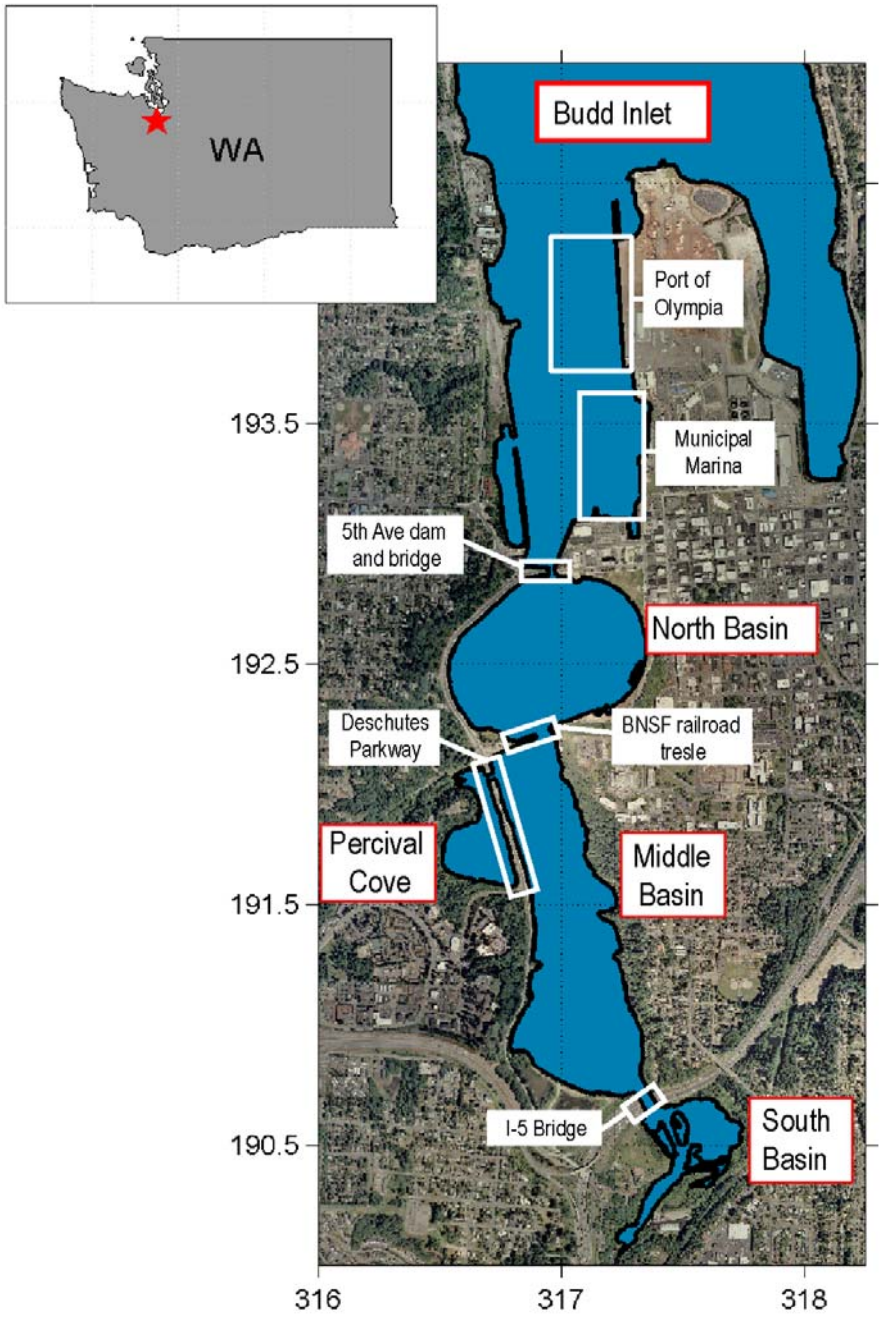

Figure 1.1. Capitol Lake and environs in 2004. The four distinct basins are South Basin, Middle Basin, Percival Cove and North Basin. The basins are connected through the labeled features. The Port of Olympia and municipal marina reside north of the 5th Avenue Dam and Bridge in Budd Inlet.

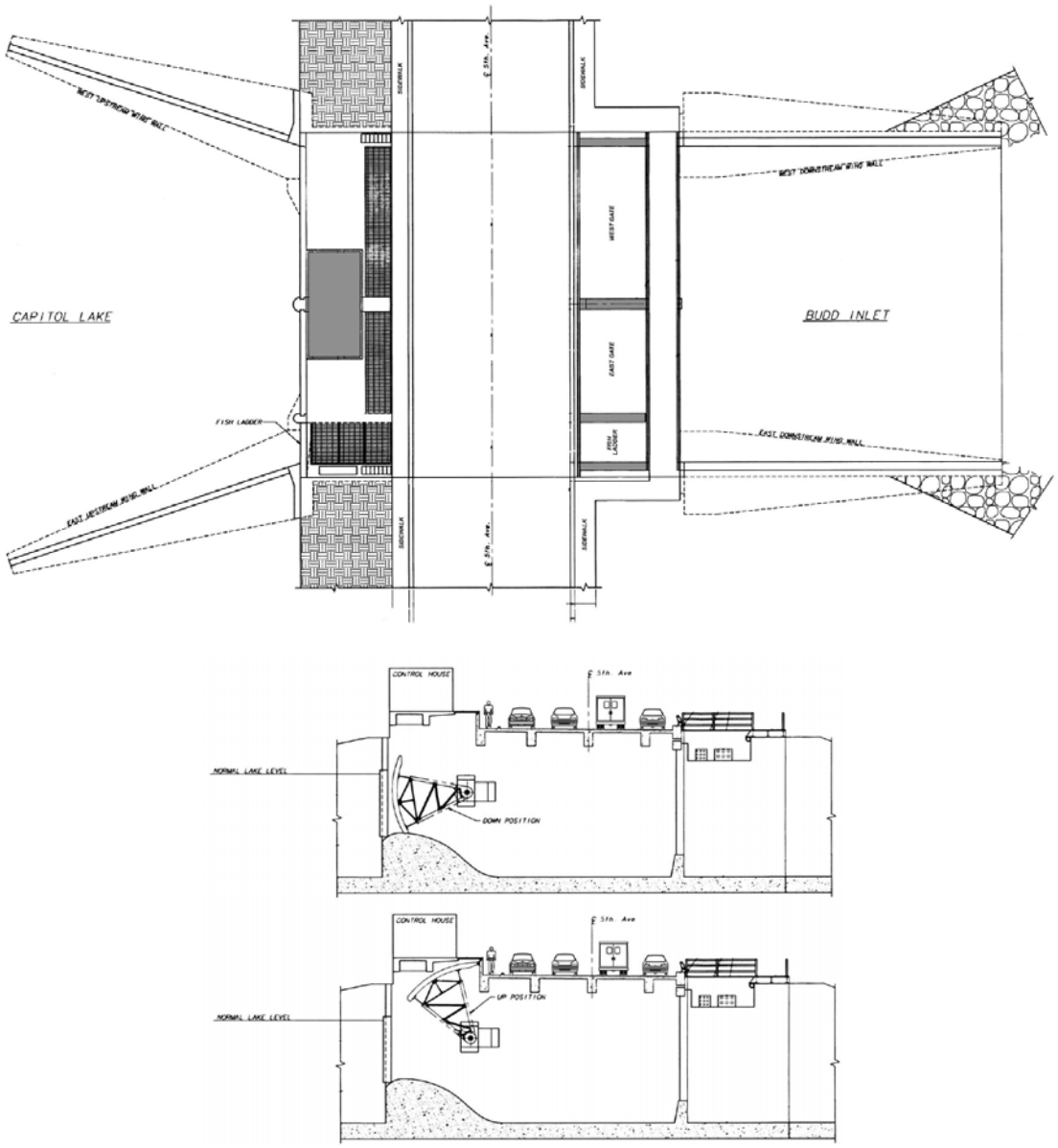

Figure 1.2. Plan (top) and side (middle, bottom) views of the 5th Avenue Bridge and Dam. From the top edge of the West Gate to the bottom edge of the Fish Ladder is approximately 25 m. The side views show the radial gate in the closed and open positions.

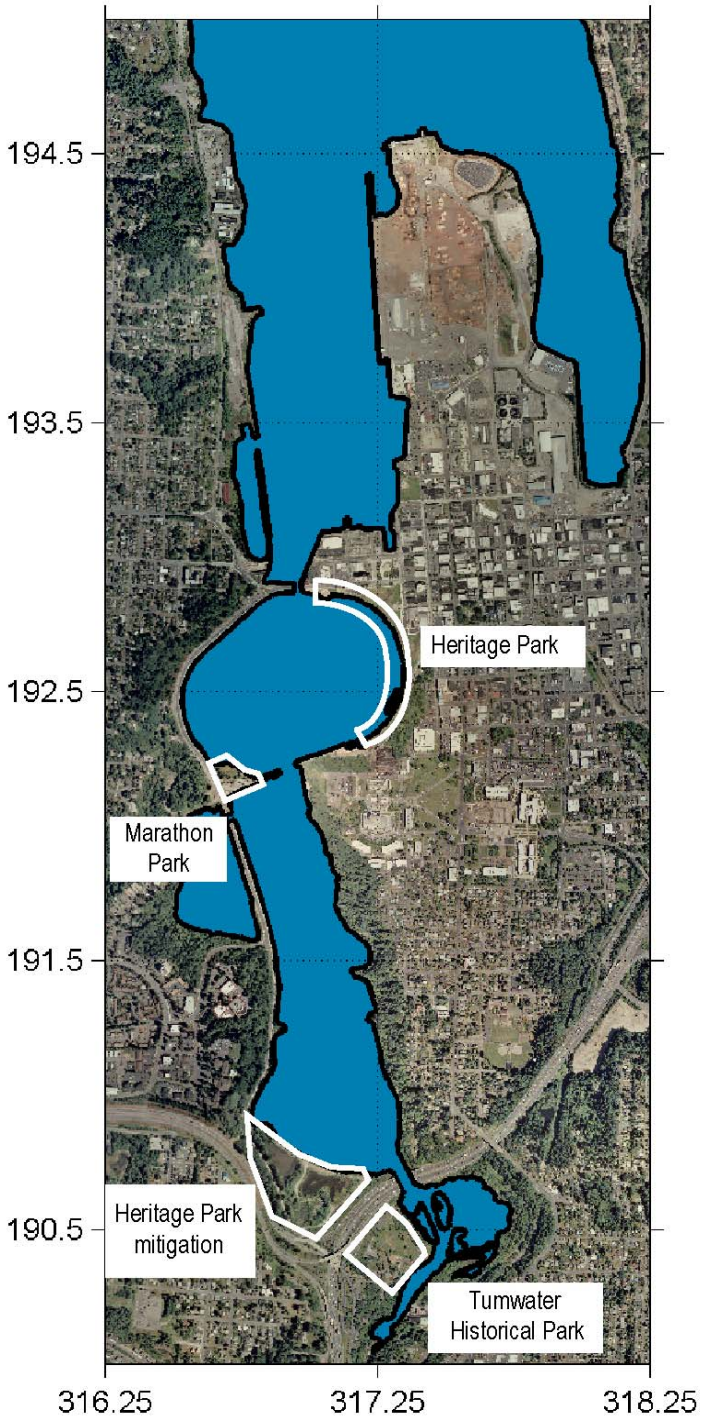

Figure 1.3. Public spaces contained within the historic Deschutes Estuary boundaries. Development of these areas has reduced the surface area of original Capitol Lake.

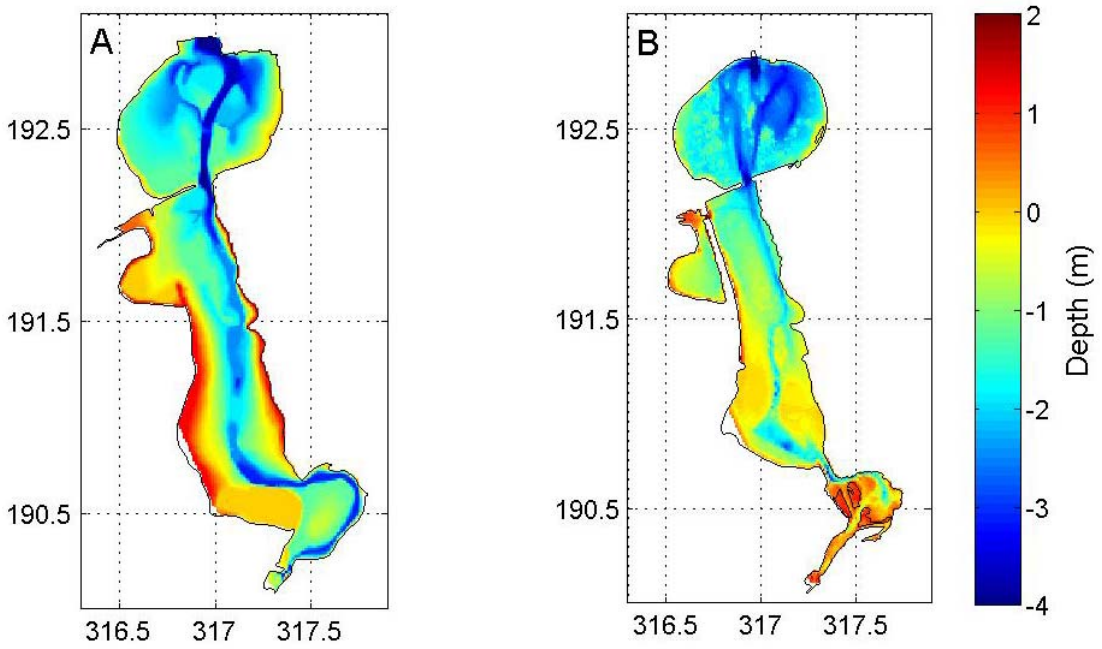

Figure 1.4. Bathymetric maps of Deschutes Estuary in 1949 (A) and Capitol Lake in 2004 (B). Blues are deeper water and reds are shallower (m MSL). Large changes to the shoreline and amount of open water are observed around Percival Cove and between South and Middle Basins.

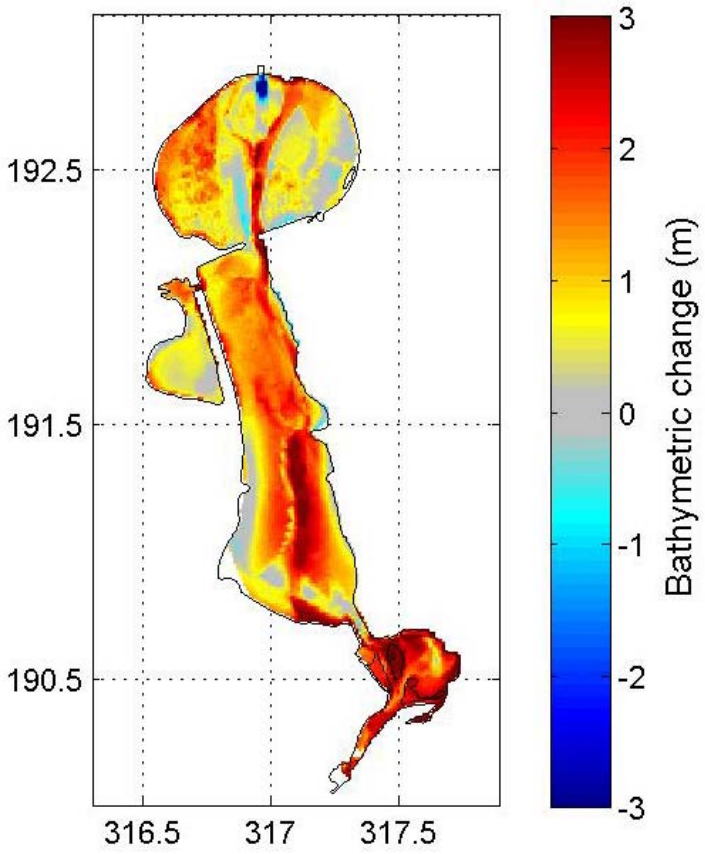

Figure 1.5. Bathymetric change within the modern Capitol Lake shoreline from 1949 to 2004. Reds are decreases in water depth, blues are increases (m). Gray represents changes less than 0.15 m and are below the resolution of the data. The largest depth decreases are observed in South and Middle Basins and in the channel of North Basin while the largest depth increase is in the scour hole due south of the 5th Ave Dam.

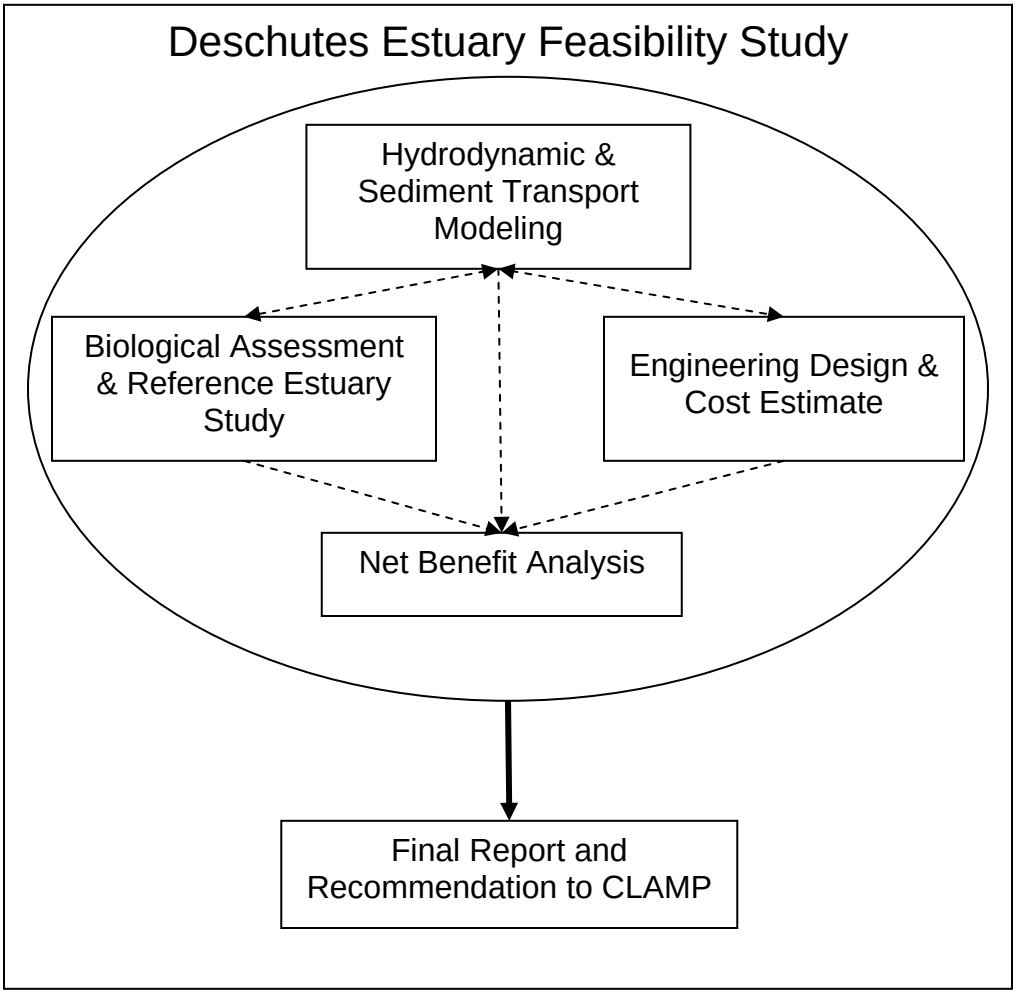

Figure 1.6. Deschutes Estuary Feasibility Study (DEFS) organizational chart. Four interacting studies comprise the feasibility study and recommendation to the Capitol Lake Adaptive Management Plan (CLAMP). Solid lines show direct contribution to the final report and dashed lines indicate contribution between the component studies. This report describes the results for the Hydrodynamic and Sediment Transport modeling component of the study.

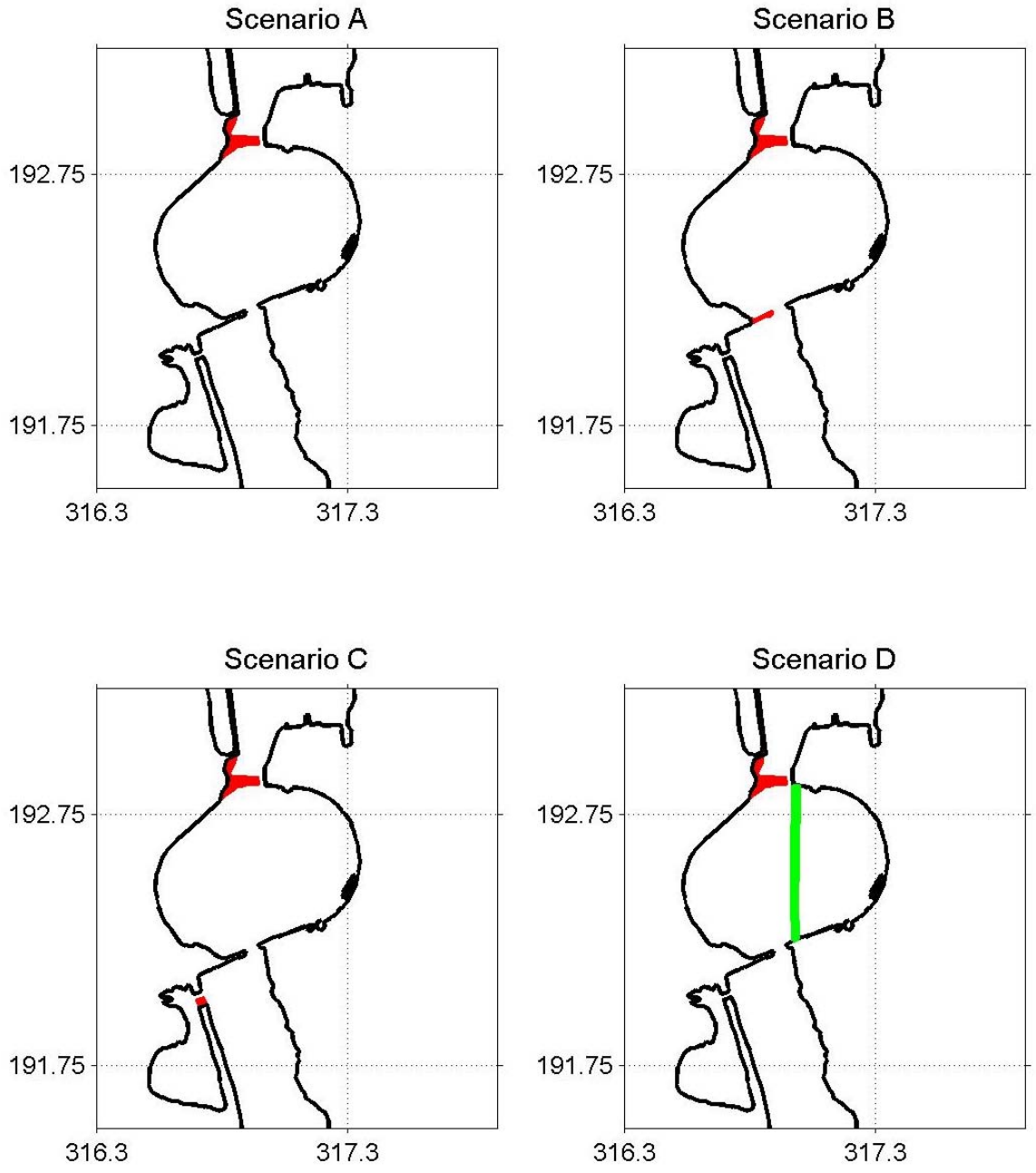

Figure 1.7. Coastlines of the four restoration scenarios. The red lines indicate removal of the current coastline and the green line in Scenario D shows the proposed dike in North Basin. The black line represents the modified coastline for each scenario.

CHAPTER 2

Methods

Modeling Requirements

The project scope as established by the DEFS Technical Committee generated a list of requirements for the hydrodynamic and sediment transport modeling program to be used. While some needs were standard, such as producing velocity fields and water levels, or allowing mixing of salinity, there were several additional specific requirements. Estuaries in this area of Puget Sound have a large tidal range and tend to be dry at low tide, requiring the model to incorporate wetting and drying. As one of the project goals was to investigate if large amounts of sediment would be exported from a restored estuary, the model needs to calculate sediment transport and perform spatially and temporally varying morphological calculations. The setting of the project in a wind-driven, wavy marine environment, with a tidally-dominated estuary and a significant freshwater river source demands a model that could be forced by several concurrent processes and be potentially run in three dimensions because of density stratification in the water column. The model also needs to incorporate multiple sediment grain sizes because the lake bed and Deschutes River contain sediment grain sizes ranging from clay and silt to sand and gravel. In short, an advanced model that could perform hydrodynamic and morphologic analyses was deemed necessary to pursue this study.

The program selected for this project was Delft3D, a numerical hydrodynamic and morphologic model from Delft Hydraulics, The Netherlands. This modeling software was first developed in the 1980s (Stelling et al., 1986) and has evolved during the past decades to be one of the premier models for sediment transport and morphology investigations in coastal environments (Sutherland et al., 2004). The Coastal and Marine Geology Program of the USGS established a co-operative agreement with Delft Hydraulics that allows access to state-of-the-art research versions of the code as well as technical support and development of customized modules.

Delft3D is composed of distinct modules, such as ecological or water quality. The hydrodynamics, including river and tidal flows, density-driven mixing and shear stress

calculations, are performed in the FLOW module. Sediment transport and morphological change routines are incorporated directly into the FLOW module (Lesser, et al., 2004).

Operationally, the FLOW module is a closed loop system. Information from input files providing bathymetry, boundary conditions and time-varying processes (e.g., a river discharge or wind field) is used to solve momentum and continuity equations. The solutions generate velocity and turbulent mixing fields. These data are combined with the constituent (salinity or sediment) properties and boundary conditions to solve the advection and diffusion equations for the constituents. Changes to constituent fields are calculated and combined with the updated hydrodynamic results. In this manner, the constituents affect the hydrodynamics. For bed morphology, the hydrodynamics control the sediment transport, which in turn determines the morphological change. The new morphology then alters the hydrodynamics (Figure 2.1). The sequence occurs at each computational time step at every active grid cell in the simulation domain.

Uncertainties in Numerical Modeling

In numerical modeling of natural systems, especially for future conditions, a number of uncertainties should be considered. The two broad categories of these uncertainties are modeling approximations and natural randomness.

Modeling approximations fall into three classes, the first being model design. Even with powerful and fast computers, design is confined by limited computational resources. Compromises are made in both the geographic domain and internal resolution of a model. By limiting the area and varying the grid cell size, an efficient and useful simulation can be created that will not exhaust computer processors or require an excessive period of time to conclude. The second approximation regards the level of understanding of complex processes. Hydrodynamic and sediment transport science are vital to this project. These physical processes have been studied for decades and the body of scientific literature is rich in discoveries. However, research continues to improve on parameterizations of fluid dynamics, turbulent mixing, erosion of mud and transport of mixed sediment. How these pieces interact is an additional area of dedicated research. The current generation of models incorporates the latest understanding and still new findings could improve the implementation of these processes.

The last set of approximations are associated with real-world knowledge, or field measurements. The data needs specific to this project that can be quantified include bathymetry, sediment grain size and tidal elevations. Many methods to collect depth information can be employed ranging from simple manual soundings at random points to acoustic echosoundings on densely spaced survey lines. Regardless of how the data are gathered, the results are a snapshot of the area and limited by the errors inherent to the collection method. The collection options for sediment data are not as numerous but the concerns are the same – a temporal freeze frame and method-associated errors. Tidal elevations can be determined from direct observation at a local site or from calculations with respect to a distant location. However, temporary effects from storms and gaps in an observation record can complicate the data. Interpolation and extrapolation are used to increase the efficacy of the data but the initial approximations affect these processing techniques.

Natural randomness, the second category of uncertainty, encompasses the stochastic behavior of natural systems. For example, long-term records of river discharge or wind patterns yield information about events in the past but any number of factors, ranging from local to global in scale, could change these processes, making their prediction less reliable. Their histories allow an estimation to be made of a river or wind climate with the understanding that significant departures may evolve over time. Standard statistical techniques improve confidence in these climatologies but cannot eliminate the uncertainties inherent in making predictions about the future.

Some sources of uncertainties cannot be reduced to an acceptable level given present knowledge (either theory or field data), therefore a sensitivity analysis should be performed. Sensitivity analyses can be performed as iterations, where a variable is tested based on previous results, or as a formalized investigation of parameter space where a matrix of values is constructed based on scientific literature. After conducting numerous simulations, if the results show no or an acceptable level of sensitivity to a variable, the uncertainty behind that variable can be considered to be small. However, if a simulation is found to be sensitive to a particular parameter, the uncertainties associated with not knowing that variable should be evaluated. Any number of steps can be tried, such as redesigning a grid, reinterpolating the bathymetry, applying different transport equations or repeating the schematization of a river climate. While the goals of a project may seek the sensitivity of a system to prescribed variations, confidence in the results improves by reducing uncertainties from the modeling inputs.

Boundary and Initial Conditions

Bathymetry

All bathymetry and topography were adjusted to NGVD29 as this was the vertical datum chosen for the project. Bathymetry contours of the Deschutes Estuary were collected in 1949 prior to construction of the dam. Depth soundings from a 1936 survey of Budd Inlet (NOS survey #H06199) were fused with the estuary data to establish a predam bathymetry (Figure 2.2). Modern bathymetry and topography for the Capitol Lake area were compiled from several surveys conducted in 2004 and 2005 (Figure 2.3). The USGS collected depth data on a high-density grid for North and Middle Basins using modern echosounder and global positioning system techniques (Eshleman et al., 2006). The Washington Department of Ecology surveyed South Basin and Percival Cove while the Washington Department of Fish and Wildlife provided data from under the I-5 bridge; both were collected in 2005. Additionally, the USGS conducted a bathymetric survey between the 5th Ave Dam and the Port of Olympia in 2005. For maintenance dredging, the US Army Corps of Engineers surveyed the port and portions of Budd Inlet in 2004. Together, these five datasets comprise the modern bathymetry. Topography was acquired from the Thurston Regional Planning Council and elevations 6.1 m (20 feet) and less were extracted for inclusion in the model.

Tides

Long-term tidal records were extracted from the National Ocean Service water level station at Gull Harbor in eastern Budd Inlet (station #9446807). Budd Inlet experiences a complex semi-diurnal tide with a maximum range of 5 m during spring tides (Figure 2.4). Twelve tidal constituents were determined to be the dominant contributors to the tide and were combined to represent the tidal height on the model boundary (Table 2.1).

Table 2.1. Significant Tidal Constituents for Budd Inlet

Constituents	Amplitude (m)	Period (hrs)
M2	1.46	12.42
O1	0.47	25.82
S2	0.35	12.00
Q1	0.07	26387
P1	0.27	24.07
K1	0.87	23.93
J1	0.05	23.10
N2	0.28	12.66
L2	0.07	12.19
K2	0.10	11.97
M4	0.05	6.21
M6	0.03	4.14

Fluvial Boundary

Two sources of freshwater enter Capitol Lake – the Deschutes River from the south and Percival Creek from the west. The 57-mile Deschutes River is monitored with several USGS river gauging stations. The gauge closest to the lake, Station #12080010 at the E Street Bridge in Tumwater, collected flow measurements from 1945 – 1954, 1957 – 1964 and 1990 – present and contains large gaps within the record (Figure 2.5). A cumulative record of almost 30 years remains after the gaps are removed. Percival Creek has no known gauging stations and consequently, no data are available to estimate flow. However, the 1984 Capitol Lake Restoration Analysis report established the freshwater and sediment contribution of the creek was significantly smaller than that from the Deschutes River. For this study, Percival Creek flow was assumed to be negligible.

The annual average flow of the Deschutes River is approximately 12 m^3/s but fluctuates widely within a year. The river exhibits a distinct wet season on average from November to April with episodic large flood events reaching above 40 m^3/s. During the dry season, spanning May to October, the river flow is approximately one magnitude less and averages approximately 3 m^3/s. The seasonal difference in river behavior heavily impacts the pattern of sediment delivery to the lake (Figure 2.6). A 1974 study established that 80-85% of the annual sediment load arrives by flood events that occur only 8% of the year (Mih and Orsborn, 1974). Therefore, even during the wet season, the majority of sediment is not constantly delivered but rather arrives during large flood events.

The sediment concentration for different river flows can be estimated by using a rating curve developed specifically for the Deschutes River. The most recent rating curve was

calculated in 1974 by Mih and Orsborn (1974). Converted to metric units, the relationship is

$$Q_s = 0.0797Q^{1.93} \quad (2.1)$$

where Q is the river discharge (m^3/s) and Q_s is sediment concentration (mg/L or g/m^3). A total sediment load of 8.6 x 10^8 kg in 30 years, or an average annual sediment load of 2.87x10^7 kg, is calculated when the river discharge data are applied to Equation 2.1. The relationship between the discharge and sediment concentration, known as a rating curve, was established during a period of logging in the Deschutes watershed and a modern rating curve may show different suspended sediment concentrations as a function of river flow. However, hydrologists have found that rating curves systematically underestimate the amount of sediment delivered by rivers (Walling, 1977; vanSickle and Beschta, 1983) and therefore, a turbid historic curve may better reflect the modern conditions than when originally developed. Regardless, the lack of a modern sediment rating curve does introduce some uncertainty into predicted estimates of sediment delivery from the river.

The annual sediment load of the Deschutes River has been discussed in many scientific and engineering studies resulting in a range of 22,000 – 42,000 m^3/yr. The 1999 CLAMP report tabulated the values reported by previous studies (Table 2.2). The primary method for calculating the sediment load was by volume decrease of the lake due to deposition and correction for the 1979 and 1986 dredging operations. This method generated an average annual load of 27,000 m^3/yr but there is no indication that the trapping rate of the fine sediment, estimated to be 60 – 80% by Entranco (1984), was factored into this value. If an additional 20 – 40% sediment load is included, the average annual load would range from 32,000 – 38,000 m^3/yr.

Table 2.2. Deschutes River sediment load and accumulation in Capitol Lake since 1952*

time frame (yrs)	sediment load (m^3/yr)	accumulation (m^3)	dredging (m^3)	total accumulation (m^3)
1952 – 1974 (22)	23,000(A)	506,000		506,000
1975 – 1979 (5)	42,000(B)	210,000	-191,000	525,000
1980 – 1983 (4)	42,000(B)	168,000		693,000
1984 – 1986 (3)	26,500(C)	79,500	-43,600	728,900
1987 – 1990 (4)	26,500(C)	106,000		834,900
1991 – 1998 (8)	22,000(D)	176,000		1,010,900
total		1,245,500	-234,600	1,010,900

* reproduced from Table 7-1, CLAMP 1999 – 2001 report; original sources: (A) – USGS, 1973; (B) – Entranco, 1984; (C) – Entranco, 1990; (D) – Entranco, 1996.

River Schematization

The constraints of numerical modeling, the difference between the time step in field data and the model simulation, and the goal of predicting future conditions do not allow direct input of river discharge and calculated sediment concentrations into the model. To effectively use any model, a time step faster than actual time that does not negatively affect the processes being studied should be employed. In the case of modeling an

"average" year, input reduction techniques are required to produce model output similar to one year but that can be calculated in a fraction of that time (de Vriend et al., 1993). Further, computational effort and hard disc space must be considered. A different set of concerns evolves from the field data. The hydrograph of the river is constructed from daily average river flows that, as calculated values, smooth the hourly variations. The long-term patterns of the river allow a general characterization yet selecting a subsample of water years would provide a widely varying behavior or randomness. An approach similar to that which has been used successfully for characterizing offshore wave climates (Gelfenbaum et al, 2003) was taken to schematize the river.

The Deschutes River hydrograph contains 10,806 daily average discharge values, and although not a continuous record, has enough data to characterize the freshwater input to the lake and estuary. However, because the hydrodynamic portion of the study has different objectives than the sediment transport section, two schematizations are used. The hydrodynamic river climatization emphasized varying the amount of constant freshwater discharge to the lake while the sediment transport schematization focused on delivery of similar sediment amounts with the actual sediment load scaled according to the frequency of the river flow.

River Schematization for Hydrodynamic Simulations

To simulate the hydrodynamics of the restored estuary for an entire year, the freshwater discharge is binned into five discharge classes (Table 2.3). Subsets of actual events were averaged to produce the selected flows and the number of required events was tallied as a percentage of the total. For example, for the dry season flow of 2.8 m^3/s, 2994 records were required, which spanned 0 – 3.7 m^3/s, and represents 27.7% of the record. When the five river flows are weighted by their respective frequency and combined, the total discharge is equivalent to an annual average calculated from the hydrograph. This schematization was designed to be used in simulations examining hydrodynamics and salinity in the predam and restored estuaries and is called 'salinity river'.

Table 2.3. Discharge classes and occurrence frequency for 'salinity river' schematization

flow type	flow (m^3/s)	range of flows (m^3/s)	daily averages (#)	time/yr (%)
dry season	2.8	0-3.7	2,994	27.7
below average	5.6	3.7-8.5	3,016	28.0
average	11.1	8.5-14.5	2,351	21.7
wet season	23.7	14.5-45	2,127	19.7
flood stage	64.4	45-230	318	2.9

River Schematization for Sediment Transport Simulations

Sediment flux from the river was calculated to be 8.6 x 10^8 kg in 30 yrs by applying the 1974 rating curve to the hydrograph. By assuming a bed density of 1,137 kg/m^3 for the sediment, an average volume of 25,200 m^3 is delivered annually. This value falls within the range of uncertainty in the reported annual sediment volumes (Table 2.2). Five river discharge classes were selected based on averaging the number of river flows needed to deliver this amount. By this technique, the sediment load brought to the lake in a few large flood events is equal to the sediment load that arrives during small quiescent flows. For example, only 12 of the extreme flood events are needed to deliver the same sediment load as 462 of the 1-yr flood events (Table 2.4).

Table 2.4. Discharge classes and occurrence frequency for sediment transport schematization

flow type	flow (m^3/s)	daily averages (#)	time/yr (%)	days/yr (#)
5-yr+ flood	146	12	0.11	0.4
2-yr flood	95	43	0.40	1.5
above average flood	66	118	1.09	4.0
1-yr flood	42	462	4.28	15.6
average flow	13	10,171	94.12	343.5

Morphological Acceleration

Modeling the relationship between hydrodynamic flows, sediment transport and morphological changes is more complicated than hydrodynamics alone. The hydrodynamics respond to changes in forcing over short time scales (10s – 100s of seconds). Morphological changes, however, occur during much longer time scales. For example, the river discharge and sediment concentration may change significantly in a few hours while the morphological response of the estuary may require weeks to months. To conduct morphological simulations for a year or longer, a technique is needed to scale from hydrodynamic to morphological time scales. For the simulations in this study, morphological time scale factor, or MORFAC, is used to scale the morphological change to significantly impact the hydrodynamics (Roelvink, 2006; Lesser et al., 2004). The scaling occurs by multiplying the depositional and erosional fluxes to and from the bed by the non-dimensional MORFAC at every computational time step. The adjusted bed changes are then incorporated into the hydrodynamic calculations. This approach is only recently used in coastal environments (Roelvink, 2006) and a similar concept is applied to the representative river discharge in this study to scale the amount of sediment delivered in each flood event and connect the tidal cycle to the river discharge. Also, because the river will be delivering sediment to the estuary, the river hydrodynamics and sediment load must be linked with the tidal hydrodynamics and morphology. Equation 2.1 shows how MORFAC is calculated to achieve these multiple goals.

$$\text{MORFAC} = \frac{\text{morphological time}}{\text{hydrodynamic time}} = \frac{(\textit{days of flow}) \times (\textit{minutes / day})}{(\textit{minutes in a tidal cycle})} \qquad (2.2)$$

For example, the largest river flow, 146 m^3/s, occurs 0.4 days in an average year. Thus,

$$\text{MORFAC} = \frac{(0.4\,\textit{days of flow}) \times (1440\,\textit{minutes / day})}{(745\,\textit{minutes / tidal cycle})} = 0.78 \qquad (2.3)$$

is the value that suspended sediment concentrations and morphological change must be scaled by to represent the impact this flow makes in an average year. Annual MORFAC values for all river flows are shown in Table 2.5. In this manner, a different percentage of sediment arrives for each discharge, with the largest amount coming from the biggest flow.

To duplicate the event-driven nature of the river, the five flows are arranged as a series of flood events. An initial high flow is followed by successively lower flows with the average discharge as an interlude between floods (Figure 2.7). Differentiating between a wet and dry season is accomplished by consecutively running the lowest flow five times after all the flood events are completed. Each flow, except the largest, is included at least twice and therefore, MORFAC values required additional scaling.

For effective model operations, the MORFAC associated with the largest flow in a flood event is used for the duration of that event. For the first event, which leads with 146 m^3/s, a MORFAC of 0.78 is applied to all following flows until the interlude (Figure 2.7). This reduces the MORFAC required for future usage of these flow magnitudes and a new value is calculated. The process is repeated four times to generate the wet season sequence. As noted above, the dry season is constructed by five runs of the lowest flow so the MORFAC is scaled appropriately. The final adjusted MORFAC values are shown in Table 2.5 and are used for all simulations involving sediment transport and morphological change. This river schematization is named 'morphological river'.

Table 2.5. MORFAC and sediment volume associated with 'morphological river' flows

flow (m^3/s)	original MORFAC (-)	scaled MORFAC (-)	volume (m^3)	total sediment delivery (%)
146	0.78	0.78	5,400	21
95	2.82	2.05	5,600	22
66	7.69	4.87	5,200	21
42	30.2	22.5	5,100	20
13	664	114	3,900	15
total			25,200	100

Bed Sediment

Characterization of the bed sediment in Capitol Lake is fundamental to accurately model sediment transport and morphological change. Much information can be gleaned from the sediment data – deposition and erosion patterns on the lakebed surface, changes to those patterns through time by examining the underlying stratigraphy, and the sediment size classes delivered by the river from calculations of the deposited grain size distributions.

Historical Data

A modest amount of sediment collection has occurred in and around Capitol Lake during the previous decades (Figure 2.8). One of the more comprehensive efforts was in 1976 when 37 cores were recovered from South and Middle Basins and Percival Cove (CH2M Hill, 1976). The cores ranged in length from <1 – 7 m. Sediments were characterized as shell, gravel, sand, silt, clay, peat, or organics and sediment horizons were identified for all cores. Prior to the present study, the most recent sediment collection occurred in 2000 in Middle Basin with cores north of the I-5 bridge (Herrera, 2000). No sediment collection has been conducted in North Basin since the construction of the 5th Ave. Dam. Consequently, only a portion of the lakebed sediments could be characterized from the 1970s and much sediment has accumulated since.

Modern Surface Grabs

As part of this study, 72 surface sediment grabs were collected in February 2005 from the three basins of Capitol Lake (Figure 2.9). In general, cross-lake transects were attempted to characterize the bed including shallow lakeside regions and primary channels. Almost half of the sample sites were located in North Basin due to the lack of information in this area. Attempts were made to reoccupy the 1976 core sites in Middle Basin but this was only marginally successful. South Basin sampling was limited by water depth. Much of South Basin was too shallow to occupy with a boat to collect a sample. No sampling occurred in Percival Cove. Approximately 500 g of sediment were collected from each site.

The samples were stored at 4°C until grain size analysis could be conducted. Protocols standardized in 1976 by the USGS Western Coastal and Marine Geology sediment analysis laboratory were followed for all samples except three which were deemed to be cobble-sized and required measurement of the individual grains by hand-held calipers (M. Torresan, pers. comm.). For all other samples, approximately 40 g of homogenized sediment was placed in a beaker with ~100 ml of deionized water and 5 ml of 30% hydrogen peroxide and allowed to stand overnight to remove organics. Any salts were removed by boiling and two centrifuge rinses. Gravel and sand fractions were separated by the 2.00 mm and 0.0625 mm sieves, respectively, dried and weighed. The cumulative percentage of material of dried sand was analyzed on the Rapid Sediment Analyzer, or settling tubes. The remaining fine-grain material was dispersed in 1000 ml of deionized water and 5 ml of calgon to disaggregate the grains. After sitting overnight, the material was agitated for two minutes and a 20 ml aliquot was taken at 20 cm depth. Using the dry aliquot weight, the sample was prepared for Sedigraph analysis by determining the required sediment density and diluting the sample accordingly. A series of centrifugations produces the desired sediment density and the sample is then analyzed by the Sedigraph. After these analyses, all the data were entered into SedSize, a customized software program that produces sediment grain size statistics and sediment class percentages. Complete sediment grain size analysis results for all of the samples are reported in Appendix A.

In general, Capitol Lake is dominated by silt-sized sediment (Figure 2.10). Areas in the lake that frequently experience higher velocities (e.g., under the I-5 bridge, near the railroad trestle, around the dam) have coarser sediment, ranging from sand to gravel (Figure 2.11). Despite the difficulty in collecting sediment in South Basin, all size classes are represented in appreciable quantities. Larger amounts of fine sediment are found in the lee of the islands (Figure 2.12) while the main river channel shows coarse sediment fractions. Large quantities of silt and clay dominate Middle Basin except near Percival Cove and the railroad trestle where the sand fraction increases. North Basin, which has experienced some of the more turbulent mixing due to drawdown and backfilling of the lake, shows two sediment patterns. Fine-grain sediment is deposited on the east and west flanks of the basin while a coarse north-south sandy and gravelly channel connects the dam and trestle areas. Gravel and mud have both deposited in the scour hole that developed just south of the dam (Figure 2.13).

Model Development

Model Grids

Delft3D uses curvilinear grids to form the skeleton of a simulation to which all other input must conform. As outlined in Chapter 1, each simulation set (predam, lakes, and restored scenarios) extends across different geographic areas. Rather than construct a single grid that would be used for all simulations, a grid unique to each set of simulations was built to maximize the efficiency of those runs (Table 2.6). However, the differences amongst the grids were kept to a minimum to allow comparison of results.

Table 2.6. Grid cell comparison for different domains

grid domain	number of grid cells
Predam	6,460
1950s lake	4,525
Modern lake	4,216
Restored scenarios	6,151

The predam grid is the largest as the historic estuary occupied more area than the lakes or restored estuary scenarios. This grid extends from the mouth of the Deschutes River to outer Budd Inlet, terminating just north of Gull Harbor (Figure 2.14). The lake grids are the smallest and cover from the mouth of the river to the 5th Ave. Dam. Some cells were removed from the 1950s lake grid (Figure 2.15) to create the modern lake grid (Figure 2.16). The restored estuary scenario grid is identical for all four scenarios and, similar to the predam grid, extends from the mouth of the river to outer Budd Inlet (Figure 2.17).

Variation of the grid cell size was necessary to resolve the details of the flow in different areas of the model domains. For example, cells in the main channels are between 100 – 200 m^2 while cells on the mudflats range from 1200 – 3500 m^2. Portions of the model where depths change slowly were given the lowest resolution (outer Budd Inlet, East Bay).

Model Bathymetry

The bathymetries for the seven individual simulations were constructed from two data sets – the 1936/1949 bathymetries for the predam and 1950s lake and the 2004/2005 bathymetries and topography for the modern lake and restored scenarios. The bathymetric data were projected onto the grids using triangular interpolation.

The predam estuary bottom (Figure 2.18) has a primary channel starting from the river mouth, meandering along the eastern bank of South Basin and then through Middle Basin to the railroad trestle. After passing under the trestle, the channel partially bifurcates halfway through North Basin and each segment curves northerly before reuniting near the modern 4th Ave Bridge. From there, the channel turns northeast and heads toward the port where dredging deepened and widened the waterway. The dredged ship channel becomes the most prominent feature in Budd Inlet.

The initial lake bathymetry is taken from the predam bathymetry with some minor adjustments (Figure 2.19). The coastline of the lake after 1957 was superimposed over the bathymetry. Regions that fell outside of the land boundary were assumed to be areas of construction (e.g., the Deschutes Parkway or Interstate-5) and the bathymetry elevated to be above water level. Fill for the I-5 overpass thrust directly into the primary channel but no information was available regarding engineered changes to the lake and no bathymetric alterations were made. Percival Cove is connected to Middle Basin only through a 30 m opening under the Deschutes Parkway.

The modern lake bathymetry shows the impacts of the dam and sediment infilling (Figure 2.20). The primary channel in South Basin is very simplified as it heads northeast from the river mouth, between two islands and intersects the old channel on the eastern bank of the basin. After passing under the I-5 bridge in a more northerly direction, the channel meanders briefly before shifting to the east side of Middle Basin. In North Basin, the simple northerly heading continues as the channel connects the trestle and dam.

The restored estuary scenarios bathymetries combine the modern lake depth with that from Budd Inlet. The municipal marina south of the Port of Olympia interrupts the old primary channel slightly but the eastern side of West Bay remains the deepest portion of the area. The port and ship channel also remain the most prominent features of the inlet.

The bathymetries of the four scenarios vary only in the locations prescribed by the DEFS Technical Committee (Figure 1.7). The depth for Restoration Scenario A is the simplest with just the dam removed and serves as a template for the other three scenarios. Bathymetry in the area of the removed dam was estimated by extrapolation of field data (Figure 2.21). All other depths are identical to the modern lake and Budd Inlet bathymetries. Restoration Scenario B, with the wider railroad trestle opening, has the same depths as Restoration Scenario A except the spit extending from Marathon Park has been replaced by extrapolated depths from field data (Figure 2.22). Restoration Scenario C is identical to Restoration Scenario A in bathymetry but an additional grid cell is active between Percival Cove and Middle Basin creating an inlet width of 60 m (Figure 2.23). The depth for Restoration Scenario D required the most redesign to split North Basin into an eastern freshwater impoundment and western estuary. A strip of lake bottom connecting the eastern points of the dam and railroad trestle was raised to 4 m (MSL) with a 2:1 slope on the banks (Figure 2.24). This closed the eastern half of North Basin to estuarine flushing while allowing tidal processes into the three southern basins.

Sediment Grain Size Classes

Sediment grain sizes of 2 μm, 31μm, 200 μm and 2000 μm were selected to represent four sediment classes for modeling sediment transport. Two vital pieces of information were produced using these grain size classes – flux of sediment for each class on the river boundary and interpolated maps of initial bed sediment distribution. Proportions of each fraction were calculated from the average percentages of the deposited sediment collected by the grab samples (15% clay, 48% silt, 33% sand, 3% gravel). The trapping rate for each sediment class was estimated from test simulations of the modern lake (Table 2.7). By combining the deposited percentage and the trapping rate, the sediment class percentages entering from the river were calculated as 28% clay, 41% silt, 28% sand and

3% gravel. The percentage differences for each class are due to the bypassing of the lake by finer sediments.

Table 2.7. Deposition and flux of selected sediment grain sizes

sediment grain size (μm)	deposited in lake (%)	trapping rate (-)	river boundary flux (%)
2 (clay)	15	0.45	28
31 (silt)	48	0.97	41
200 (sand)	33	1.00	28
2000 (gravel)	3	1.00	3

Total concentration of sediment load for the five river flows of the 'morphological river' was calculated from the rating curve (Table 2.8). The expected flux percentage of each sediment class was multiplied by the total concentration to produce the sediment class concentrations. These values are used in conjunction with the morphological river.

Table 2.8. Concentrations of sediment classes at 'morphological river' flows

river flow (m^3/s)	total concentration (kg/m^3)	2 μm concentration (kg/m^3)	31μm concentration (kg/m^3)	200 μm concentration (kg/m^3)	2000 μm concentration (kg/m^3)
146	1.20	0.34	0.49	0.34	0.04
95	0.52	0.15	0.21	0.15	0.02
66	0.26	0.07	0.11	0.07	0.01
42	0.11	0.03	0.04	0.03	0.00
13	0.01	0.003	0.005	0.003	0.00

* component concentrations may not sum to total concentrations because of rounding

Initial sediment grain size maps were generated only for the Capitol Lake region as no sediment data are available for Budd Inlet. Maps for each sediment class were produced by interpolating the percentage of the clay, silt, sand and gravel classes between grab sample locations onto the grid (Figures 2.25, 2.26, 2.27). A fifth map was generated to provide the amount of sediment in terms of thickness at each grid cell location. Most of the Capitol Lake bed sediment thickness was set at 10 m to provide sediment in excess of the erosion that was expected. Areas that grab sample data indicated to be coarser than 2000 μm or where sediment data were not available were 'bed hardened' by setting the sediment thickness to 0. Grid cells that were hardened (i.e., bed sediment thickness set to 0) were also labeled as 100% gravel despite containing no sediment (Figure 2.28). The initial distribution and thickness maps were used in sediment transport/morphological simulations of the estuary restoration scenarios only.

Constants

Delft3D uses a combination of data input files and constants to solve the transport and momentum equations. The data files are designed by the user while the constants can be set to any value within a prescribed range. A constant wind field of 5 m/s from the south was constructed based on averaged data from Deerfield Park/Tolmie State Park in Olympia. A uniform wave field ($H_{1/3}$ = 10 cm; T_s = 2 sec) was built from test simulations

of the lake. Bottom roughness was set to 65 $m^{1/2}/s$ in the u- and v-directions (Chèzy formulation). The wave height is automatically reduced in very shallow gridcells where even these very small waves would be expected to break.

Sensitivity Analyses

Vertical Resolution

Delft3D can be operated in three-dimensional (3D) or two-dimensional horizontal (2DH) mode, which simulates vertically averaged flows. The difference between operating the model in 2DH and 3D has significant implications for the computational time of each simulation. Simulations were tested in 3D for evidence of salinity-driven density differences through the water column of a restored estuary. Simulations with the larger river flows showed an increase in the vertical density stratification.

In general, estuaries can be characterized as well-mixed, where water density is vertically uniform and the salinity gradient is constantly increasing from the head of the estuary to the marine environment, or partially mixed, where a surface layer of freshwater overlays more saline water at depth. In well-mixed estuaries, turbulence homogenizes the water column and blends the outgoing freshwater with the incoming seawater. The partially mixed estuary, however, uses entrainment, or the mixing of the lower strata of surface freshwater and upper layer of bottom seawater, to produce a blended brackish layer of water in the middle of the water column. Depending on the river flow, test cases of a restored estuary exhibited both estuarine types.

According to test simulations, Middle Basin is typically partially mixed (Figure 2.29). The stratification breaks down in North Basin and by the marina, the distribution is better described as well-mixed. The average salinity in a 3D simulation is also more saline than in 2D simulation by approximately 5 – 8 ppt. Tests showed that 2D simulations are not completely capturing the estuarine circulation. Enough stratification occurs as to require some discrete resolution in the vertical direction. A significant difference in computational times (7.5 hrs for 2D, 331 hrs for 3D) resulted from the increased number of calculations and the decreased time step (6 sec for 2D, 2.4 sec for 3D). The smaller time step is necessary to keep the 3D simulations stable. A number of basic sensitivity analyses were conducted to determine the most efficient 3D simulation with the objective of reducing computational time and maintaining accuracy.

The first analysis focused on the number of layers in the vertical direction. Results from five test simulations with a range of layers (3, 5, 7, 10, and 20) were compared. Time-series plots of salinity showed the 3- and 5-layer simulations produced unacceptably different results than the other three simulations (Figure 2.30). The 7-layer simulation is only slightly different in the salinity recorded in the bottom strata and nearly identical in the surface as the 10- and 20-layer simulations. Because of the similar results to higher resolution models and the shorter computational time for a 3-day test run (Table 2.9), the 7-layer design was selected for further use.

Table 2.9. Comparison of computational time for simulating a 3-day period using 3D runs with varying numbers of layers

number of layers	computational time (hrs)
3	7.25
5	12.0
7	14.5
10	22.3
20	44.3

The second sensitivity analysis examined the distribution of the seven layers in the water column. Four arrangements were tested: high resolution in the surface and bottom layers, high resolution in the bottom layer only, high resolution in the middle of the water column and a uniformly-spaced distribution. Differences of less than 2 ppt in salinity (approximately 10%) were seen between the four designs (Figure 2.31) and as the computational times were similar, the uniformly-spaced distribution was selected.

The last sensitivity analysis regarding 3D simulations involved an operational value for background viscosity and diffusivity. In the 3D simulations, eddy viscosity and diffusivity are calculated within the model, but a background value must be set. The resulting viscosity and diffusivity is the larger number between the input value and calculated value from the turbulence equation. If the background value is consistently larger than the calculated one, the mixing is not being accurately represented. Recommended values of 10^{-3} – 10^{-4} m^2/s are suggested as a suitable range for stratified lakes and estuaries. A test range of 10^{-2} – 10^{-6} m^2/s was examined. Salinity distributions were observed to be better mixed with higher background values but no other discernable patterns emerged (Figure 2.32). The more conservative value of 10^{-4} m^2/s was selected from the suggested range to be used in all 3D simulations. No field data were available to test the model results for this parameter setting.

Erodibility of Mud

Several additional constants and input files are needed for sediment transport and morphological simulations. Some sediment parameters are difficult to quantify in a mixed grain size sample, including the densities of individual size classes, the sediment erosion rate and the critical shear stress for erosion. Information from the scientific literature was used to produce reasonable ranges of parameters expected to be valid for Capitol Lake sediment.

Different values of sediment bulk density are needed for the four sediment classes selected to be simulated. The bulk densities for sand and gravel were held constant at 1,600 kg/m^3. The density of mud will change with depth through the sediment layers in the bed but information related to the porosity of mud was not gathered from field data. Based on observations of estuarine mud found in the scientific literature, a density of 1,000 kg/m^3 was selected to represent the silt and clay fractions in a majority of the simulations (van Rijn, 1993). However, densities have been observed to be as low as 100 kg/m^3 in areas where mud has not yet consolidated. Therefore, to represent looser mud conditions for one specific type of simulation, a density of 500 kg/m^3 was selected for the silt and clay fractions.

As fine-grain sediment consolidates on the bed, the deposits become more resistant to erosion (van Rijn, 1993). Sediment erodibility has been the subject of intense research in the recent past. Early work suggested that the physical properties of sediments such as particle size and water content were the primary factors controlling erodibility (Hjulstrom, 1939; Postma, 1967; Einsele et al., 1974). The physical characteristics of the bed continue to be recognized as important determinants of erodibility (Amos et al., 1997), but alone cannot be used to make accurate predictions (Dade et al., 1992). A consideration of biological processes must be included.

Numerous studies have been undertaken to investigate the effect of benthic biology on the erodibility of marine sediments. By perturbing the sediment-water interface in a variety of ways, benthic flora and fauna have the capability of both increasing and decreasing sediment erodibility (Rhoads et al., 1978). As a result, marine sediments having similar physical properties often respond differently to applied bottom stresses because of a biological overprint (Jumars and Nowell, 1984; Stevens et al., In Press). For instance, decreases in sediment erodibility have been observed as a result of binding by benthic diatoms and bacteria via secretion of mucus (e.g., Grant and Gust, 1987; Paterson et al., 2000; Lelieveld et al., 2003). On the other hand, increases in sediment erodibility have been observed in connection with the production of fecal pellets (Andersen, 2001) and by increasing the surface micro-topography (de Deckere et al., 2001).

Field data to quantify the erodibility of the Capitol Lake sediment were not acquired and therefore, scientific literature was used to guide the input values for the mud fractions. The erosion settings for clay and silt involved varying two parameters - the sediment erosion rate and the critical shear stress for erosion. Conservative ranges for each were selected from observations of natural muds published by van Rijn (1993) and test simulations were designed accordingly (Table 2.10). The ranges for critical shear stress and erosion rate fall within the bounds of other published data from the Fraser River delta, Canada (Amos et al., 1997) and from the Hollandsch Diep freshwater system in the Netherlands (Andersen et al., 2002).

Table 2.10. Erodibilities tested during the sensitivity analysis for the mud fraction

erodibility level	critical shear stress for erosion (N/m^2)	erosion rate ($kg/m^2/s$)
extreme low	0.4	$1x10^{-5}$
mid-level	0.3	$25x10^{-5}$
extreme high	0.2	$50x10^{-5}$

Recent modeling of fine grain size sediment transport in the Yellow River, China, found that formulations that treat silt size classes as non-cohesive sediment produce more reliable results than when silt is modeled as cohesive (B. van Maren, pers. comm.). These findings encouraged adding a fourth test case to the erodibility where the clay fraction is the only sediment class treated as cohesive.

The four test simulations were run for one year in the Restoration Scenario A estuary with initial bed sediment distributions. Spatially, the extreme low erodibility appeared to transport unacceptably small amounts of sediment while the three other test cases

produced noticeable morphologic change. Cumulative sediment transport through cross-sections in the estuary showed the four test cases produce widely ranging results (Figure 2.33). The extreme high erodibility parameter as chosen from the literature and non-cohesive silt transport comparable sediment amounts, particularly through the I-5 bridge and trestle. The mid-level erodibility moves approximately half as much sediment as the extreme high while the extreme low erodibility conveys less than 10% of the mid-level. Because three of the test cases (extreme high, non-cohesive silt and mid-level) yield sediment amounts of similar magnitudes, the extreme low erodibility was determined to be unreasonably small and removed from further consideration. However, the wide range of test results and uncertainty discussed in the scientific literature still warranted a conservative approach. Therefore, both the mid-level and extreme high erodibilities were selected to bracket the most likely erodibilities for mud that may be present in the Capitol Lake sediment. The chosen erodibilities were reclassified as lower (from mid-level) and higher (from extreme high) erodibility (Table 2.11).

Table 2.11. Erodibility parameter space for sediment transport/morphology simulations

erodibility level	critical shear stress for erosion (N/m^2)	erosion rate ($kg/m^2/s$)
lower	0.3	$25x10^{-5}$
higher	0.2	$50x10^{-5}$

While other factors could be expanded in similar fashion to create a multivariate analysis, reporting a large number of results as ranges is undesirable. However, the erodibility level that is investigated as outlined above is among the most important variables for accurate sediment transport and morphological modeling.

Modeling Approach

The project objectives of investigating both hydrodynamics/salinity and sediment transport/morphology allowed development of two categories of simulations (Table 2.12). Additionally, a specific set of simulations were conducted to investigate extreme hydrologic events.

Hydrodynamics/salinity Simulations

For hydrodynamics/salinity, 3D models were built with uniformly-spaced 7-layer domains with a 2.4 sec time step to accurately capture turbulent mixing. A complex tide comprised of the dominant components and the ‘salinity river’ are the hydrodynamic forcings. A salinity of 28 ppt was used in Budd Inlet and 0 in the Deschutes River. These simulations were run for two weeks (the spring-neap tidal cycle) for each river discharge class and scaled and summed to represent a full year. These simulations were run only on the predam or restored scenario estuary domains.

Sediment transport/morphology Simulations

Sediment transport/morphology runs were operated in 2D with a 6 sec time step as they were required to simulate significantly longer times (years as compared to weeks). A

simple tide was used to remove the need to simulate the complex semi-diurnal inequality during the spring-neap tidal cycle (Latteux, 1995). The amplitude of the largest component, M2, was multiplied by 1.1 and a harmonic 'morphological tide' was generated for tidal forcing (Figure 2.34). The 'morphological river' was used as the fluvial forcing with the four sediment sizes and associated concentrations. Initial sediment distribution and thickness maps were included in restoration scenario but not predam or lake simulations. Underlying stratigraphy was used in all simulations to track the evolution of the relative grain size fractions through time. In salt water, cohesive sediment tends to flocculate to form sediment flocs, with the degree of flocculation depending on the salinity of the water. These flocs are much larger than the individual sediment particles and settle at a faster rate. Delft3D handles flocculation of fine sediment by requiring a salinity value when all particles are flocculated and a settling velocity for the flocs. For estuarine simulations when saline water would be causing flocculation, the salinity value was set at 10 ppt and the settling velocity was set at 1 mm/s (Hill, 1998). The constant wind and wave fields were included in the sediment transport/morphology simulations. All estuary simulations were examined according to the erodibilities in Table 2.11.

Table 2.12. Comparison of design and operation of simulation categories

Parameter	Hydrodynamics/salinity	Sediment transport/morphology
dimension	3D, 7 uniformly-spaced layers	2D
timestep (sec)	2.4	6
tidal forcing	complex tide	morphological tide
fluvial forcing	'salinity river'	'morphological river'
domain	predam estuary and restoration scenarios	predam estuary, initial and modern lakes, restoration scenarios
scale of simulated time	weeks	years
length of runs	300 hrs for 2 weeks	70 hrs for 3 years
additional details	salinity: 0 ppt on river, 28 ppt in Budd Inlet	four sediment classes, underlying stratigraphy, maximum flocculation at 10 ppt, wind and waves included, two erodibilities

Extreme hydrologic events

Five extreme hydrologic events were developed to simulate the highest water levels and fastest velocities resulting from episodic incidents (Table 2.13). High tide heights and flood events were combined to reproduce observed storm events and statistically rare occurrences. Measured river discharge and tide height at Olympia (Figure 2.35) for a large storm (December 1977) were extracted from a published report (URS Group, Inc., 2003). One of the largest tidal oscillations on record, which occurred at the end of December 1986, was identified at Seattle from NOAA archival data and the tide heights were adjusted for Olympia (Figure 2.36). Specific flood event volumes for the 100-year flood (341 cms) and two-year flood (113 cms) were acquired from a published flood analysis report (CLAMP Phase One – Task 2, 2000). The dry season flow calculated

from the hydrograph (2.8 cms) was also used to investigate a large tidal oscillation without significant river discharge.

Table 2.13. Descriptions of the five extreme hydrologic events

event	description	tide height	river discharge
I	observed 1977 tide and storm	1977 tide	1977 storm
II	observed 1977 tide and 100-yr flood	1977 tide	341 cms
III	largest tidal oscillation and 100-yr flood	1986-87 tide	341 cms
IV	largest tidal oscillation and 2-yr flood	1986-87 tide	113 cms
V	largest tidal oscillation and dry season	1986-87 tide	2.8 cms

The extreme hydrologic event simulations were conducted on bathymetry that evolved after three-year morphological runs to allow investigation of water levels and velocities after the initial transformation phase from Capitol Lake to a restored estuary. Evolved bathymetry results from the lower erodibility level only were extracted and the five extreme events were simulated for Restoration Scenarios A, B and D.

Model Validation

The objective of the DEFS is to predict conditions in an environmental setting that does not exist, so no model calibration data are available to test or adjust model parameters. However, hydrodynamic and water quality measurements were acquired in Budd Inlet in 1996-1997 by a research consortium for the LOTT Wastewater Management Partnership (1998). Hydrodynamic/salinity validation runs were conducted in 3D on the Budd Inlet grid and depth section using Capitol Lake discharge from the LOTT report (Figure 2.37). Measured salinity cross-sections were compared to model results for winter and summer. Both comparisons showed the simulations qualitatively reflect the field observations in outer Budd Inlet (Figure 2.38). The modeled salinity values closely match the measured data with a range of 23 – 27 ppt. Fresher layers of water overlay a mixed saltier layer on the eastern side of the inlet. Stratification is the strongest in the east with vertical salinity fronts along the cross-section ending in a well-mixed water column on the west side. The hydrodynamic/salinity test case increases confidence for several aspects of the model design and operation – grid and vertical resolution, mixing parameters, initial conditions and time step. While an exhaustive analysis would use the measured data to extensively calibrate the model to match the observations, this exercise was to establish a degree of realism, not reproduce Budd Inlet. The test cases were very successful and encouraged a transition from the model development stage to the results production stage. Validation was not possible for sediment transport as no data were found against which to test. Therefore, the sediment erodibility range should be viewed as an envelope that characterizes the sensitivity of sediment transport to user-defined parameters.

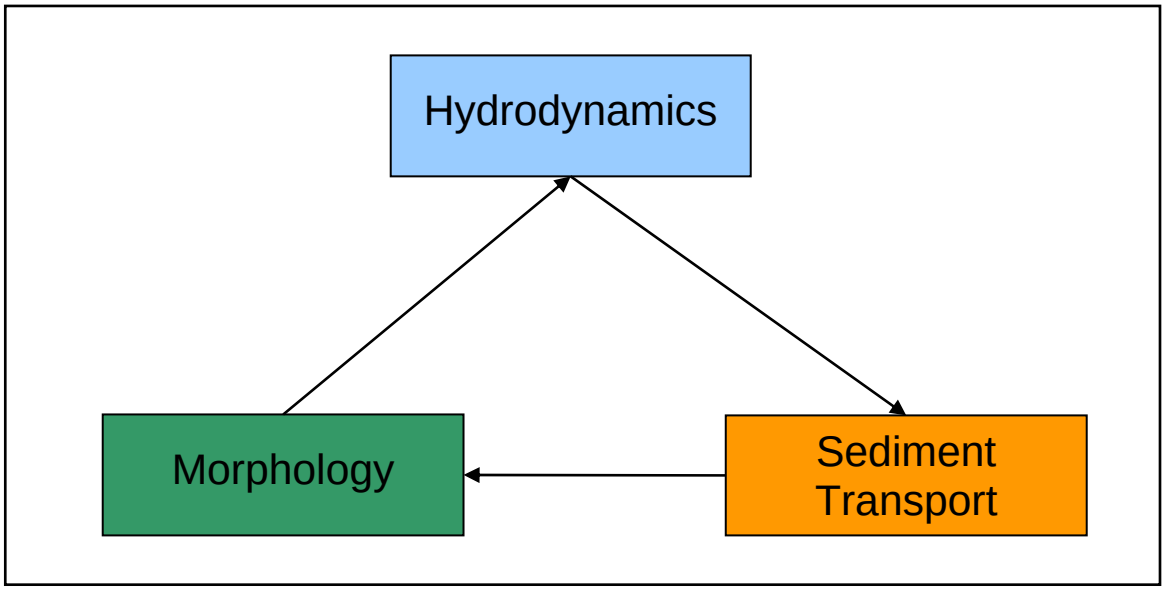

Figure 2.1. Schematic of the hydrodynamic, sediment transport and morphology interaction in the Delft3D FLOW module. The hydrodynamics control the sediment transport, which in turn determines the morphological change. The morphology is updated and fed back into the hydrodynamics. The cycle then continues with the next time step.

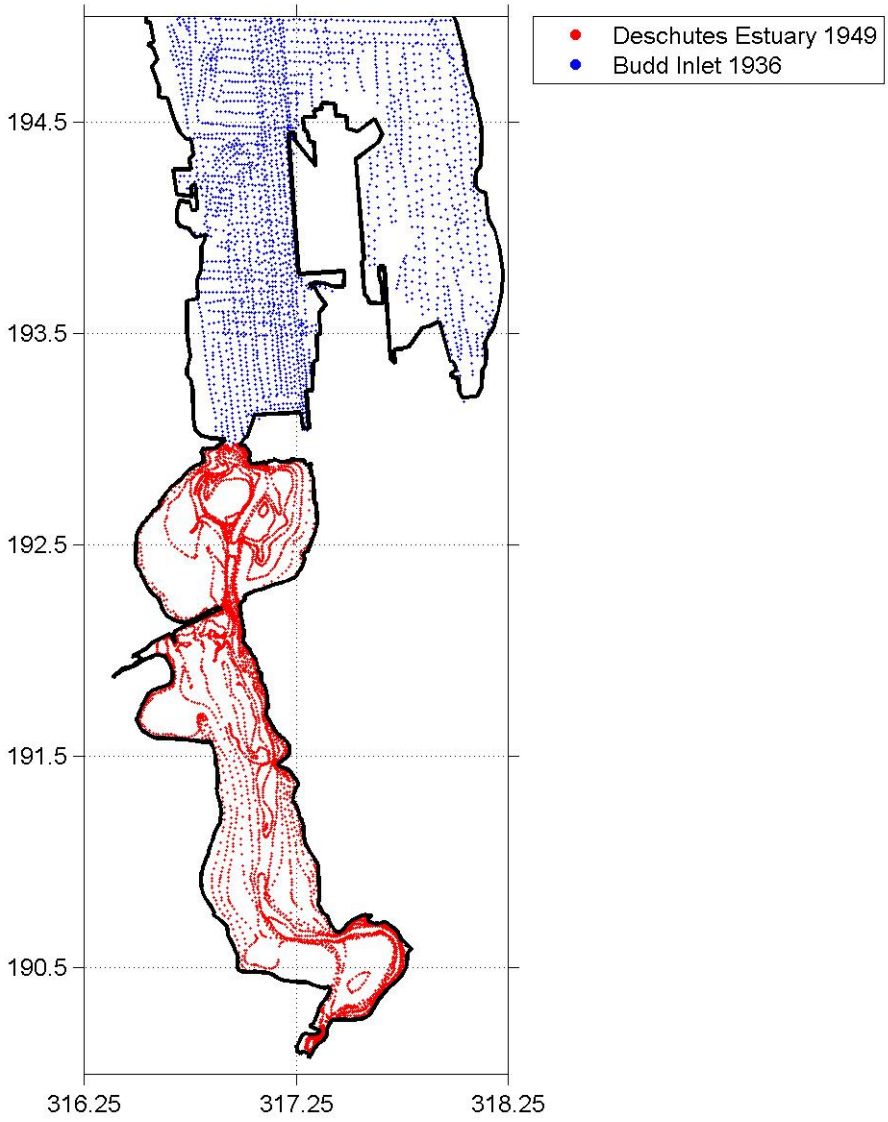

Figure 2.2. Bathymetric surveys that provided data to compile predam bathymetry for the Deschutes Estuary and lower Budd Inlet. All datasets were adjusted to NGVD29, meters.

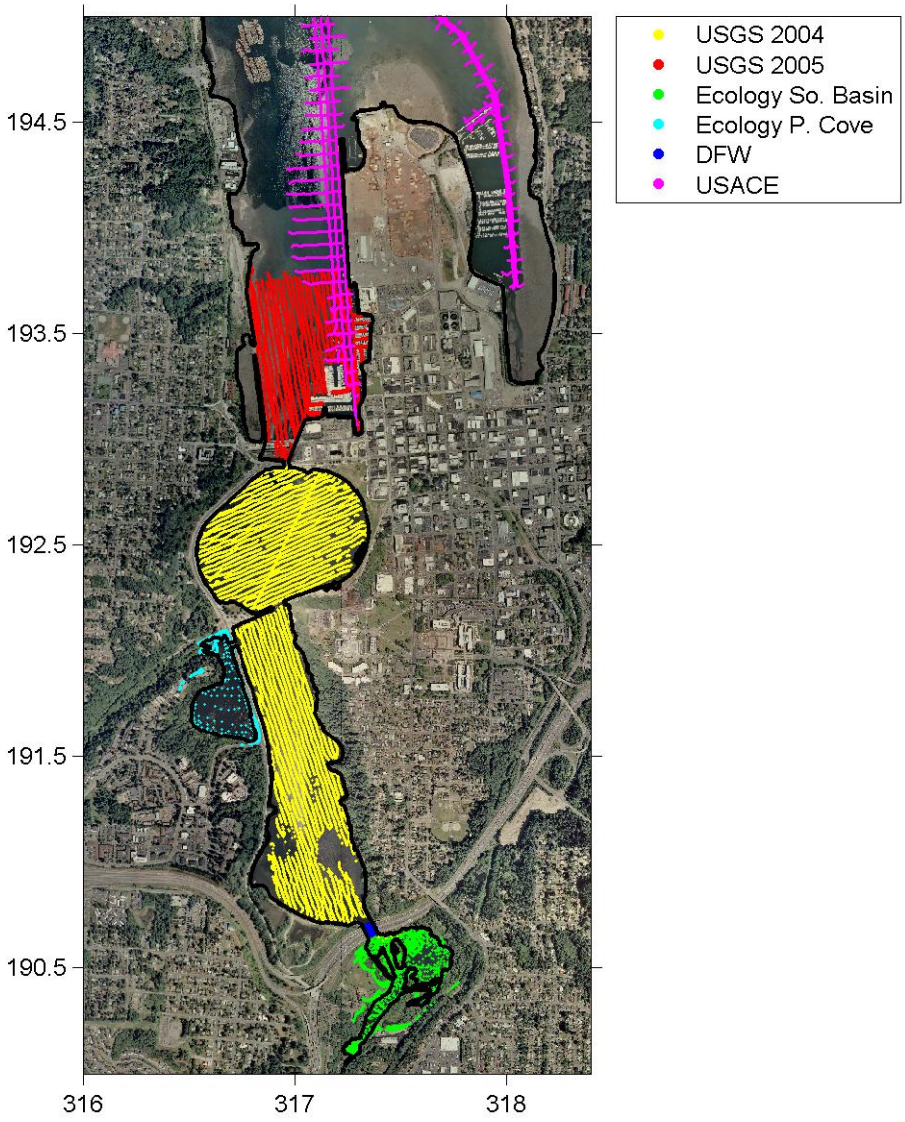

Figure 2.3. Bathymetric surveys that provided data to compile modern bathymetry for Capitol Lake and lower Budd Inlet. All datasets were adjusted to NGVD29, meters. Areas in Budd Inlet that do not have recent data were supplemented with the 1936 Budd Inlet survey.

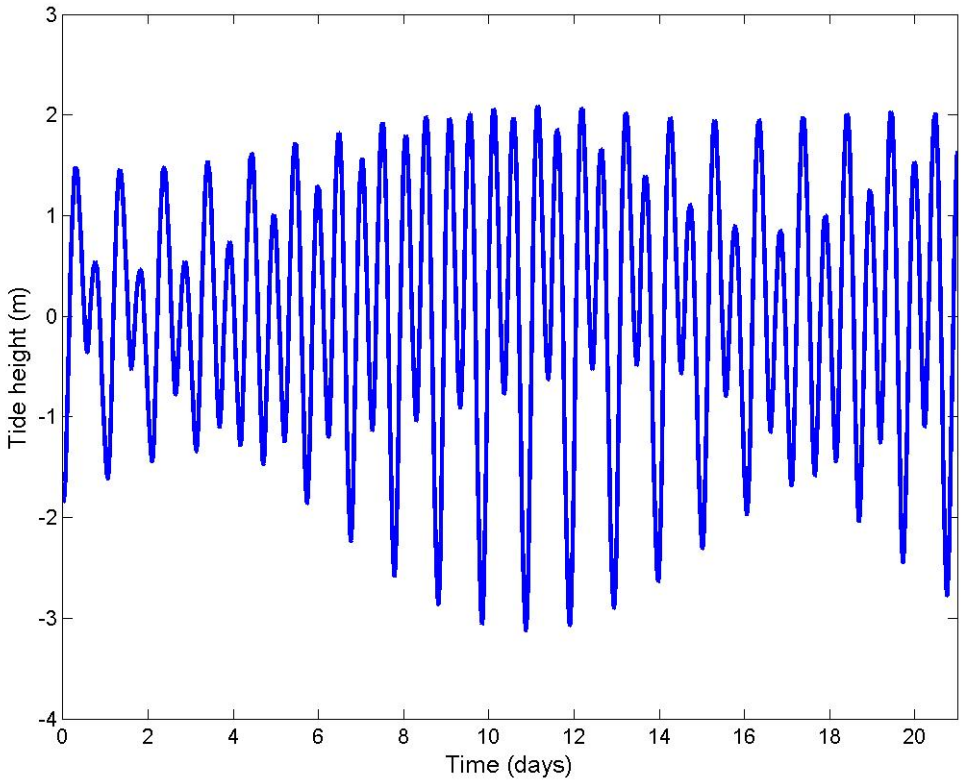

Figure 2.4. Semi-diurnal spring-neap tidal record (m MSL) extracted from the National Ocean Service water level station at Gull Harbor in eastern Budd Inlet (station #9446807). The maximum range during a normal tidal cycle is 5 m but seasonal extreme tides can temporarily cause larger ranges.

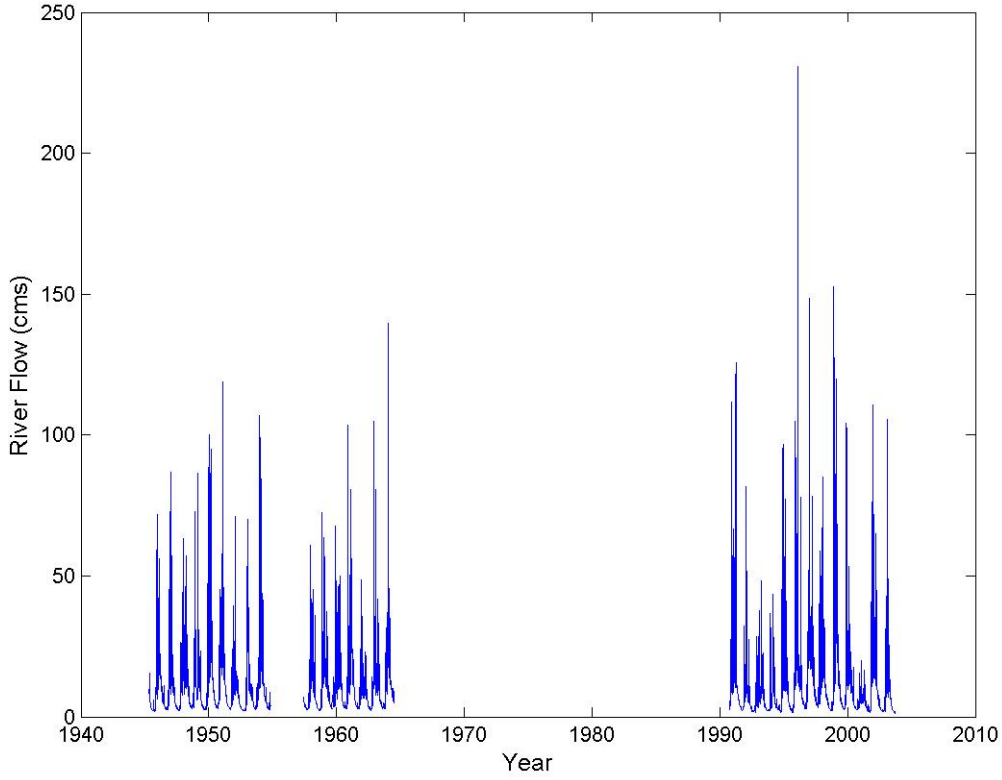

Figure 2.5. Deschutes River hydrograph record from USGS Station #12080010 at the E Street Bridge in Tumwater. A cumulative record of almost 30 years remains after the three data gaps are removed.

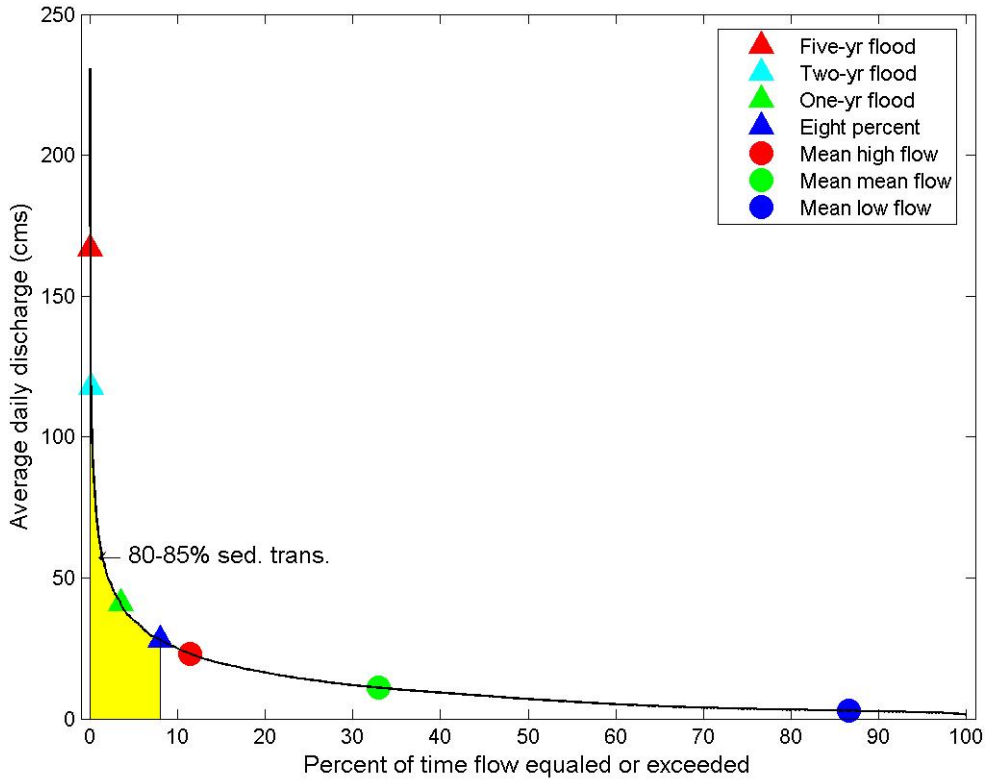

Figure 2.6. Deschutes River flows as percent of the year and majority of associated sediment transport. The yellow region represents 80 – 85% of the annual sediment load, which is delivered by flows that occur only 8% of the year. Key river flows are also identified, showing the frequency and discharge of particular events.

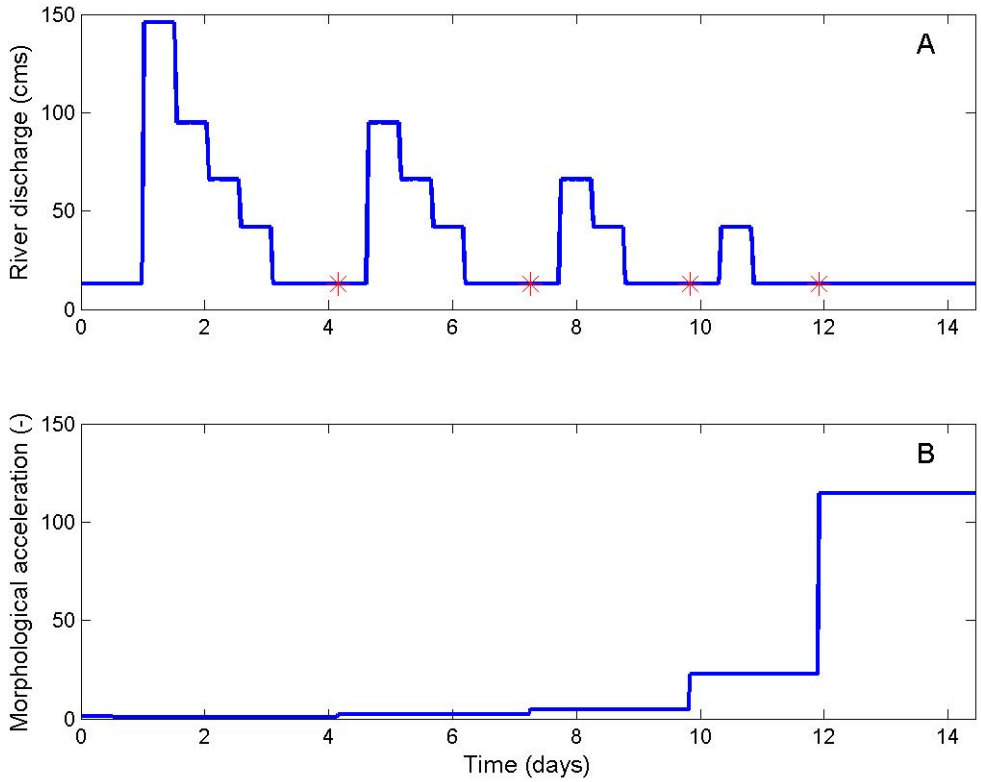

Figure 2.7. Arrangement of flood events (A) and morphological acceleration factor (B) for the 'morphological river'. Red stars in A indicate when MORFAC changes. An initial high flow is followed by successively lower flows with the average discharge as an interlude between floods. A dry season succeeds the wet season and the entire hydrograph can be repeated to create multi-year 'morphological river' simulations. See Table 2.5 for MORFAC values.

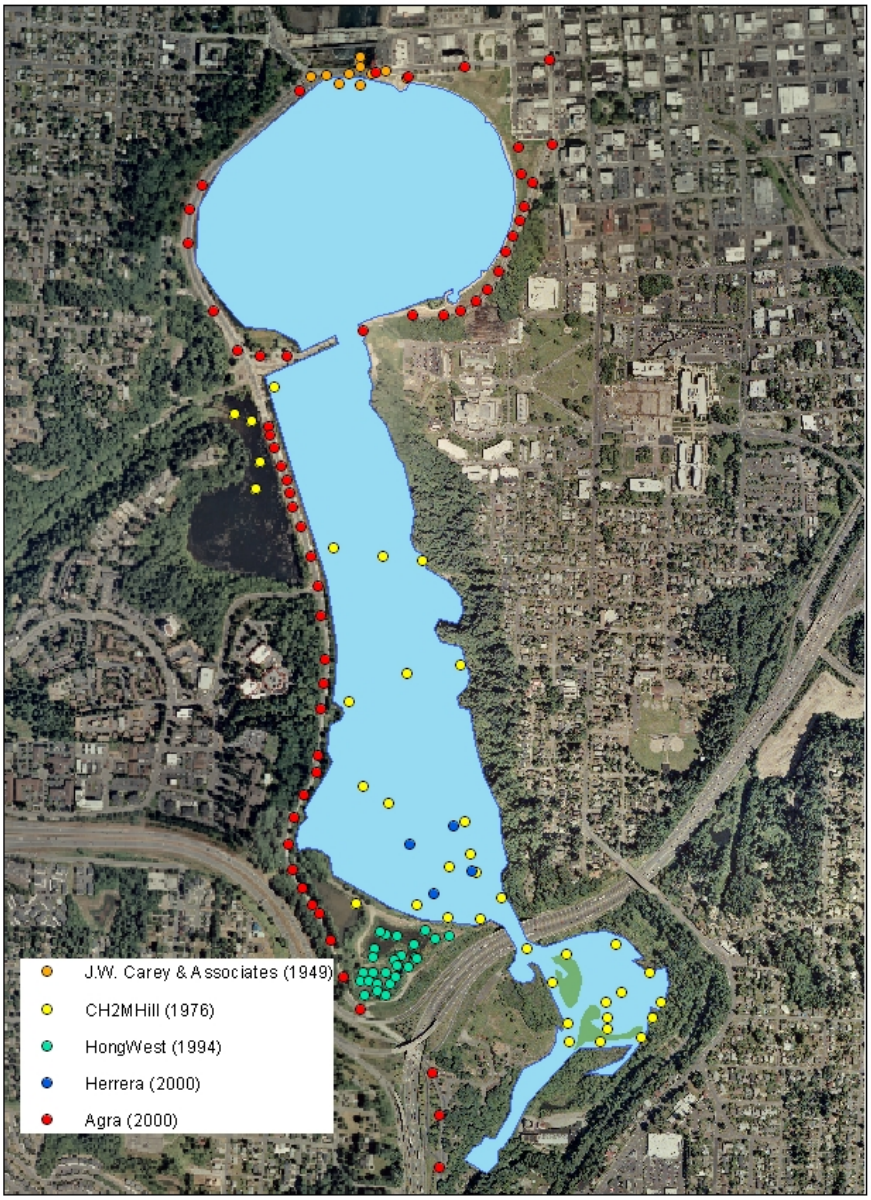

Figure 2.8. Historical sediment collection in and around Capitol Lake since 1949. North Basin has not been sampled since the creation of the lake from the Deschutes Estuary.

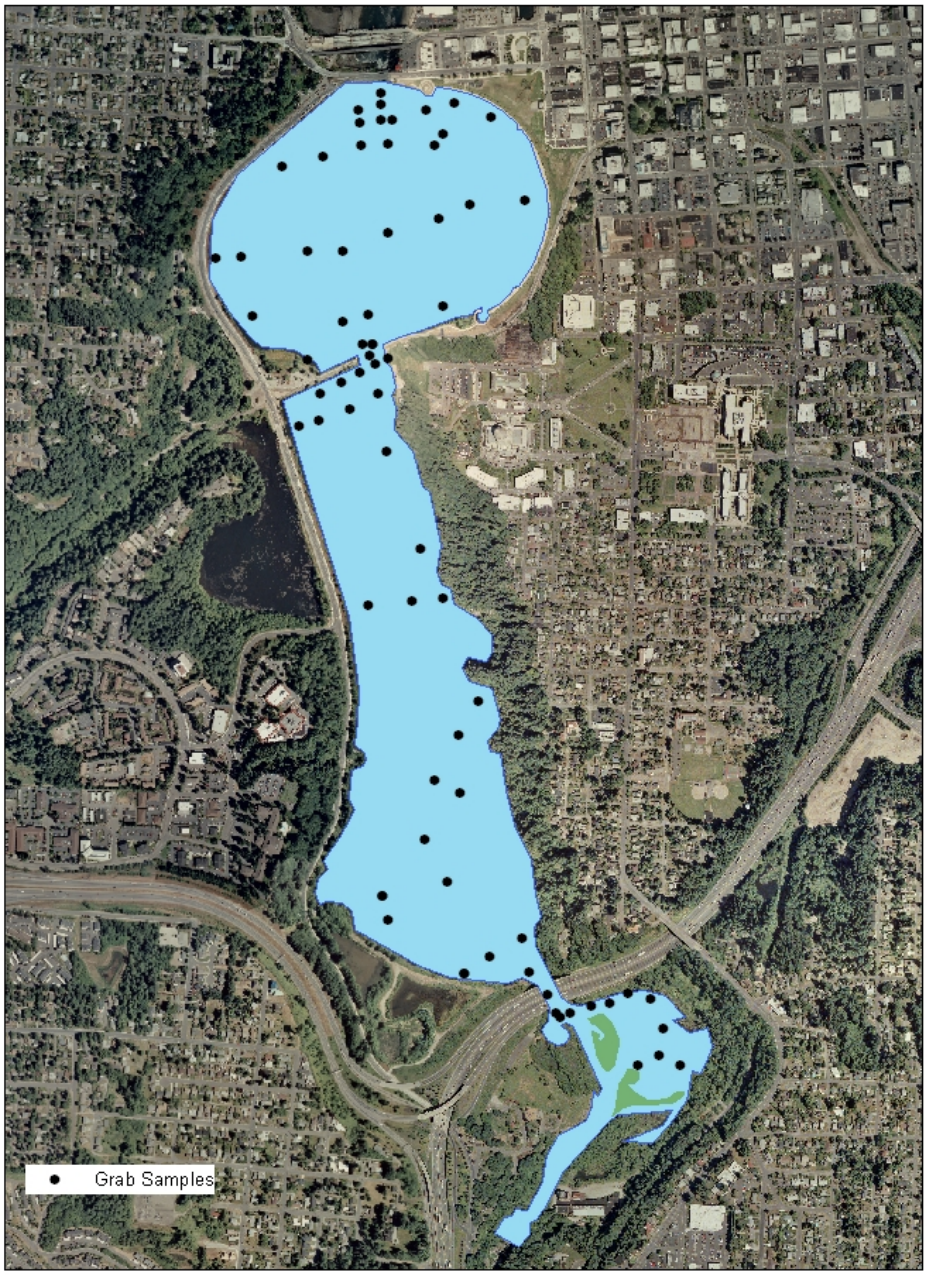

Figure 2.9. Surface sediment samples collected in February 2005 for this study. Approximately 500 g of sediment were gathered from 72 grab samples in North, Middle and South Basins. No samples were taken from Percival Cove or outside of the lake.

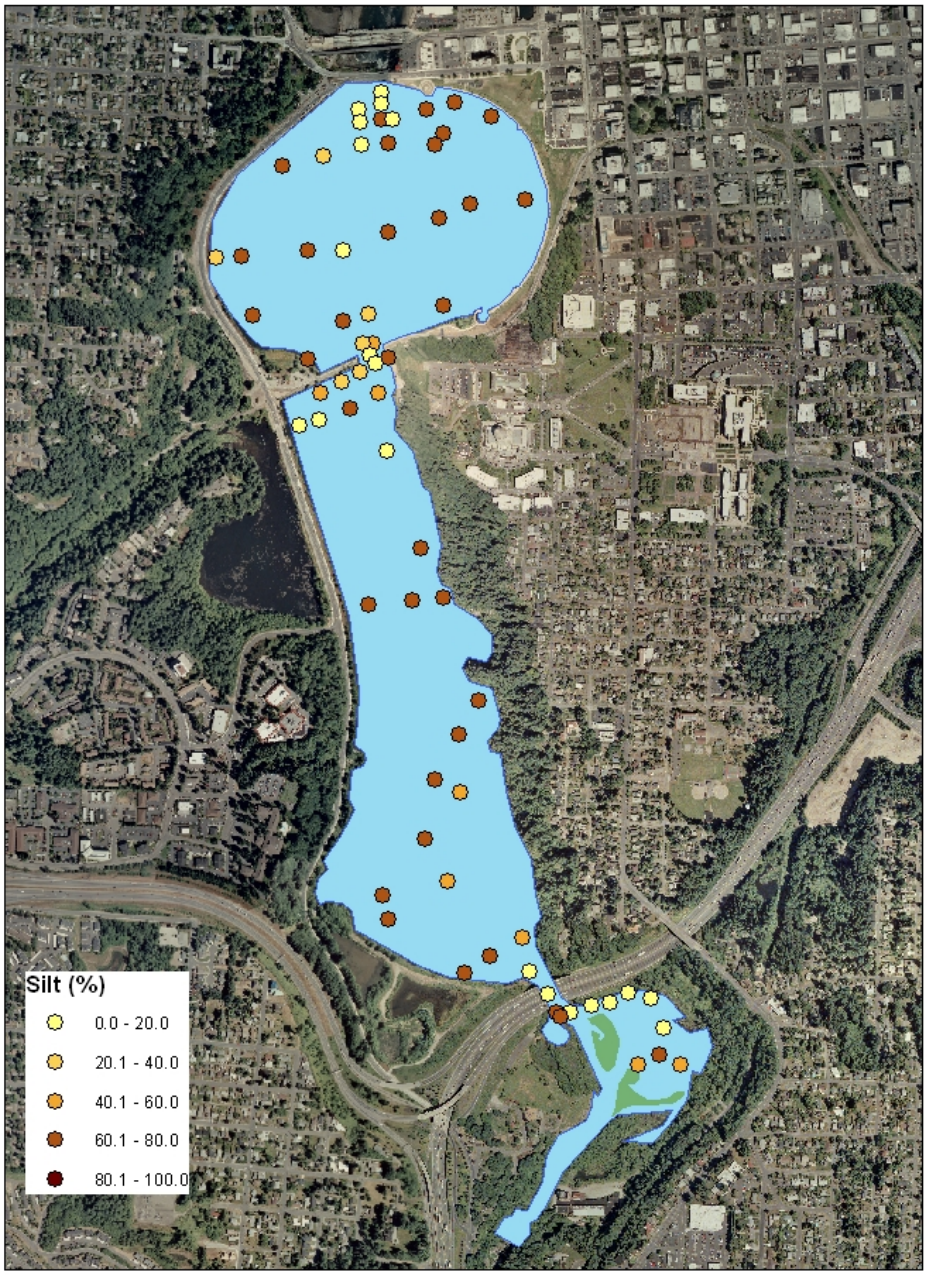

Figure 2.10. Silt percentages in the 2005 grab samples. Yellow indicates low quantities of silt while dark brown shows high quantities. Middle Basin and parts of North Basin are silt-dominated.

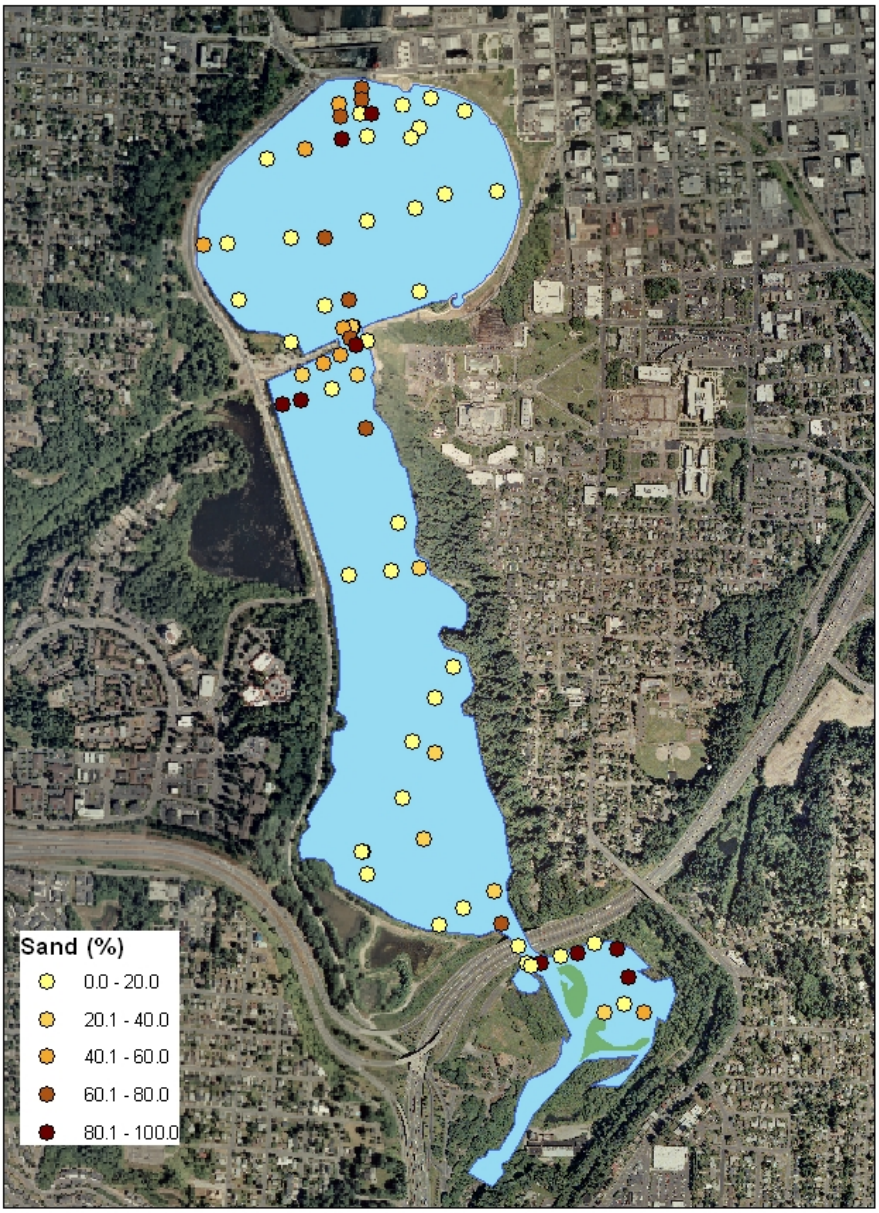

Figure 2.11. Sand percentages in the 2005 grab samples. Yellow indicates high quantities of sand while dark brown shows low quantities. Central North Basin and the trestle area are sand-dominated.

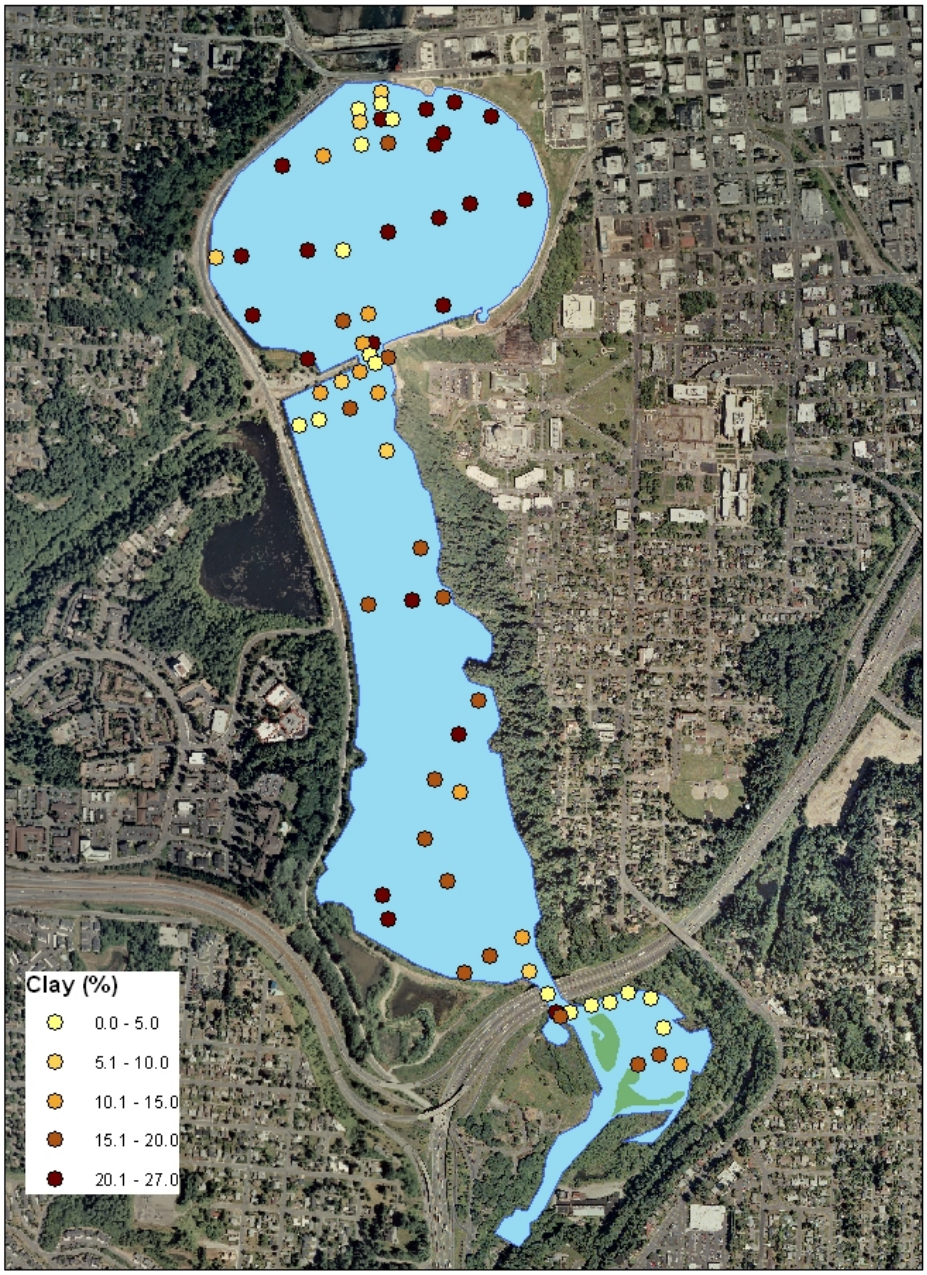

Figure 2.12. Clay percentages in the 2005 grab samples. Yellow indicates low quantities of clay while dark brown shows high quantities. Middle Basin and parts of North Basin show large amounts of clay.

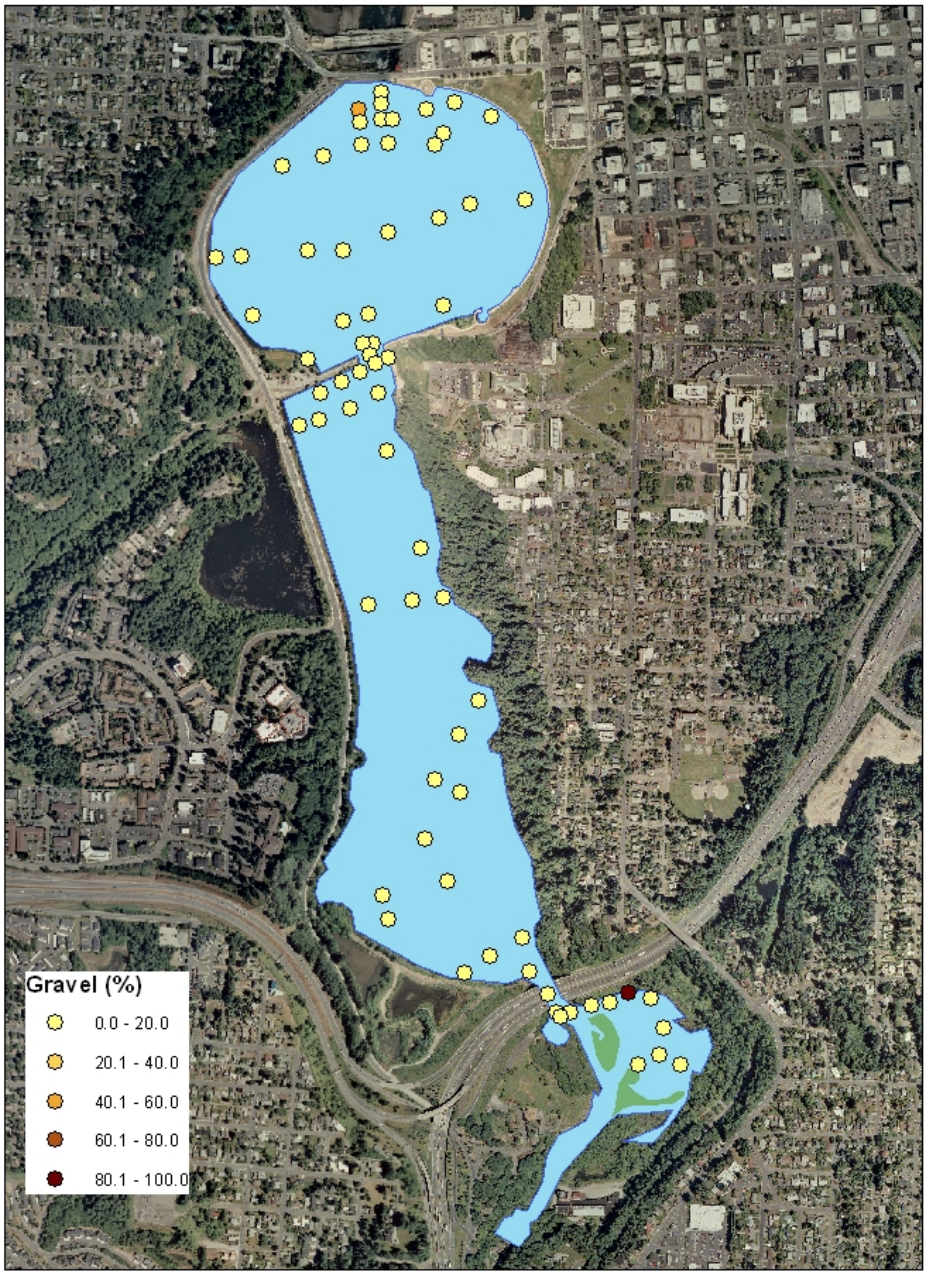

Figure 2.13. Gravel percentages in the 2005 grab samples. Yellow indicates low quantities of gravel while dark brown shows high quantities.

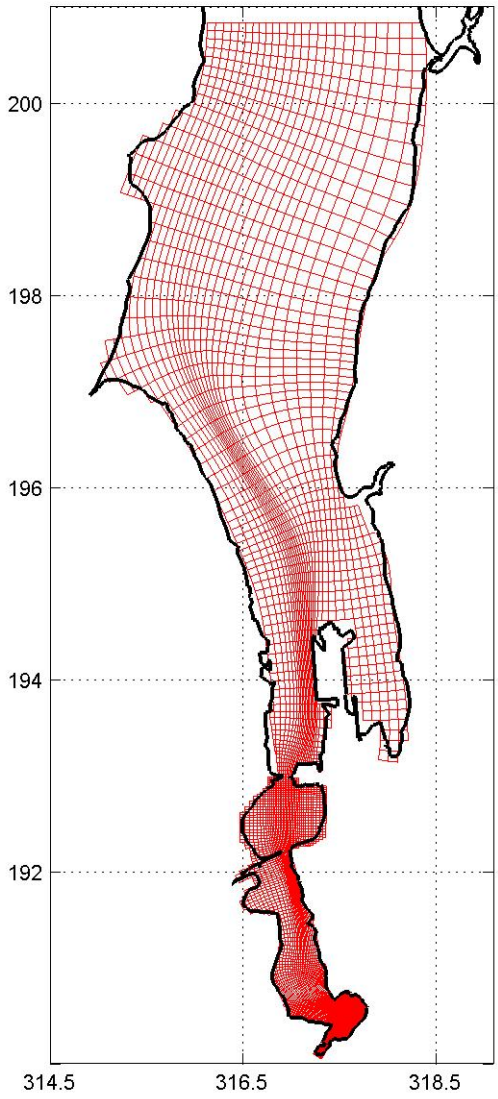

Figure 2.14. Predam estuary grid of Deschutes Estuary and Budd Inlet. The axes are in Washington State Plane South (km). Resolution is higher in the estuary, port region and ship channel while other areas have lower resolution.

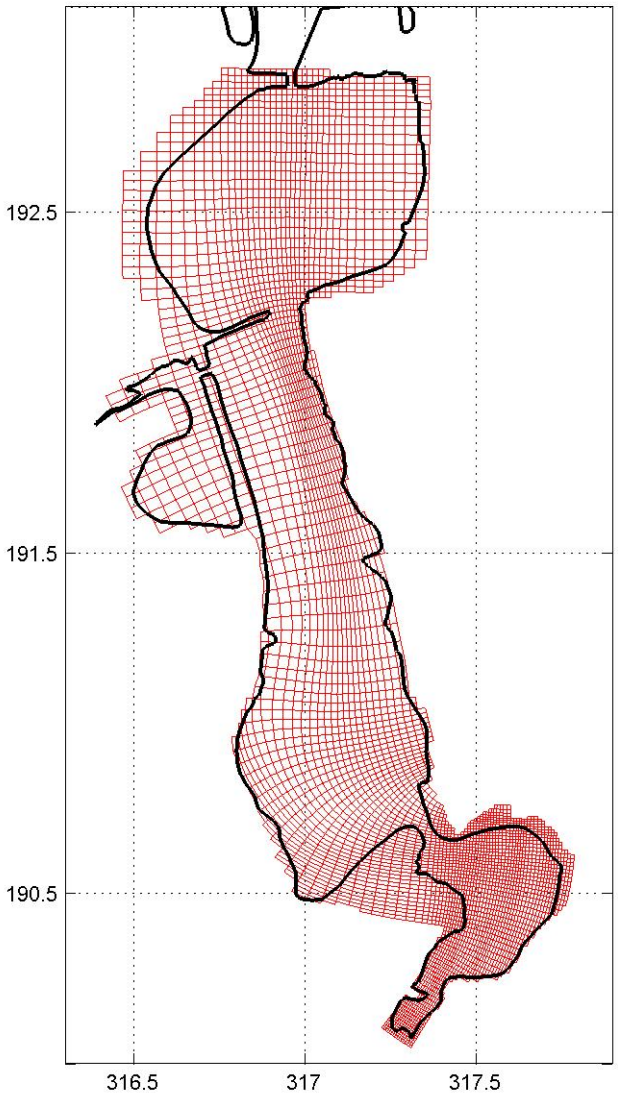

Figure 2.15. Initial lake grid for Capitol Lake after completion of the I-5 bridge in 1957. The axes are in Washington State Plane South (km). Resolution is higher in South Basin and around the trestle while other areas have lower resolution.

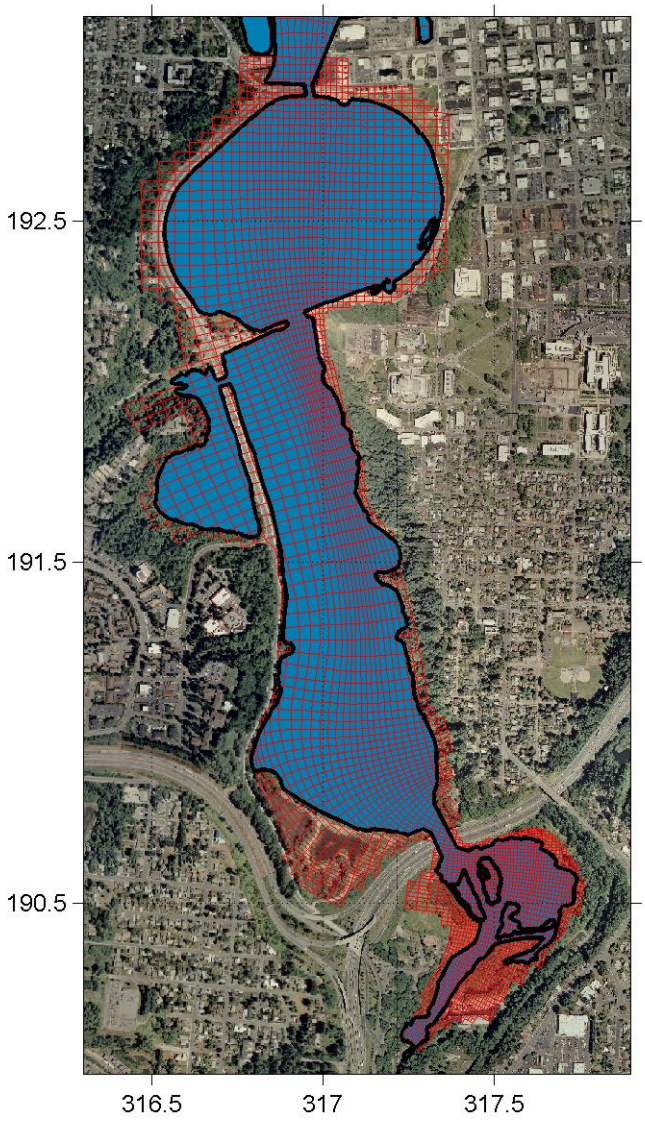

Figure 2.16. Modern lake grid for Capitol Lake in 2005. The axes are in Washington State Plane South (km). Resolution is higher in South Basin and around the trestle while other areas have lower resolution.

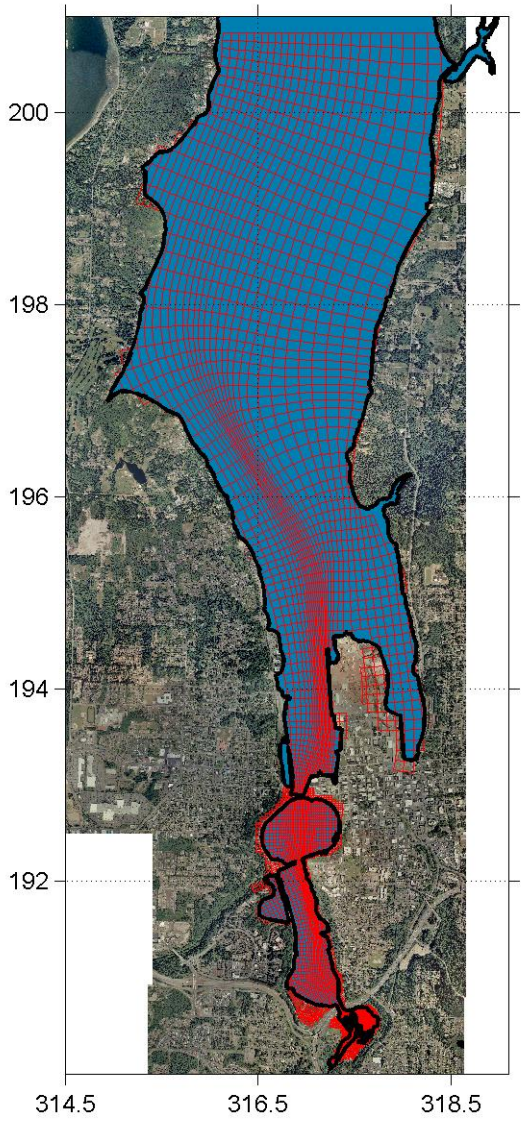

Figure 2.17. Restoration scenario grid for a restored Deschutes Estuary and Budd Inlet. The axes are in Washington State Plane South (km). Resolution is higher in the estuary, port region and ship channel while other areas have lower resolution.

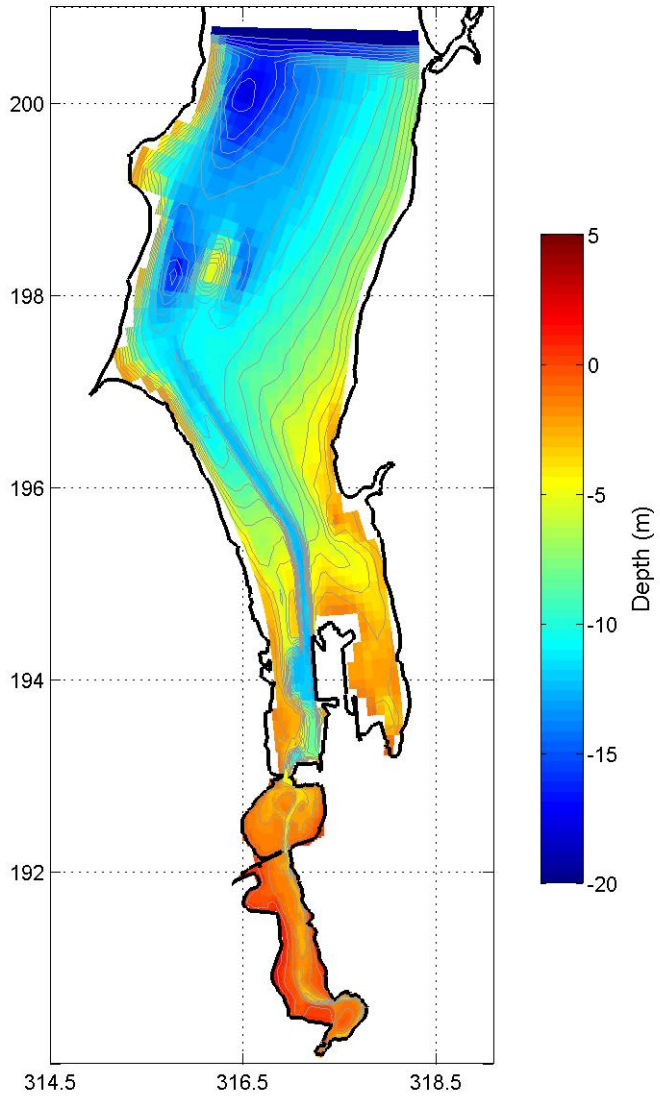

Figure 2.18. Predam bathymetry of Deschutes Estuary and Budd Inlet. The axes are in Washington State Plane South (km) and bathymetry contours are in 1 m increments from – 20 to 4 m MSL. Blues are deeper water and reds are shallow.

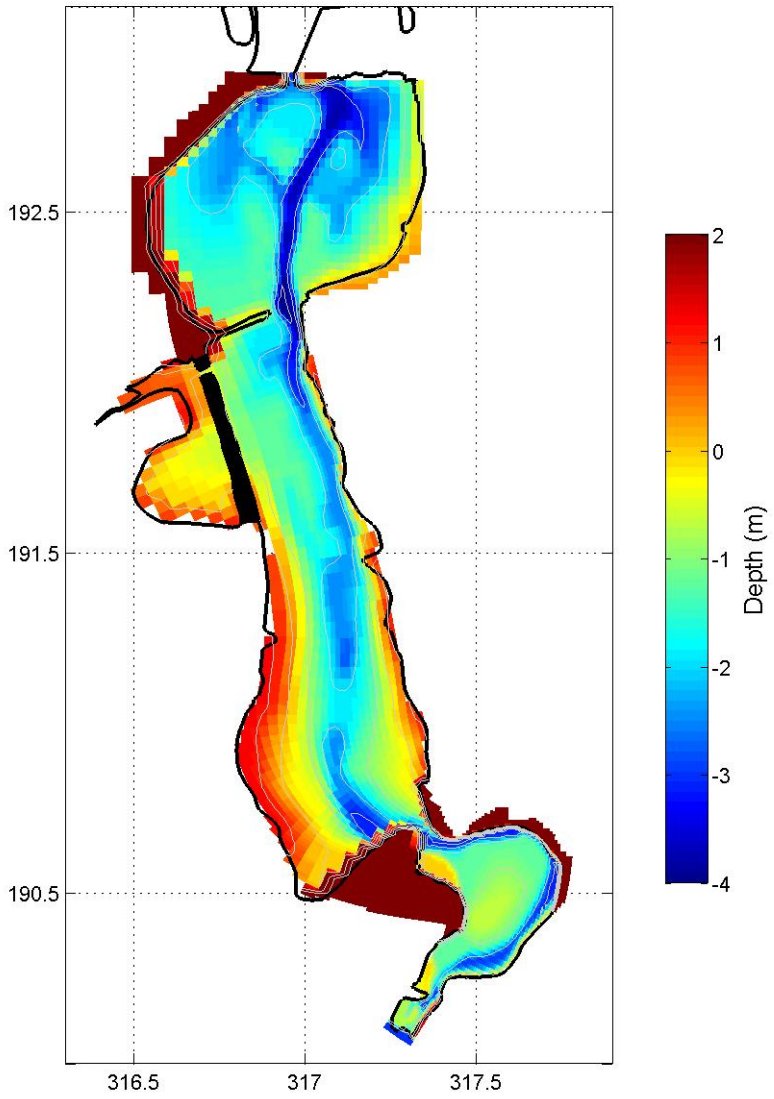

Figure 2.19. Bathymetry of Capitol Lake after completion of the I-5 bridge in 1957. The axes are in Washington State Plane South (km) and bathymetry contours are in 1 m increments from – 4 to 2 m MSL. Blues are deeper water and reds are shallow. The channel of the historic Deschutes Estuary is altered by the construction of the I-5 bridge between South and Middle Basins. Percival Cove is connected to Middle Basin only through a 30 m opening under the Deschutes Parkway.

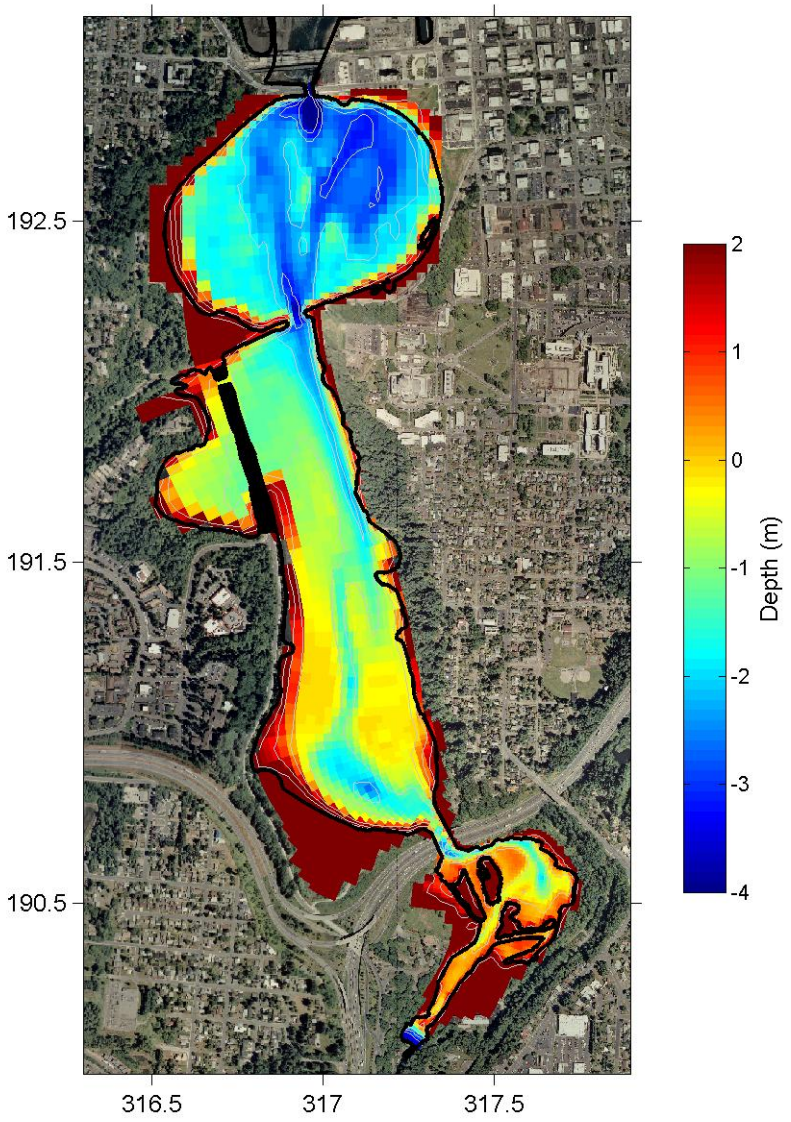

Figure 2.20. Bathymetry of Capitol Lake in 2005. The axes are in Washington State Plane South (km) and bathymetry contours are in 1 m increments from – 4 to 2 m MSL. Blues are deeper water and reds are shallow. The scour hole south of the 5th Ave. Dam is approximately 8 m while the islands of South Basin are approximately 3 m.

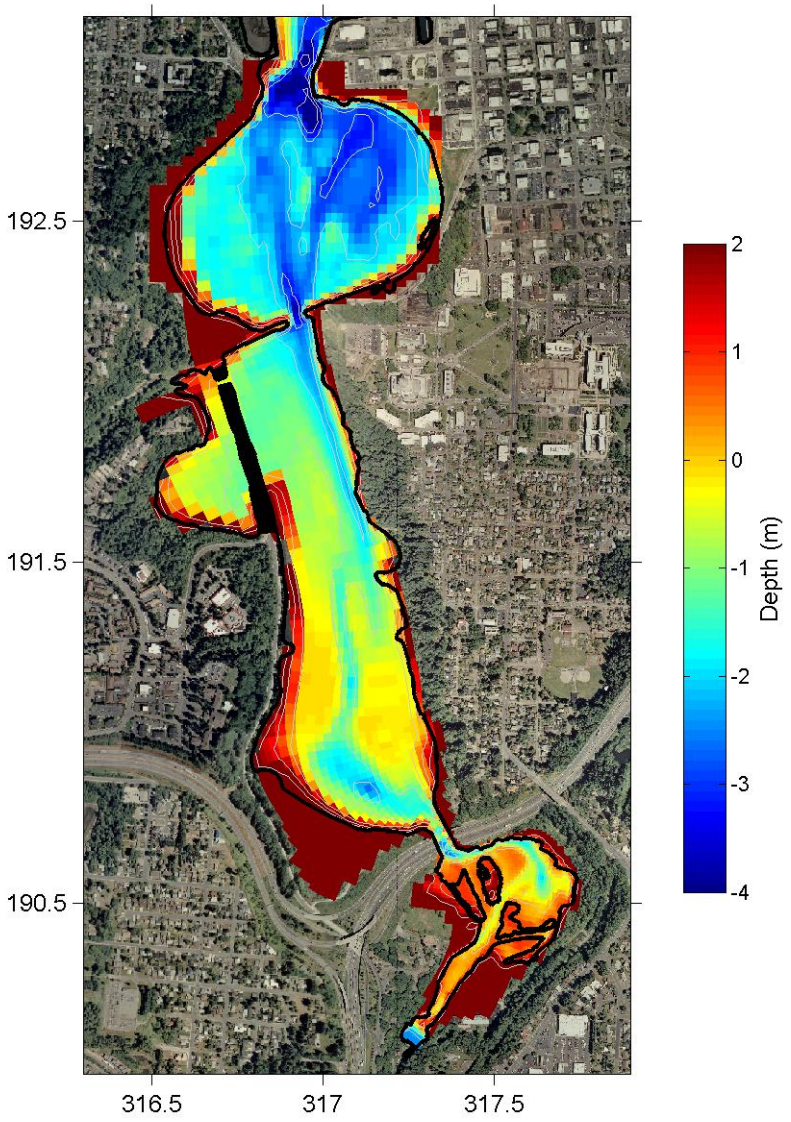

Figure 2.21. Bathymetry of Restoration Scenario A for the estuary only. The 5th Ave. Dam and Bridge have been removed and depths interpolated to connect the estuary to Budd Inlet through a 150 m wide opening. The axes are in Washington State Plane South (km) and bathymetry contours are in 1 m increments from – 4 to 2 m MSL. Blues are deeper water and reds are shallow.

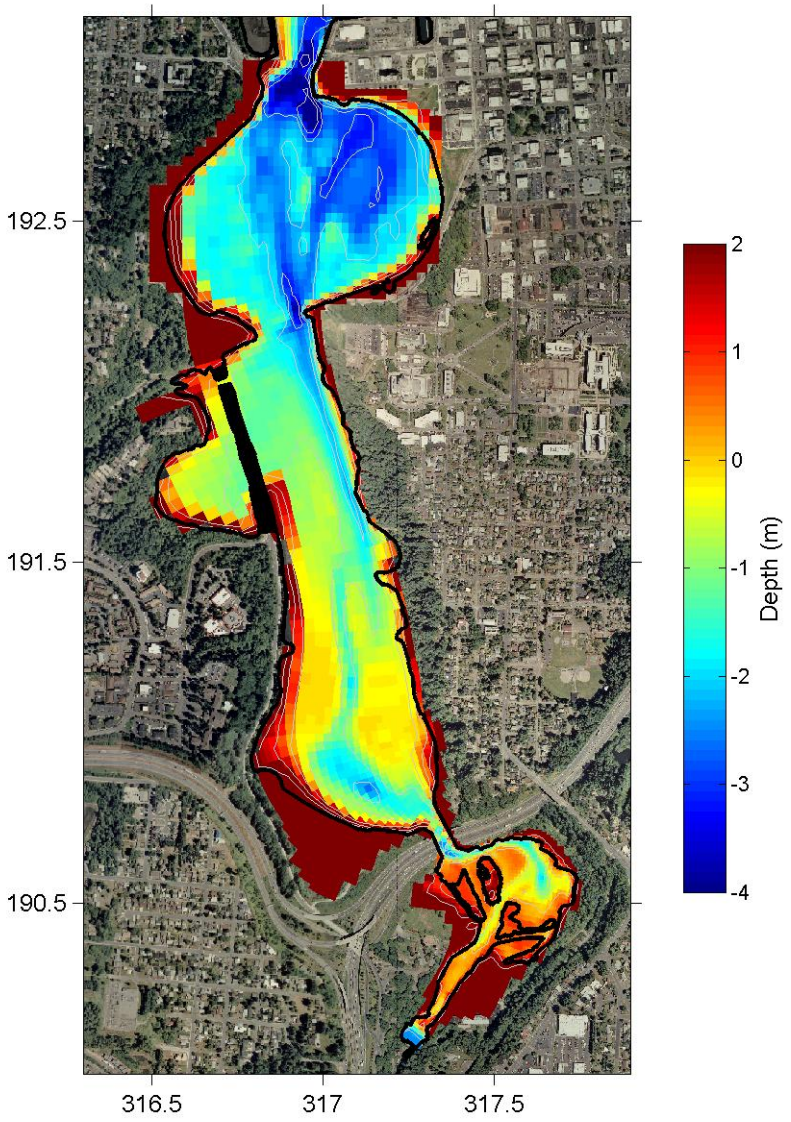

Figure 2.22. Bathymetry of Restoration Scenario B for the estuary only. The 5th Ave. Dam and Bridge have been removed and depths interpolated to connect the estuary to Budd Inlet through a 150 m wide opening. The railroad trestle opening has been widened to 150 m and depths interpolated across the new connection. The axes are in Washington State Plane South (km) and bathymetry contours are in 1 m increments from – 4 to 2 m MSL. Blues are deeper water and reds are shallow.

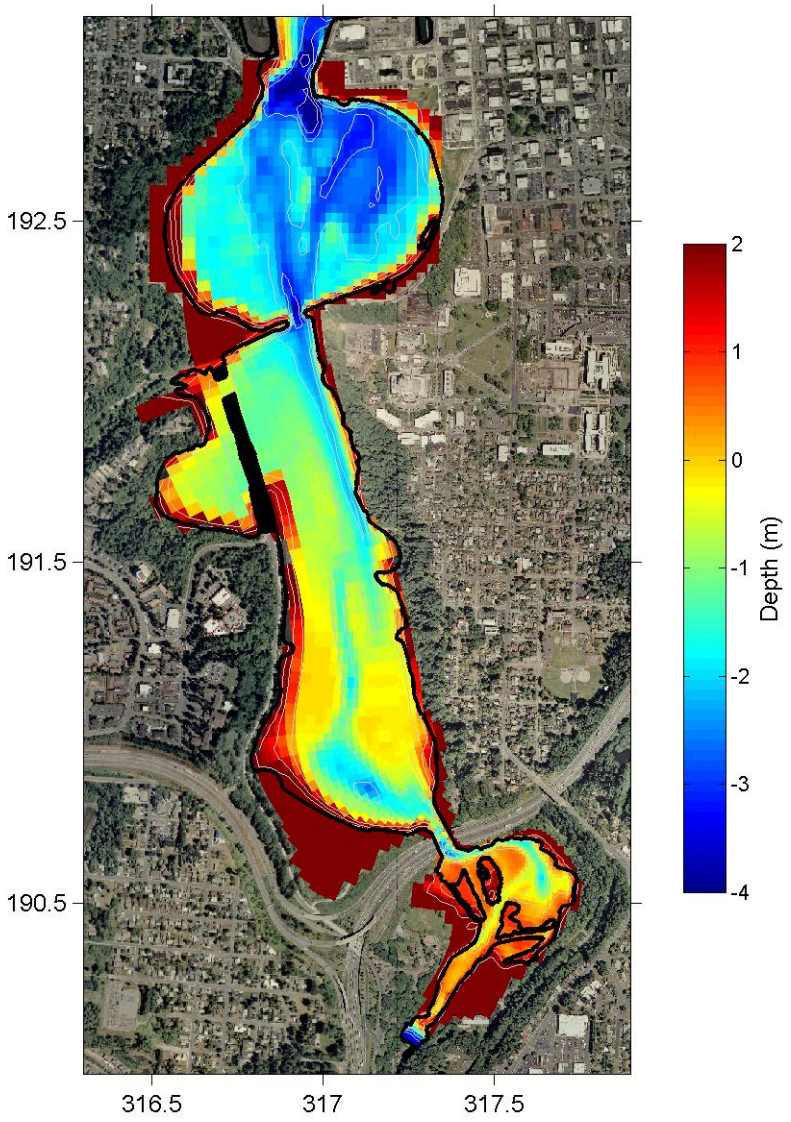

Figure 2.23. Bathymetry of Restoration Scenario C for the estuary only. The 5th Ave. Dam and Bridge have been removed and depths interpolated to connect the estuary to Budd Inlet through a 150 m wide opening. The opening to Percival Cove has been widened to 60 m and depths interpolated across the new connection. The axes are in Washington State Plane South (km) and bathymetry contours are in 1 m increments from – 4 to 2 m MSL. Blues are deeper water and reds are shallow.

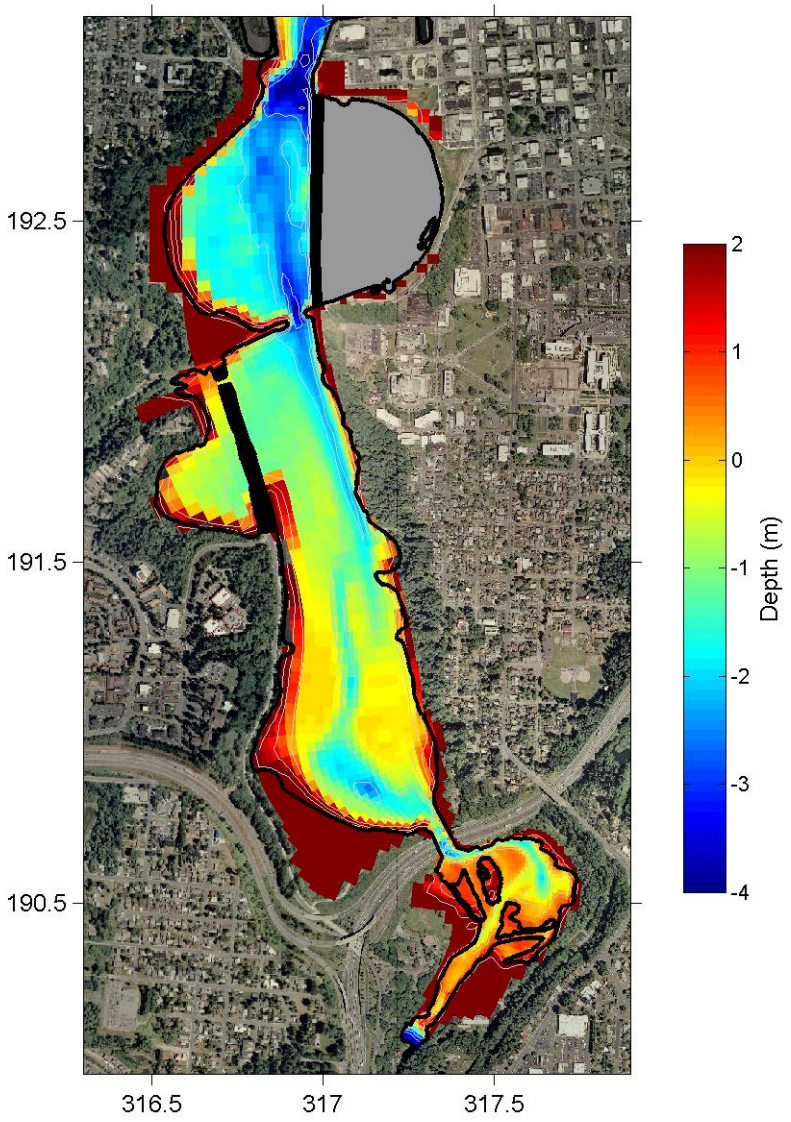

Figure 2.24. Bathymetry of Restoration Scenario D for the estuary only. The 5th Ave. Dam and Bridge have been removed and depths interpolated to connect the estuary to Budd Inlet through a 150 m wide opening. The eastern half of North Basin has been separated from the estuary by a 2:1 sloped 4-m high retaining wall. The axes are in Washington State Plane South (km) and bathymetry contours are in 1 m increments from – 4 to 2 m MSL. Blues are deeper water and reds are shallow.

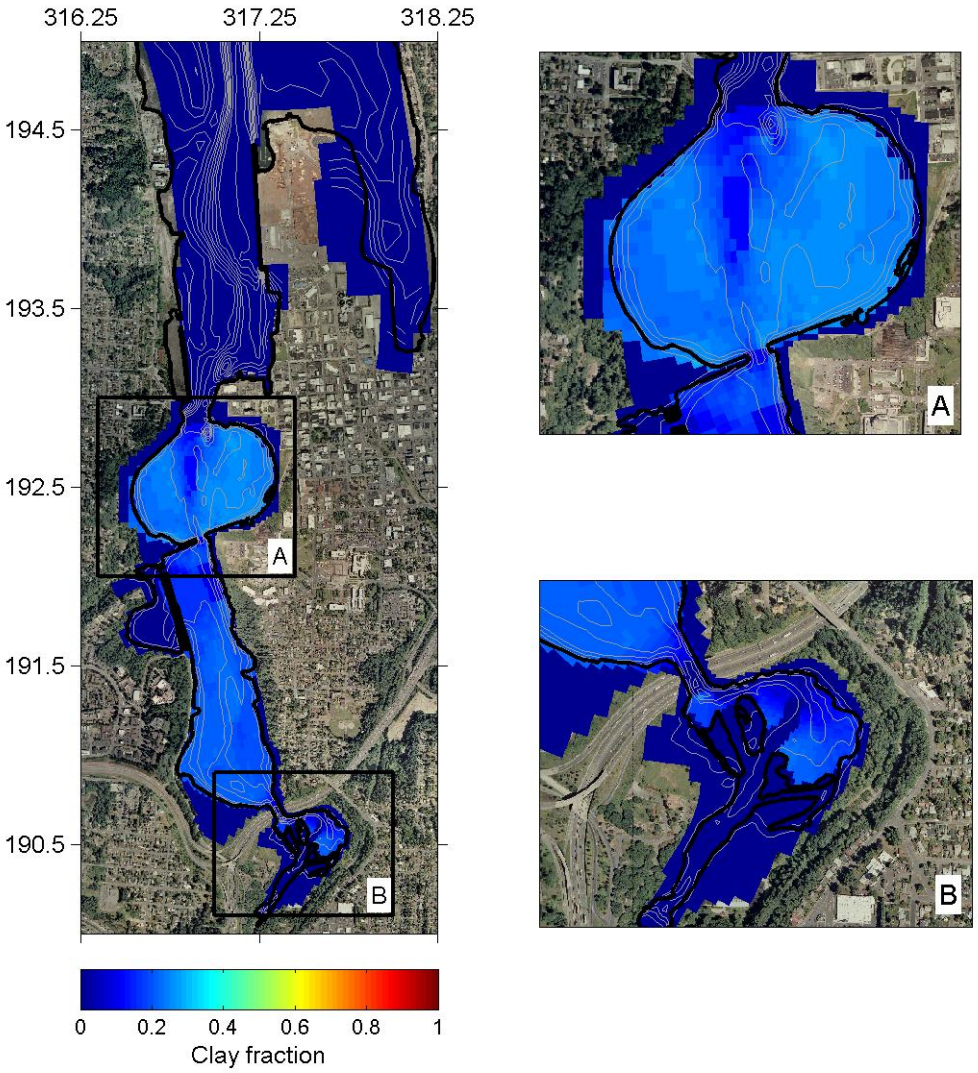

Figure 2.25. Initial clay fraction map for the restoration scenarios. The axes are in Washington State Plane South (km) and bathymetry contours are in 1 m increments from – 10 to 2 m MSL. Clay fraction based on the 2005 sediment grab sample data was interpolated onto the grids. Blues are lower percentages of clay and reds are larger.

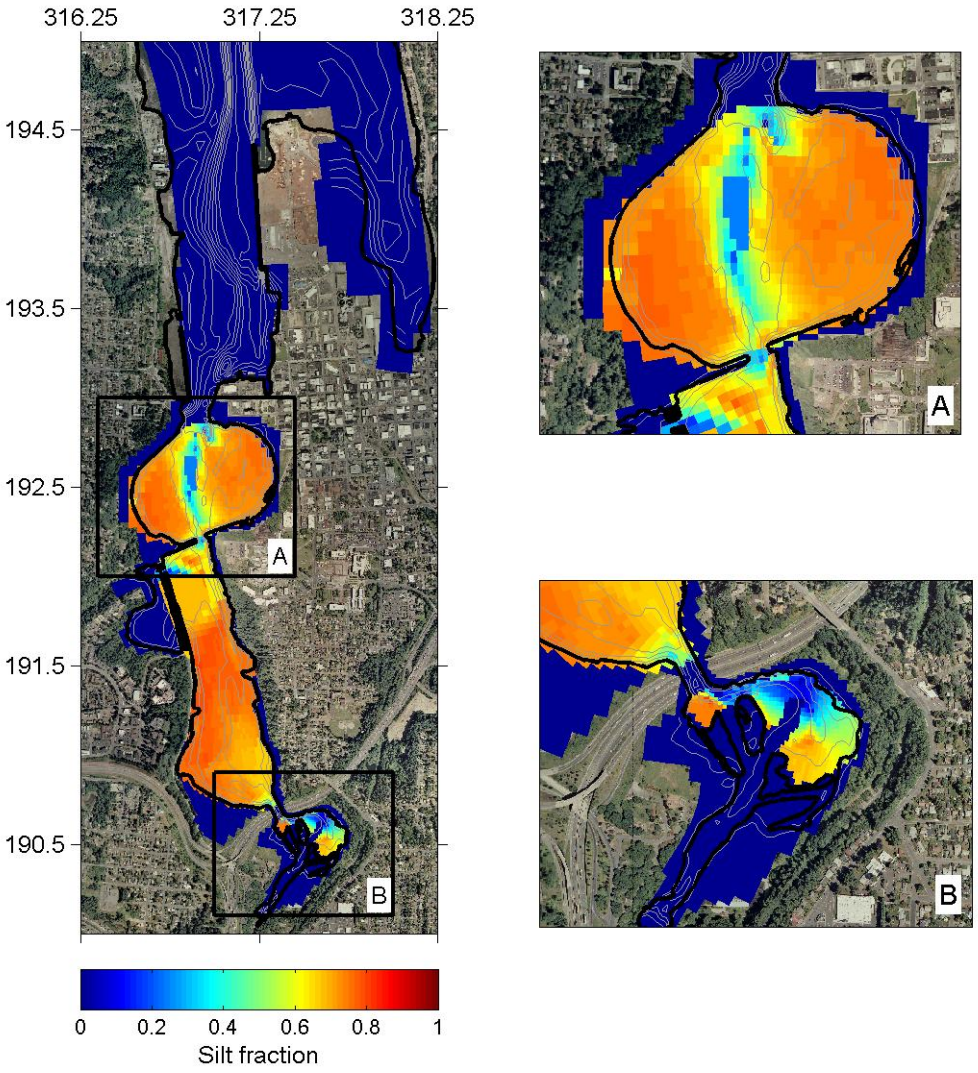

Figure 2.26. Initial silt fraction map for the restoration scenarios. The axes are in Washington State Plane South (km) and bathymetry contours are in 1 m increments from – 10 to 2 m MSL. Silt fraction based on the 2005 sediment grab sample data was interpolated onto the grids. Blues are lower percentages of silt and reds are larger.

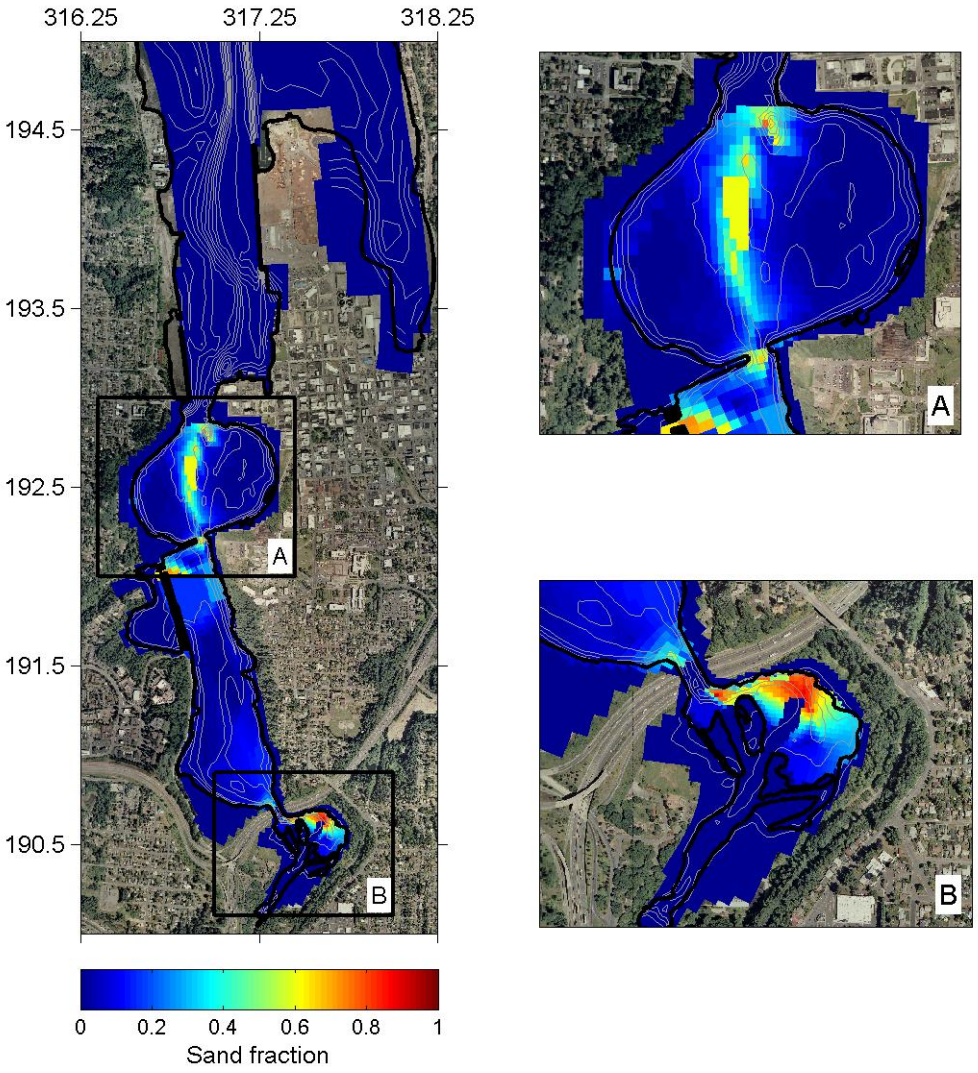

Figure 2.27. Initial sand fraction map for the restoration scenarios. The axes are in Washington State Plane South (km) and bathymetry contours are in 1 m increments from – 10 to 2 m MSL. Sand fraction based on the 2005 sediment grab sample data was interpolated onto the grids. Blues are lower percentages of sand and reds are larger.

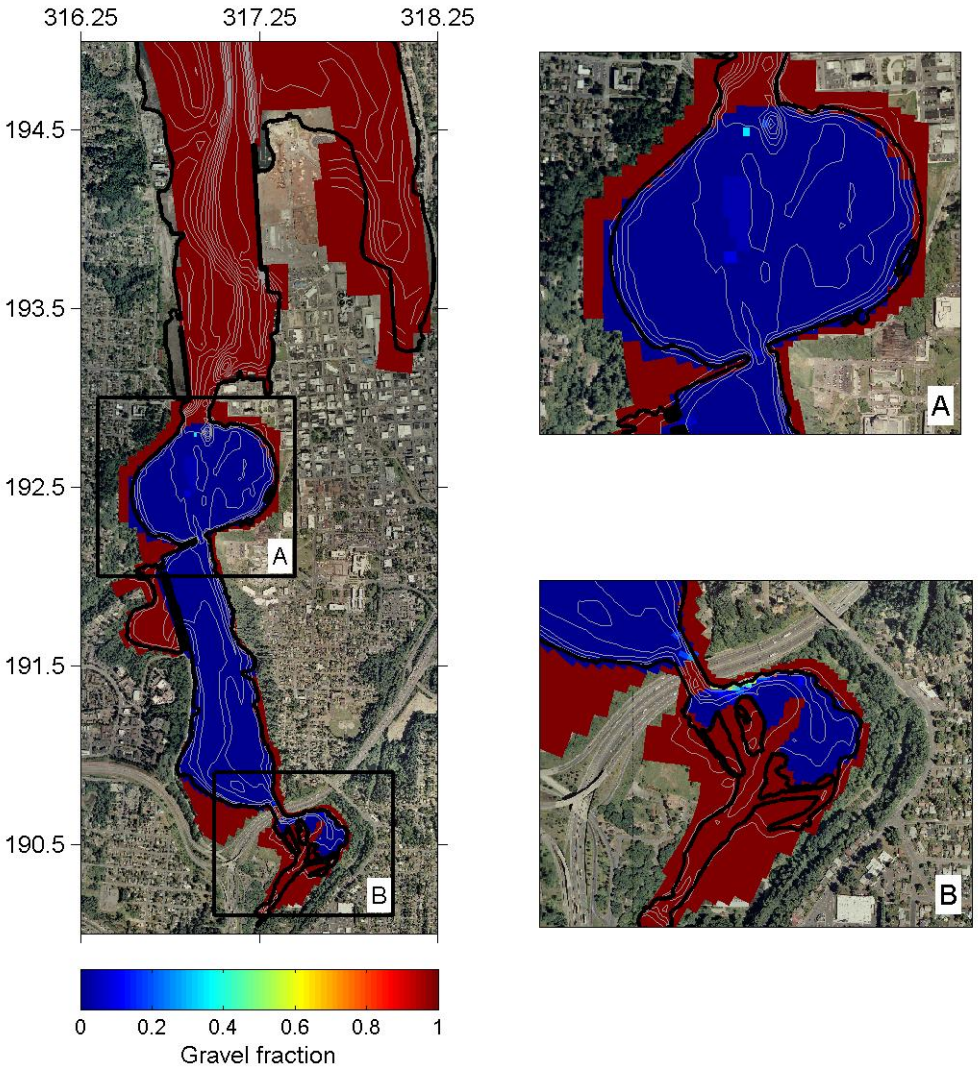

Figure 2.28. Initial gravel fraction map for the restoration scenarios. The axes are in Washington State Plane South (km) and bathymetry contours are in 1 m increments from – 4 to 2 m MSL. Gravel fraction based on the 2005 sediment grab sample data was interpolated onto the grids. Blues are lower percentages of gravel and reds are larger. Regions without sediment data or required to be hardened are set to 100% gravel and have a sediment thickness of 0, resulting in no bed sediment available of any size class in those locations.

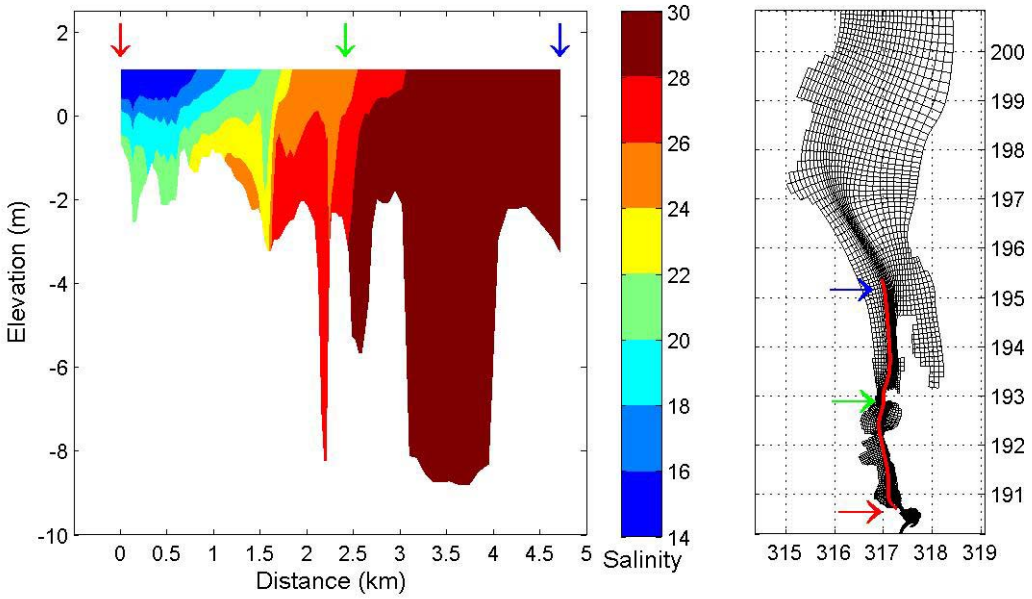

Figure 2.29. Cross-section of salinity distribution from 3D test case of a restored estuary. The arrows represent benchmarks on the model domain along the red line. Middle Basin shows a vertical distribution typical of a partially mixed estuary while the distributions of North Basin and the Port of Olympia are better described as well-mixed.

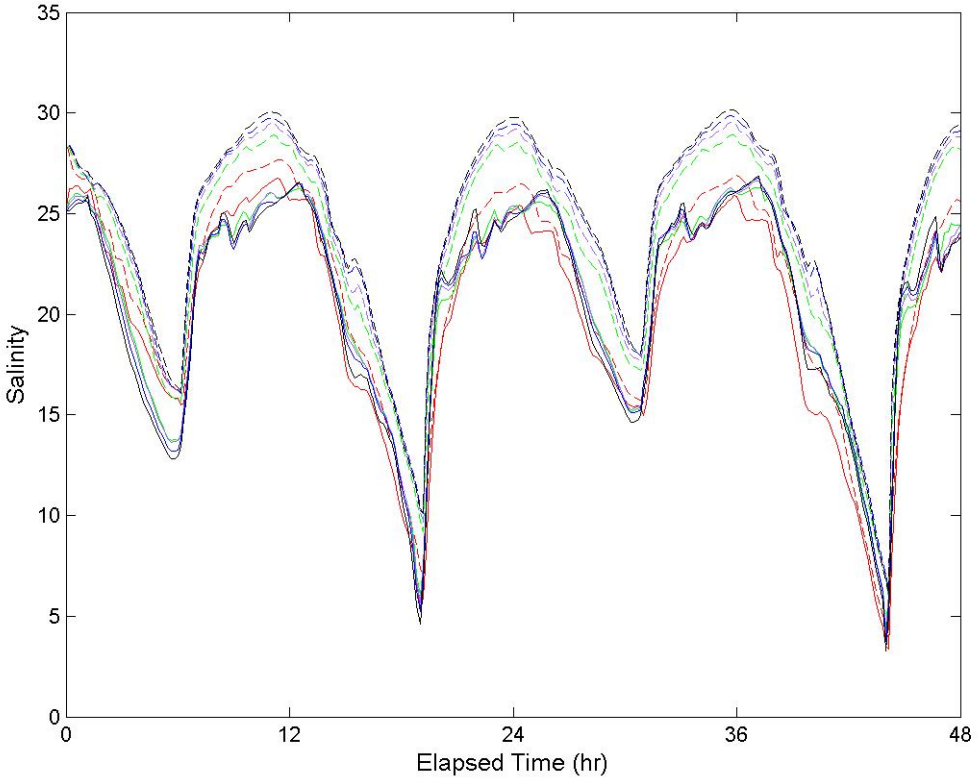

Figure 2.30. Salinity results from a test case to examine the number of layers in a 3D simulation. Solid lines are the surface layer and dashed lines are the bottom layer. Five numbers of layers were tested – 3 (red), 5 (green), 7 (purple), 10 (blue), and 20 (black). The 3- and 5-layer simulations produced unacceptably different results than the other three simulations. The 7-layer simulation was selected for further use.

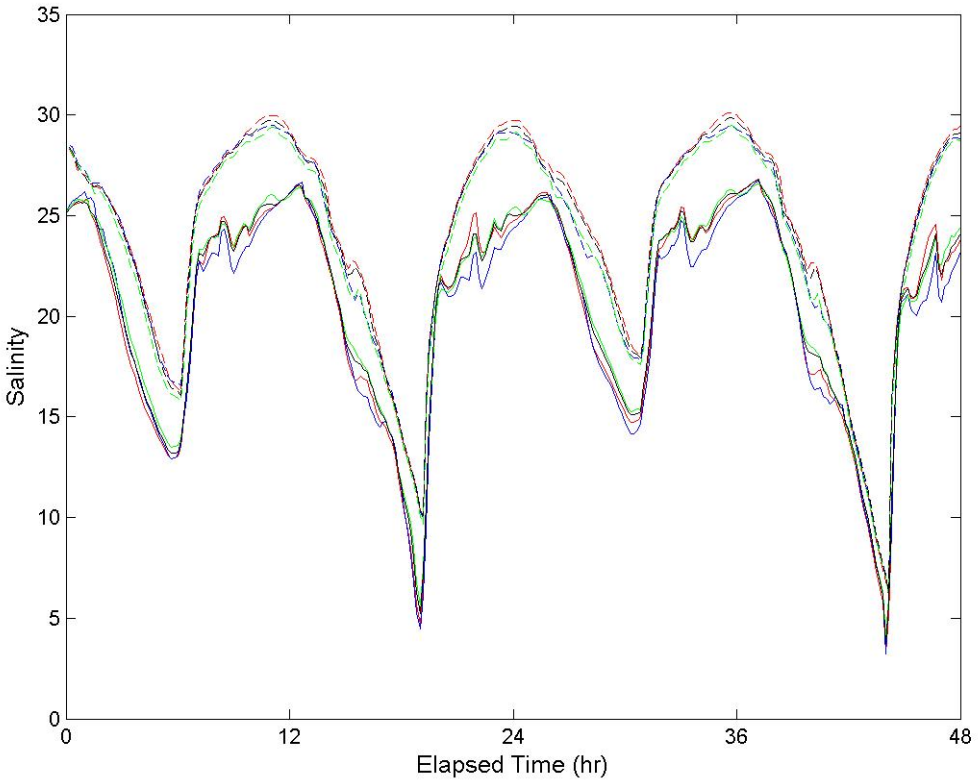

Figure 2.31. Salinity results from a test case to examine the distribution of layers in a 3D simulation. Solid lines are the surface layer and dashed lines are the bottom layer. Four distribution of layers were tested - high resolution in the surface and bottom layers (red), high resolution in the bottom layer only (blue), high resolution in the middle of the water column (green) and a uniformly-spaced distribution (black). Differences of less than 2 ppt in salinity (approximately 10%) are seen among the four designs and the uniformly-spaced distribution was selected for further use.

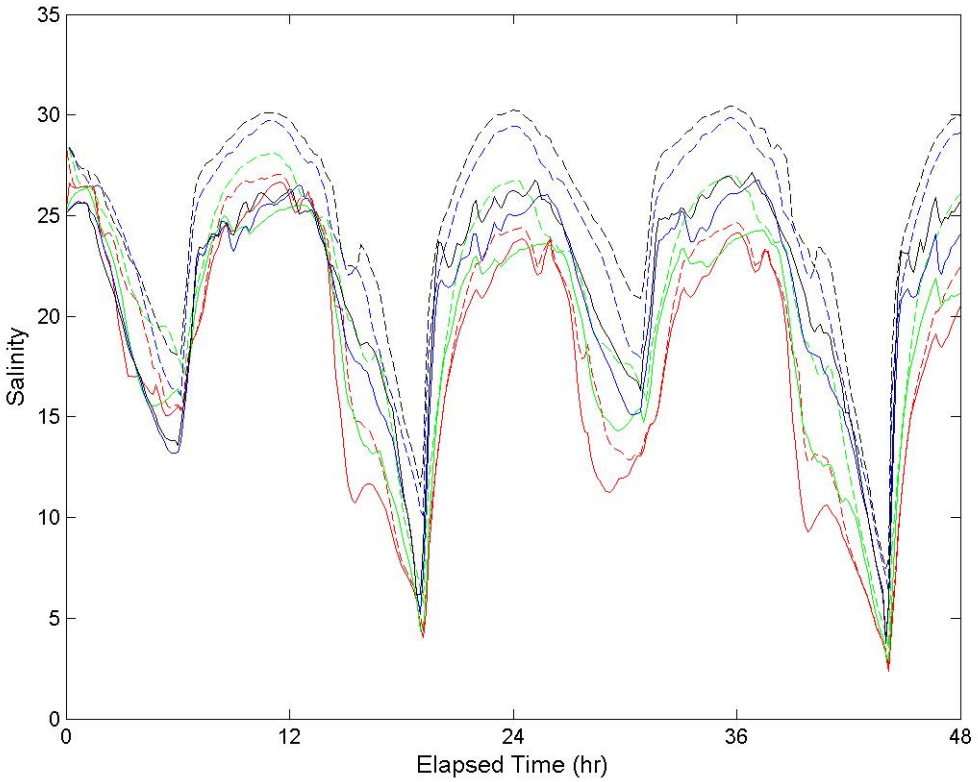

Figure 2.32. Salinity results from a test case to examine the background viscosity and diffusivity in a 3D simulation. Solid lines are the surface layer and dashed lines are the bottom layer. Four values were tested – 10^{-2} m^2/s (red), 10^{-3} m^2/s (green), 10^{-4} m^2/s (blue), and 10^{-6} m^2/s (black). Salinity distributions are observed to be better mixed with higher background values but no other discernable patterns are evident. The moderately conservative value of 10^{-4} m^2/s was selected for further use.

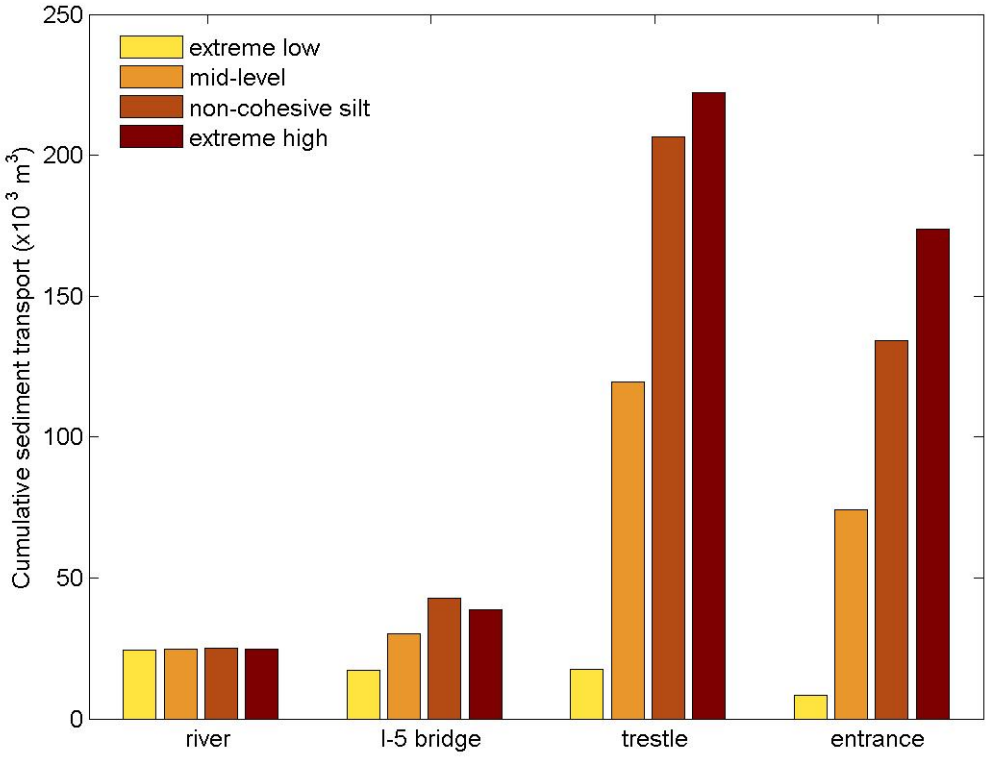

Figure 2.33. Comparison of cumulative sediment transport after one year through four cross-sections in a sensitivity analysis for different erodibilities and treatments of silt. Sediment was supplied from the bed and the river. The non-cohesive silt and extreme high erodibility cases have comparable sediment transport while the extreme low erodibility has lower sediment transport fluxes. The mid-level erodibility produces sediment transport fluxes in the same magnitude as the non-cohesive silt and extreme high erodibility. The extreme low erodibility case was deemed undesirable and not included in further analyses. Both the mid-level and extreme high erodibility parameters were selected to bracket the most likely erodibilities for mud that may be present in the Capitol Lake sediment.

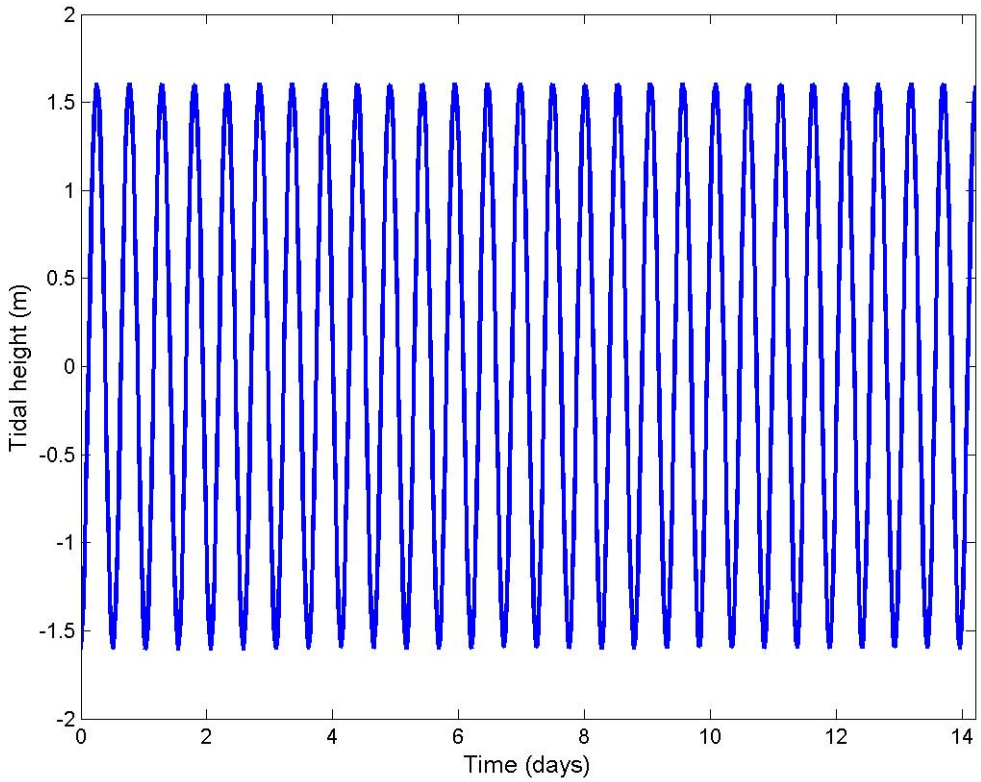

Figure 2.34. Morphological tide used for forcing sediment transport/morphology simulations. The M2 component of the semi-diurnal tide was multiplied by 1.1 to produce the harmonic tide to be combined with the 'morphological river'.

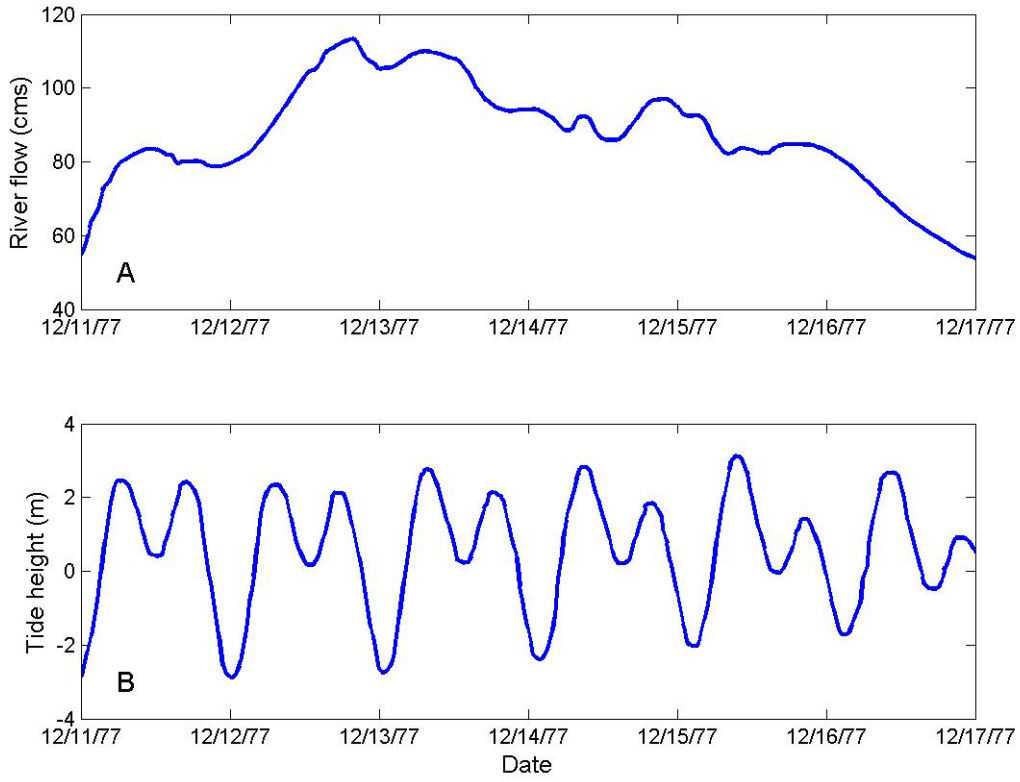

Figure 2.35. River flow (A) and tide height (B) for the 1977 extreme hydrologic event. Data were extracted from observations reported by URS Group, Inc. (2003). The tide height was also combined with a constant river discharge equivalent to the 100-yr flood.

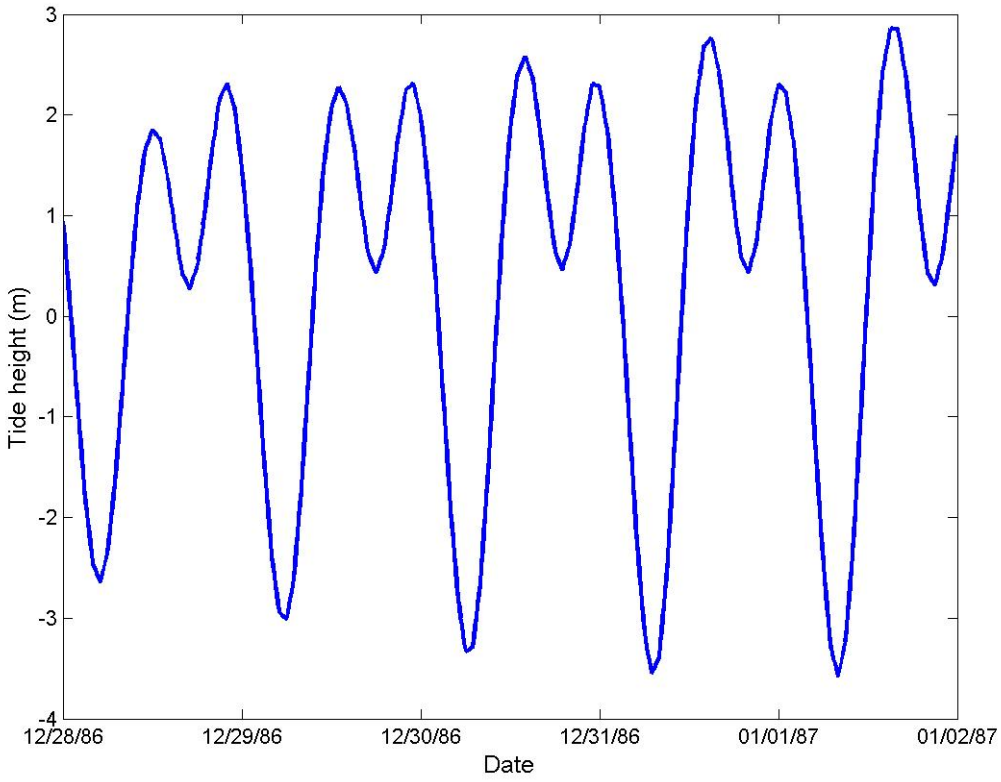

Figure 2.36. Tide height for the 1986 extreme hydrologic event. These data were combined with three different constant river discharges (see Table 2.13).

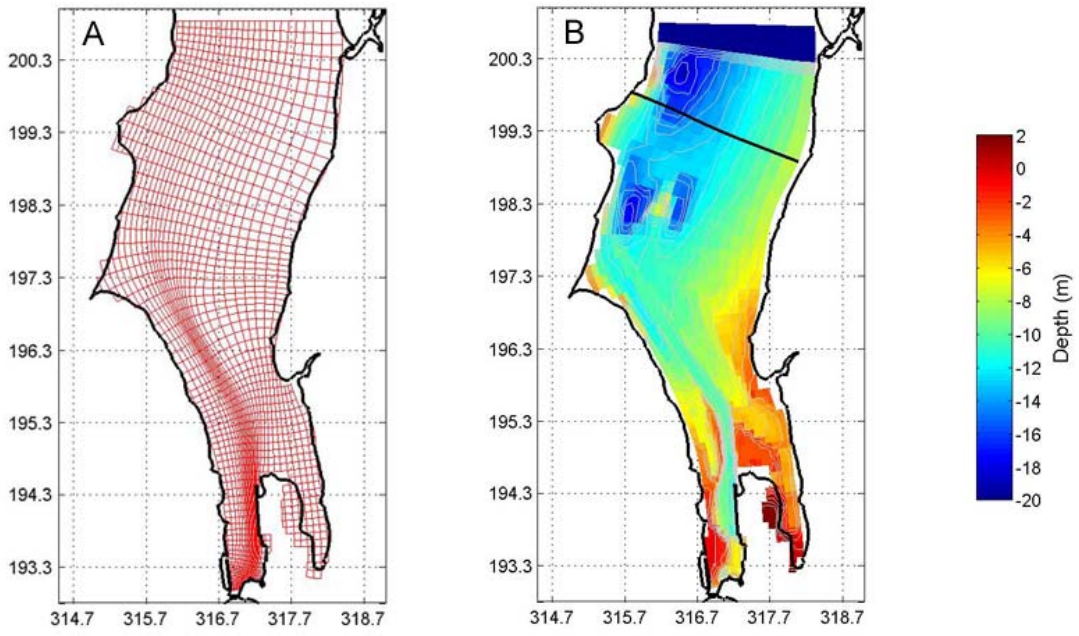

Figure 2.37. Grid (A) and bathymetry (B) used for the validation analyses. Model observation stations are located as near as possible to field observation sites used in the LOTT Wastewater Management Partnership study. The cross-inlet transect in B (black line) is investigated in a subsequent plot.

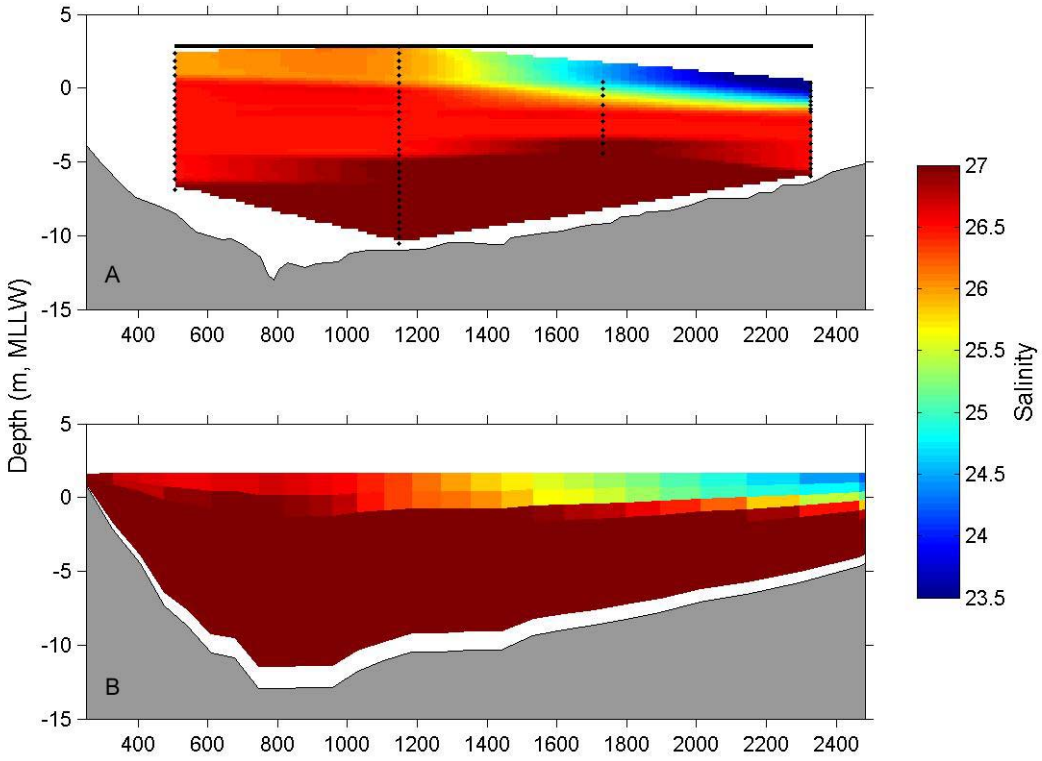

Figure 2.38. Measured (A) and modeled (B) salinity cross-sections along a transect (see Figure 2.37). Blues are fresher water and reds are saltier. In A, black dots are sample locations and the black line is the water level. Fresher layers of water overlay a mixed saltier layer on the eastern side of the inlet in both the measured and modeled results.

CHAPTER 3

Results

Modeling results are organized into simulations conducted to address hydrodynamic and salinity predictions and simulations conducted to address sediment transport and morphology predictions. Hydrodynamic/salinity simulations provide circulation pattern, velocity, inundation frequency and near-bed salinity data. Sediment transport/morphology runs supply cumulative movement of sediment through specific cross-sections, erosion and deposition of sediment, evolution of sediment grain size classes and long-term changes to the shape of the estuary. A large number of model simulations were run to explore a range of conditions and possible outcomes and the uncertainty in a few key parameters.

The current velocities observed during four flow conditions are examined to determine the range of velocities that might be found during an average year in the predam and restored estuaries. The maximum speeds during the ebb and flood tidal stages are identified for the lowest (2.8 m^3/s) and highest (64 m^3/s) river flows of the 'salinity river'. A simple nomenclature is used to describe the four hydrodynamic combinations (Table 3.1). Two tidal stages were selected because of the asymmetrical shape of the tide in Southern Puget Sound.

Table 3.1. Hydrodynamic combinations of river discharge and tidal stage

river discharge	tidal stage	descriptor
lowest (2.8 m^3/s)	ebb	low-ebb
	flood	low-flood
highest (64 m^3/s)	ebb	high-ebb
	flood	high-flood

Model results from simulations using the 'morphological river' are used to analyze sediment transport through the estuary and lake. Erosion and deposition and evolution of the sediment grain size classes are quantified using two erodibility levels (Table 2.11). A range of possible mud erodibilities is explored because of the complete paucity of field data from Capitol Lake for these parameters. Taken from the literature, the selected range

is believed to provide the widest possible, yet realistic set of erodibility conditions for the lake. The conditions chosen do not necessarily have equal probability of occurrence either spatially or temporally.

Predam Estuary Results

Hydrodynamics and Salinity
Hydrodynamic simulations run on the 1949 bathymetry provide estimates of the flow and salinity in the estuary prior to dam construction. Circulation patterns during low river flow and an ebb tide (low-ebb) show the estuary draining first from Middle Basin followed by South Basin and lastly North Basin. When the velocity peaks at the trestle, all of the flow vectors point north towards the entrance with no eddies forming (Figure 3.1). The highest velocities are observed under the trestle and north of the entrance where they exceed 1 m/s. A northerly strip of high velocities is observed in North Basin. The circulation patterns for low-flood indicate the estuary fills the main channel and then overtops the banks to complete inundation of the basin. During the peak velocity at the trestle, eddies form on the flanks of North Basin and in South Basin (Figure 3.2). A southerly band of high velocities stretches from the entrance to the center of Middle Basin. Velocities are largest at the entrance and trestle, exceeding 1 m/s, although areas in Middle Basin also experience large flows. During the low river flow simulation, the fastest velocities observed at the trestle are approximately 1.1 m/s and occur halfway between low and high tide; velocities approach decrease to near 0 m/s at both slack tides with a residual flow from the river discharge (Figure 3.3). Other locations follow a similar trend, such as at the entrance (peak velocity 1.1 m/s), in Middle Basin (peak velocity 1.2 m/s) and at the boundary between South and Middle Basins (peak velocity 0.6 m/s).

The effect of the high river flow on circulation in the predam estuary is clearly seen in both high-ebb and high-flood simulations. During ebb, the river flow follows the channel although the width of the active channel is larger than during low-ebb (Figure 3.4). Current velocities exceeding 1 m/s extend from the trestle to beyond the entrance and form a jet into Budd Inlet. Time-series of velocity magnitude at different locations in the estuary show the fastest current speeds in South and Middle Basin when the tide height is lowest. The fast velocities would be caused from a shallower flow depth than during higher tide levels, resulting in an accelerated flow speed. During high-flood, circulation is chaotic in South Basin and southern Middle Basin as the incoming tide collides with the outgoing river flow (Figure 3.5). The tide overruns the river from North Basin through Middle Basin and opposing circulation cells develop off the main channel in the North Basin with the western cell spinning clockwise and eastern cell counterclockwise. During the high river flow simulation, the fastest velocities observed at the trestle are approximately 1.3 m/s and occur during a falling tide; velocities approach almost 0 m/s at high slack tide (Figure 3.6). However, velocities at low slack tide appear to be governed by the river flood and reach a constant speed of 0.8 m/s. This pattern is similar at other locations, such as in Middle Basin (peak velocity 1.7 m/s, flood velocity 1.7 m/s) and at the boundary between South and Middle Basins (peak velocity 1 m/s, flood velocity 1 m/s). The entrance (peak velocity 1 m/s) does not show a high velocity during low slack tide.

Although the river discharge affects the circulation and velocity patterns, the estuary is still tidally-dominated for wetting and drying of the mudbanks as noted in the percent inundation. No noticeable differences are observed between the annual and dry season conditions. During an average year, all of North Basin, most of South Basin and approximately 50% of Middle Basin are underwater at least 70% of the time (Figure 3.7). Large mudflats are exposed adjacent to the central channel along most of Middle Basin. Elevations above 2 m are inundated less than 50% of the year but get submerged at least once during the highest spring tide. Some localized pooling of water appears outside of the main channel, although this does not represent a large portion of the estuary.

The near-bed salinity is greatly affected by the river flow. According to predam simulations, the annual mean salinity shows a nearly uniform gradient from freshwater at the river mouth to above 25 ppt at the entrance (Figure 3.8). Northern South Basin and most of Middle Basin exhibit brackish water with salinities between 10 – 20 ppt. North Basin shows a slightly fresher channel than the flanks. The salinity distribution is saltier during the dry season (low river flow) than during times of river flooding (Figure 3.9). The steepest salinity gradients occur in South Basin between the river mouth and where the northern section exceeds 15 ppt. The majority of the estuary is above 18 ppt with the flanks of North Basin above 25 ppt.

Sediment Transport

Predam estuary sediment movement for one year is investigated by analyzing the amount of sediment passed through the basins and exported to Budd Inlet. Observational cross-sections record the volume of each sediment grain size class at every time step during the simulation and the data are summed to produce a final volume. Sediment grain size data are not available from this time period so no initial bed sediment distribution is provided and the Deschutes River yields all the sediment for the predam estuary simulations. Three cross-sections demonstrate the movement of sediment through the basins after the 'morphological river' supplies approximately 25,000 m^3 of sediment to the predam estuary (Table 3.2). A cross-section along the location of the future I-5 bridge shows approximately 16,000 m^3 of sediment pass into Middle Basin and the trestle section records approximately 11,000 m^3 of sediment exporting out of the basin. The entrance cross-section shows approximately 8,300 m^3 exits the estuary. Combining these values indicate the basins of the predam estuary are accumulating more than half of the sediment supplied by the river with South Basin garnering 9,000 m^3, Middle Basin 5,000 m^3 and North Basin 2,700 m^3 of sediment for a total of 16,700 m^3.

Table 3.2. Sediment transport (m^3) through the predam estuary cross-sections

cross-section	sediment load
river	25,000
I-5	16,000
trestle	11,000
entrance	8,300

Lake Simulation Results

A series of lake simulations were run to help guide the investigation of sediment transport in the lake prior to restoration. The lake simulations assist in understanding sediment transport through the initial and modern lakes and how the four selected sediment size classes behave in the lake environment.

The initial lake sediment transport simulation was conducted with a hardened bed similar to the predam sediment transport simulations with all sediment supplied by the river. Sediment fractions on the lakebed after five years show clay and silt dominate most of the lake with sand and gravel accumulating closest to the river (Figure 3.10). Percival Cove appears to collect only the clay fraction but that may be a result of no freshwater input from Percival Creek to introduce coarser fractions to the cove.

The modern lake sediment transport simulation was performed with initial sediment fraction distributions on the lakebed similar to the restoration scenario simulations. Hence, some redistribution of the sediment fractions was bound to occur in addition to the introduction of sediment from the Deschutes River. The clay fraction decreases in South and Middle Basins but increases in North Basin after five years of simulation (Figure 3.11). Similar to the initial lake simulation, Percival Cove accumulates the clay fraction almost exclusively. The silt fraction is largest in Middle and South Basins and is small in areas of constriction (e.g., trestle, I-5 bridge, main channels in South Basin). The sand fraction is largest in the central portion of South Basin and in constricted areas while the gravel fraction accumulates primarily in main stem of the river upstream of the South Basin islands.

The lake simulations indicate clay and silt increase in concentration on the lakebed from south to north and large amounts of sand in South Basin and in constricted areas. These results are consistent with the field observations of sediment grain size from the grab samples at selected sites. These simulations were used to assist in the interpolation and extrapolation of the grain size distributions from the field samples. In addition, estimates of sediment trapping and grain size distributions at the river boundary were made based on these simulations (Table 2.7).

Restoration Scenario Results

The restoration scenarios simulations were constructed and run as similarly as possible to each other and to the predam estuary to allow comparison of the results. The scenarios are described in Table 1.2 and will be referenced accordingly. Each scenario experiences tidal flow after removal of the dam, which when combined with the freshwater discharge of the Deschutes River, produces an estuarine environment. Hydrodynamics are examined in a similar manner for the restoration scenarios as for the predam estuary. The identical hydrodynamic combinations are used for investigating velocity and circulation patterns (Table 3.1). Inundation frequency and salinity used the same river flows to define ‘annual’ and ‘dry season’ conditions. However, morphological changes to the bed, which were not produced for the predam estuary, provide additional results. Three year

simulations generated sediment transport data that will be used to compare to the one year predam estuary results.

Restoration Scenario A

The Restoration Scenario A estuary connects to Budd Inlet through a 150 m opening with all other features of modern Capitol Lake still intact.

Hydrodynamics and Salinity
Circulation patterns for Restoration Scenario A initially develop in response to the modern lake shape and constriction zones. During low-ebb, the flow is confined to the main channel in South Basin and slightly increases in speed under the I-5 bridge (Figure 3.12). Current velocities throughout Middle Basin are northward at approximately 0.4 m/s until the trestle where the narrow opening causes the water to accelerate beyond 1 m/s. Current speed out of Percival Cove reaches 0.6 m/s. In North Basin, a band of high velocity water connects the trestle to the entrance. Immediately north of the estuary entrance, the velocities peak above 1 m/s. The patterns during low-flood differ by basin. A southerly band of high velocity water enters North Basin and extends into central Middle Basin (Figure 3.13). A strong counterclockwise eddy develops on the eastern side of North Basin while a slower moving clockwise cell appears on the west side. The jet of fast water into Middle Basin decelerates from 1.5 m/s to approximately 0.3 m/s although velocities exceeding 0.5 m/s are observed entering Percival Cove. Velocities slow before the I-5 bridge and then enter South Basin at about 0.5 m/s, where the flow turns to the east. The water moves up channel and effectively stalls the river flow between the two northern islands and southern island. During the low river flow simulation, the fastest velocities observed at the trestle are approximately 1.3 m/s and occur halfway between high and low tides; current velocities approach 0 m/s at high tide and are small at low tide (Figure 3.14). This pattern is similar at other locations, such as the entrance (peak velocity 1.1 m/s), in Middle Basin (peak velocity 0.7 m/s) and at the I-5 bridge (peak velocity 0.4 m/s).

The high-ebb and high-flood conditions are dominated by the high river flow. The main channel of South Basin contains most of the flow at up to 1 m/s but some water is directed between the two northern islands in a shallow secondary channel during high-ebb (Figure 3.15). The current accelerates to almost 1.5 m/s under the I-5 bridge before slowing to 0.4 – 0.6 m/s throughout Middle Basin. The fastest velocities, exceeding 1.5 m/s, occur at the trestle and north of the entrance with a northerly band of high velocity water that stretches between them. The ability of the river discharge to block the incoming tide is demonstrated in simulations under high-flood conditions (Figure 3.16). Circulation patterns are similar to high-ebb for South Basin and into southern Middle Basin. However, central Middle Basin shows velocities slower than 0.2 m/s and opposing current vectors from the north and south. Velocities at the trestle are southerly but slower than 1 m/s. Currents entering Percival Cove exceed 0.8 m/s. A weak counterclockwise circulation cell develops in eastern North Basin bounded by a relatively slow southerly flow from Budd Inlet. During the high river flow simulation, the fastest velocities observed at the trestle are approximately 1.7 m/s and occur halfway between high and low tide; velocities approach almost 0 m/s at high slack tide (Figure 3.17). However, velocities at low slack tide are governed by the high river flow and reach a constant speed

of 1.3 m/s. This pattern is similar at other locations, such as the entrance (peak velocity 0.7 m/s, flood velocity 0.3 m/s), in Middle Basin (peak velocity 1.7 m/s, flood velocity 1.7 m/s) and at the I-5 bridge (peak velocity 1.4 m/s, flood velocity 1.3 m/s).

With restored estuarine processes, inundation of the tide flats in Restoration Scenario A is tidally controlled and responds very little to changing river flows. Predictions of percent inundations averaged over a year and over just the low flow time period are essentially the same. The main channel of the estuary, most of Percival Cove, northern Middle Basin and all of North Basin are submerged at least 70% of the time (Figure 3.18). The banks of the channel in Middle Basin and large portions of South Basin are underwater approximately 50% of the time with the islands getting inundated less than 30% of the time. Although parts of the Heritage Park mitigation site are below the mean tidal level, none of the wetlands get submerged, possibly due to the earthen berm separating the region from the estuary.

The differences in near-bed salinity between the annual and dry season conditions can be accounted for by the river flow. Averaged over a year, a salinity gradient develops from freshwater at the river mouth to approximately 15 ppt at the trestle (Figure 3.19). Percival Cove is saltier than Middle Basin, possibly due to the limited influx of freshwater into the cove from Middle Basin and the absence of Percival Creek in the model. North Basin shows an intrusion of 15 – 18 ppt water from Middle Basin into a fairly uniform 18 – 20 ppt brackish water. The salinity distribution during the dry season is substantially different (Figure 3.20). While South Basin remains mostly fresh, Middle Basin contains water with salinities from 10 – 20 ppt. The main channel is fresher than the flanks in the center of the basin while salinities in Percival Cove and North Basin are almost uniformly above 20 ppt. The slightly fresher intrusion into North Basin from Middle Basin appears to dissipate rapidly.

Extreme Hydrologic Events

The five extreme hydrologic events (Table 2.13) produce a variety of maximum water levels and maximum velocities within the estuary. Events I and II were driven by an observed 1977 tide with the observed river discharge and a 100-year flood event, respectively. Events III, IV and V were driven by the largest tidal oscillation on record and river discharges associated with the 100-year flood, the 2-year flood and a dry season flow, respectively. The highest water level and fastest velocity for each grid cell during a simulation was recorded and spatially assembled to create maxima maps for both variables. Maximum water levels for Event I and Event II range from 3 – 3.5 m and 3 – 4 m, respectively (Figure 3.21). The highest water levels are observed in South Basin while the lowest are in Budd Inlet. Tumwater Historical Park, the lower sections of the Heritage Park mitigation site and areas of Marathon Park all become submerged during these two event simulations. Maximum velocities across the domain for Event I show speeds of 0 – 4 m/s with the fastest velocities outside of the entrance and within the primary channel (Figure 3.22). In general, the spatial pattern of the maximum velocities is similar for Event II but the speeds are faster and range from 0 – 6 m/s. Events III, IV and V show progressively lower water levels and slower velocities with respect to each other, reflecting the effect of different river discharges. Maximum water levels in Event III, the largest river flood, range from 3 – 4 m while ranging from 3.3 – 2.7 m for Event IV and remaining between 2.75 – 3 m for Event V (Figure 3.23). Less area outside of the estuary

boundary gets inundated during these events compared to Events I and II, such as at Marathon Park. Maximum velocities decrease from Event III to Event IV then Event V. While the locations of the higher flow speeds are near constant, such as outside the entrance, near the trestle and I-5 bridge and in the channel, Event III shows maximum velocities of up to 6 m/s, but Event IV velocities peak near 4 m/s and Event V at less than 2 m/s (Figure 3.24).

To explore the water levels and water level gradients from these events, a 5-km long maximum water level profile for each event was generated from the Deschutes River through the Port of Olympia (Figure 3.25). Event I shows a gradual decline through Middle and North Basins for a net change of less than 0.2 m (Figure 3.26). Events II and III, the 100-yr flood event simulations, show the steepest gradient within South Basin; the net change of almost 0.8 m for Event III is the largest among all the events. The gradients and net changes for Events IV and V are the smallest. The largest water level gradients are associated with constrictions in the estuary (i.e., near the I-5 bridge, the trestle, the entrance). The bathymetry along the transect plays a minor role relative to the constrictions in the estuary in affecting the water levels.

Observation stations recorded water levels and velocities throughout the estuary (Figure 3.27) and the highest water levels (Table 3.3) and fastest velocities (Table 3.4) during an event show Events II and III produce the most dynamic conditions.

Table 3.3. Maximum water levels (m MSL) for Scenario A extreme hydrologic events

Station	Event I	Event II	Event III	Event IV	Event V
I5Bridge	3.47	3.54	3.12	3.11	3.00
PC2MB	3.34	3.46	3.12	3.11	3.01
trestle	3.31	3.42	3.08	3.08	2.98
NBasin5	3.29	3.37	3.07	3.08	2.98
NBasin6	3.28	3.37	3.07	3.08	2.97
NBasin7	3.30	3.36	3.07	3.08	2.98
entrance	3.26	3.35	3.07	3.07	2.97
Fourth Ave	3.24	3.33	3.06	3.06	2.97
MPark	3.33	3.38	*	*	*
RRNorth	3.31	3.40	3.06	3.08	2.98
RRSouth	3.32	3.43	3.10	3.09	2.98
PC2	3.35	3.46	3.13	3.11	3.01
MBA	3.42	3.52	3.13	3.10	3.00
MBB	3.41	3.52	3.12	3.11	3.01
Miti1	3.44	3.59	3.13	3.12	3.00
Miti2	*	*	*	*	*
I52	3.45	3.53	3.12	3.11	3.01
SBW	3.50	3.63	3.35	3.15	3.02
SBE	3.50	3.75	3.48	*	3.03

* - station does not get inundated

Table 3.4. Maximum velocities (m/s) for Scenario A extreme hydrologic events

Station	Event I	Event II	Event III	Event IV	Event V
I5Bridge	3.4	5.1	5.1	3.5	1.5
PC2MB	0.8	0.9	0.5	0.6	0.6
trestle	2.3	2.4	2.4	1.4	1.0
NBasin5	0.6	0.6	0.3	0.3	0.3
NBasin6	1.5	1.9	1.5	1.1	0.8
NBasin7	0.4	0.3	0.2	0.3	0.2
entrance	2.3	1.7	1.6	1.2	1.5
Fourth Ave	3.0	5.3	5.3	3.3	1.8
MPark	0.4	0.2	0.0	0.0	0.0
RRNorth	2.1	2.4	2.0	1.3	1.1
RRSouth	2.1	2.0	2.0	1.1	0.9
PC2	0.9	1.0	0.5	0.6	0.5
MBA	0.5	0.7	0.6	0.3	0.3
MBB	0.5	0.5	0.3	0.2	0.2
Miti1	0.1	0.3	0.1	0.1	0.1
Miti2	0.0	0.0	0.0	0.0	0.0
I52	0.7	2.0	1.9	0.7	0.4
SBW	0.3	0.4	0.3	0.2	0.2
SBE	0.2	0.1	0.1	0.0	0.2

Sediment Transport

Sediment movement for the first year of the sediment transport/morphology simulations is investigated by analyzing the amount of sediment passed through the basins and exported to Budd Inlet. Observational cross-sections record the volume of each sediment grain size class at every time step during the simulation and the data are summed to produce a final flux. Sediment is supplied by the Deschutes River (25,000 m^3/yr) and from the estuary bed but not from Budd Inlet. Sediment fluxes through cross-sections at four constrictions show both redistribution of bed sediment and accumulation of the fluvial load in the basins (Table 3.5). Given the uncertainty in the erodibility characteristics of the mud, simulations were carried out with lower and higher erodibility conditions (Table 2.11). The I-5 cross-section shows a likely range of approximately 30,000 to 39,000 m^3/yr of sediment passing under the bridge, depending on mud erodibility. Approximately 120,000 to 222,000 m^3/yr of sediment is transported through the trestle. The cross-section at the entrance to Percival Cove exhibits 2,200 to 4,400 m^3/yr of sediment movement into the cove. Sediment exported from the estuary through the entrance is approximately 74,000 m^3/yr for the lower erodibility and 174,000 m^3/yr for the higher erodibility. Changes to the individual basins are described in the morphology results below.

Table 3.5. Sediment transport (m^3/yr) through Restoration Scenario A cross-sections during the first year after dam removal

cross-section	lower erodibility	higher erodibility
river	25,000	25,000
I-5	30,000	39,000
trestle	120,000	222,000
Percival Cove	2,200	4,400
entrance	74,000	174,000

First Year Morphology Change

Changes to the estuary bed after the dam is removed occur in all basins. For the lower erodibility sediment conditions, South and Middle Basins experience large amounts of erosion between 0.5 – 1 m (Figure 3.28). Localized deposition of up to 0.6 m occurs in South Basin and north of the I-5 bridges. A broad but thin deposit forms to the east of the Deschutes Parkway near Percival Cove. North Basin shows a mix of erosion and deposition. Depths increase around the trestle and in patches along a north-south axis to the entrance. On both sides of the erosion, however, large deposits of up to 1 m thick form. The western deposit is nearly parallel to the eroded channel while the eastern deposit is somewhat patchy. Very little change is observed closer to the shoreline. Sediment accumulates in the scour hole south of where the dam was and to the west of the new opening. No elevation changes are seen in the region between the estuary and the marina. The marina and the port experience the broadest decrease in depth, with changes from 0.2 – 0.5 m across the eastern side of West Bay.

The substantial amount of sediment transport and morphological change that occurs after the dam is removed is accompanied by changes in the bed sediment grain size. The initial surface sediment distribution for each size class changes radically in the first post-dam year. What was a silt-dominated lake with sand deposits becomes an estuary that is silt-dominated on the flanks, sand-dominated in the channels and with clay and gravel fractions considerably smaller than the silt or sand. The clay fraction ranges from 0 – 0.3 for South and Middle Basins (Figure 3.29). The western side of Percival Cove acquires dominating clay fractions greater than 0.5 while the North Basin clay fraction is the largest on the flanks of the basin. Lower fractions are observed in the marina and port while dominating fractions are seen in Budd Inlet and East Bay. The silt class dominates most of the estuary with fractions above 0.5 (Figure 3.30). Some portions of the basin have low amounts of silt, such as northern South Basin, under the I-5 bridge, along the channel in Middle and North Basins and around the trestle. Dominating fractions of silt are found in the marina and port. The sand distribution appears to be the inverse of the silt fraction (Figure 3.31). The channels and northern South Basin exhibit the largest fraction of sand, mostly above 0.5. The flanks of the estuary show low percentages not exceeding 20%. Gravel shows the least presence of the size classes with some accumulation around the I-5 bridges and near the trestle (Figure 3.32).

Short-term Morphology Change

Erosion and deposition patterns in the Restoration Scenario A estuary resemble those after one year but with more deposition in North Basin, the marina and port and more

widespread erosion in Middle Basin (Figure 3.33). Three cross-estuary transects demonstrate how the rate of bed change decreases and new sediment distributions evolve. In Middle Basin, the main channel deepens by several meters and widens by 300 m in the first year but does not change much in subsequent years. Although the size remains the same, the larger channel coarsens and sand becomes the dominant fraction in year two. By year three, grain size distribution in the channel has evolved to approximately 50% sand-50% mud (Figure 3.34). A similar pattern is seen in North Basin where the shape of the bed by year three is not substantially different than after year one (Figure 3.35). The off channel zones accumulate fine sediment while the channel becomes predominately sand. A more complicated shift to the bed occurs in the marina where a new channel may be developing to the west of the original one (Figure 3.36). Approximately 2 – 3 m of sediment accumulates in the marina with wholly fine grain sizes on the eastern side and sand mixed into the deposit on the western half.

A bed with higher erodibility results in more erosion throughout the estuary. More erosion occurs in one year if the bed has higher erodibility than in three years with a bed of lower erodibility. Erosion in Middle Basin is extensive, removing at least the top 0.5 m from most of the basin (Figure 3.37). A somewhat patchy pattern of erosion develops in North Basin while appreciable amounts of deposition between 0.5 – 1.5 m are observed on the eastern half of the basin. More than 3 m of sediment is seen to accumulate in the marina and a lesser amount in the port. The cross-estuary transects show the rate of change to the bed as starting to slow but evolution still occurring. Sections B and C indicate less change between years two and three than one and two in the depth profiles (Figures 3.38 and 3.39, respectively). Sediment grain size fractions are still adjusting with the channels coarsening along Section B to almost 100% sand. Section A, however, indicates sediment continues to accumulate in the marina and the channel noticeably coarsening between years two and three (Figure 3.40).

Whether the bed has lower or higher erodibility produces different results in both sediment transport and morphology. After three years, the simulations with a lower erodibility bed appear to be approaching a dynamic equilibrium as most of the changes occur in the first year after dam removal. The higher erodibility still causes shifts in morphology although changes in the upstream portion of the estuary are beginning to slow. The two erodibilities represent discrete sedimentological settings for the estuary whereas actual spatial variability in these parameters would likely result in a range of erodibilities between the selected lower and higher values co-existing within the estuary.

Long-term Morphology Change

A ten-year simulation using the lower level of erodibility and a looser mud density of 500 kg/m^3 is used to investigate when dynamic equilibrium is achieved in a restored estuary. The looser mud density was selected to simulate a more conservative estimate of mud density, or a worst-case scenario in terms of erosion. Five years after dam removal widespread erosion in Middle Basin and large depth changes in the channel are observed (Figure 3.41). In North Basin, sediment continues to accumulate on both sides of the primary channel with more depositing in the eastern half of the basin. More sediment deposits in the marina and port region. Ten years after dam removal, some areas of the port and marina accumulate more than 2 m of sediment while eastern North Basin continues to accrete (Figure 3.41). Some deepening of the primary channel and more

widespread erosion occurs in Middle Basin. Southeastern Middle Basin experiences the most severe erosion during the time period from five to ten years after dam removal. In South Basin, approximately 0.5 m of sediment deposits in the lee of the islands.

Cross-estuary transects and sediment grain size fractions indicate that most change occurs within the first three years with additional adjustments slowing by year five after dam removal. In Section A, the primary channel gets shallower by approximately 2 m and a secondary channel forms to the west of the main deposition center (Figure 3.42). The surface sediment fractions show a sandy silt channel develops within the first five years and minimal changes in the subsequent five years. Two trends are observed during 10 years of morphological evolution after dam removal for Section B bathymetry in North Basin – a deepening channel and accreting mudflats to the east (Figure 3.43). The surface sediment fractions do not appear to change substantially after the first three years when the channel coarsens to almost 100% sand and the flats become silt-dominated platforms. The bathymetry of Section C, in Middle Basin, shows an initial deepening of the channel within the first five years followed by widening to the west and a slight shallowing by 10 years (Figure 3.44). The gradual broadening of the channel can be tracked in the surface sediment grain size evolution. At year three, the channel is centrally located in the middle of Middle Basin and the sediment is approximately 50% sand. By year five, the sand fraction is increasing to the west and decreasing to the east, culminating in year 10 with a sandy channel extending along the western half of the basin and a mudflat to the east.

Time-series of bed depth after each year of morphological simulation at observation stations throughout the estuary reveal the rate of bathymetric change slows substantially between two and four years after dam removal (Figure 3.45). Only the port station shows a nearly constant accretion rate with a net deposition of approximately 1 m of sediment at this site in the decade after dam removal. Station NB6, in the channel of North Basin, erodes more than 0.6 m in the first year, accretes 0.2 m during the second year, and then remains almost unchanged for the next eight years, resulting in a net erosion of approximately 0.4 m. This contrasts with Station NB7 on the western mudflats of North Basin which accretes in the first year before minimally eroding for the next nine years, producing an erosion of less than 0.1m. The trestle station shows the largest net change in depth, eroding almost 4 m with the majority of erosion occurring within the first four years. The bed depth at Station MB4, on the eastern side of Middle Basin, behaves similarly to Station NB6 by eroding in the first year and accreting for the next several years. The rate of accretion slows by year five to an almost imperceptible pace. The thalweg, or deepest point of the channel along Transect C, erodes almost 1.5 m in the first year followed by very little change for the next nine years.

The long-term morphology simulation indicates that a dynamic equilibrium is reached within the first three to five years after dam removal. The rate of change slows noticeably even though change continues, such as a meander of the primary channel or accretion in eastern North Basin. Coarsening of the channels by increasing sand fraction prevents extreme scour once a sustainable bed depth is reached. The one exception to a slowing rate of change is in the port region where sediment, supplied by the river and possibly from the estuary, continuously accumulates.

Restoration Scenario B

The Restoration Scenario B estuary connects to Budd Inlet through a 150 m opening and has a wider opening of 150 m between North and Middle Basins at the railroad trestle.

Hydrodynamics and Salinity

The hydrodynamics of Restoration Scenario B are remarkably similar to those of Restoration Scenario A except around the trestle and Percival Cove. During low-ebb, currents through the widened trestle opening reach 0.6 m/s, which are slower than in Restoration Scenario A (Figure 3.46). Currents exceed 0.6 m/s into Percival Cove during low-flood. The opposing circulation cells in North Basin develop as before despite the increased area for water to flow into Middle Basin during low-flood (Figure 3.47). During the low river flow simulation, the fastest velocities observed at the trestle occur halfway between high and low tides while velocities approach 0 m/s at high tides (Figure 3.48). The other stations show nearly similar velocities as Restoration Scenario A.

The high-ebb and high-flood conditions are also dominated by the high river flow in Restoration Scenario B at the trestle and Percival Cove. The high-ebb velocity at the trestle exceeds 1 m/s, while at Percival Cove, currents remain under 1 m/s. During high-flood, velocities at the trestle are southerly but slower than 1 m/s. Currents entering Percival Cove do not exceed 0.8 m/s. During the high river flow simulation, the fastest velocities observed at the trestle occur during low slack tide when the river flood is dominate over the tides (Figure 3.49). The other stations show nearly similar velocities as Restoration Scenario A.

The fraction of the time the bed is inundated for Restoration Scenario B varies from that of Restoration Scenario A only where the trestle is removed (Figure 3.50). The results do not indicate a more complete draining of the estuary with the wider trestle opening. The near-bed salinity distribution, however, shows the water properties are affected by the wider opening. Averaged over an entire year, South Basin is fresh, Middle Basin is filled with brackish water between 5 – 15 ppt and Percival Cove is almost uniformly 18 ppt (Figure 3.51). North Basin shows a wide intrusion of fresher water across the entire trestle and the maximum basin salinity does not exceed 20 ppt. During the dry season, fresher water extends along the main channel into central Middle Basin (Figure 3.52). The salinities in North Basin approach 25 ppt but are marginally fresher than those in Restoration Scenario A, possibly due to the increased trestle width allowing more water to exchange and mix.

Extreme Hydrologic Events

Overall, the five hydrologic events (Table 2.13) produce similar maximum water levels and maximum velocities for Restoration Scenario B as for Restoration Scenario A (Tables 3.6 and 3.7, respectively). The only notable exception is the velocities around the trestle. Events I and II show slower velocities at the trestle although the higher river flood of Event II still results in relatively fast currents (Figure 3.53). Stations RRNorth and RRSouth (Figure 3.27) are consistently slower for all the events and remain as low as 0.5 m/s in Event V (Figure 3.54). The 5-km long maximum water level transect for Restoration Scenario B shows very little difference from Restoration Scenario A, except

around the trestle where water surface gradients are smaller with the wider trestle opening (Figure 3.55).

Table 3.6. Maximum water levels (m MSL) for Scenario B extreme hydrologic events

Station	Event I	Event II	Event III	Event IV	Event V
I5Bridge	3.49	3.52	3.16	3.16	3.03
PC2MB	3.35	3.43	3.14	3.11	3.00
trestle	3.31	3.40	3.11	3.10	3.01
NBasin5	3.29	3.36	3.11	3.09	3.00
NBasin6	3.29	3.37	3.11	3.09	3.00
NBasin7	3.29	3.37	3.11	3.09	3.00
entrance	3.27	3.34	3.10	3.09	3.00
Fourth Ave	3.25	3.32	3.08	3.08	3.00
MPark	3.30	3.42	3.11	*	*
RRNorth	3.30	3.39	3.11	3.10	3.01
RRSouth	3.32	3.41	3.12	3.10	3.01
PC2	3.36	3.43	3.14	3.11	3.01
MBA	3.43	3.50	3.16	3.13	3.02
MBB	3.43	3.49	3.15	3.13	3.02
Miti1	3.45	3.58	3.17	3.14	3.04
Miti2	*	*	*	*	*
I52	3.47	3.52	3.16	3.15	3.03
SBW	3.53	3.62	3.36	3.18	3.06
SBE	3.54	3.73	3.49	*	3.06

* - station does not get inundated

Table 3.7. Maximum velocities (m/s) for Scenario B extreme hydrologic events

Station	Event I	Event II	Event III	Event IV	Event V
I5Bridge	3.4	5.1	5.1	3.5	1.6
PC2MB	0.9	1.0	0.5	0.6	0.6
trestle	1.7	2.5	2.5	1.4	0.8
NBasin5	0.6	0.5	0.3	0.2	0.3
NBasin6	1.7	1.6	1.6	1.2	0.7
NBasin7	0.4	0.3	0.2	0.2	0.2
entrance	2.3	1.7	1.6	1.2	1.5
Fourth Ave	3.1	5.2	5.2	3.3	1.9
MPark	0.4	0.3	0.3	0.0	0.0
RRNorth	1.5	1.7	1.3	0.9	0.7
RRSouth	1.1	1.5	1.5	1.0	0.5
PC2	0.9	1.0	0.5	0.6	0.5
MBA	0.5	0.8	0.7	0.3	0.3
MBB	0.5	0.5	0.4	0.2	0.2
Miti1	0.2	0.2	0.1	0.1	0.5
Miti2	0.0	0.0	0.0	0.0	0.0
I52	0.8	1.6	1.9	0.8	0.4
SBW	0.4	0.4	0.3	0.2	0.2
SBE	0.1	0.1	0.1	0.0	0.1

Sediment Transport

Sediment movement for the first year of the sediment transport/morphology simulations is investigated similar to that of Restoration Scenario A. Sediment is supplied by the Deschutes River (25,000 m^3/yr) and from the estuary bed but not from Budd Inlet. Sediment fluxes through cross-sections at four constrictions show both redistribution of bed sediment and accumulation of the fluvial load in the basins (Table 3.8). The I-5 cross-section shows approximately 30,000 to 39,000 m^3/yr of sediment passing under the bridge. Approximately 118,000 to 219,000 m^3/yr of sediment is transported through the trestle. The cross-section at the entrance to Percival Cove exhibits 2,400 to 5,000 m^3/yr of sediment movement into the cove. Sediment exported from the estuary through the entrance is approximately 68,000 m^3/yr under the lower erodibility conditions and 172,000 m^3/yr under the higher erodibility conditions. Changes to the individual basins are described in the morphology results below.

Table 3.8. Sediment transport (m^3/yr) through Restoration Scenario B cross-sections during the first year after dam removal

cross-section	lower erodibility	higher erodibility
river	25,000	25,000
I-5	30,000	39,000
trestle	118,000	219,000
Percival Cove	2,400	5,000
entrance	68,000	172,000

First Year Morphology Change
Morphological changes after one year for Restoration Scenario B are similar to those of Restoration Scenario A (Figure 3.56). The most noticeable difference occurs around the trestle. Deposition of approximately 1 m occurs on the eastern side of the widened constriction while erosion, which is skewed to the north, occurs on the west side. The bathymetry changes in North Basin curve slightly to the northeast although a nearly parallel pattern of deposition-erosion-deposition is maintained across the basin. The marina and port accumulate 0.2 – 0.5 m of sediment, with larger amounts observed in the marina.

The bed sediment grain size distributions are also similar to those of Restoration Scenario A although North Basin and the trestle show the effects of the wider opening. The clay fraction in North Basin is largest north of Marathon Park and extends along the parkway. The broader open area of the trestle exhibits low silt fractions of 0 – 0.3 (Figure 3.57) and dominating sand fractions larger than 0.6 (Figure 3.58). The gravel distribution is nearly identical to Restoration Scenario A with slight accumulation around the I-5 bridge.

Short-term Morphology Change
The morphology results for the lower erodibility after three years follow the same trend as one year with increased amounts of erosion and deposition and larger regions of bed change. Erosion across the larger trestle opening is more widespread and deposition covers almost the entire eastern half of North Basin. More than 1 m of sediment accumulates in some areas of the marina while less deposits in the port (Figure 3.59). Similar to Restoration Scenario A, the rate of change is decreasing through time as seen in cross-estuary depth profiles and grain size distributions. Section B in North Basin shows the tendency for channels to get sandier and the flanks to become muddier (Figure 3.60). Once the main channel is established, the sand fraction approaches 100% while areas that get shallower increase in mud fraction.

Results from the higher erodibility simulation show similar patterns observed for the higher erodibility case of Restoration Scenario A. Deposition is reduced and erosion enhanced in western North Basin due to the wider trestle opening (Figure 3.61). The main channel in North Basin does not erode as deeply in Restoration Scenario B although the remainder of the estuary exhibits erosion of up to 1 m. Cross-estuary transects indicate a decreasing rate of change through time and coarsening of the main channel.

The morphology for Restoration Scenario B after three years appears to be similar to that of Restoration Scenario A except around the trestle. Distinct results are produced depending on the erodibility. As with Restoration Scenario A, a range of erodibilities could co-exist in the estuary, which would generate patterns not observed from the simple singular erodibilities used in the simulations.

Long-term Morphology Change
Deposition and erosion patterns throughout most of the estuary are nearly identical between Restoration Scenarios A and B for the ten-year simulation (lower erodibility and looser mud density of 500 kg/m^3). The only notable differences in morphological change are in western North Basin and at the trestle. In North Basin, slight erosion of approximately 1 m is observed immediately north of the wider trestle opening while at

the original trestle opening, very little erosion occurs (Figure 3.62). Surface sediment grain sizes are nearly identical in Restoration Scenario B as they are to Restoration Scenario A after 10 years. The two North Basin and trestle observation stations show the effect of the wider trestle (Figure 3.63). Station NB6 erodes almost 0.75 m in the first year and remains close to 2 m in depth until the fourth year when a slight accretion begins. The accumulation is temporary though and by the tenth year, the bed has eroded down to 2 m again. Station NB7 shows a long-term trend of accretion and erosion which results in a net change of less than 0.2 m. Bed depth at the trestle station, located in a deep section of the original trestle opening, decreases in the first year followed by a gradual increase as erosion dominates for the next nine years; a net change of almost 0 m results.

As with Restoration Scenario A, the long-term morphology simulation indicates that a dynamic equilibrium is reached within the first three to five years after dam removal for Restoration Scenario B. The wider trestle opening produces localized effects, such as erosion immediately north in North Basin and little change to the original bed depth at the trestle.

Restoration Scenario C

The Restoration Scenario C estuary connects to Budd Inlet through a 150 m opening and has a wider opening of 60 m between Middle Basin and Percival Cove. Simulations for the extreme hydrologic events and ten-year morphology were not conducted for Restoration Scenario C.

Hydrodynamics and Salinity

The hydrodynamics, inundation frequencies and near-bed salinity distributions for Restoration Scenario C so closely resemble those from Restoration Scenario A that only a few differences require highlighting. Current velocities under the Percival Cove bridge tend to be slower in Restoration Scenario C due to the wider opening. For example, in high-flood, currents entering Percival Cove remain less than 0.5 m/s while in Restoration Scenario A, speeds are almost double (Figure 3.64). Circulation patterns and velocities throughout the rest of the estuary mimic those of Restoration Scenario A. Minimal differences around the Percival Cove entrance are observed for inundation frequency (Figure 3.65). Percival Cove is almost imperceptibly fresher in the annual near-bed salinity distribution than would occur in Restoration Scenario A (Figure 3.66).

Sediment Transport

Sediment movement for the first year of the sediment transport/morphology simulations is investigated similar to that of Restoration Scenario A. The results are analogous to those of Restoration Scenario A, even around Percival Cove. Sediment is supplied by the Deschutes River (25,000 m^3/yr) and from the estuary bed but not from Budd Inlet. Data from cross-sections at four constrictions show both redistribution of bed sediment and accumulation of the fluvial load in the basins (Table 3.9). The I-5 cross-section shows approximately 30,000 to 39,000 m^3/yr of sediment passing under the bridge. Approximately 119,000 to 222,000 m^3/yr of sediment is transported through the trestle. The cross-section at the entrance to Percival Cove exhibits 2,300 to 4,600 m^3/yr of sediment movement into the cove. Sediment exported from the estuary through the

entrance is approximately 74,000 m^3/yr for the lower erodibility and 173,000 m^3/yr for the higher erodibility. Changes to the individual basins are described in the morphology results below.

Table 3.9. Sediment transport (m^3/yr) through Restoration Scenario C cross-sections during the first year after dam removal

cross-section	lower erodibility	higher erodibility
river	25,000	25,000
I-5	30,000	39,000
trestle	119,000	222,000
Percival Cove	2,300	4,600
entrance	74,000	173,000

First Year Morphology Change
The morphological changes after one year are also extremely similar to those of Restoration Scenario A with the exception that the region near the Percival Cove bridge erodes more than 1 m (Figure 3.67). South and Middle Basin and the central channel of North Basin exhibit the largest erosion while deposition occurs on the flanks of North Basin, and in the marina and port. As the sediment grain size distributions are essentially similar to those of Restoration Scenario A, refer to the discussion above for detailed descriptions of the clay, silt and gravel classes. The only addendum is that larger fractions of sand are observed under the widened opening for Percival Cove.

Short-term Morphology Change
As with the other investigated variables, long-term morphology for Restoration Scenario C is similar to Restoration Scenario A except near Percival Cove. Only the differences will be discussed to reduce redundant descriptions.

Erosion occurs under the wider Percival Cove bridge after three years for both sets of erodibility conditions. The amount does not appear to depend on the erodibility – between 0.5 – 1 m of erosion – but the fate of the sediment varies. For the higher erodibility, no deposition occurs near Percival Cove in Middle Basin (Figure 3.68). All other aspects of the morphology and sediment grain size evolution can be understood from the Restoration Scenario A discussion.

Restoration Scenario D

The Restoration Scenario D estuary connects to Budd Inlet through a 150 m opening and has a freshwater impoundment in the eastern half of North Basin.

Hydrodynamics and Salinity
The hydrodynamics of Restoration Scenario D are similar to those of Restoration Scenario A but modified by the retaining wall that splits North Basin. For all four hydrodynamic combinations of river flow and tides, circulation patterns and velocities in South and Middle Basins and Percival Cove are essentially the same in Restoration Scenario D as in Restoration Scenario A. North Basin exhibits slightly lower velocities but without the counterclockwise eddy in the eastern half of the basin at low-flood

(Figure 3.69). Currents are also slower entering the estuary. A similar pattern is observed during high-flood (Figure 3.70). The velocity time-series for low and high river flows at the entrance, trestle, in Middle Basin and at the I-5 bridge are similar for Restoration Scenario D as Restoration Scenario A.

Except for the freshwater impoundment in eastern North Basin, the inundation fraction of Restoration Scenario D is identical to that of Restoration Scenario A (Figure 3.71). Additional flooding or draining of the estuary does not appear to result from the North Basin split. Near-bed salinity distribution in Percival Cove and North Basin, though, is different for Restoration Scenario D. The cove is fresher by 2 – 3 ppt and the fresher water intrusion into North Basin extends almost to the entrance for the annual average conditions (Figure 3.72). During the dry season, fresher water in the channel reaches beyond central Middle Basin (Figure 3.73). Salinities range from 18 – 24 ppt in North Basin, making it slightly fresher than in Restoration Scenario A.

Extreme Hydrologic Events

Different observation stations are necessary in North Basin for Restoration Scenario D (Figure 3.74). Overall, the five hydrologic events (Table 2.13) produce similar maximum water levels and maximum velocities for Restoration Scenario D as for Restoration Scenario A except in central North Basin (Tables 3.10 and 3.11, respectively). Velocities in North Basin are modified by the freshwater impoundment in the eastern half of the basin. The dike causes currents to accelerate to approximately 2 m/s along a north-south axis extending from the trestle to the entrance (Figure 3.75). In Events IV and V, speeds are closer to 1 m/s (Figure 3.76). The maximum water level gradients are nearly identical for Restoration Scenario D as for Restoration Scenario A.

Table 3.10. Maximum water levels (m MSL) for Scenario D extreme hydrologic events

Station	Event I	Event II	Event III	Event IV	Event V
I5Bridge	3.48	3.52	3.11	3.12	3.01
PC2MB	3.34	3.46	3.11	3.11	2.98
trestle	3.33	3.41	3.07	3.08	2.99
NBasin3	3.28	3.37	3.06	3.09	2.98
NBasin6	3.28	3.37	3.06	3.08	2.98
NBasin7	3.29	3.36	3.06	3.08	2.99
NBasin9	3.25	3.34	3.06	3.07	2.98
entrance	3.24	3.34	3.06	3.07	2.98
Fourth Ave	3.24	3.35	3.05	3.06	2.97
MPark	3.31	3.39	*	*	*
RRNorth	3.32	3.40	3.06	3.09	2.98
RRSouth	3.33	3.43	3.09	3.09	2.98
PC2	3.35	3.47	3.11	3.11	2.99
MBA	3.42	3.54	3.11	3.10	3.01
MBB	3.42	3.53	3.11	3.11	3.01
Miti1	3.45	3.56	3.12	3.11	3.01
Miti2	*	*	*	*	*
I52	3.46	3.56	3.11	3.11	3.01
SBW	3.52	3.64	3.34	3.16	3.03
SBE	3.53	3.75	3.48	3.16	3.02

* - station does not get inundated

Table 3.11. Maximum velocities (m/s) for Scenario D extreme hydrologic events

Station	Event I	Event II	Event III	Event IV	Event V
I5Bridge	3.5	5.1	5.1	3.6	1.6
PC2MB	0.7	0.9	0.5	0.6	0.6
trestle	2.4	2.5	2.4	1.4	1.1
NBasin3	1.6	1.9	1.5	0.9	0.8
NBasin6	1.3	1.7	1.4	1.3	0.7
NBasin7	0.5	0.5	0.3	0.3	0.2
NBasin9	2.6	1.7	1.7	2.6	0.8
entrance	1.6	1.7	1.7	1.1	1.1
Fourth Ave	2.7	4.9	5.0	3.3	1.5
MPark	0.3	0.1	0.0	0.0	0.0
RRNorth	2.2	2.6	1.9	1.2	1.0
RRSouth	2.4	1.9	1.9	1.1	1.0
PC2	0.9	0.9	0.5	0.5	0.5
MBA	0.5	0.7	0.6	0.3	0.3
MBB	0.4	0.5	0.3	0.2	0.2
Miti1	0.1	0.3	0.2	0.1	0.3
Miti2	0.0	0.0	0.0	0.0	0.0
I52	0.7	1.7	1.6	0.7	0.4
SBW	0.3	0.4	0.4	0.2	0.2
SBE	0.1	0.1	0.1	0.1	0.0

Sediment Transport

Sediment movement for the first year of the sediment transport/morphology simulations is investigated similar to that of Restoration Scenario A. Sediment is supplied by the Deschutes River (25,000 m^3/yr) and from the estuary bed but not from Budd Inlet. Sediment fluxes through cross-sections at four constrictions show both redistribution of bed sediment and accumulation of the fluvial load in the basins (Table 3.12). The I-5 cross-section shows approximately 30,000 to 38,000 m^3/yr of sediment passing under the bridge. Approximately 121,000 to 222,000 m^3/yr of sediment is transported through the trestle. The cross-section at the entrance to Percival Cove exhibits 2,500 to 5,000 m^3/yr of sediment movement into the cove. Sediment exported from the estuary through the entrance is approximately 101,000 m^3/yr for the lower erodibility and 222,000 m^3/yr for the higher erodibility. Changes to the individual basins are described in the morphology results below.

Table 3.12. Sediment transport (m^3/yr) through Restoration Scenario D cross-sections during the first year after dam removal

cross-section	lower erodibility	higher erodibility
river	25,000	25,000
I-5	30,000	38,000
trestle	121,000	222,000
Percival Cove	2,500	5,000
entrance	101,000	222,000

First Year Morphology Change
Morphological change after one year shows erosion in South and Middle Basin of 0.2 – more than 1 m in similar areas as Restoration Scenario A; deposition patterns are also similar (Figure 3.77). North Basin patterns also resemble those of Restoration Scenario A, despite the removal of the eastern half. A channel parallel to the retaining wall emerges but no area erodes more than 0.6 m. Patchy areas of deposition occur along the wall. Sediment grain size distributions mostly follow those of Restoration Scenario A as well. The region adjacent to the retaining wall shows large fractions of sand (Figure 3.78) and low fractions of silt or clay (Figure 3.79). Gravel distributions are nearly identical to those of Restoration Scenario A.

Short-term Morphology Change
The three-year morphology results for Restoration Scenario D are mostly similar to those from Restoration Scenario A. North Basin is the only part of the estuary that shows unique patterns. Deposition is spread across the southwestern quadrant of the basin while erosion parallel to the retaining wall is patchy for the lower erodibility (Figure 3.80). The marina and port accumulate more than 1 m of sediment. As with the previous restoration scenarios, changes to the bed slow after one year even though the sediment grain size continues to evolve. In cross-estuary Section B, which cuts through the freshwater impoundment, a distinct sand-dominated channel develops while the western flanks become finer (Figure 3.81).

Results from the higher erodibility case show most of Middle Basin and parts of South Basin erode by at least 0.5 m after three years (Figure 3.82). Deposition is scattered throughout the estuary: in South Basin, Percival Cove and a small area north of Marathon Park. Deposition and erosion patterns also run parallel to the retaining wall in North Basin. More than 2 m of sediment accumulate in the marina and port. The bed continues to change in depth although not as abruptly between years two and three as between years one and two. The cross-estuary transect of Section B shows a sandy narrow channel forming along the retaining wall and stripping the fine fractions in the center of North Basin (Figure 3.83). Section C demonstrates unique behavior in Middle Basin (Figure 3.84). During the first year, the flanks and channel erode between 1 – 2 m, but after the second year, the channel begins to accumulate sediment. The flanks continue to erode for another year while the channel gets shallower. By the third year, the profile does not show a defined channel or flanks but rather a broad flat estuary with varying amounts of sand mixed with a silt-dominated bed.

Similar to the other three restoration scenarios, the morphology of Restoration Scenario D shows variability depending on the erodibility. The impact of the freshwater impoundment and retaining wall on the resulting estuarine morphology is less severe than the uncertainty in the bed erodibility.

Long-term Morphology Change
Deposition and erosion patterns throughout most of the estuary are nearly identical between Restoration Scenarios A and D for the ten-year simulation (lower erodibility and looser mud density of 500 kg/m^3). North Basin and the marina and port areas are heavily impacted by the freshwater impoundment of the eastern half of the basin (Figure 3.85). Along the dike, erosion continues through the fifth year and slows substantially during

the next five years. The southwestern part of the basin accretes approximately 0.5 m of sediment and widespread regions of the marina and port accumulate more than 2 m of sediment.

The two northern cross-estuary transects of bathymetry and surface sediment grain size fractions show different behavior in Restoration Scenario D than in Restoration Scenario A. In Section A, the surface sediment fraction remains mud-dominated despite the formation of a slightly sandy channel by the tenth post-dam year (Figure 3.86). The sediment fraction in Section B, already explored in the short-term morphology discussion, shows sand dominating the transect through year ten (Figure 3.87). Few differences are observed for Section C between Restoration Scenarios D and A. Station NB6 shows erosion of more than 1 m within the first two years before the bed depth stabilizes at approximately 2.8 m for the next eight years (Figure 3.88). The rate of bed depth change slows within the first two to four years for all of the stations, which is similar to observations from Restoration Scenario A.

The long-term morphology simulation indicates that a dynamic equilibrium is reached within the first three to five years after dam removal for Restoration Scenario D. The freshwater impoundment of the eastern half of North Basin impacts the sediment transport and morphologic change of the basin and deposition amounts in the marina and port.

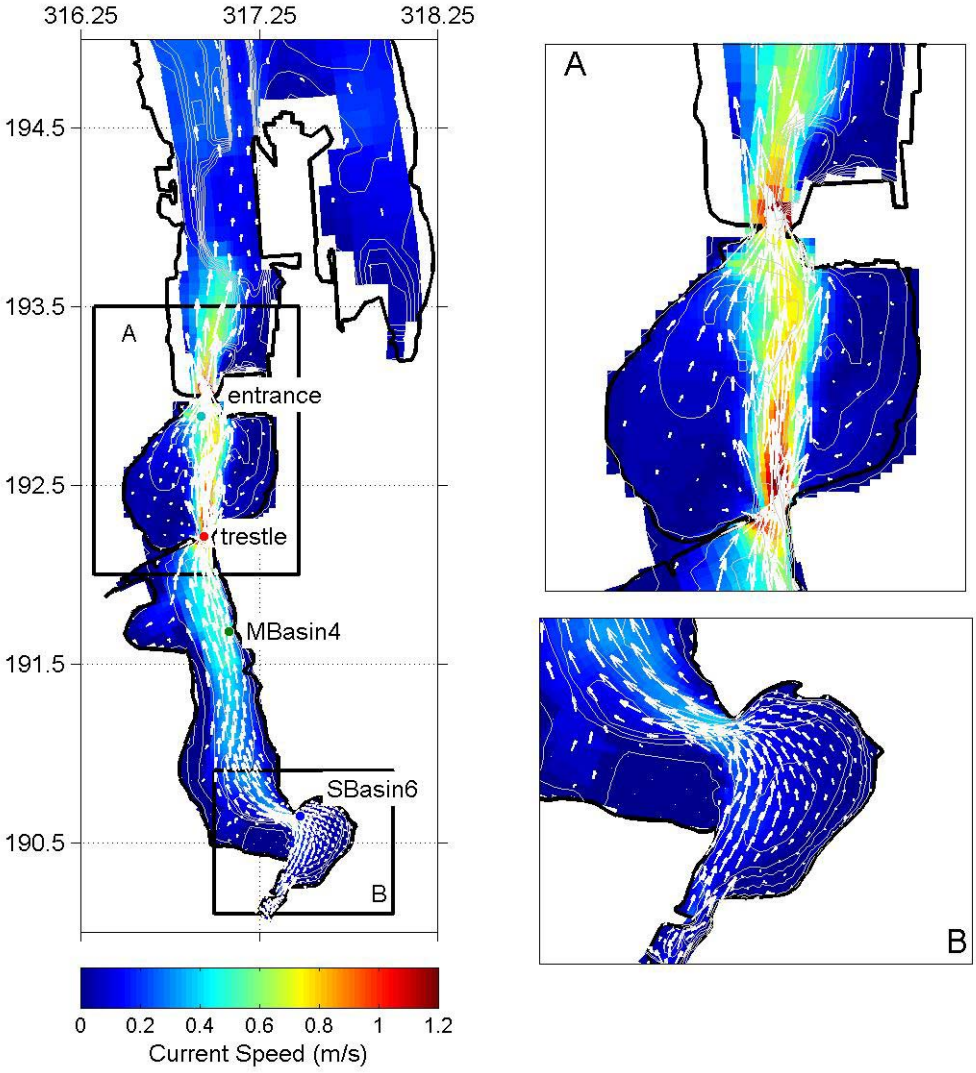

Figure 3.1. Maximum velocity magnitude and vectors during low river flow at ebb tide for the predam estuary. The axes are in Washington State Plane South (km) and bathymetric contours in 1 m increments. Blues indicate slow velocities and reds show the fastest speeds. The fastest currents are observed through the trestle and entrance while speeds decrease in Middle Basin and are slowest in South Basin.

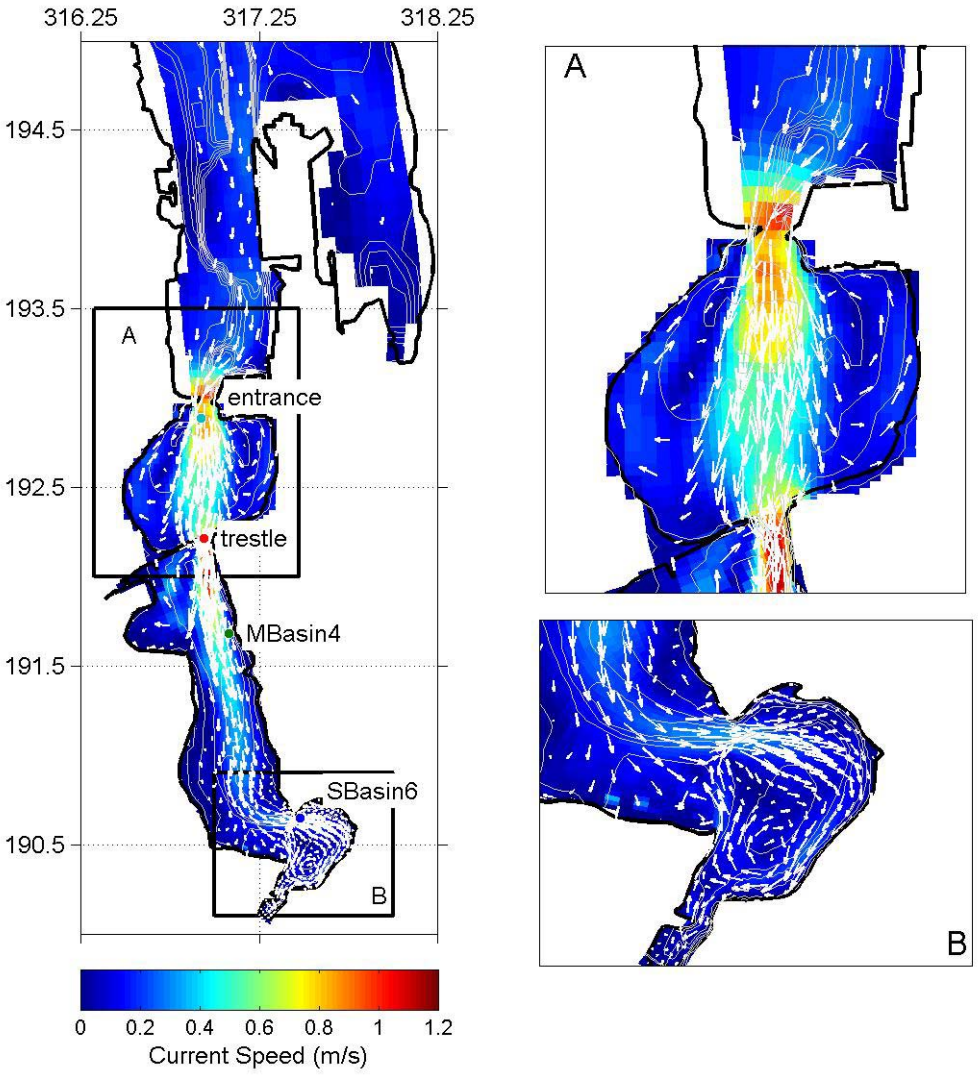

Figure 3.2. Maximum velocity magnitude and vectors during low river flow at flood tide for the predam estuary. The axes are in Washington State Plane South (km) and bathymetric contours in 1 m increments. Blues indicate slow velocities and reds show the fastest speeds. The fastest currents are observed through the trestle and entrance while speeds decrease in Middle Basin and are slowest in South Basin.

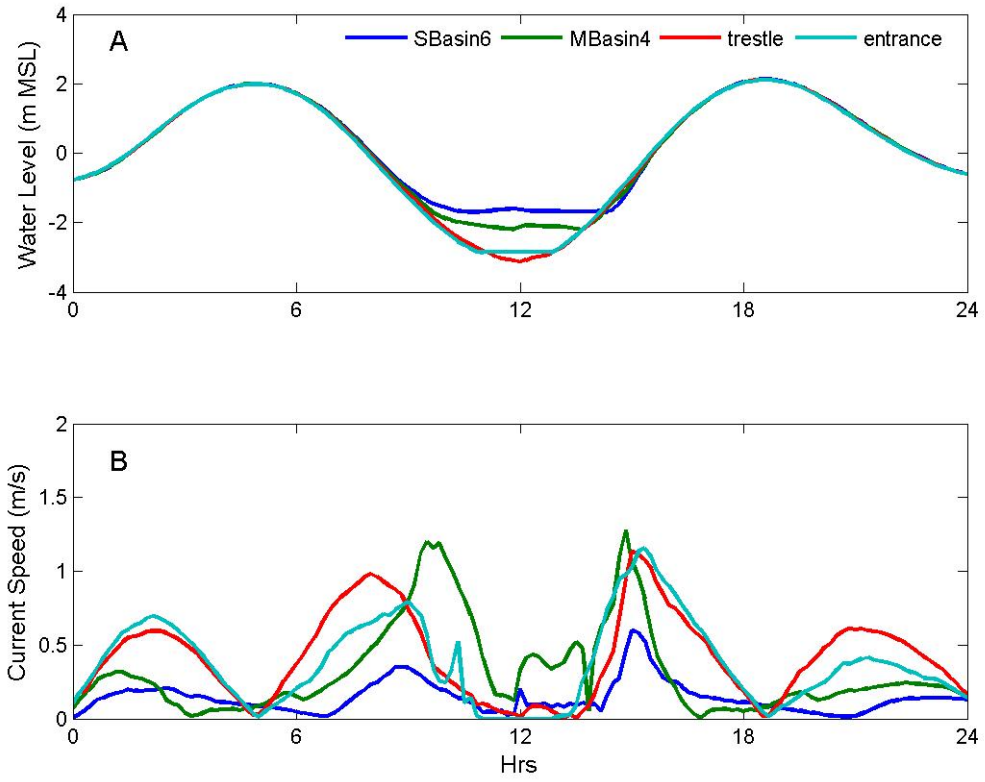

Figure 3.3. Water level and current speed at four stations during the low river flow for the predam estuary. See Figure 3.1 for locations of the stations. The fastest velocities are observed halfway between slack tides and the slowest are seen at high or low tide.

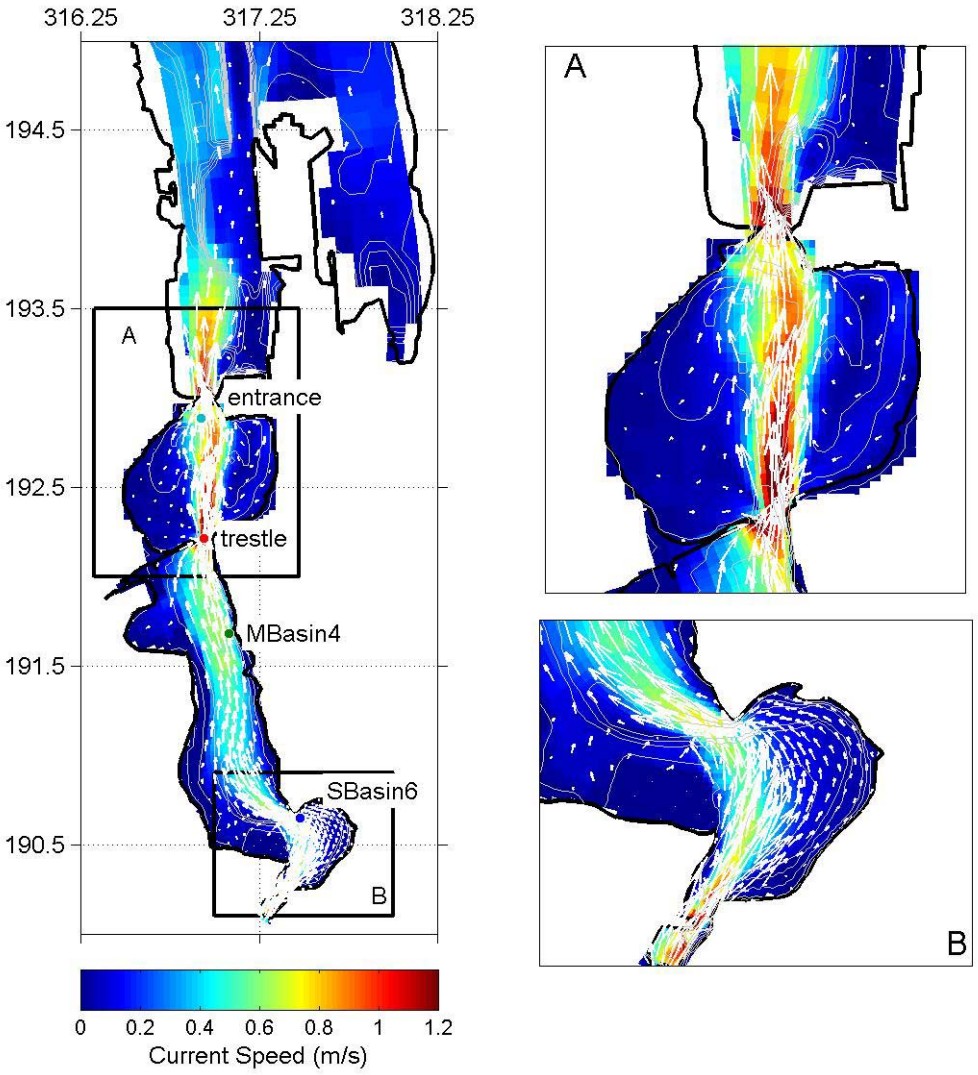

Figure 3.4. Maximum velocity magnitude and vectors during high river flow at ebb tide for the predam estuary. The axes are in Washington State Plane South (km) and bathymetric contours in 1 m increments. Blues indicate slow velocities and reds show the fastest speeds. The fastest currents are observed through the trestle and entrance while speeds decrease in Middle Basin. Flow in South Basin is fast mainly due to the Deschutes River.

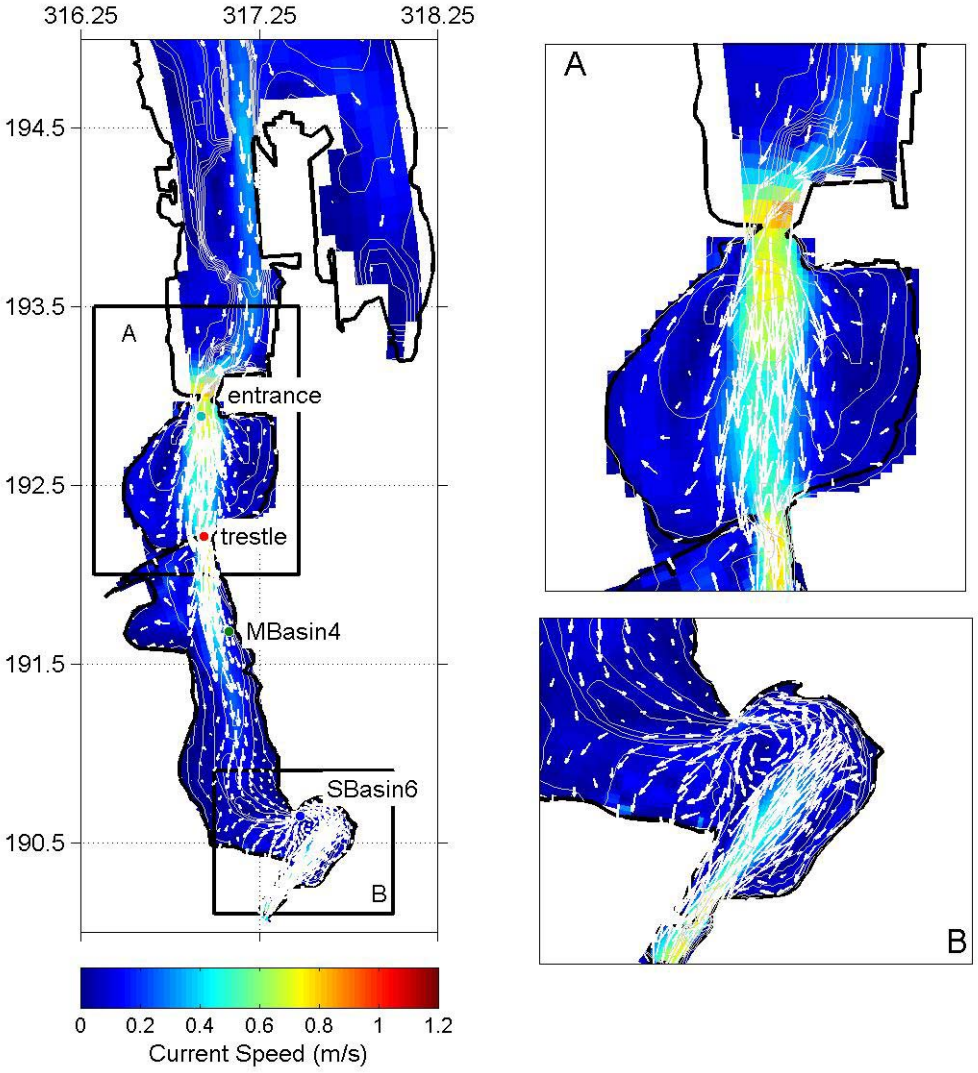

Figure 3.5. Maximum velocity magnitude and vectors during high river flow at flood tide for the predam estuary. The axes are in Washington State Plane South (km) and bathymetric contours in 1 m increments. Blues indicate slow velocities and reds show the fastest speeds. The fastest currents are observed through the trestle and entrance but speed decreases in Middle Basin as the incoming tide encounters the outgoing river flow. South Basin shows chaotic circulation patterns from the tide-river interaction.

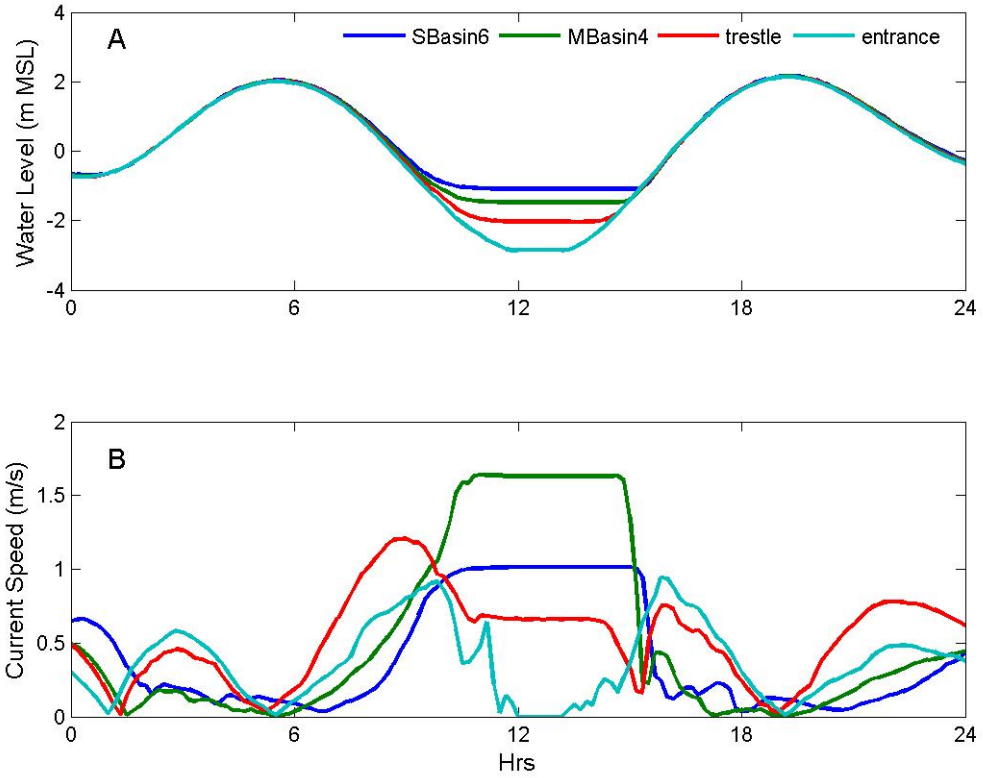

Figure 3.6. Water level and current speed at four stations during the high river flow for the predam estuary. See Figure 3.1 for locations of the stations. The fastest velocities are observed halfway between slack tides and the slowest are seen at high tide. At low tide for stations inside the estuary, the high river flow dominates the velocity magnitude signal with a constant speed.

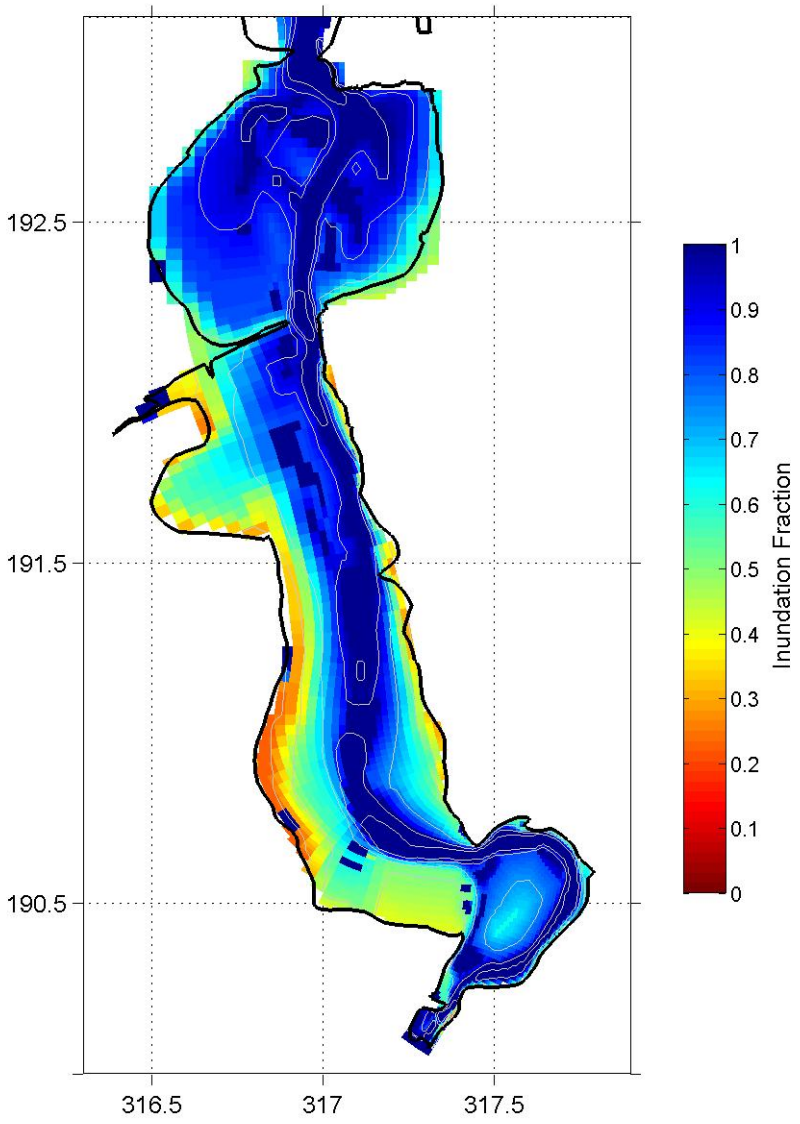

Figure 3.7. Annual mean inundation fraction for the predam estuary. Blues indicate continuous submersion and reds show continuous exposure. The main channel appears to be underwater at all times of the year while elevations above 2 m are wet less than 50% of the time.

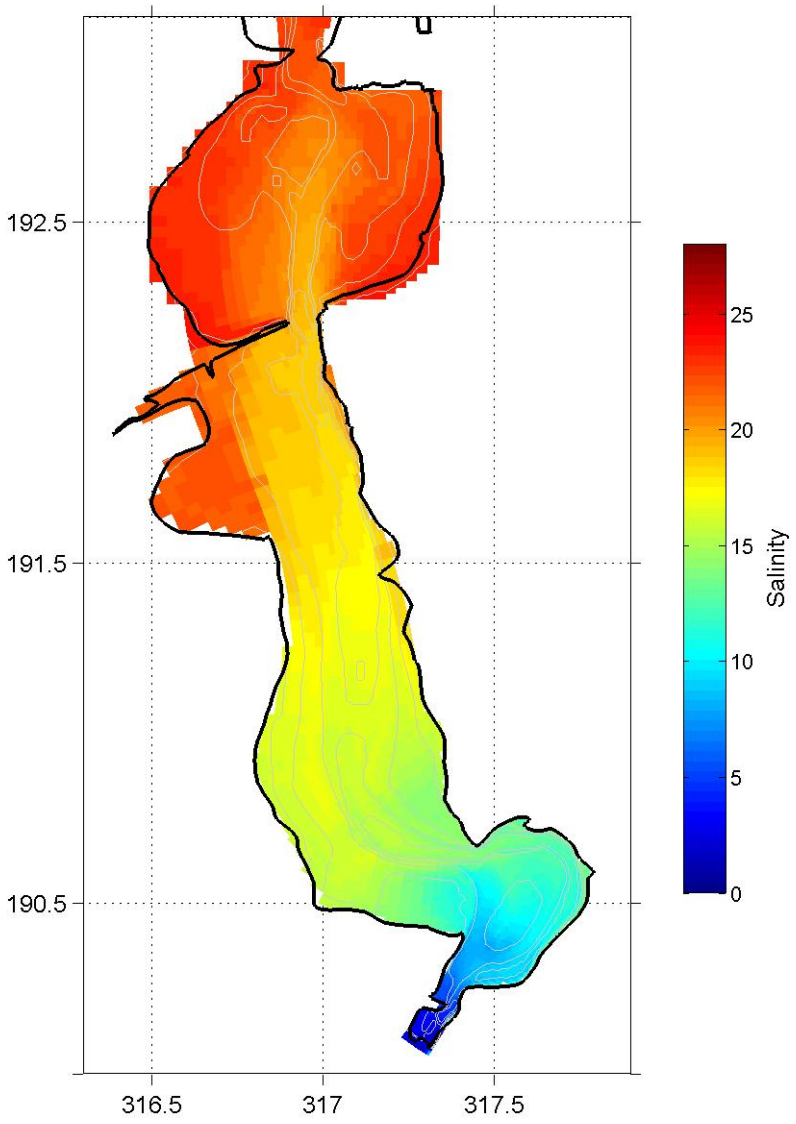

Figure 3.8. Annual mean near-bed salinity for the predam estuary. Blues indicate freshwater and reds show the most saline water. Northern South Basin and most of Middle Basin exhibit brackish water with salinities between 10 – 20 ppt. North Basin shows a slightly fresher channel than the flanks.

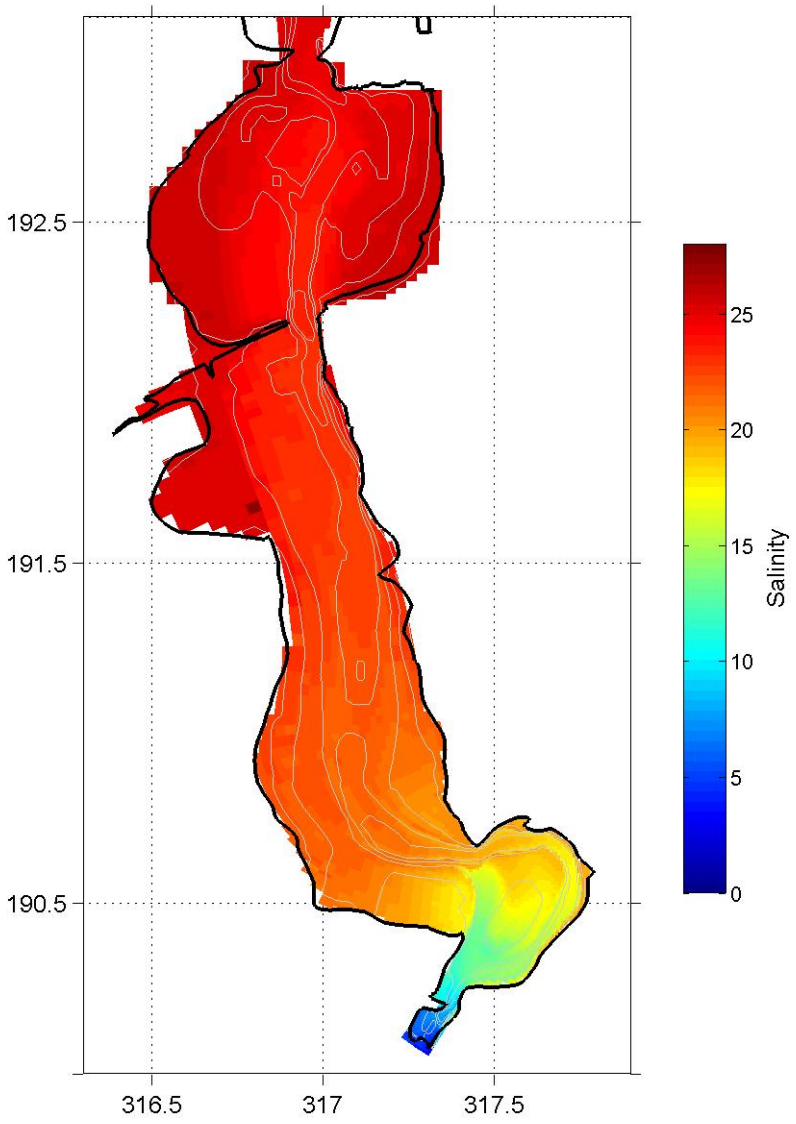

Figure 3.9. Dry season (low river flow)mean near-bed salinity for the predam estuary. Blues indicate freshwater and reds show the most saline water. The steepest salinity gradient occurs in South Basin between the river mouth and where the northern section exceeds 15 ppt. The majority of the estuary is above 18 ppt with the flanks of North Basin above 25 ppt.

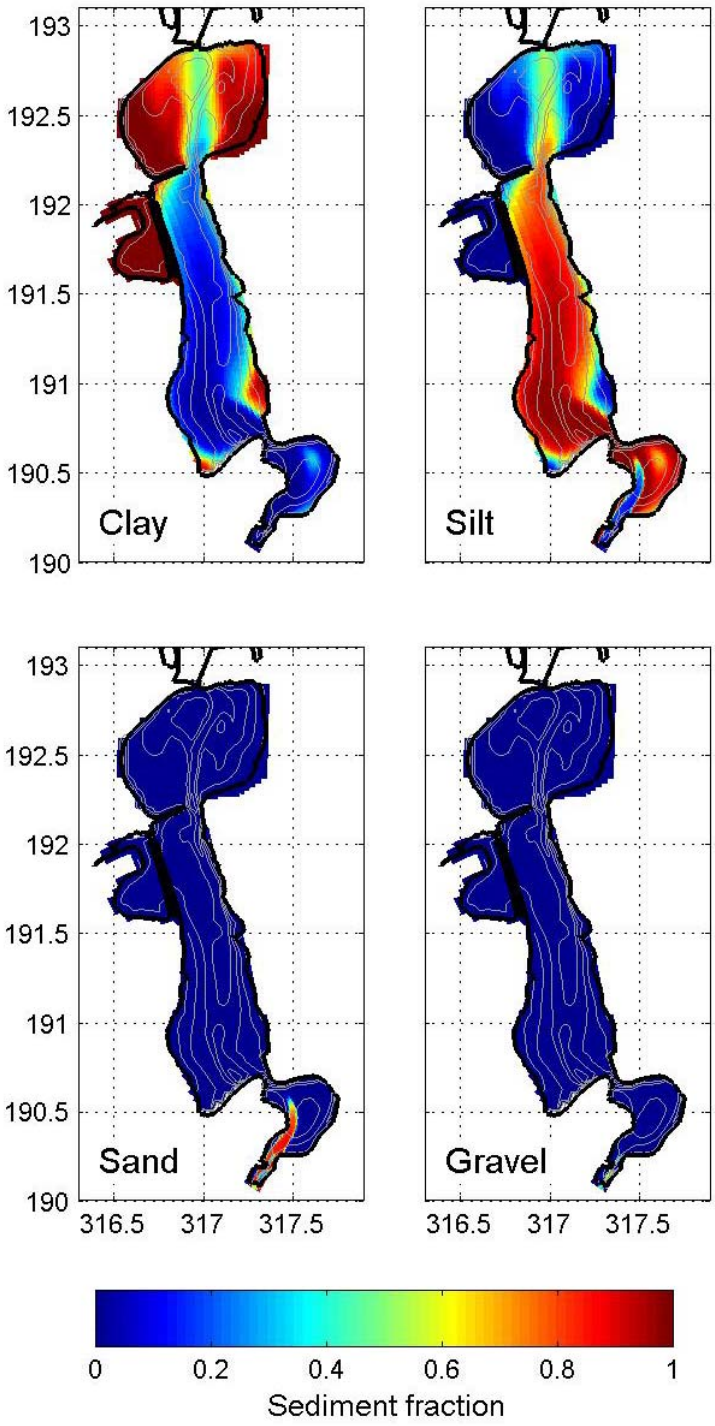

Figure 3.10. Surface sediment fraction distributions after a five-year simulation in the initial lake after construction of the I-5 bridge in 1957. Clay dominates in North Basin and Percival Cove and silt covers the bed in Middle Basin and most of South Basin. Sand accumulates in the channel immediately downstream of the Deschutes River. Gravel amounts are negligible.

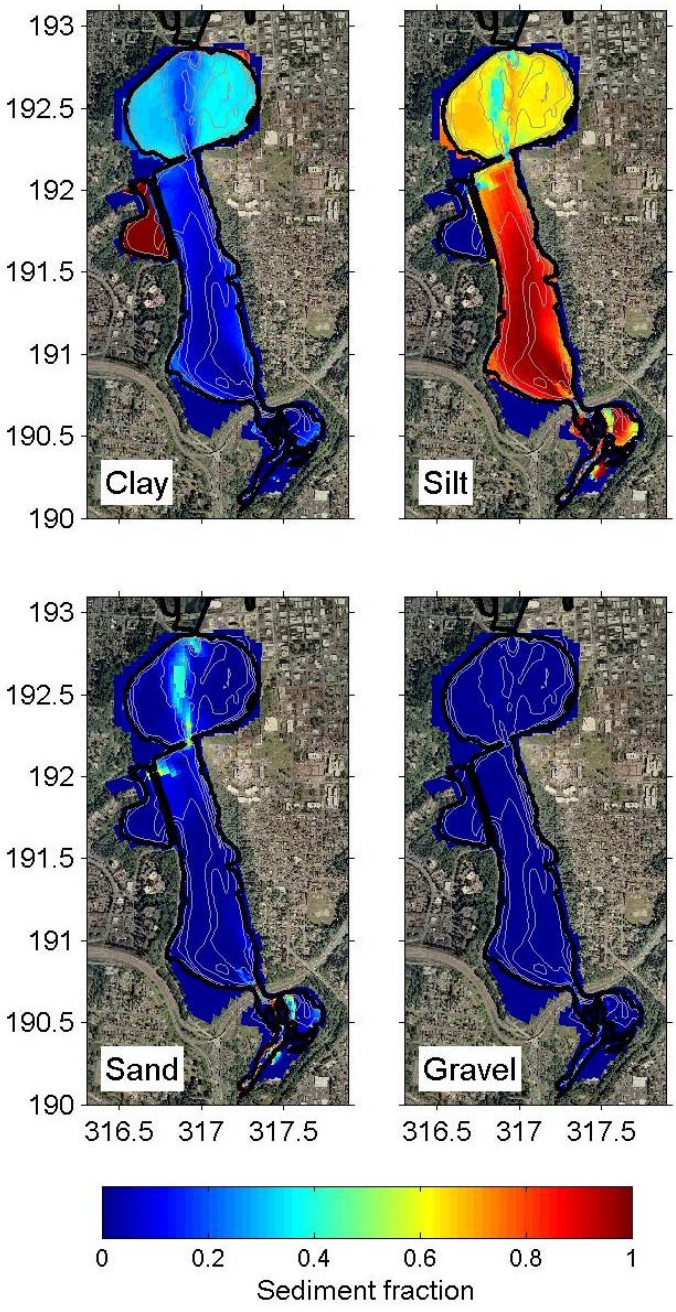

Figure 3.11. Surface sediment fraction distributions after a five-year simulation in the modern lake (2005 bathymetry) with initial distributions of sediment on the bed. The clay fraction on the bed in North Basin is approximately 0.4 but almost 100% in Percival Cove. Silt dominates the bed in Middle Basin and most of South Basin. Sand accumulates in the channels and in areas of higher velocities, such as around the trestle. Gravel amounts are negligible.

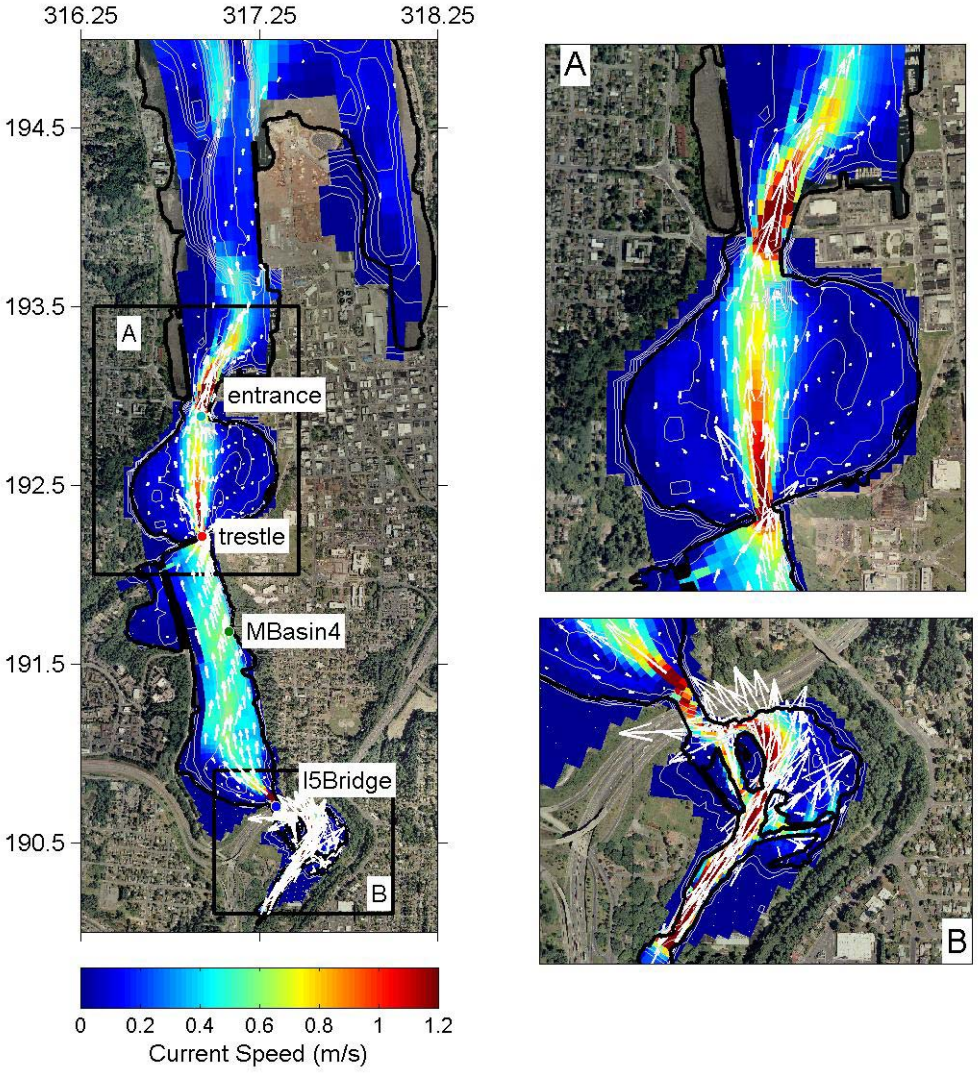

Figure 3.12. Maximum velocity magnitude and vectors during low river flow at ebb tide for the Restoration Scenario A estuary. The axes are in Washington State Plane South (km) and bathymetric contours in 1 m increments. Blues indicate slow velocities and reds show the fastest speeds. The fastest currents are observed through the trestle and entrance while speeds decrease in Middle Basin. Speeds under the I-5 bridge are less than 0.5 m/s.

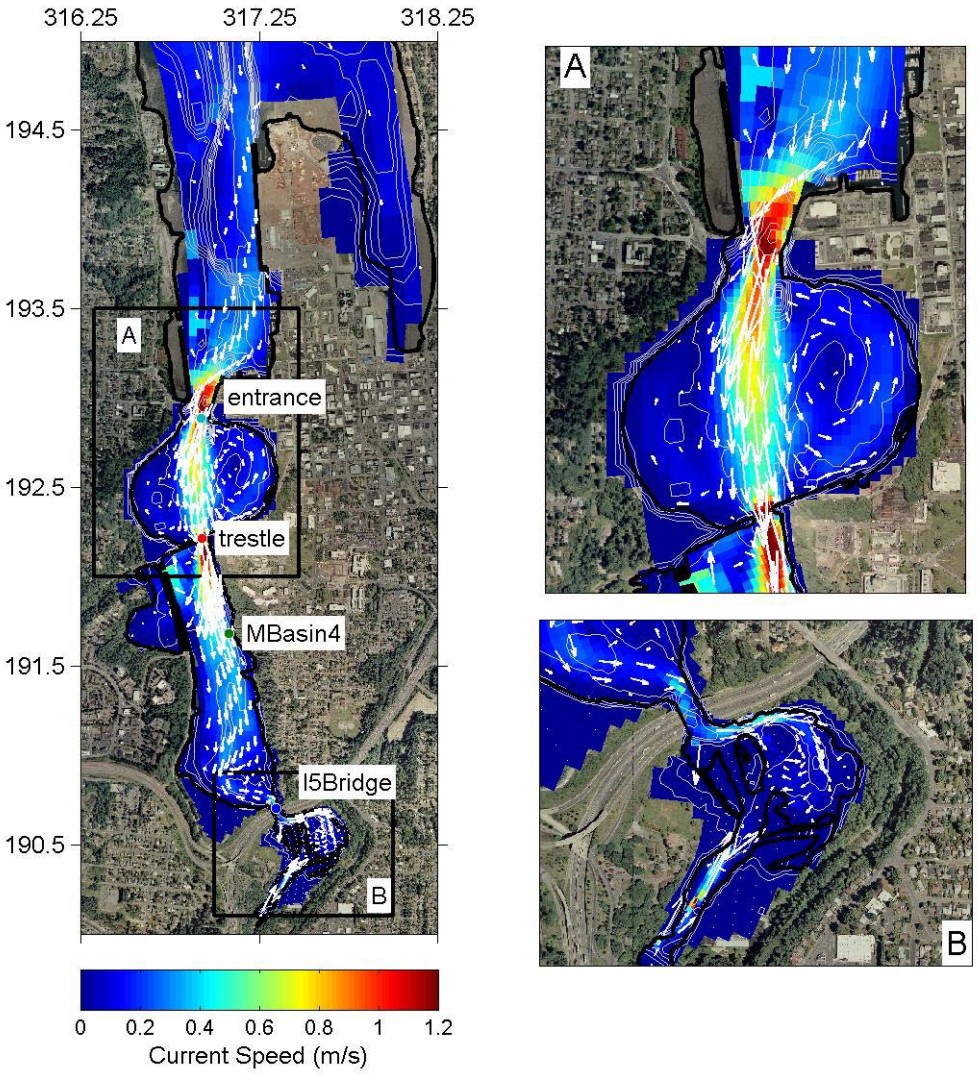

Figure 3.13. Maximum velocity magnitude and vectors during low river flow at flood tide for the Restoration Scenario A estuary. The axes are in Washington State Plane South (km) and bathymetric contours in 1 m increments. Blues indicate slow velocities and reds show the fastest speeds. The fastest currents are observed through the trestle and entrance while speeds decrease in Middle Basin. Speeds under the I-5 bridge are less than 0.5 m/s. Opposing circulation eddies are seen in North Basin.

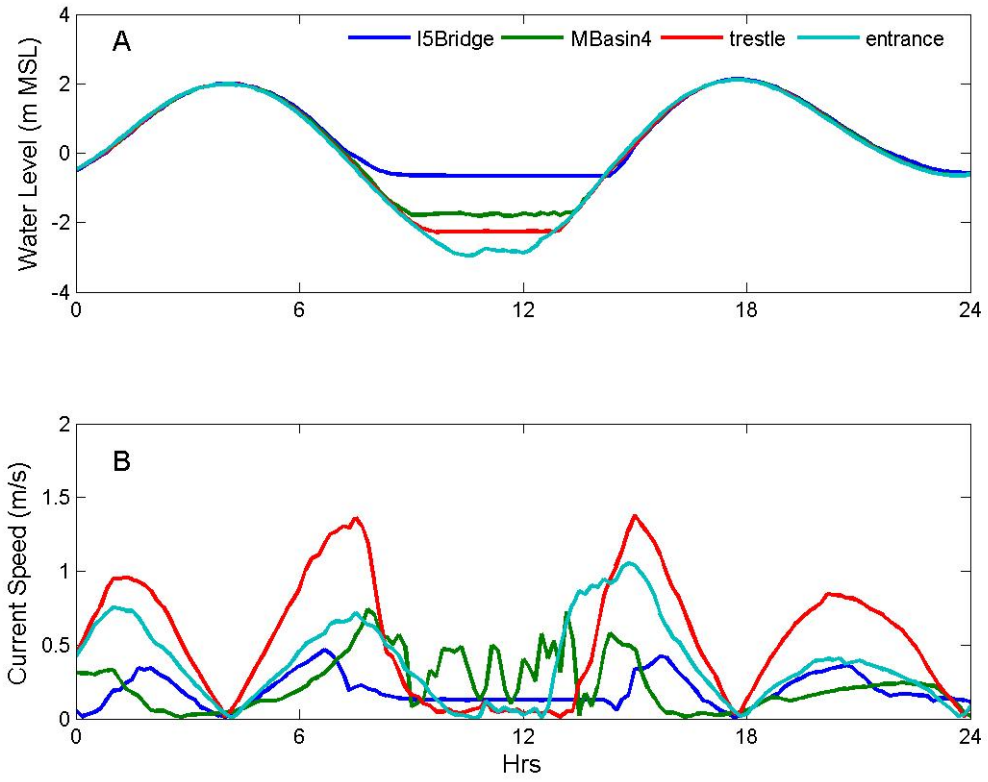

Figure 3.14. Water level and current speed at four stations during the low river flow for the Restoration Scenario A estuary. See Figure 3.12 for locations of the stations. The fastest velocities are observed halfway between slack tides and the slowest are seen at high or low tide.

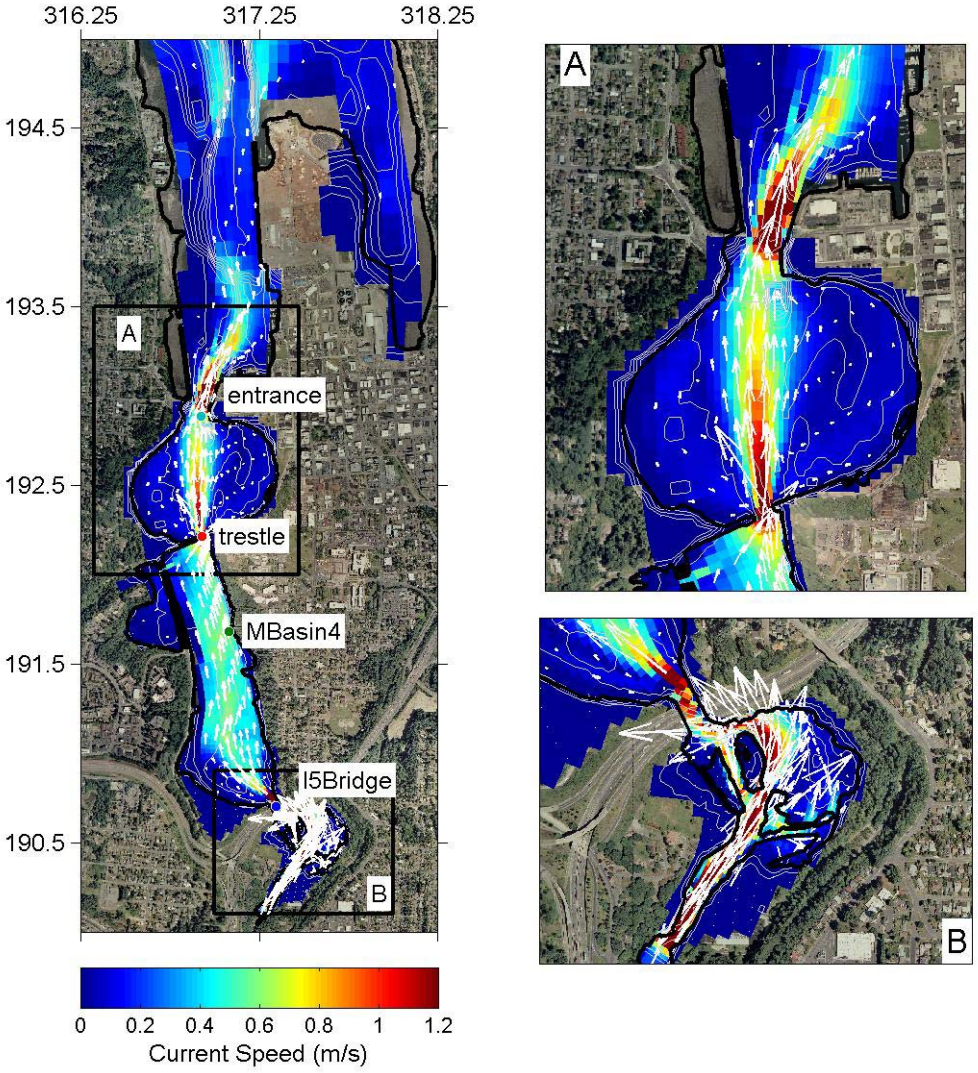

Figure 3.15. Maximum velocity magnitude and vectors during high river flow at ebb tide for the Restoration Scenario A estuary. The axes are in Washington State Plane South (km) and bathymetric contours in 1 m increments. Blues indicate slow velocities and reds show the fastest speeds. The fastest currents are observed through the trestle and entrance while speeds decrease in Middle Basin but remain above 0.5 m/s. Speeds under the I-5 bridge are faster than 1 m/s.

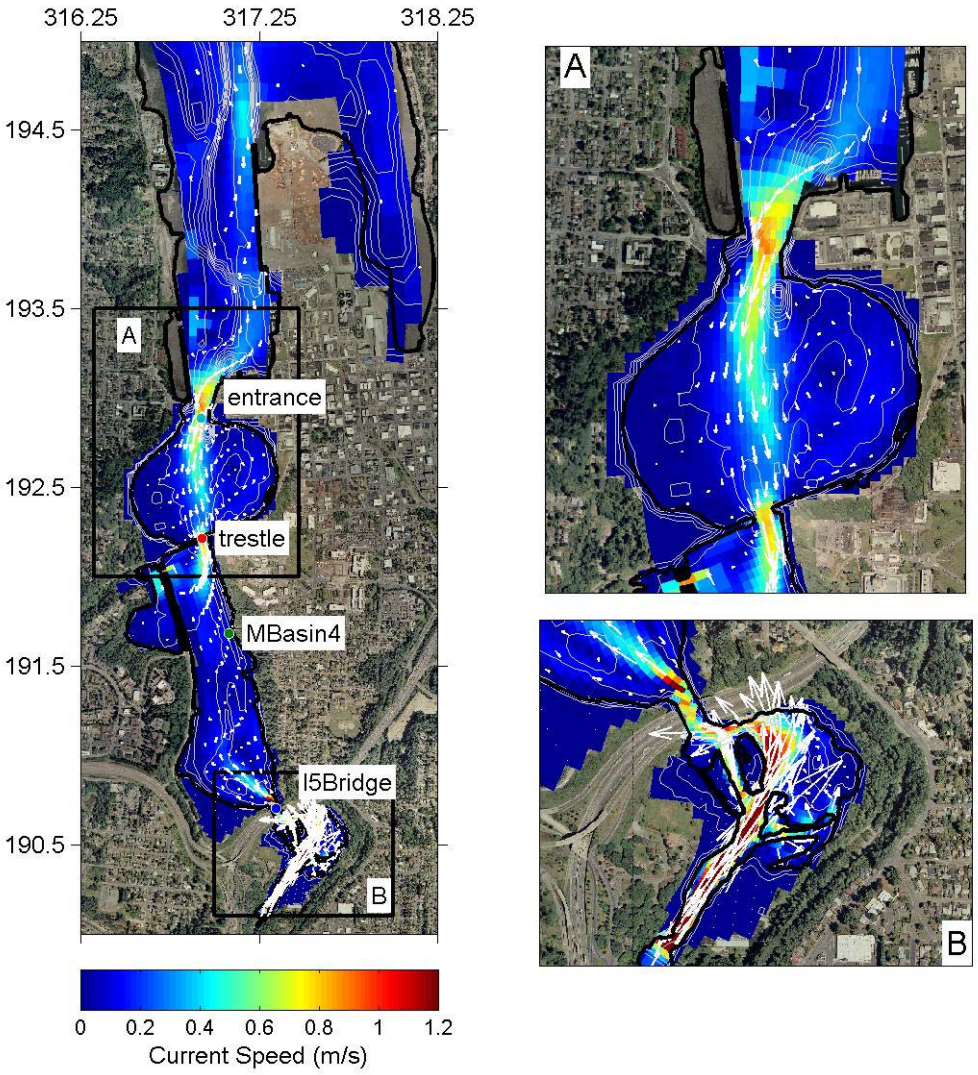

Figure 3.16. Maximum velocity magnitude and vectors during high river flow at flood tide for the Restoration Scenario A estuary. The axes are in Washington State Plane South (km) and bathymetric contours in 1 m increments. Blues indicate slow velocities and reds show the fastest speeds. The fastest currents are observed through the trestle and entrance and under the I-5 bridge. Speeds are slow throughout the estuary as the incoming tide encounters the outgoing river flow. South Basin shows chaotic circulation patterns from the tide-river interaction.

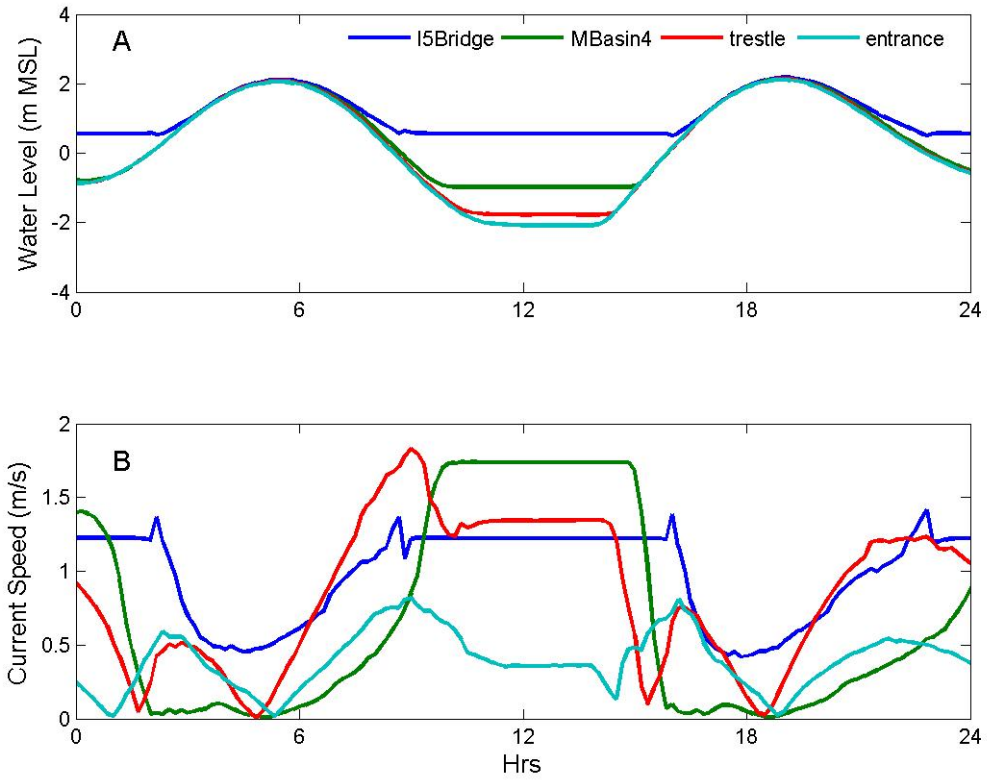

Figure 3.17. Water level and current speed at four stations during the high river flow for the Restoration Scenario A estuary. See Figure 3.12 for locations of the stations. The fastest velocities are observed halfway between slack tides and the slowest are seen at high tide. During low tide, the river flow dominates the velocity magnitude signal with a constant speed.

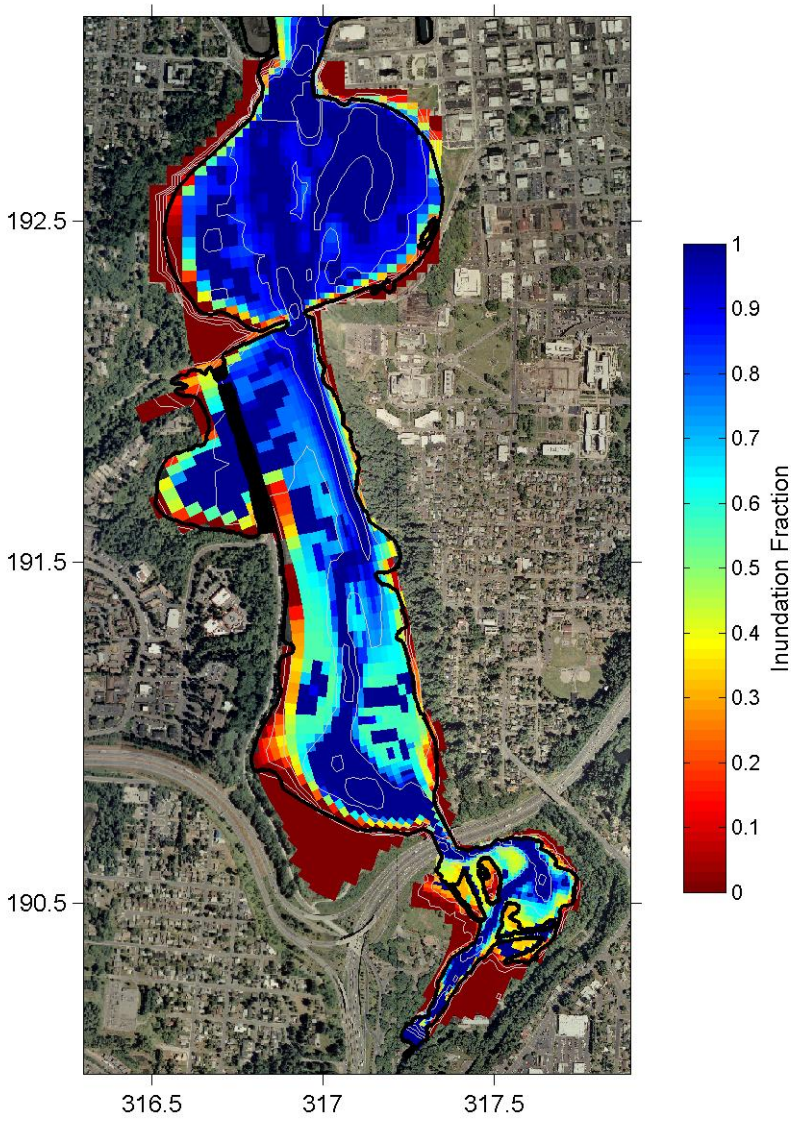

Figure 3.18. Annual mean inundation fraction for the Restoration Scenario A estuary. Blues indicate continuous submersion and reds show continuous exposure. The main channel, North Basin and part of Middle Basin appear to be underwater at least 80% of the year while elevations above 2 m are wet less than 50% of the time. Portions of the South Basin islands get submerged about 30 – 40% of the year.

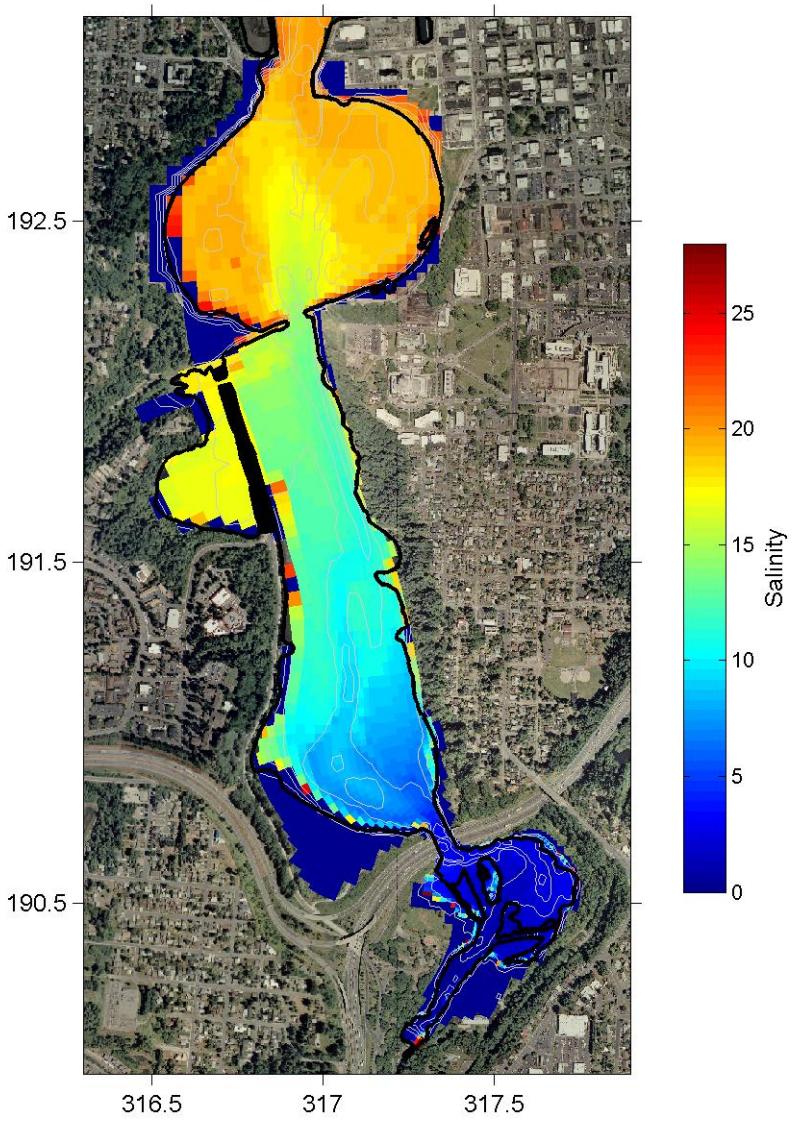

Figure 3.19. Annual mean near-bed salinity for the Restoration Scenario A estuary. Blues indicate freshwater and reds show the most saline water. A steady salinity gradient is observed from freshwater at the river mouth to approximately 15 ppt at the trestle. Percival Cove is saltier than Middle Basin, possibly due to the limited influx of freshwater into the cove from Middle Basin and the absence of Percival Creek in the model. North Basin shows an intrusion of 15 – 18 ppt water into a fairly uniform basin of 18 – 20 ppt brackish water.

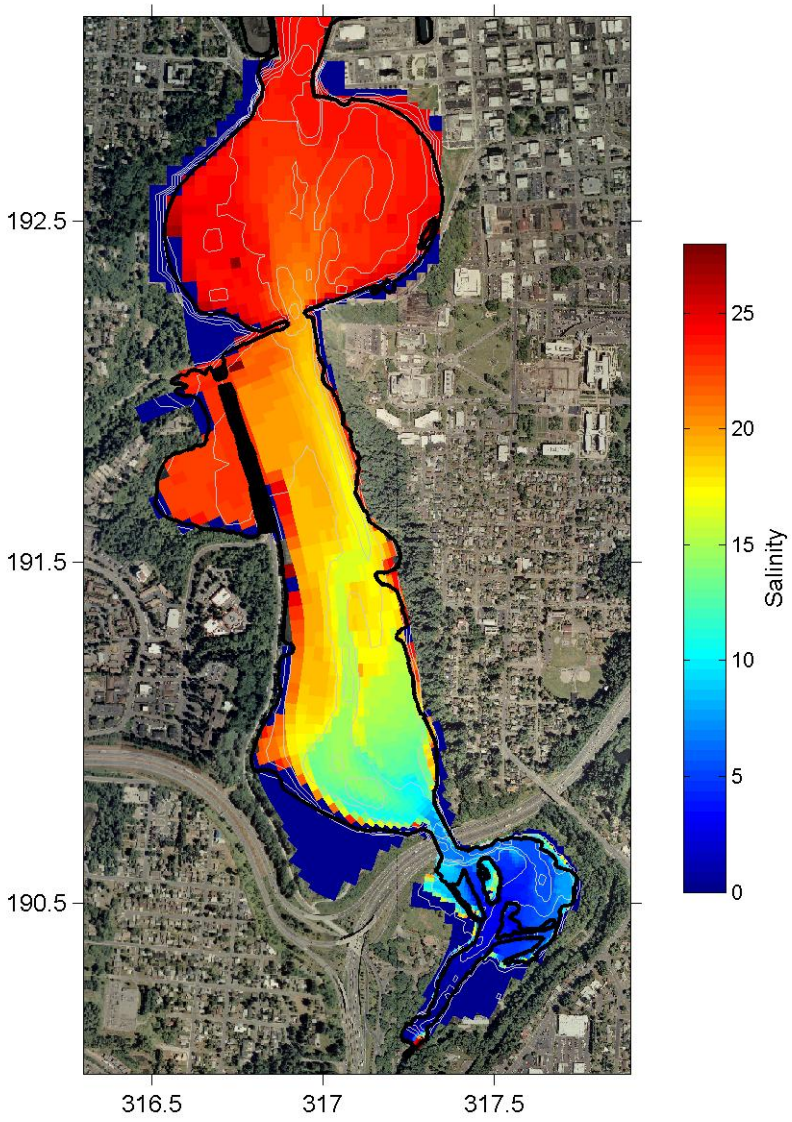

Figure 3.20. Dry season mean near-bed salinity for the Restoration Scenario A estuary. Blues indicate freshwater and reds show the most saline water. South Basin remains mostly fresh and Middle Basin contains water with salinities from 10 – 20 ppt. The main channel is fresher than the flanks in the center of the basin while salinities in Percival Cove and North Basin are almost uniformly above 20 ppt.

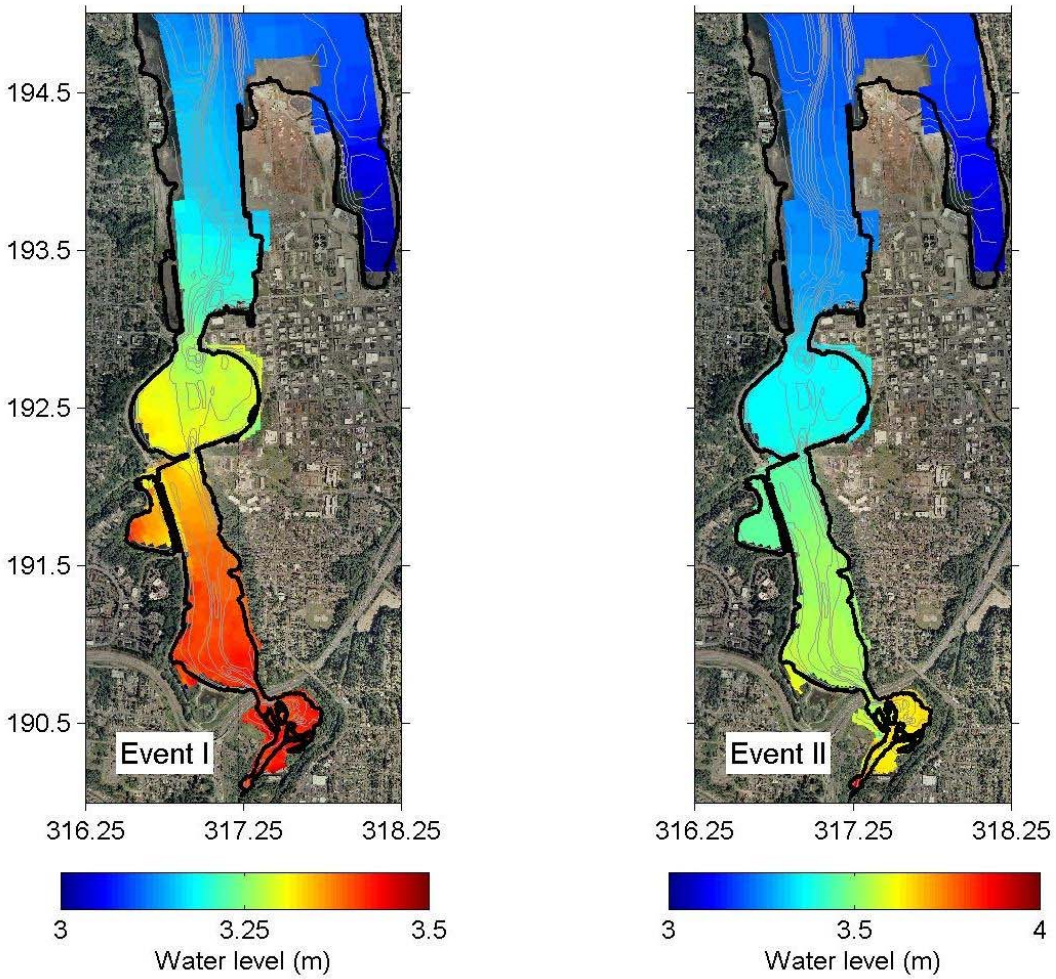

Figure 3.21. Maximum water levels for Events I and II in the Restoration Scenario A estuary (scales vary by event). The highest water levels are observed in South Basin. Tumwater Historical Park, the lower sections of the Heritage Park mitigation site and areas of Marathon Park all get submerged during the events.

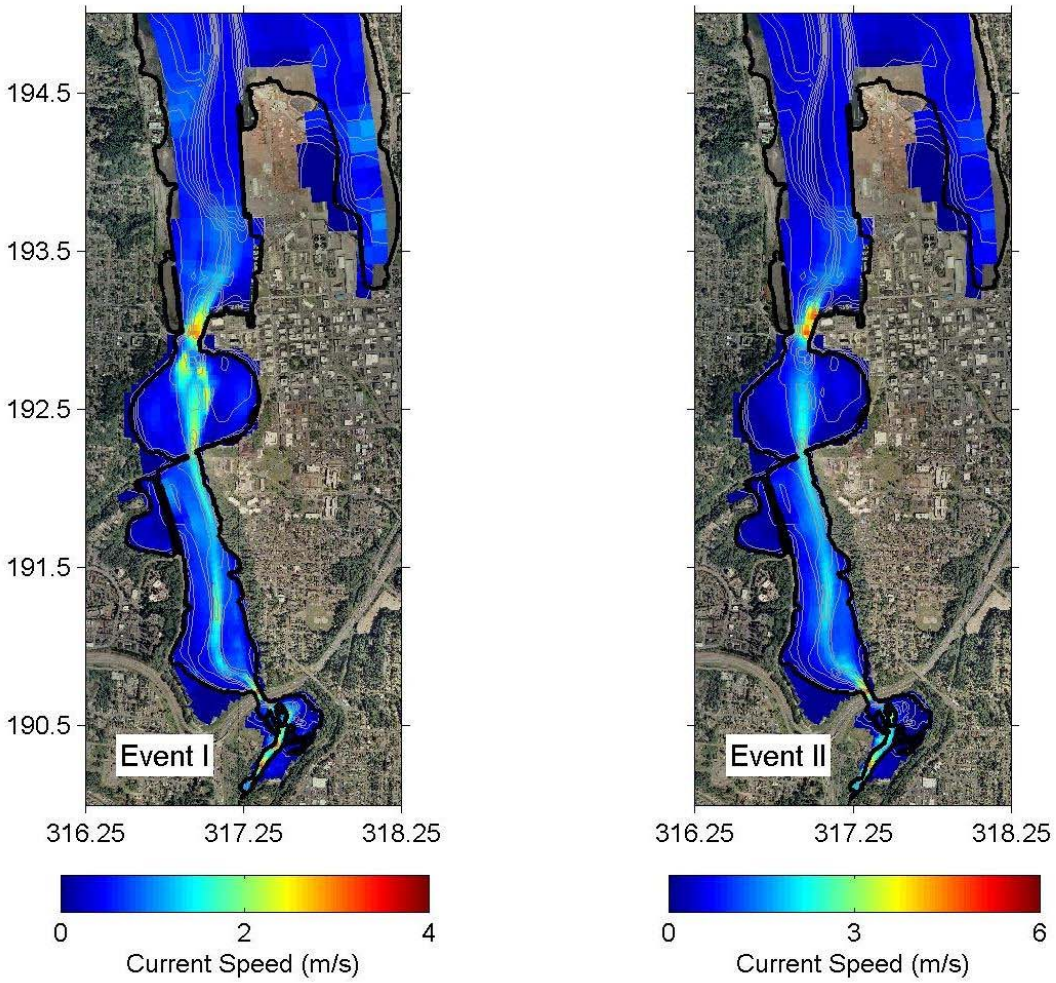

Figure 3.22. Maximum velocities for Events I and II in the Restoration Scenario A estuary. Blues are slower speeds and reds are faster (scales vary by event). Velocity magnitudes are largest immediately north of the estuary and under the I-5 bridge.

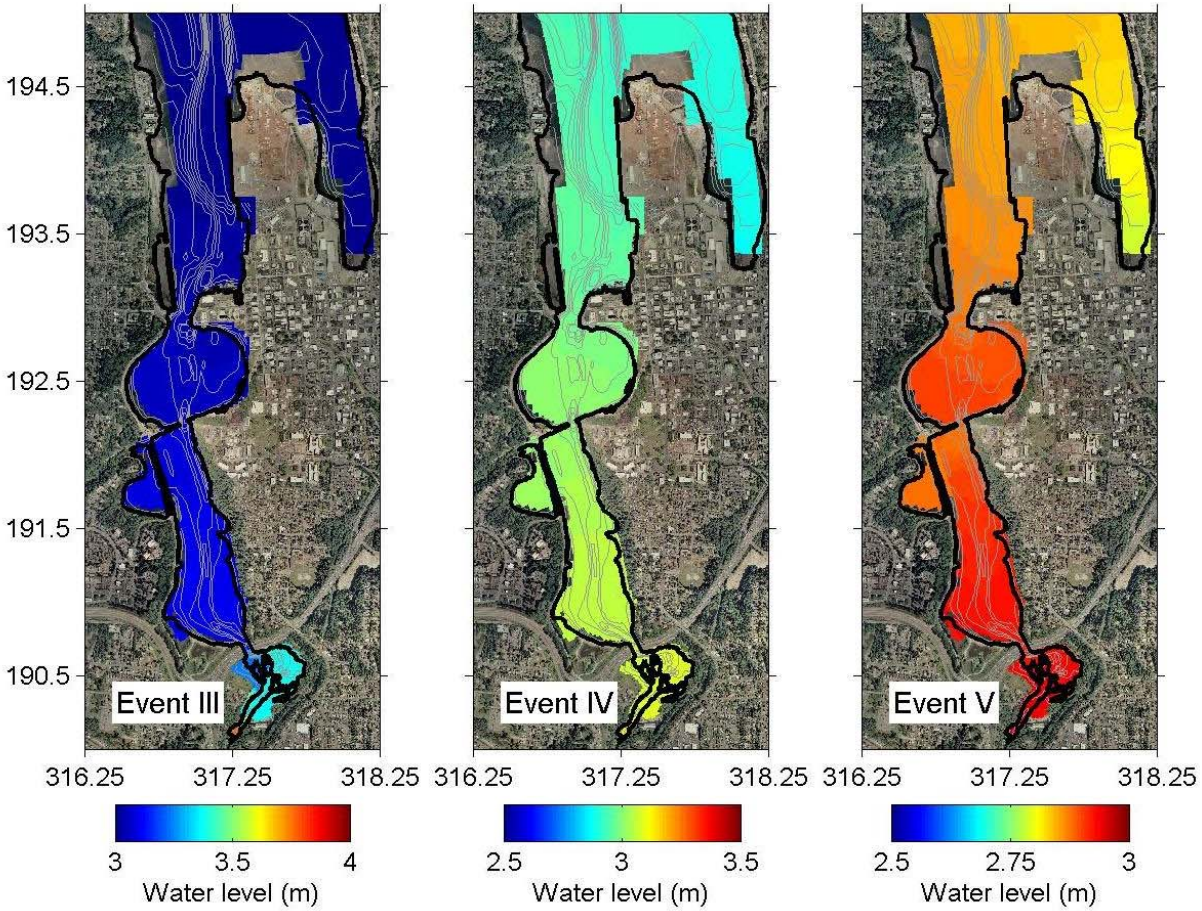

Figure 3.23. Maximum water levels for Events III, IV and V in the Restoration Scenario A estuary(scales vary by event). The highest water levels are observed in South Basin. Tumwater Historical Park, the lower sections of the Heritage Park mitigation site and areas of Marathon Park all get submerged during all events, but to a lesser amount in Event V.

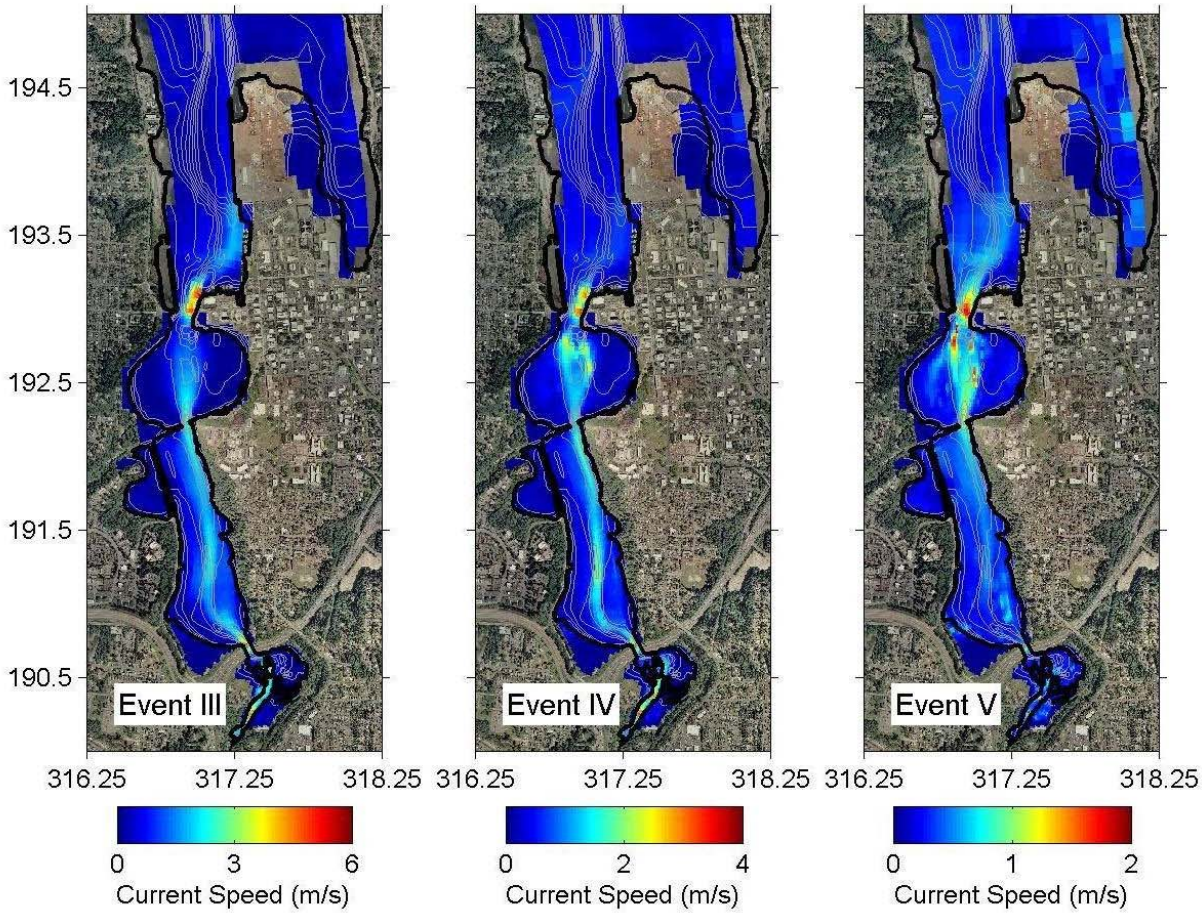

Figure 3.24. Maximum velocities for Events III, IV and V in the Restoration Scenario A estuary. Blues are slower speeds and reds are faster (scales vary by event). Velocity magnitudes are largest immediately north of the estuary and under the I-5 bridge with the fastest velocities observed in Event III.

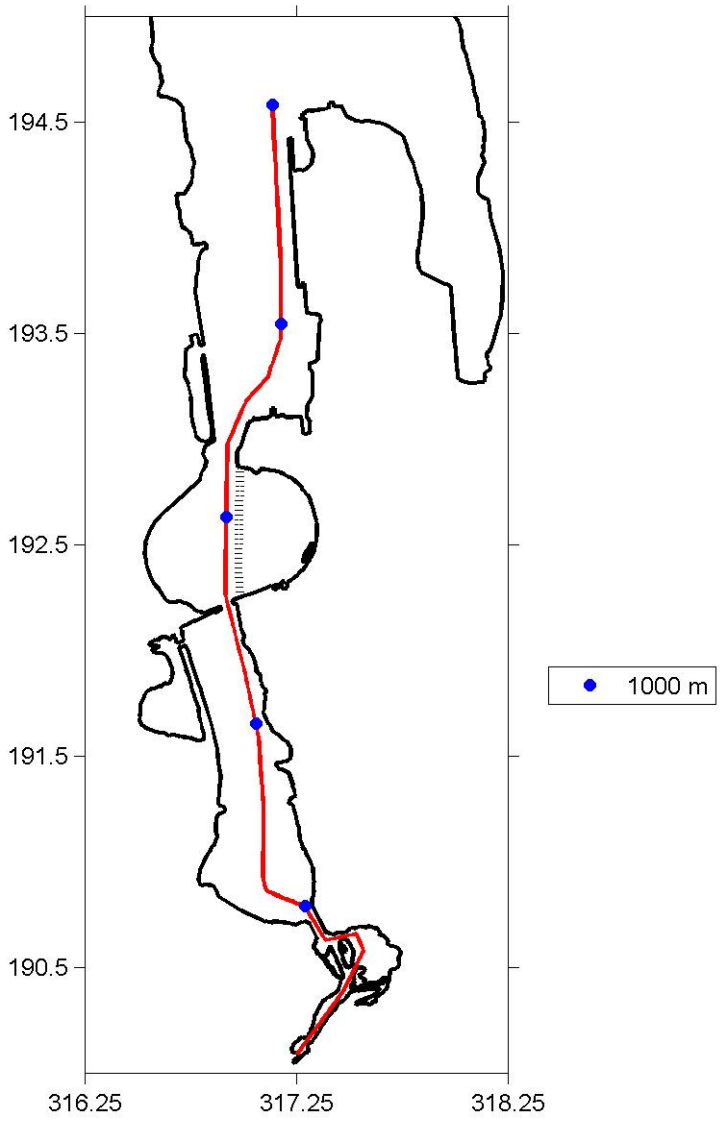

Figure 3.25. The 5,000-m transect selected for investigating the maximum water level gradient during the extreme hydrologic events. Blue dots are in 1,000 m intervals. The transect was identical for Restoration Scenarios A, B and D, with the proposed dike in Restoration Scenario D identified as the black hashed line.

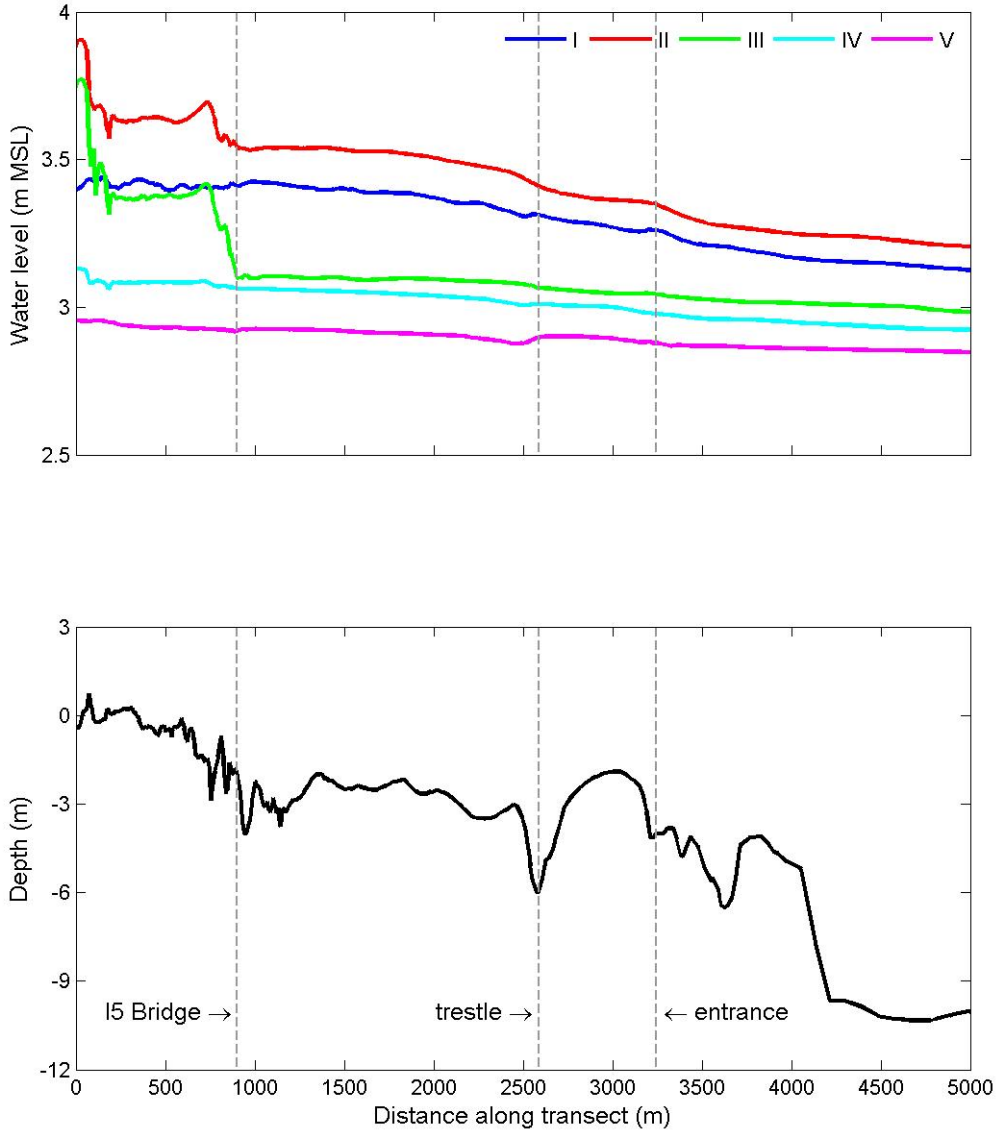

Figure 3.26. Maximum water level profile for the five extreme hydrologic events and bathymetry along the transect in Figure 3.25 for the Restoration Scenario A estuary. Events II and III show the steepest gradients in South Basin with Event III having the largest change overall. Water levels decrease gradually north of the I-5 bridge.

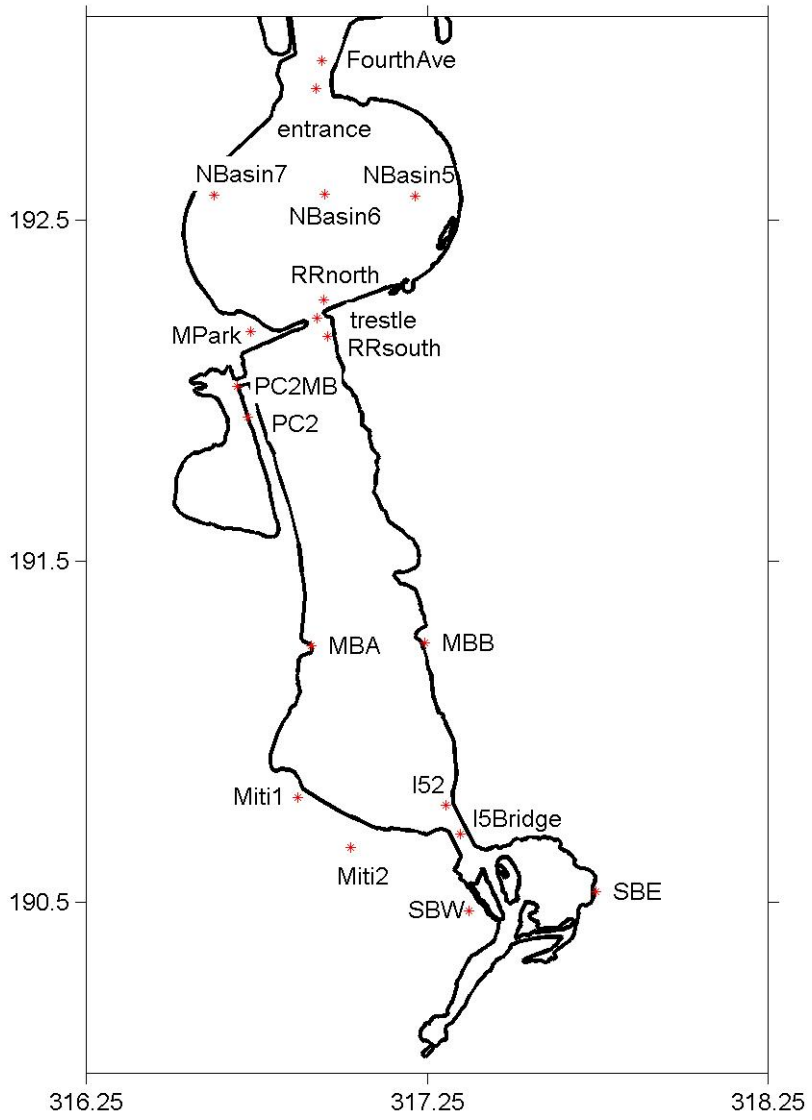

Figure 3.27. Observation stations used in Restoration Scenarios A and B to record water levels and velocities during the five extreme hydrologic events. See tables in the text for maximum values.

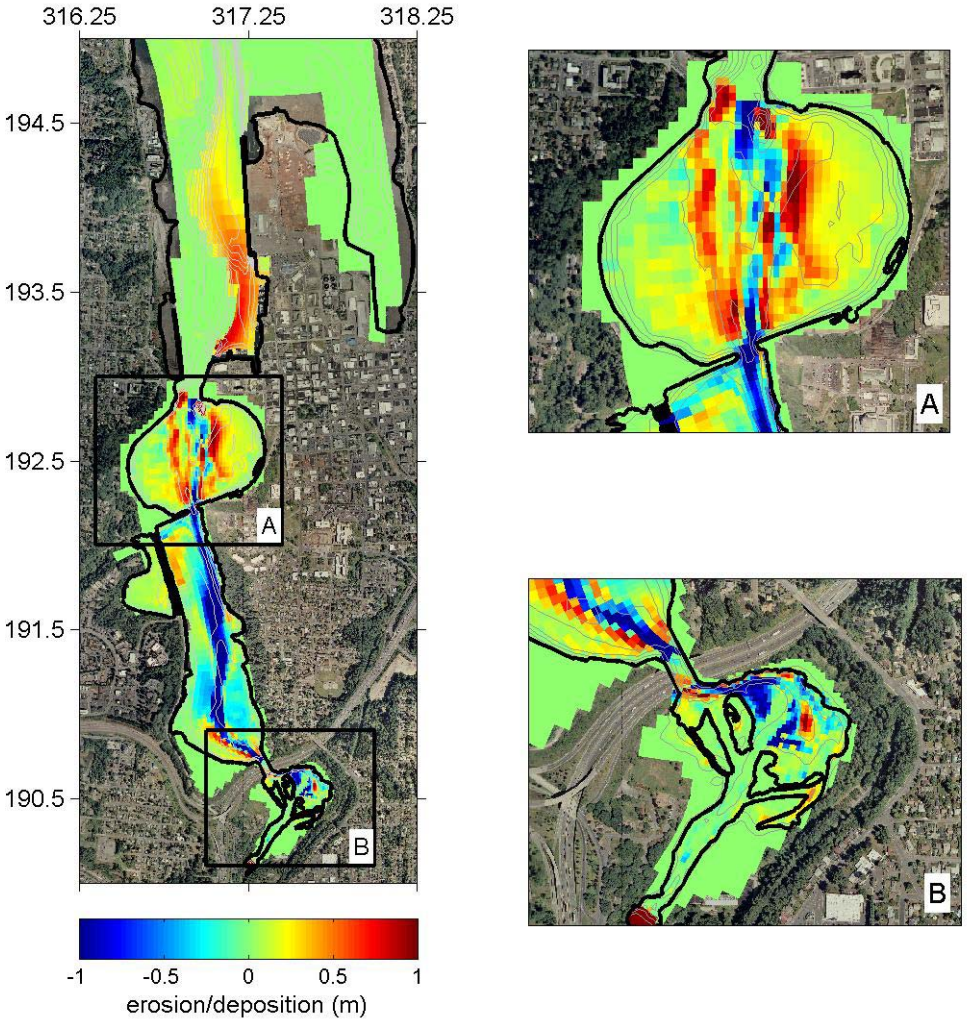

Figure 3.28. Erosion and deposition after the first post-dam year for the Restoration Scenario A estuary under lower erodibility conditions. The axes are in Washington State Plane South (km) and bathymetric contours in 1 m increments. Blues indicate erosion and reds show deposition.

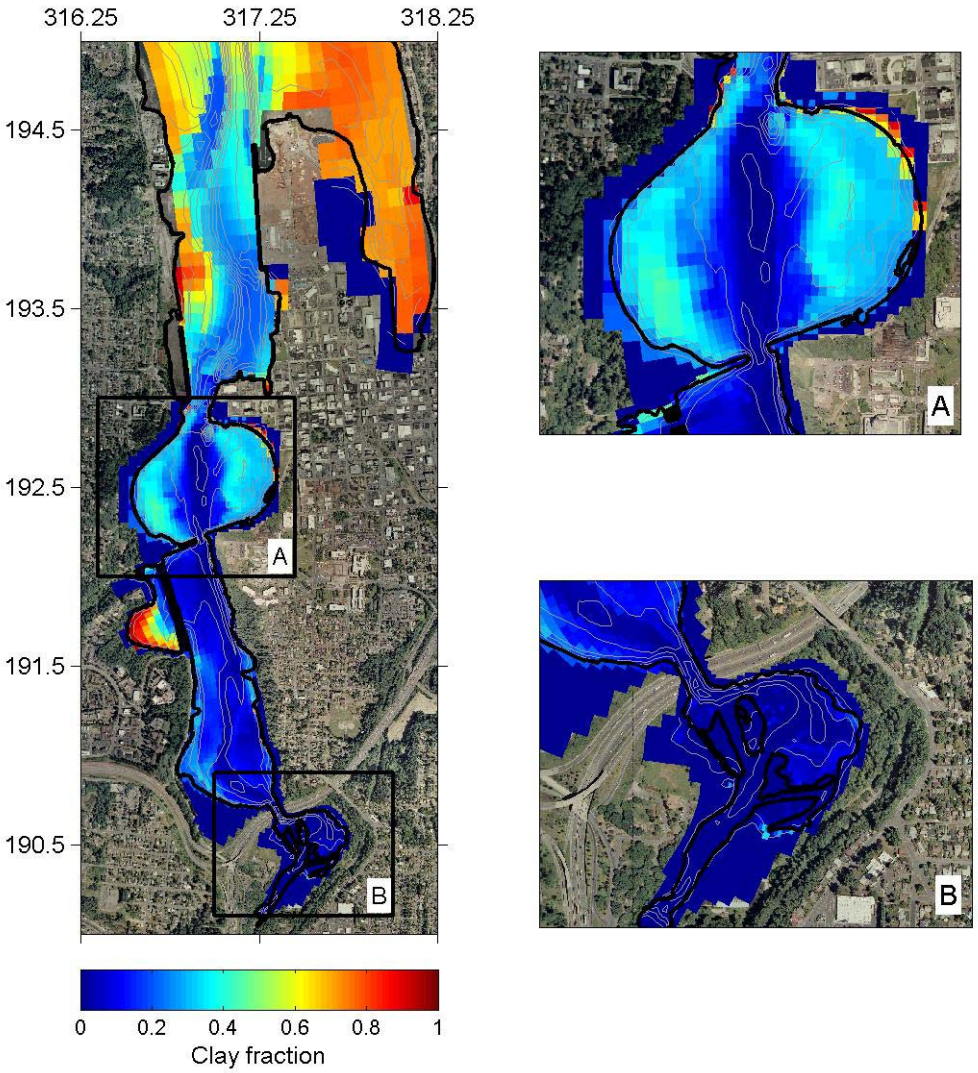

Figure 3.29. Clay fraction distribution after the first post-dam year for the Restoration Scenario A estuary under lower erodibility conditions. The axes are in Washington State Plane South (km) and bathymetric contours in 1 m increments. Blues indicate small and reds show large amounts of clay.

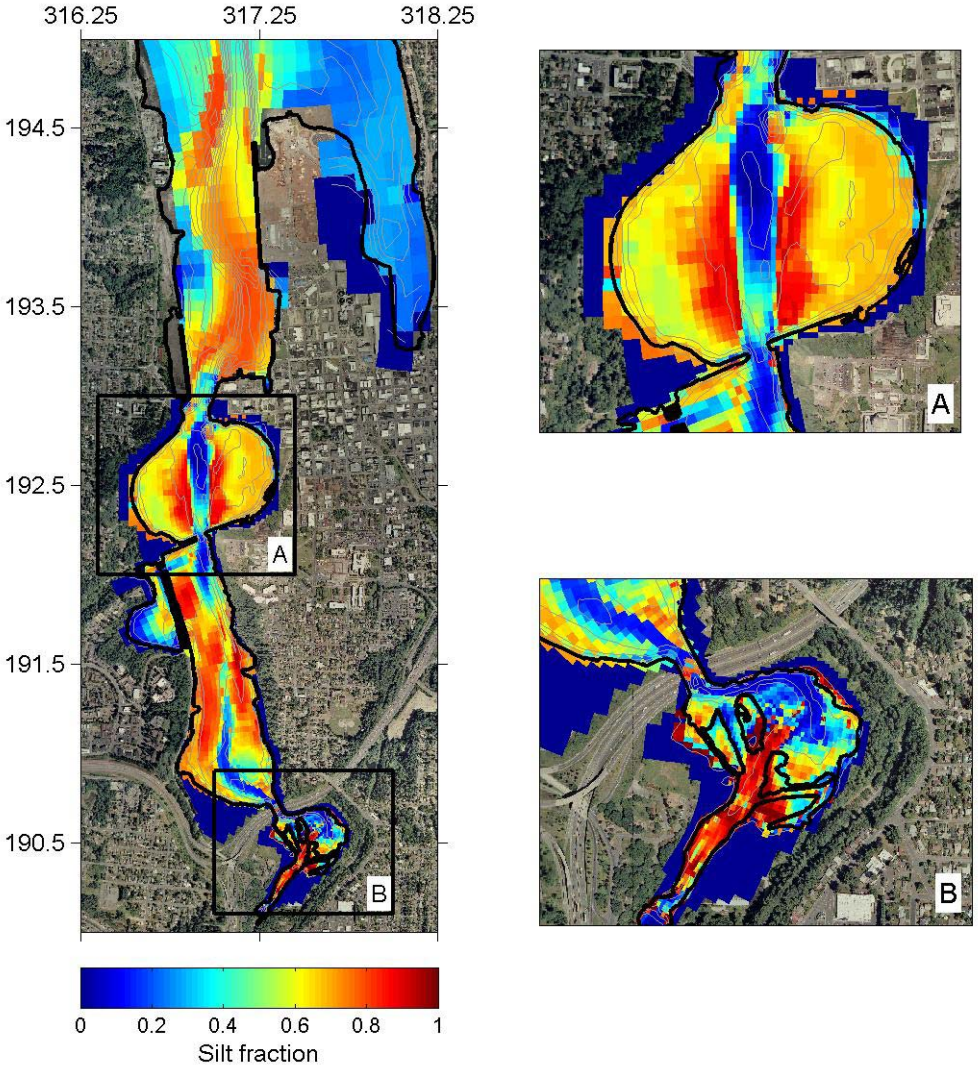

Figure 3.30. Silt fraction distribution after the first post-dam year for the Restoration Scenario A estuary under lower erodibility conditions. The axes are in Washington State Plane South (km) and bathymetric contours in 1 m increments. Blues indicate small and reds show large amounts of silt.

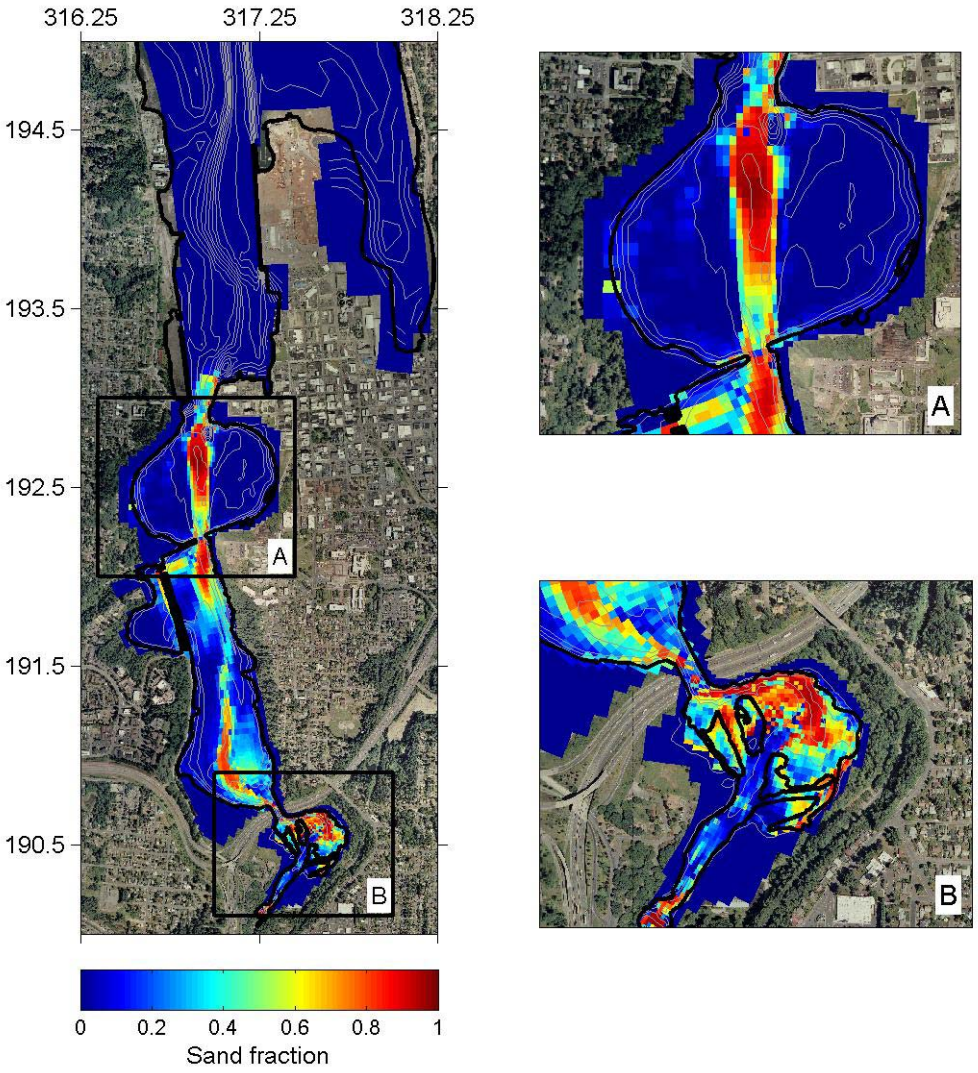

Figure 3.31. Sand fraction distribution after the first post-dam year for the Restoration Scenario A estuary under lower erodibility conditions. The axes are in Washington State Plane South (km) and bathymetric contours in 1 m increments. Blues indicate small and reds show large amounts of sand.

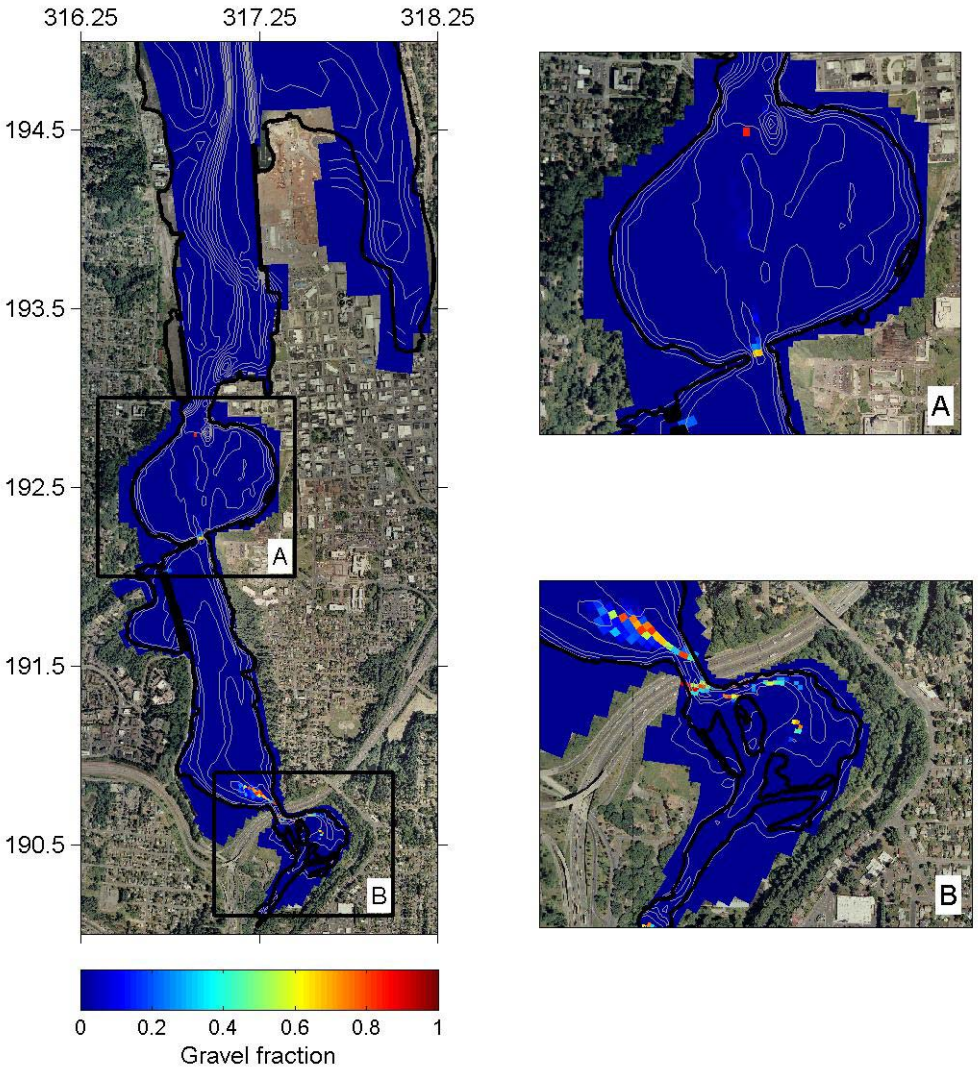

Figure 3.32. Gravel fraction distribution after the first post-dam year for the Restoration Scenario A estuary under lower erodibility conditions. The axes are in Washington State Plane South (km) and bathymetric contours in 1 m increments. Blues indicate small and reds show large amounts of gravel.

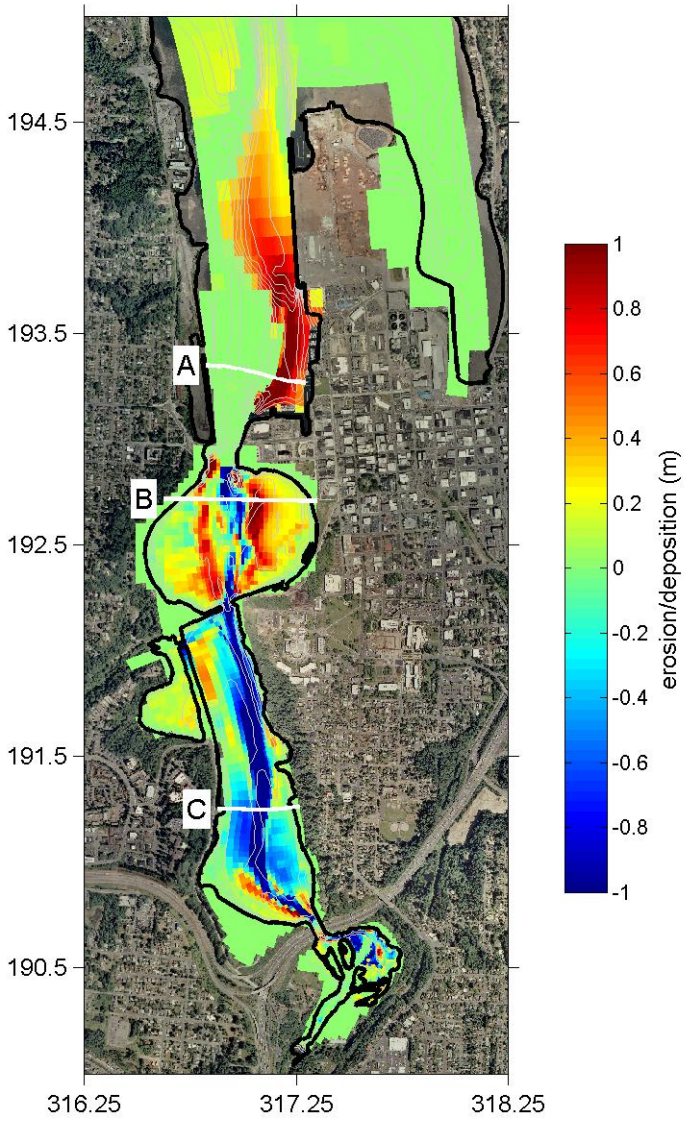

Figure 3.33. Erosion and deposition three years after dam removal for the Restoration Scenario A estuary under lower erodibility conditions. The axes are in Washington State Plane South (km) and bathymetric contours in 1 m increments. Blues indicate erosion and reds show deposition. Cross-estuary transects A, B and C will be examined in subsequent plots.

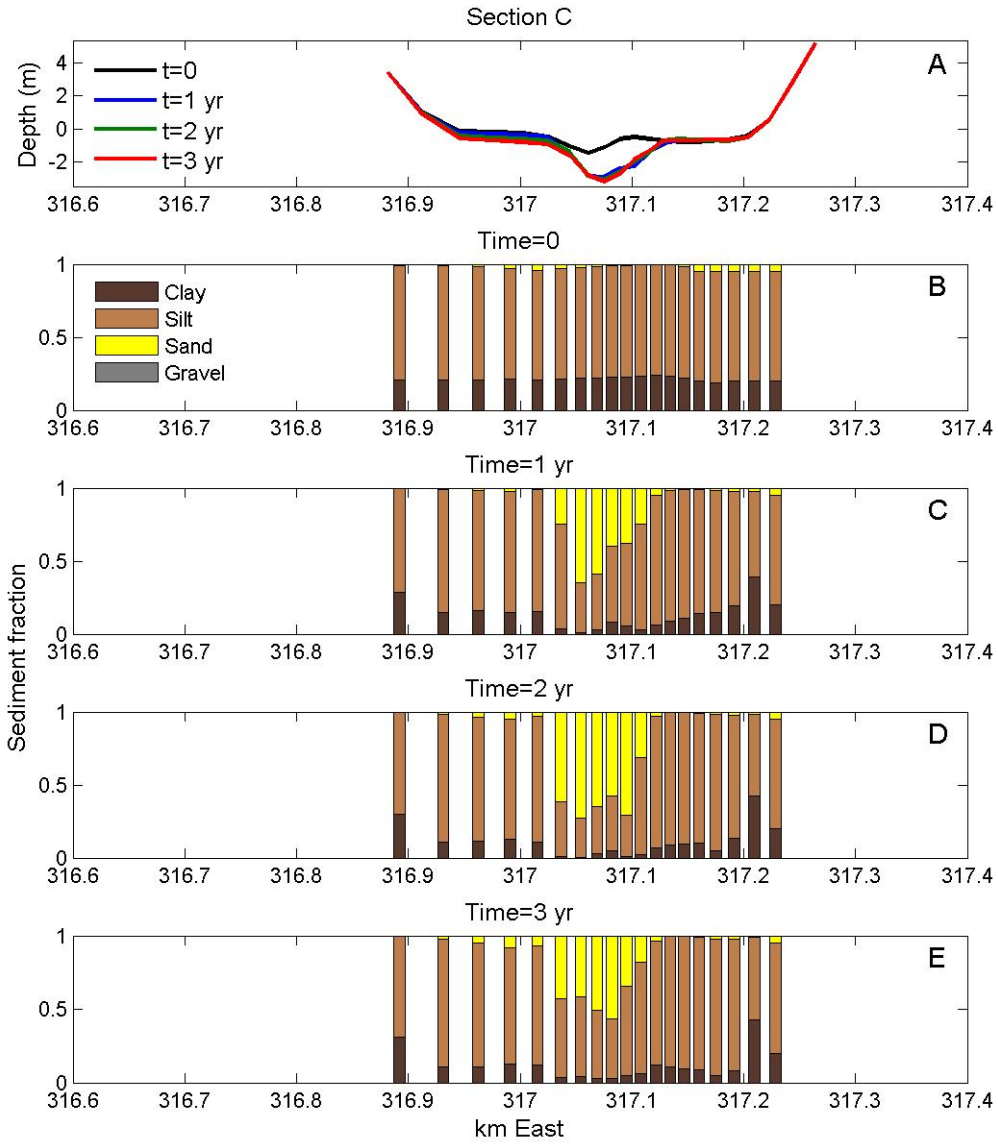

Figure 3.34. Cross-estuary transect Section C for the Restoration Scenario A estuary under lower erodibility conditions. Depth profiles show changes each year (Panel A). Surface sediment grain size fractions for the initial bed (B), first post-dam year (C), second post-dam year (D) and third post-dam year (E) show coarsening of the channel and fining of the flanks.

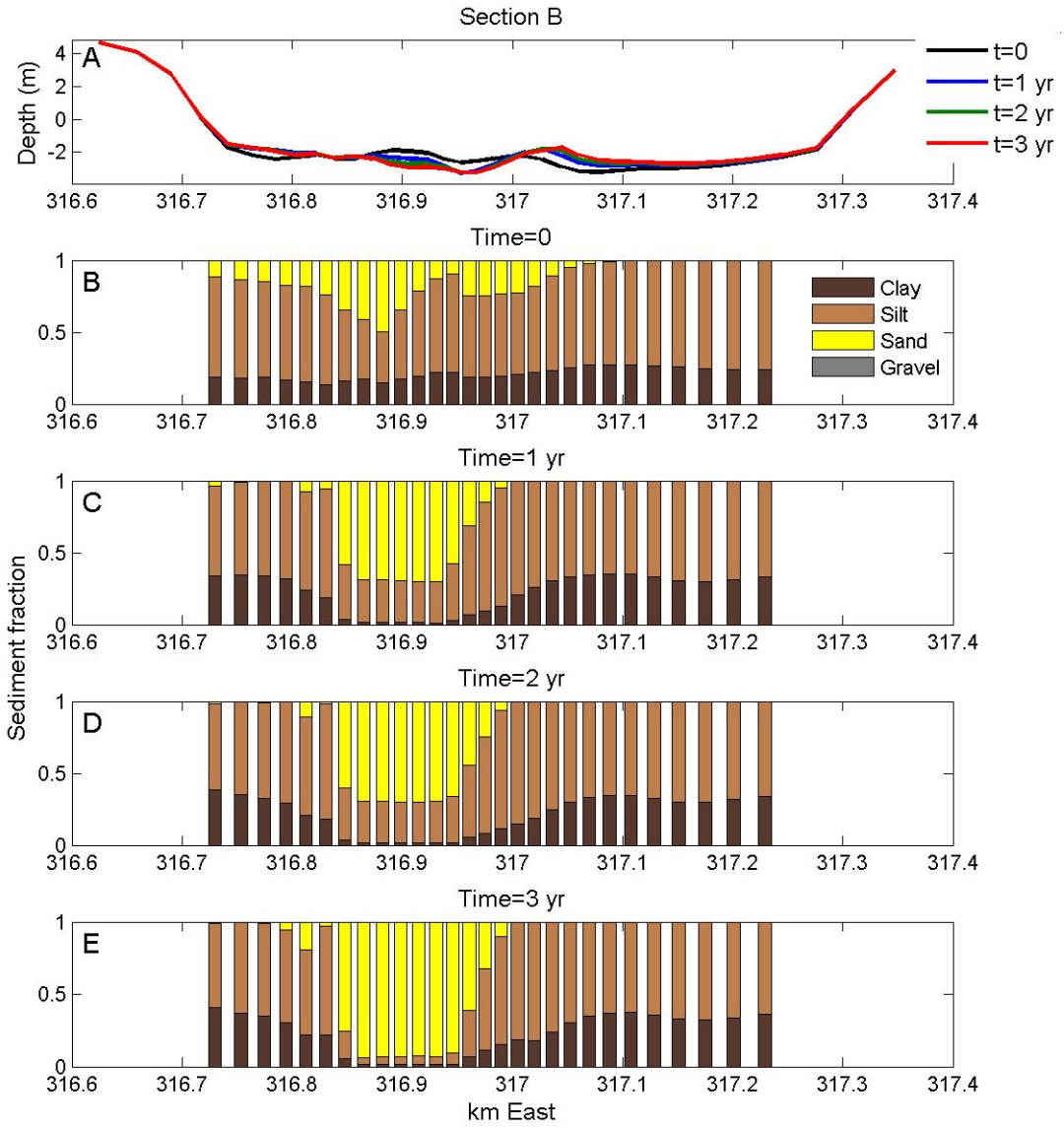

Figure 3.35. Cross-estuary transect Section B for the Restoration Scenario A estuary under lower erodibility conditions. Depth profiles show changes each year (Panel A). Surface sediment grain size fractions for the initial bed (B), first post-dam year (C), second post-dam year (D) and third post-dam year (E) show coarsening of the channel and fining of the flanks.

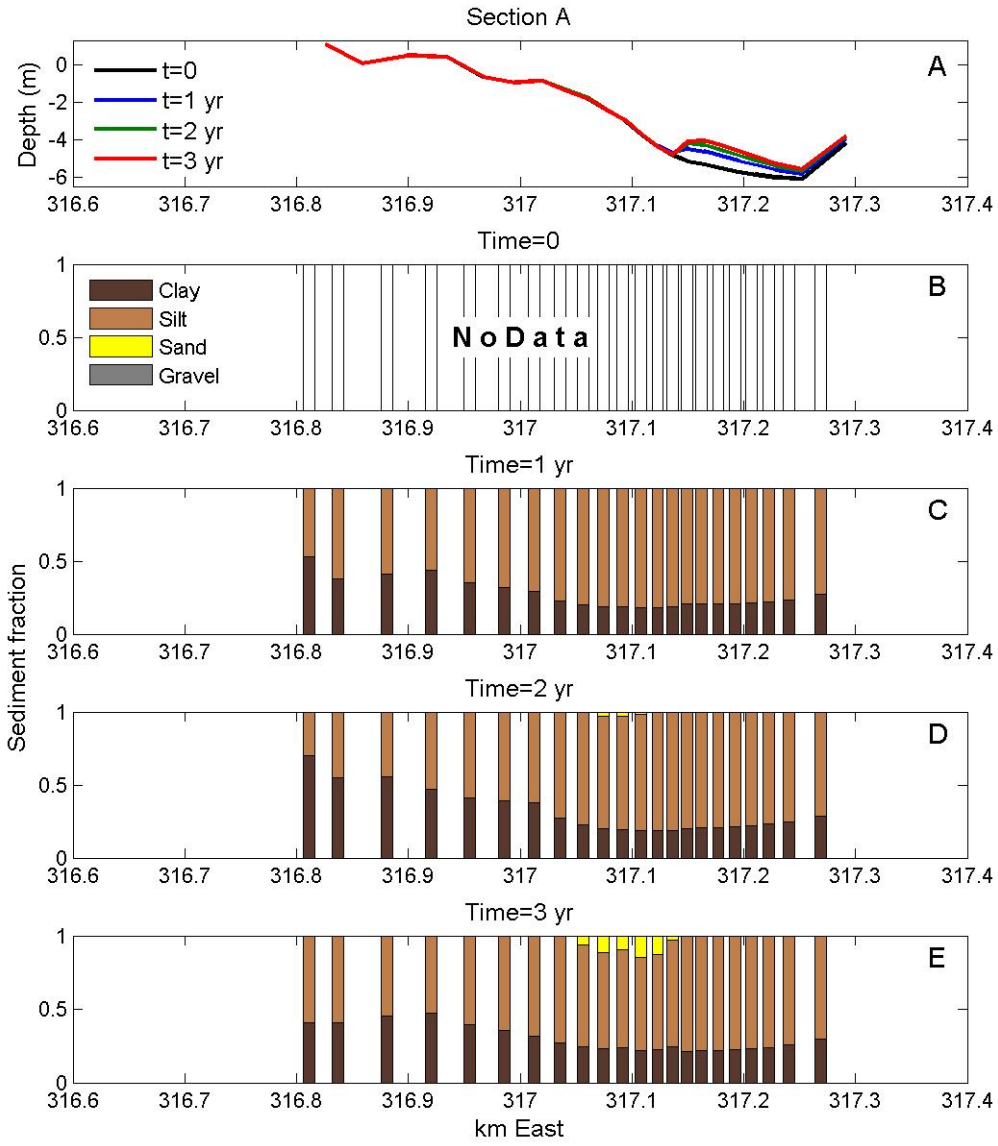

Figure 3.36. Cross-estuary transect Section A for the Restoration Scenario A estuary under lower erodibility conditions. Depth profiles show changes each year (Panel A). No initial surface sediment distribution was designed (B) but sediment grain size fractions for the first post-dam year (C), second post-dam year (D) and third post-dam year (E) show coarsening of the channel and fining of the flanks.

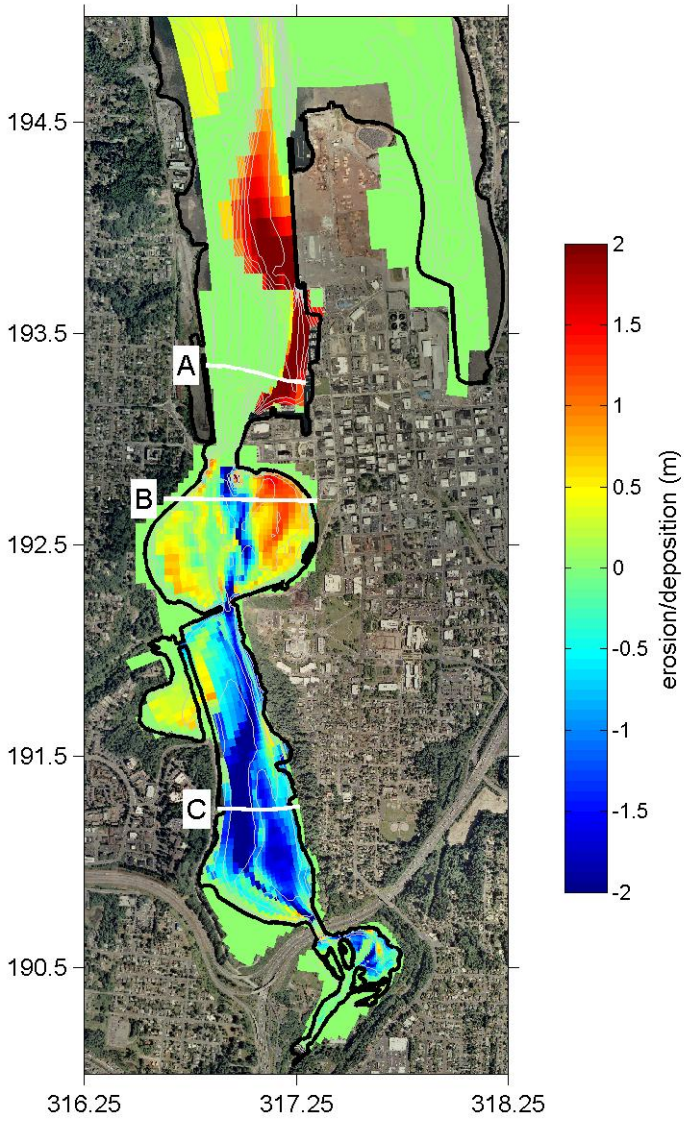

Figure 3.37. Erosion and deposition three years after dam removal for the Restoration Scenario A estuary under higher erodibility conditions. The axes are in Washington State Plane South (km) and bathymetric contours in 1 m increments. Blues indicate erosion and reds show deposition. Cross-estuary transects A, B and C will be examined in subsequent plots.

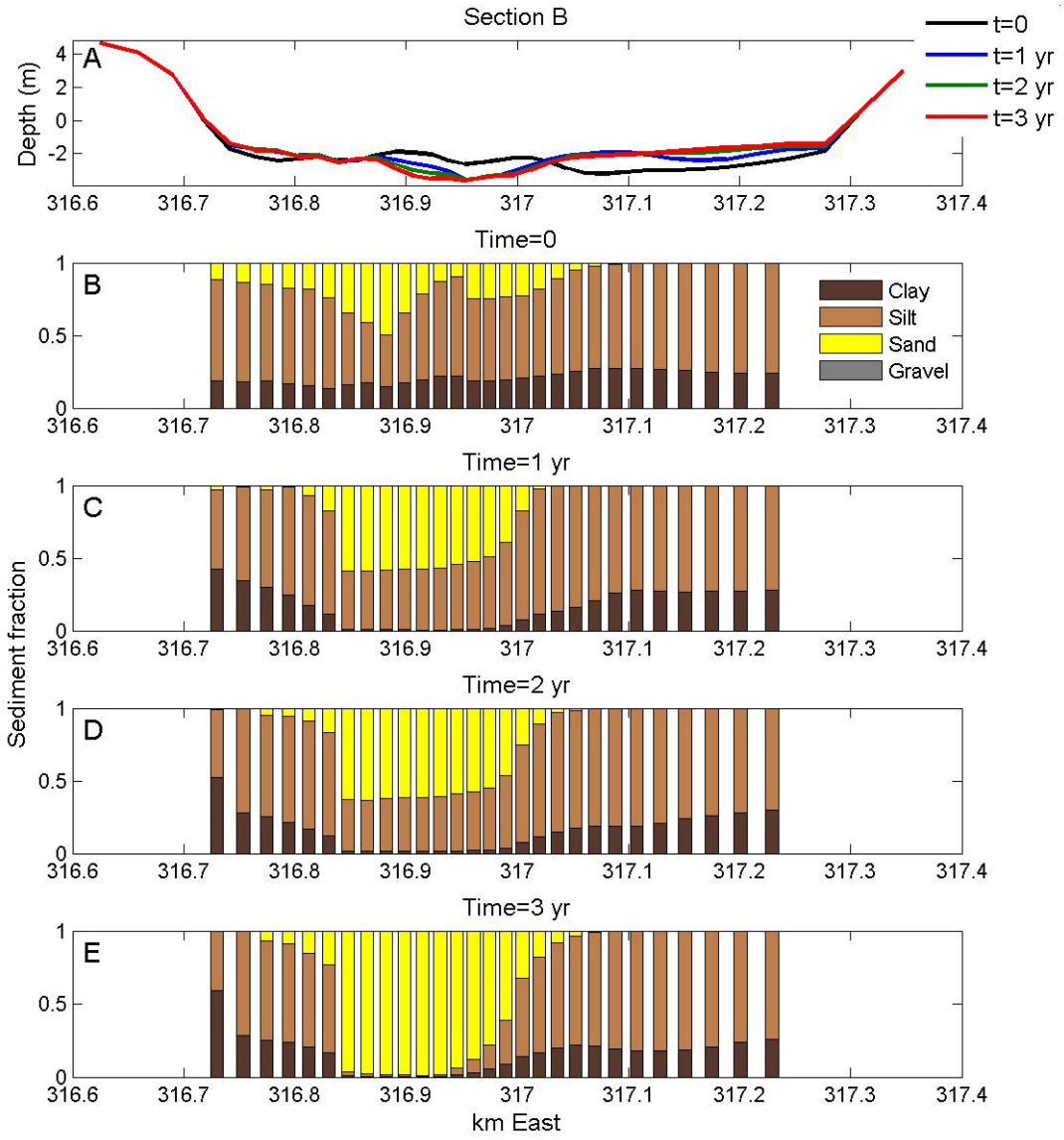

Figure 3.38. Cross-estuary transect Section B for the Restoration Scenario A estuary under higher erodibility conditions. Depth profiles show changes each year (Panel A). Surface sediment grain size fractions for the initial bed (B), first post-dam year (C), second post-dam year (D) and third post-dam year (E) show coarsening of the channel and fining of the flanks.

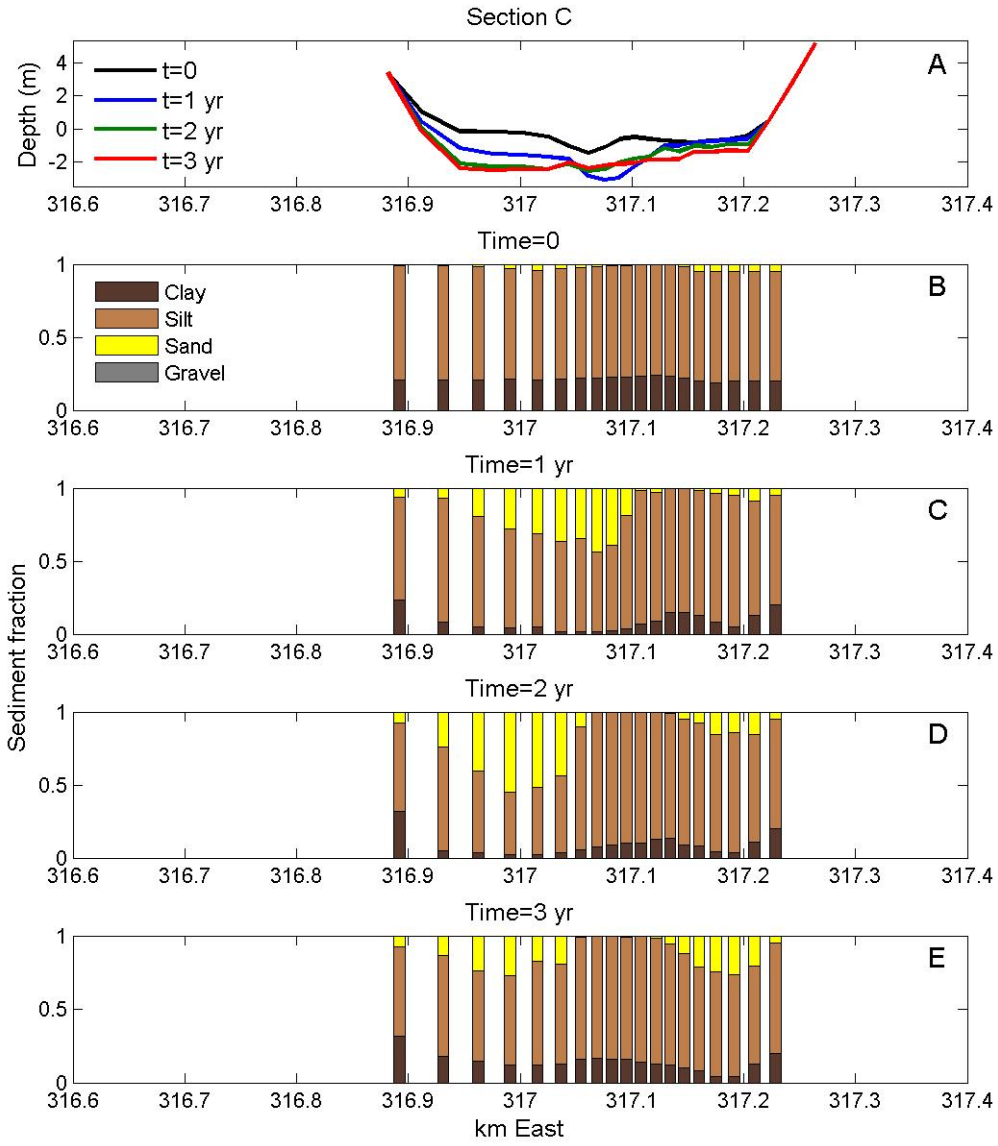

Figure 3.39. Cross-estuary transect Section C for the Restoration Scenario A estuary under higher erodibility conditions. Depth profiles show changes each year (Panel A). Surface sediment grain size fractions for the initial bed (B), first post-dam year (C), second post-dam year (D) and third post-dam year (E) show coarsening of the channel and fining of the flanks.

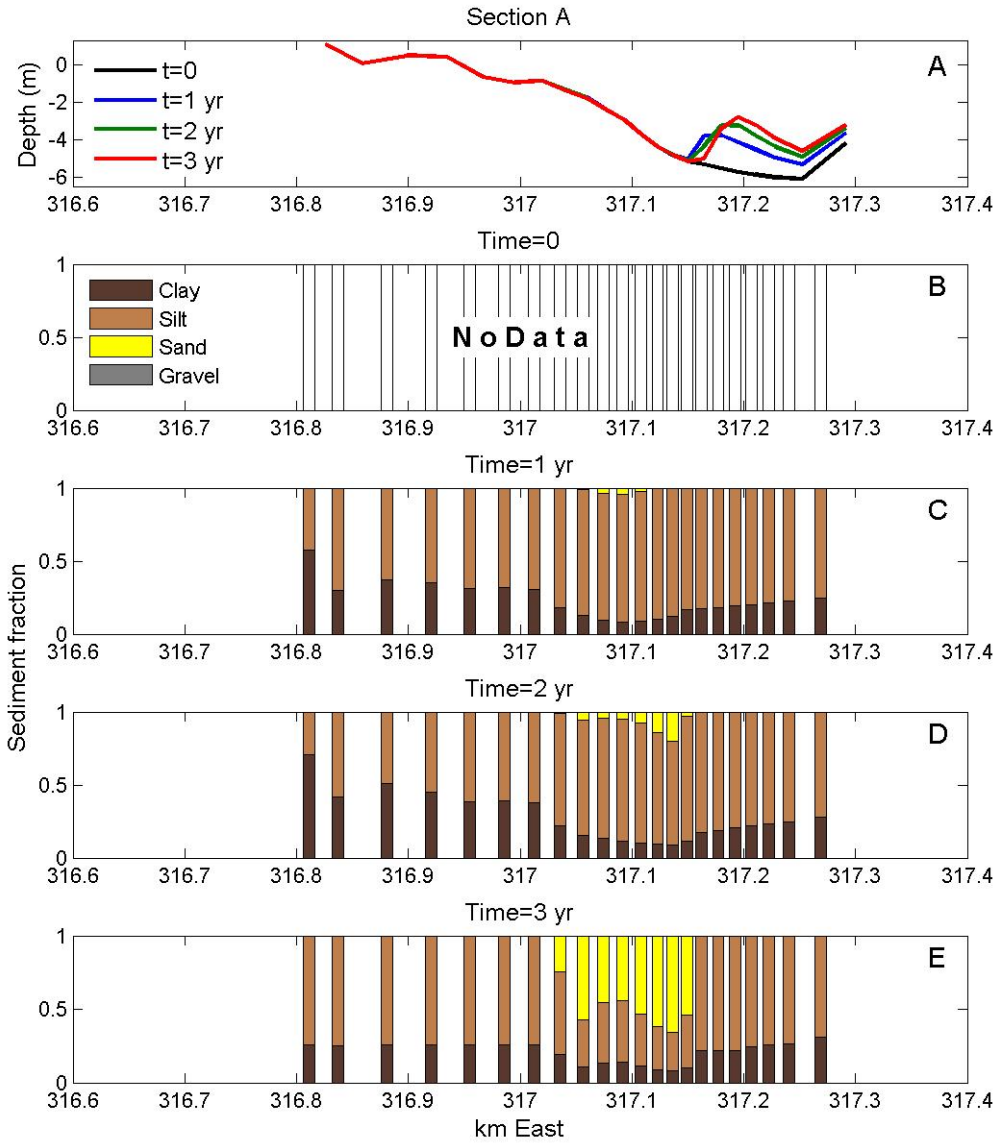

Figure 3.40. Cross-estuary transect Section A for the Restoration Scenario A estuary under higher erodibility conditions. Depth profiles show changes each year (Panel A). No initial surface sediment distribution was designed (B) but sediment grain size fractions for the first post-dam year (C), second post-dam year (D) and third post-dam year (E) show coarsening of the channel and fining of the flanks.

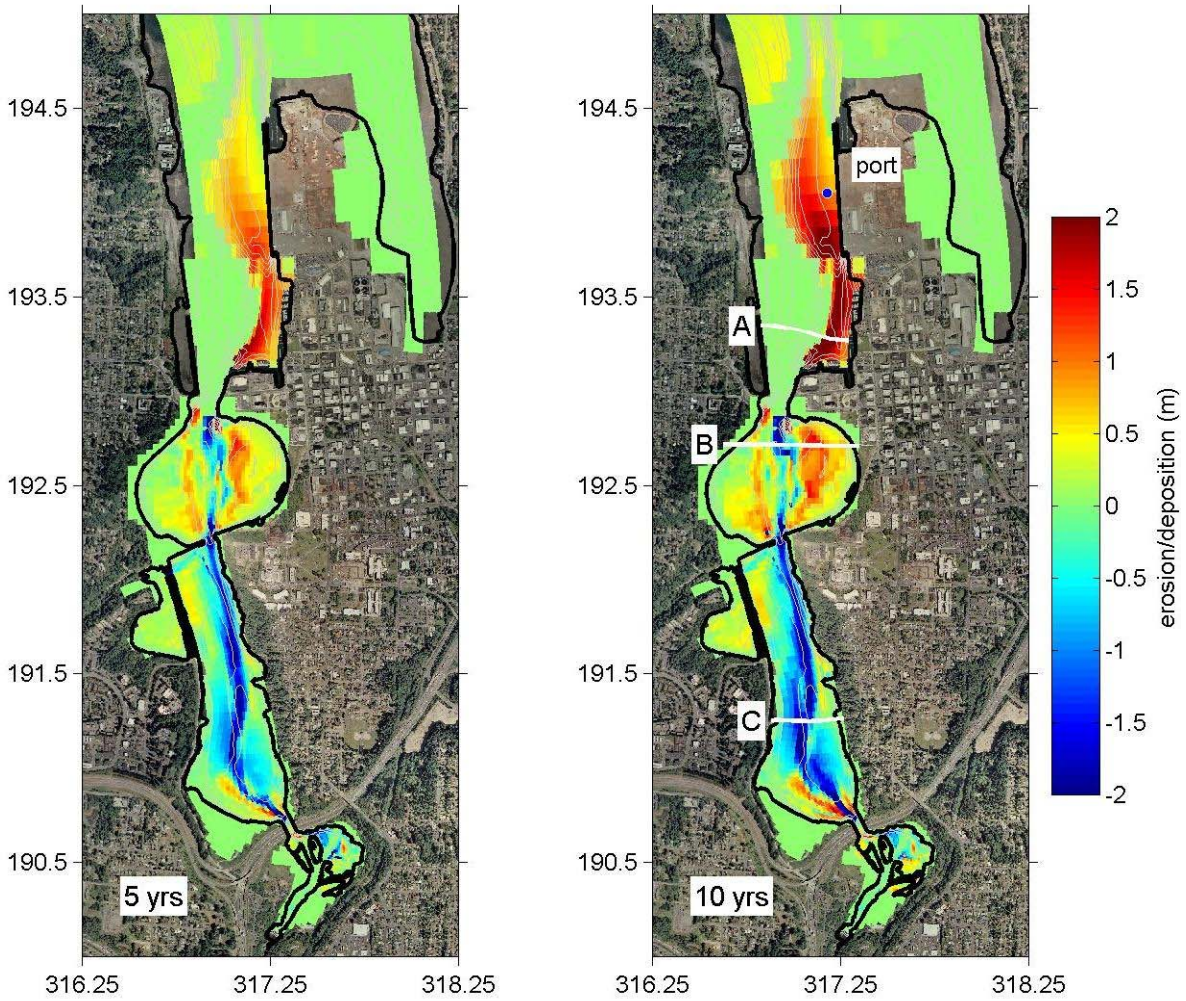

Figure 3.41. Erosion and deposition five and 10 years after dam removal for the Restoration Scenario A estuary under lower erodibility conditions with a lower density of mud. Blues indicate erosion and reds show deposition.

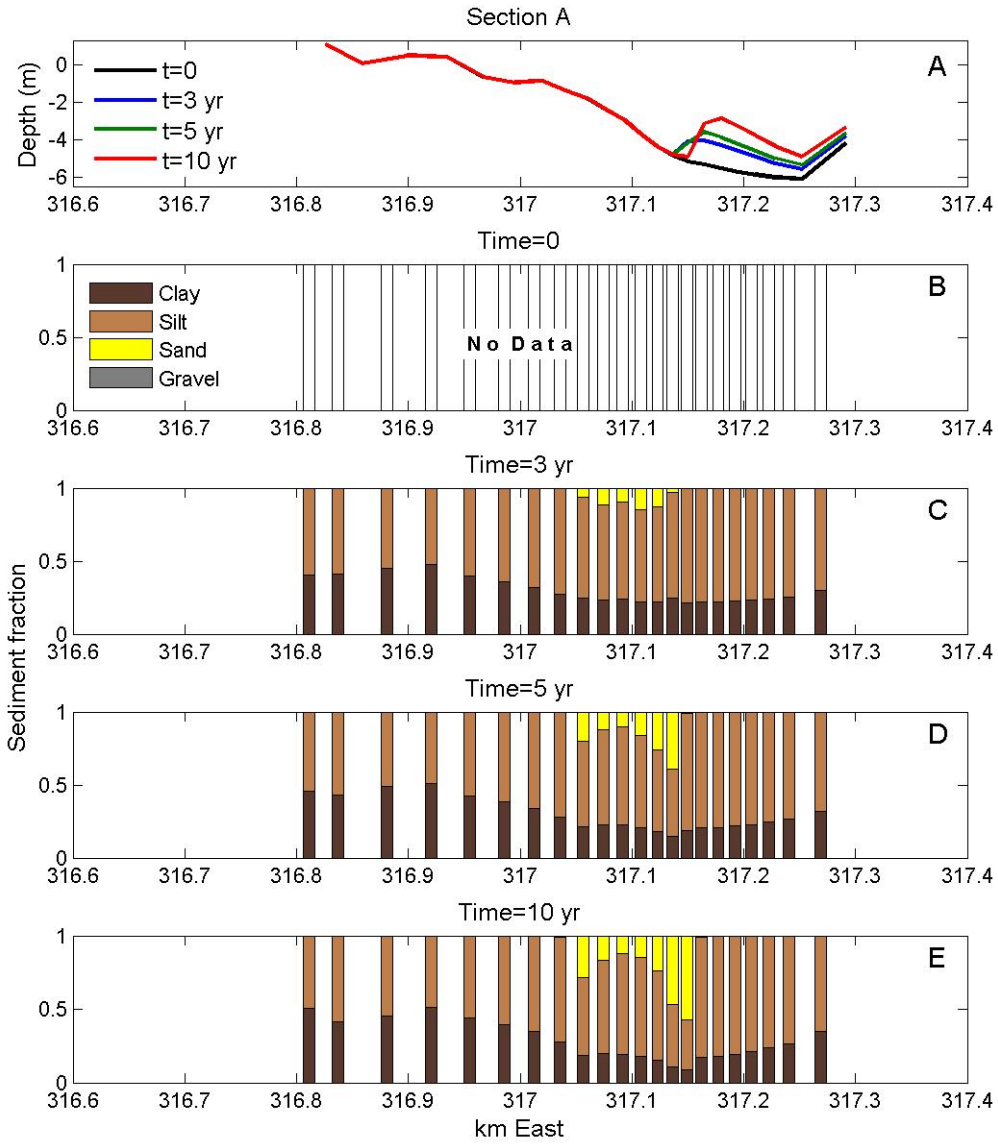

Figure 3.42. Cross-estuary transect Section A for the Restoration Scenario A estuary under lower erodibility conditions with a lower density of mud. Depth profiles show changes each year (Panel A). No initial surface sediment distribution was designed (B) but sediment grain size fractions for the third post-dam year (C), fifth post-dam year (D) and tenth post-dam year (E) show coarsening of the channel.

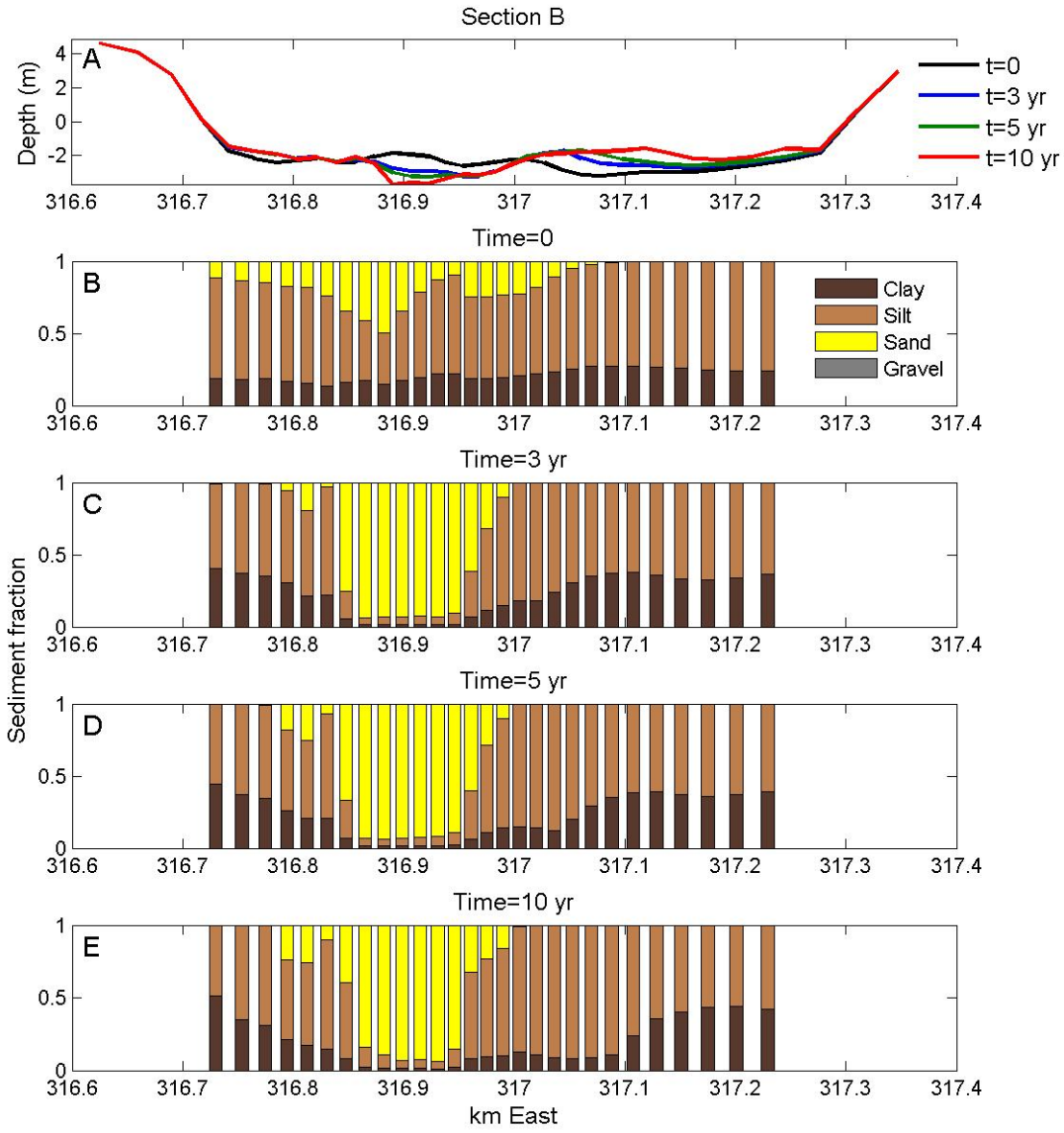

Figure 3.43. Cross-estuary transect Section B for the Restoration Scenario A estuary under lower erodibility conditions with a lower density of mud. Depth profiles show changes each year (Panel A). Surface sediment grain size fractions for the initial bed (B), third post-dam year (C), fifth post-dam year (D) and tenth post-dam year (E) show coarsening of the channel and fining of the flanks.

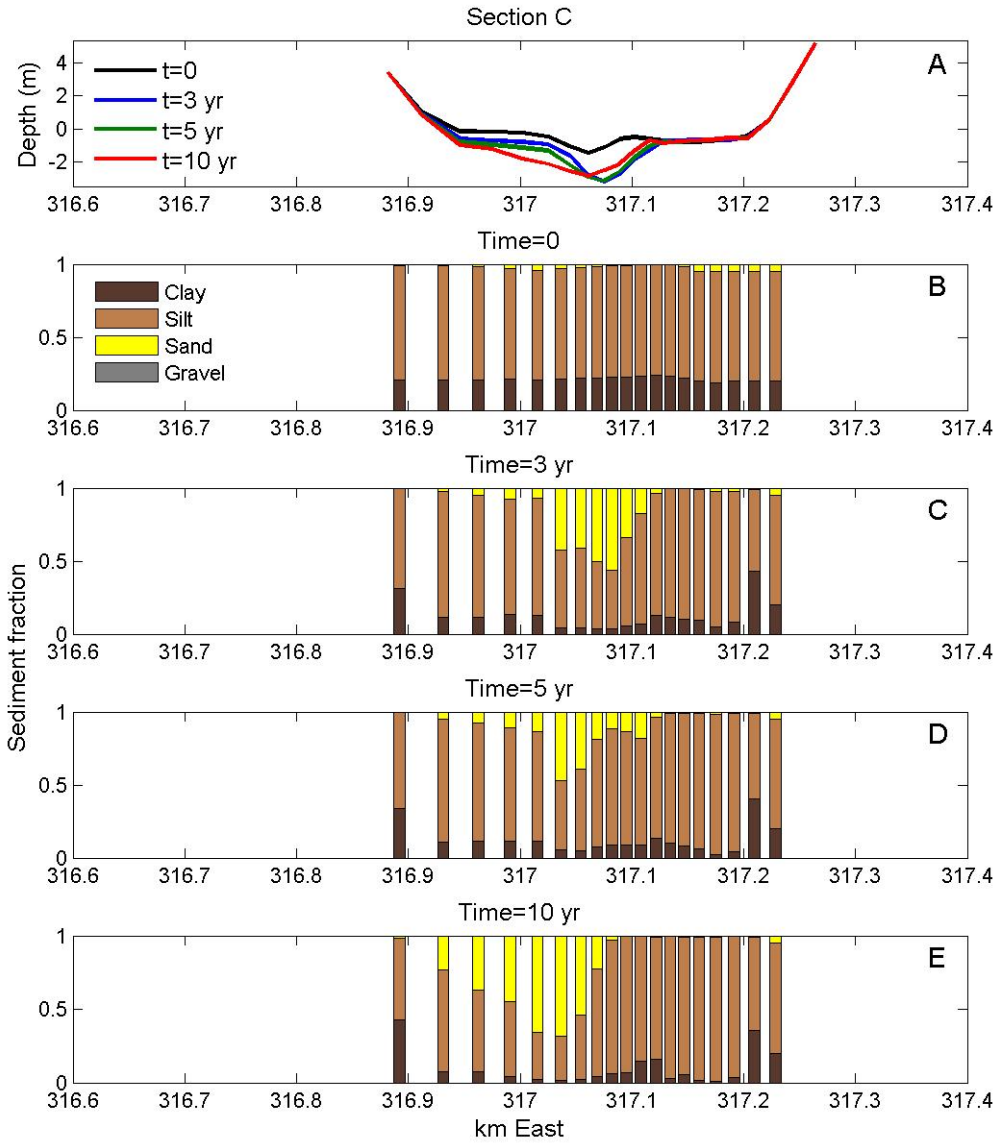

Figure 3.44. Cross-estuary transect Section C for the Restoration Scenario A estuary under lower erodibility conditions with a lower density of mud. Depth profiles show changes each year (Panel A). Surface sediment grain size fractions for the initial bed (B), third post-dam year (C), fifth post-dam year (D) and tenth post-dam year (E) show coarsening of the channel and fining of the flanks.

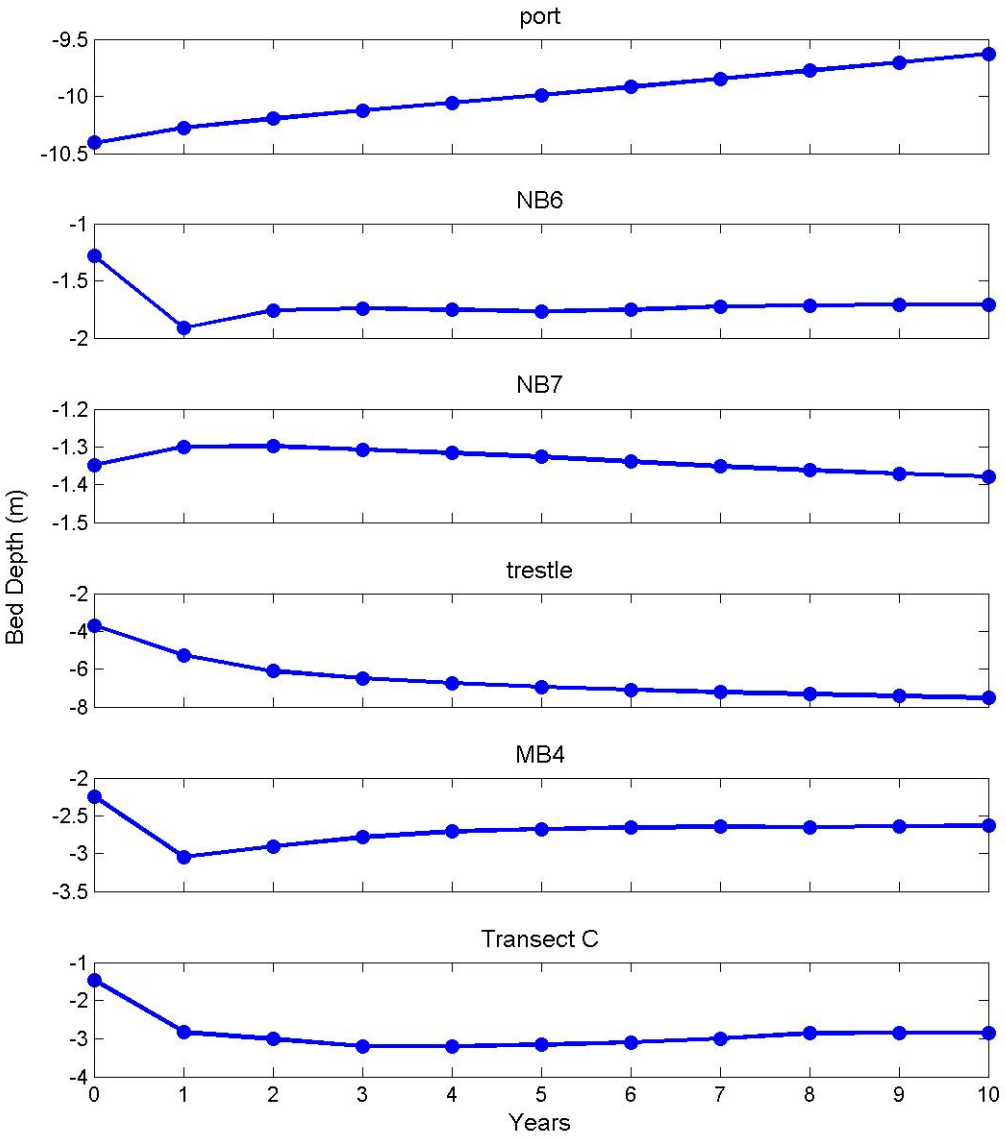

Figure 3.45. Bed depth at selected stations for the Restoration Scenario A estuary under lower erodibility conditions with a lower density of mud (scales vary by station). See Figures 3.27 and 3.41 for locations. The depth of the deepest point along Transect C is monitored in the final panel. With the exception of the port, most changes to the stations' bed depth occur within the first two to four years. The trestle shows the largest change while the flanks of North Basin (NB7) show the least.

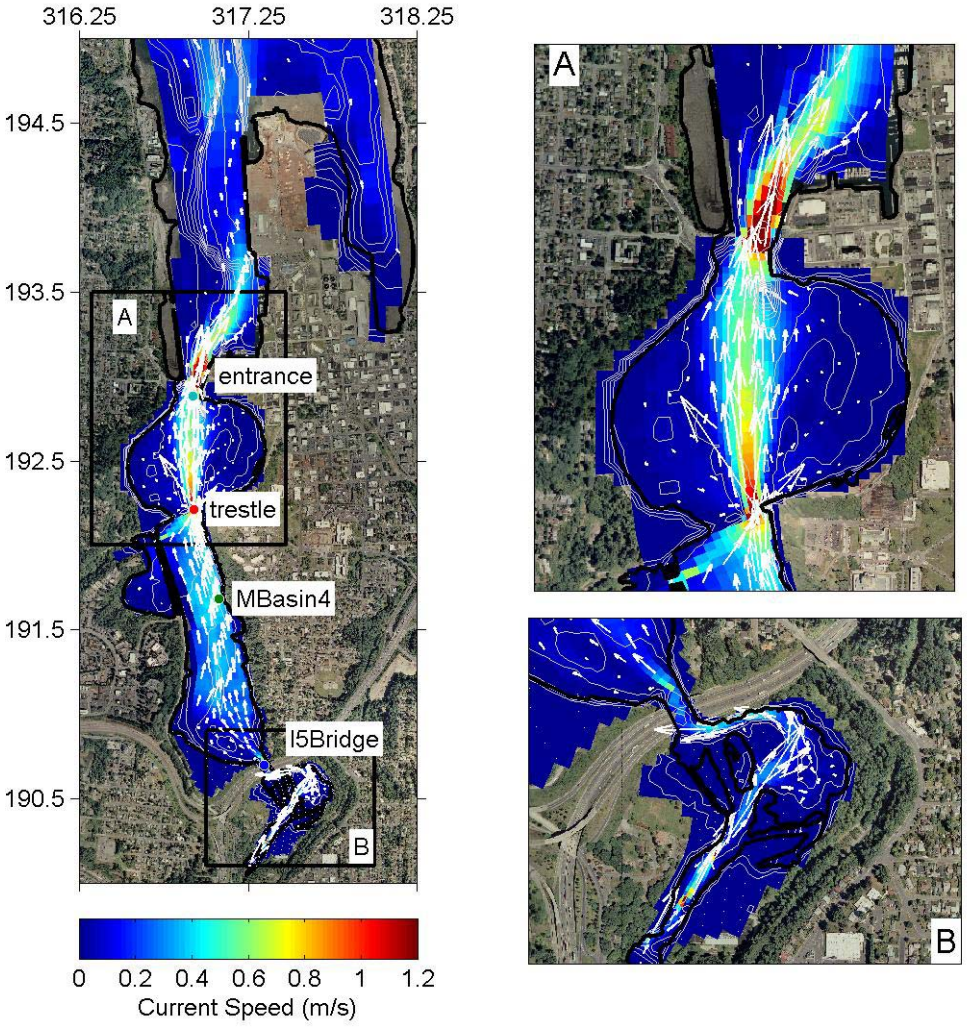

Figure 3.46. Maximum velocity magnitude and vectors during low river flow at ebb tide for the Restoration Scenario B estuary. The axes are in Washington State Plane South (km) and bathymetric contours in 1 m increments. Blues indicate slow velocities and reds show the fastest speeds. The fastest currents are observed through the entrance while speeds decrease in Middle Basin. The wider trestle opening shows velocities of approximately 0.5 m/s. Speeds under the I-5 bridge are less than 0.5 m/s.

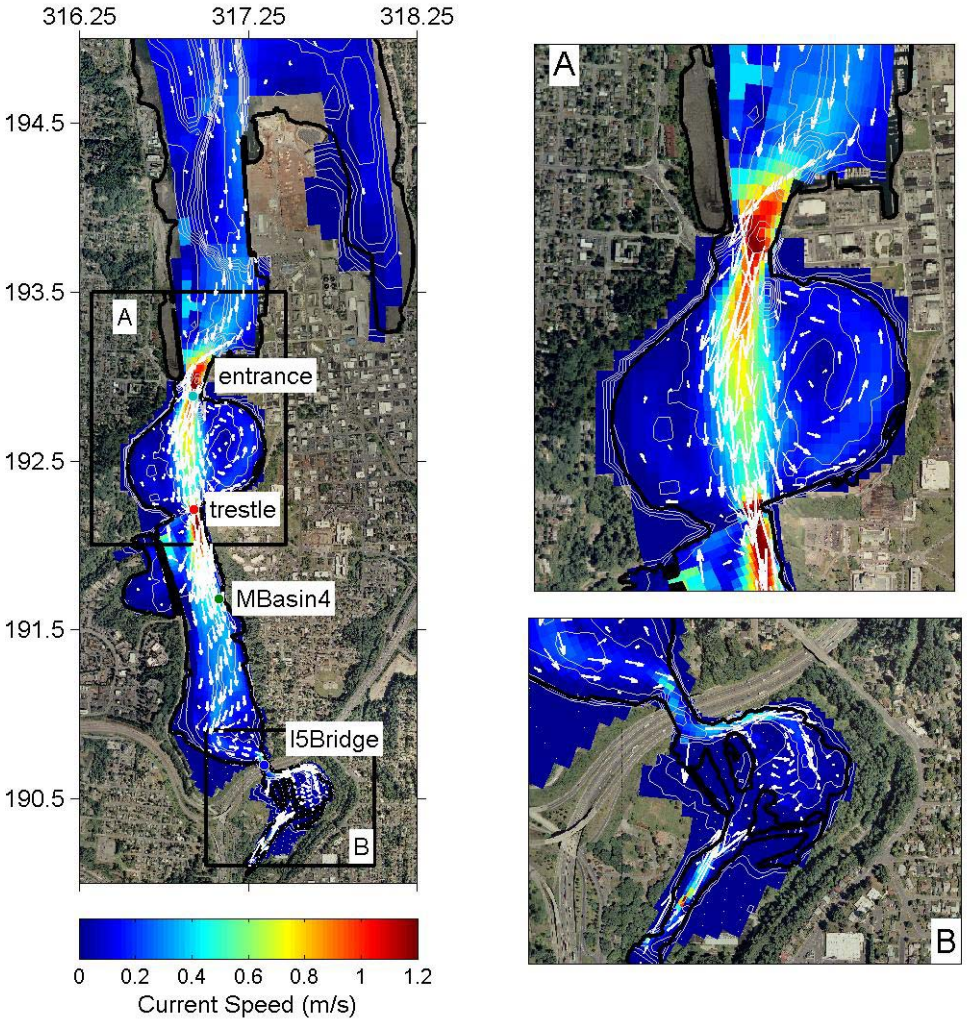

Figure 3.47. Maximum velocity magnitude and vectors during low river flow at flood tide for the Restoration Scenario B estuary. The axes are in Washington State Plane South (km) and bathymetric contours in 1 m increments. Blues indicate slow velocities and reds show the fastest speeds. The fastest currents are observed through the entrance while speeds decrease in Middle Basin. The wider trestle opening shows velocities of approximately 0.5 m/s. Speeds under the I-5 bridge are less than 0.5 m/s.

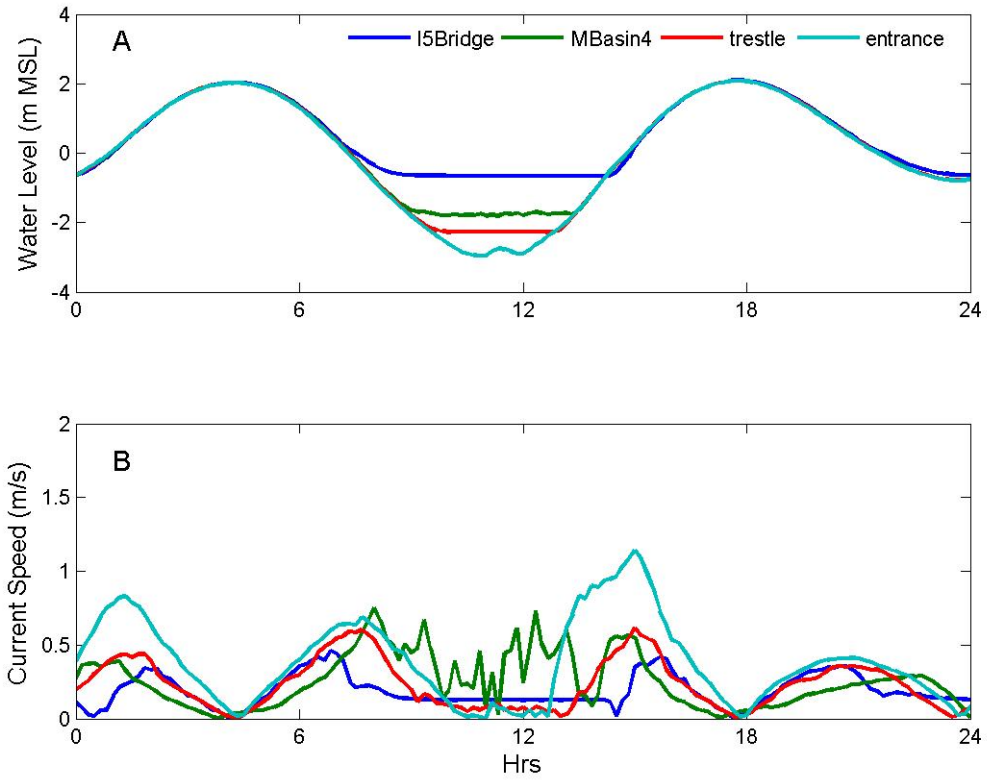

Figure 3.48. Water level and current speed at four stations during the low river flow for the Restoration Scenario B estuary. See Figure 3.12 for locations of the stations. The fastest velocities are observed halfway between slack tides and the slowest are seen at high or low tide.

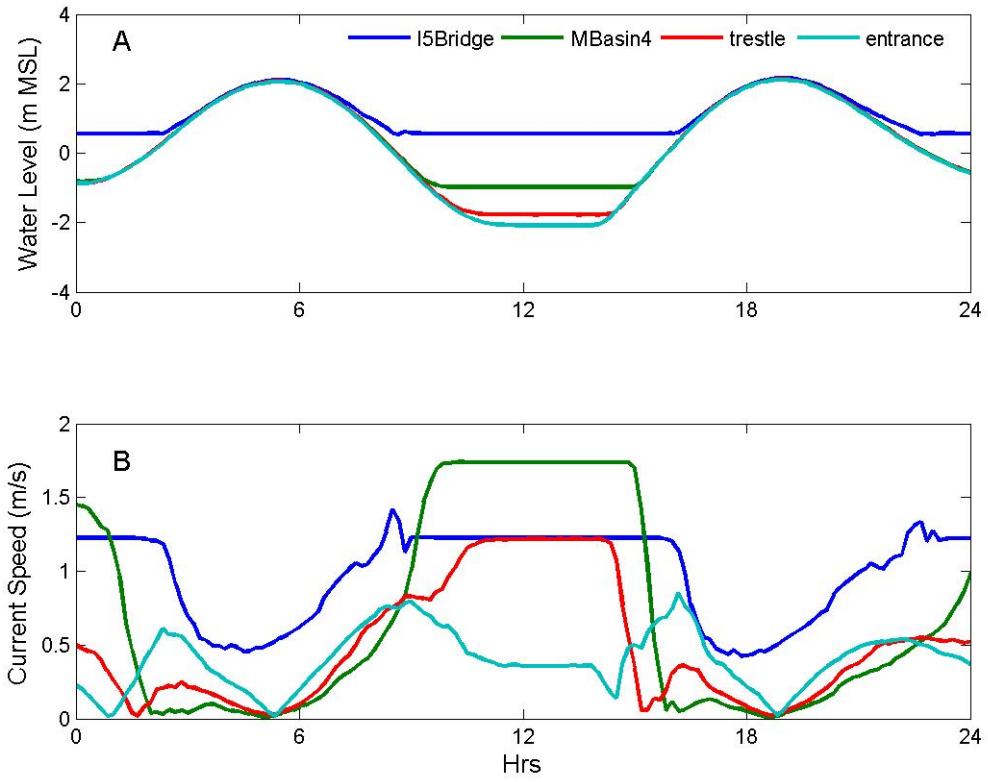

Figure 3.49. Water level and current speed at four stations during the high river flow for the Restoration Scenario B estuary. See Figure 3.12 for locations of the stations. Faster velocities are observed halfway between slack tides and the slowest are seen at high tide. During low tide, the river flow dominates the velocity magnitude signal with a constant speed.

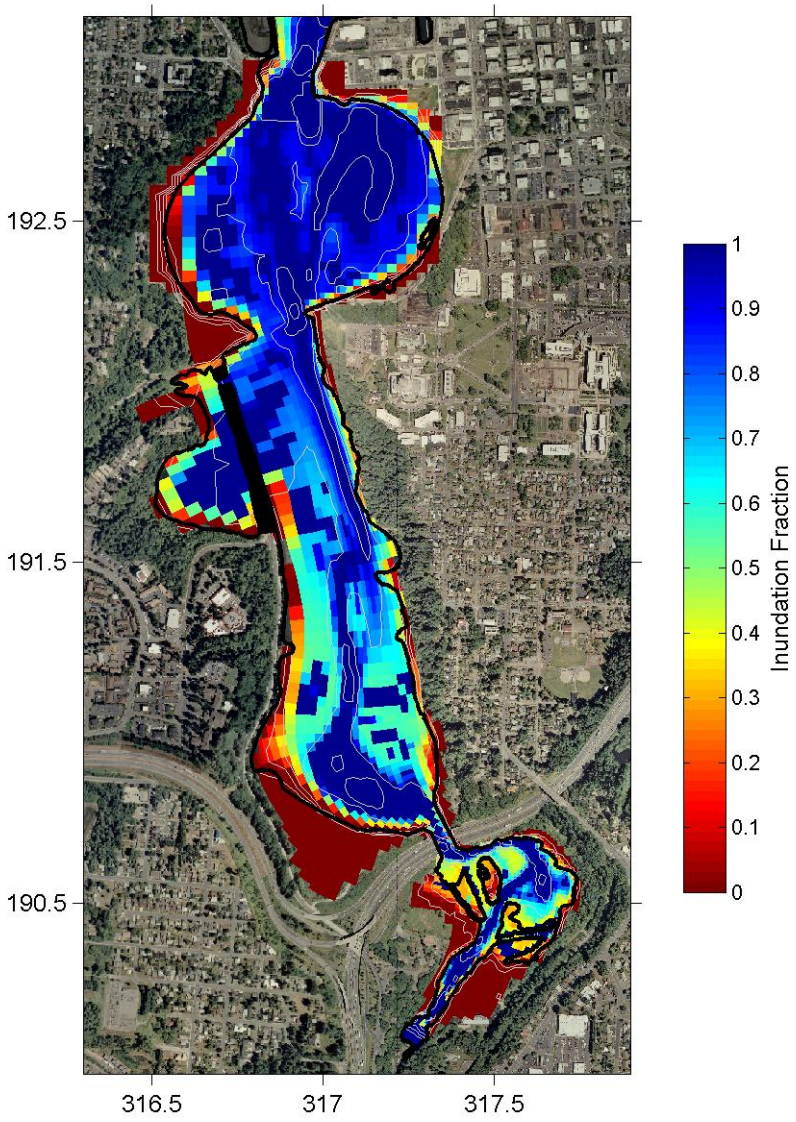

Figure 3.50. Annual mean inundation fraction for the Restoration Scenario B estuary. Blues indicate continuous submersion and reds show continuous exposure. The main channel, North Basin and part of Middle Basin appear to be underwater at least 80% of the year while elevations above 2 m are wet less than 50% of the time. Portions of the South Basin islands get submerged about 30 – 40% of the year.

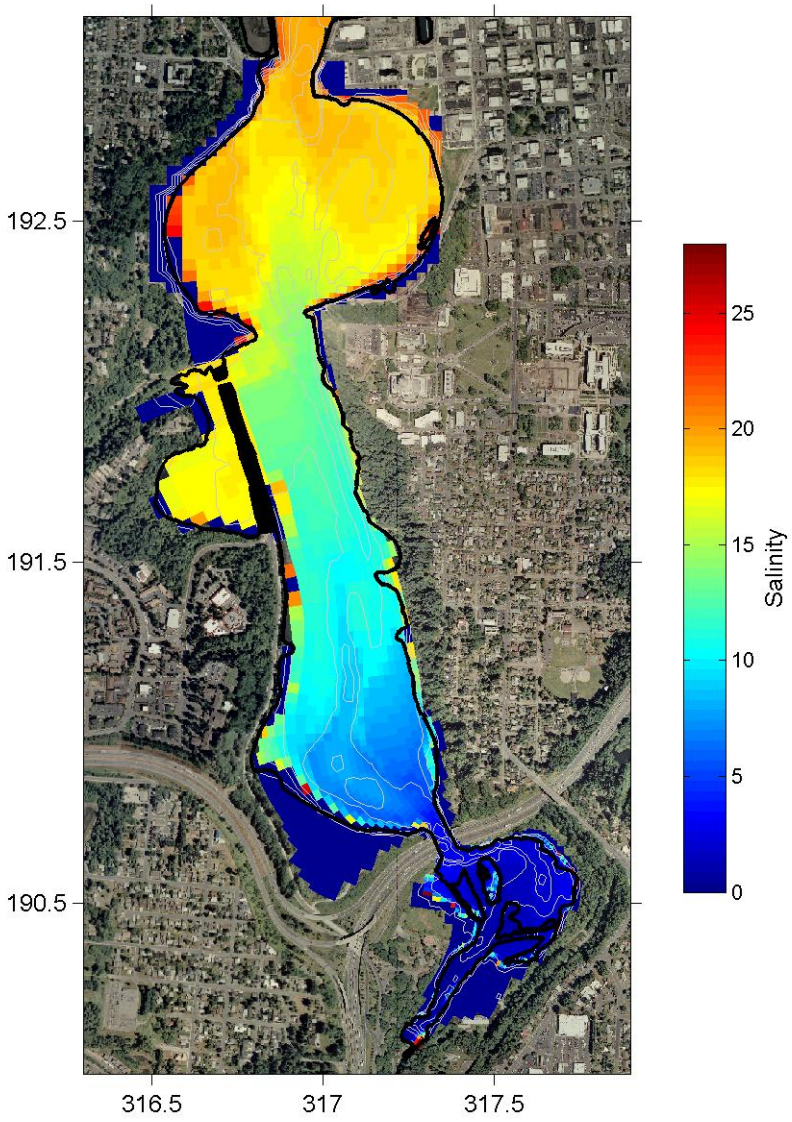

Figure 3.51. Annual mean near-bed salinity for the Restoration Scenario B estuary. Blues indicate freshwater and reds show the most saline water. A steady salinity gradient is observed from freshwater at the river mouth to approximately 15 ppt at the trestle. Percival Cove is saltier than Middle Basin, possibly due to the limited influx of freshwater into the cove from Middle Basin and the absence of Percival Creek in the model. North Basin shows an intrusion of 15 – 18 ppt water into a fairly uniform basin of 18 – 20 ppt brackish water.

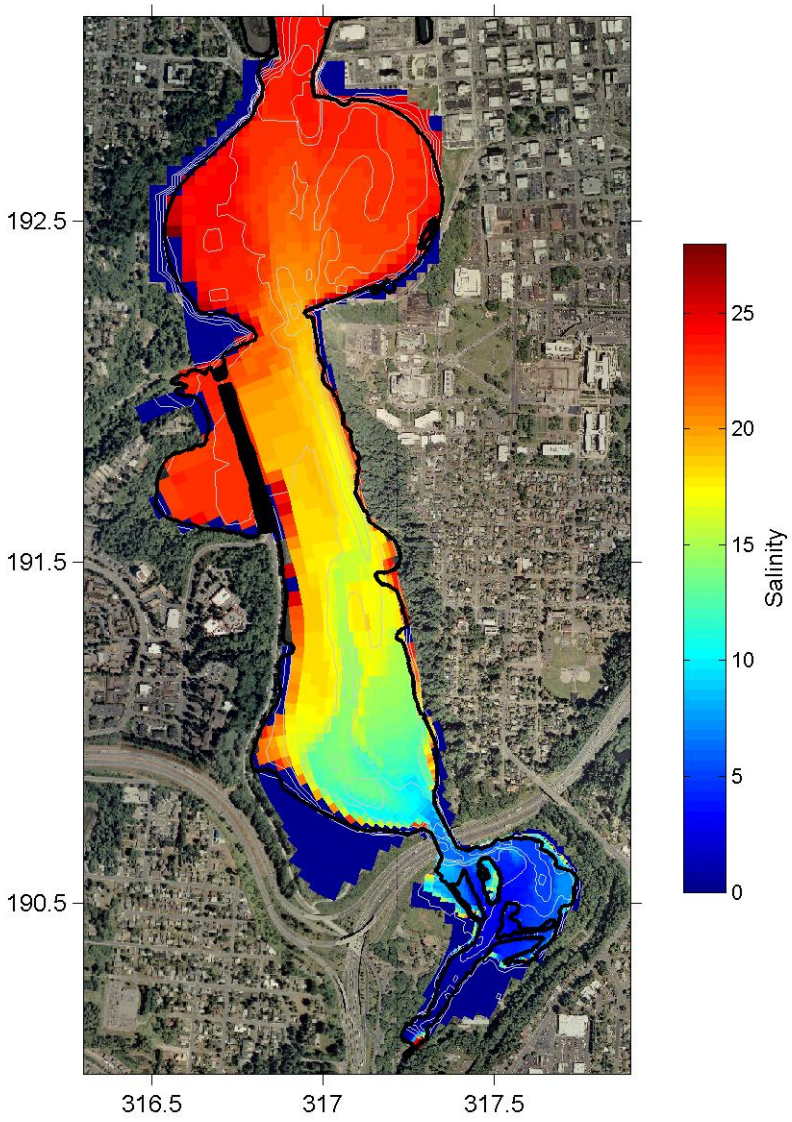

Figure 3.52. Dry season mean near-bed salinity for the Restoration Scenario B estuary. Blues indicate freshwater and reds show the most saline water. South Basin remains mostly fresh and Middle Basin contains water with salinities from 10 – 20 ppt. The main channel is fresher than the flanks in the center of the basin while salinities in Percival Cove and North Basin are almost uniformly above 20 ppt.

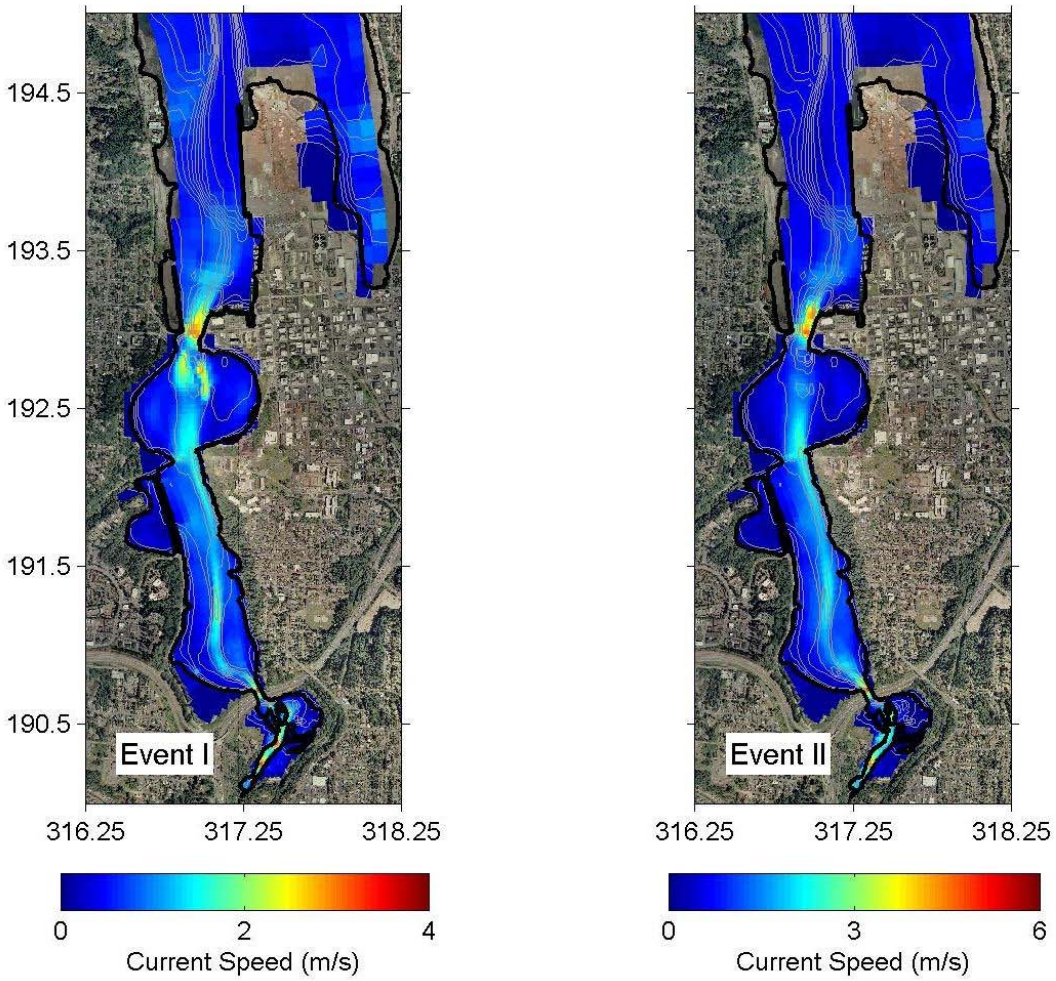

Figure 3.53. Maximum velocities for Events I and II in the Restoration Scenario B estuary. Blues are slower speeds and reds are faster (scales vary by event). Velocity magnitudes are largest immediately north of the estuary and under the I-5 bridge. The wider trestle shows slower velocities than observed in Restoration Scenario A.

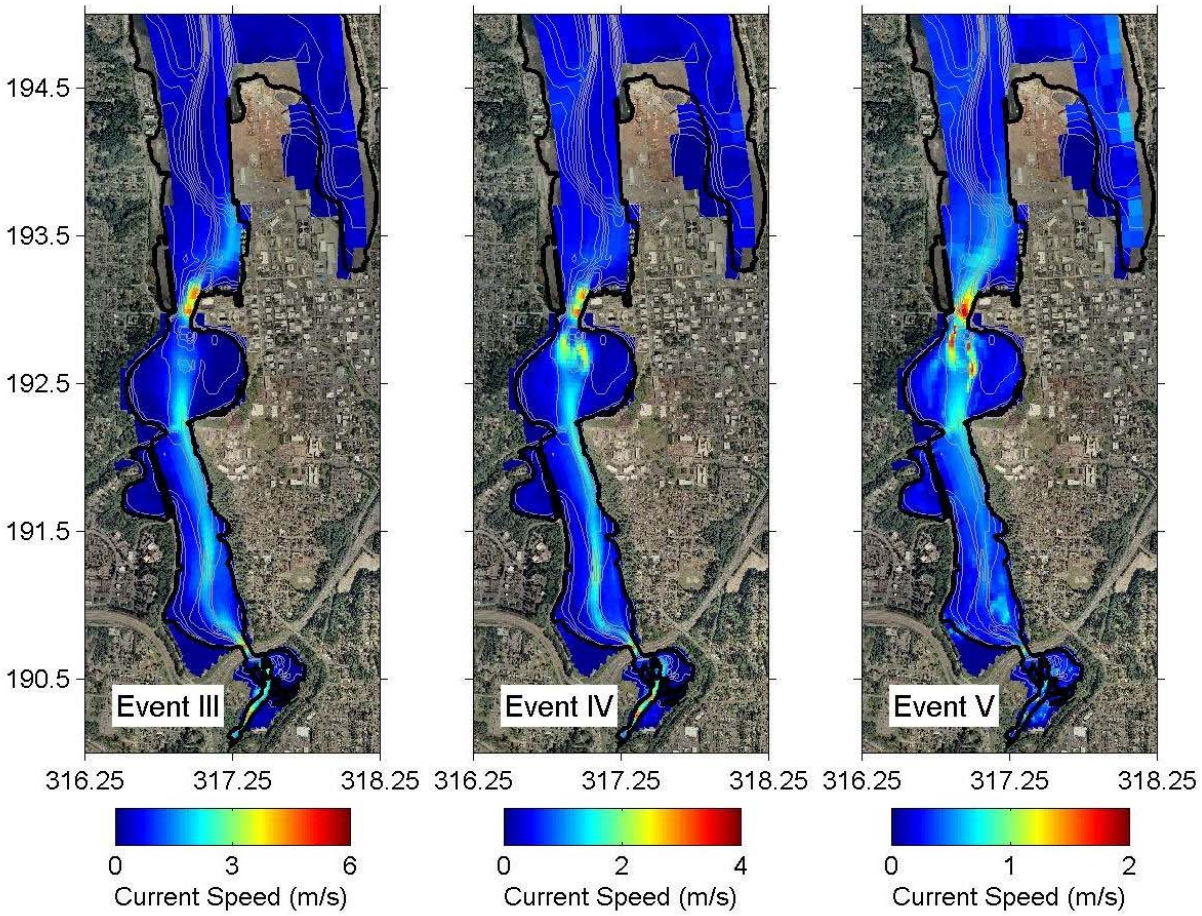

Figure 3.54. Maximum velocities for Events III, IV and V in the Restoration Scenario B estuary. Blues are slower speeds and reds are faster (scales vary by event). Velocity magnitudes are largest immediately north of the estuary and under the I-5 bridge. The wider trestle shows slower velocities than observed in Restoration Scenario A.

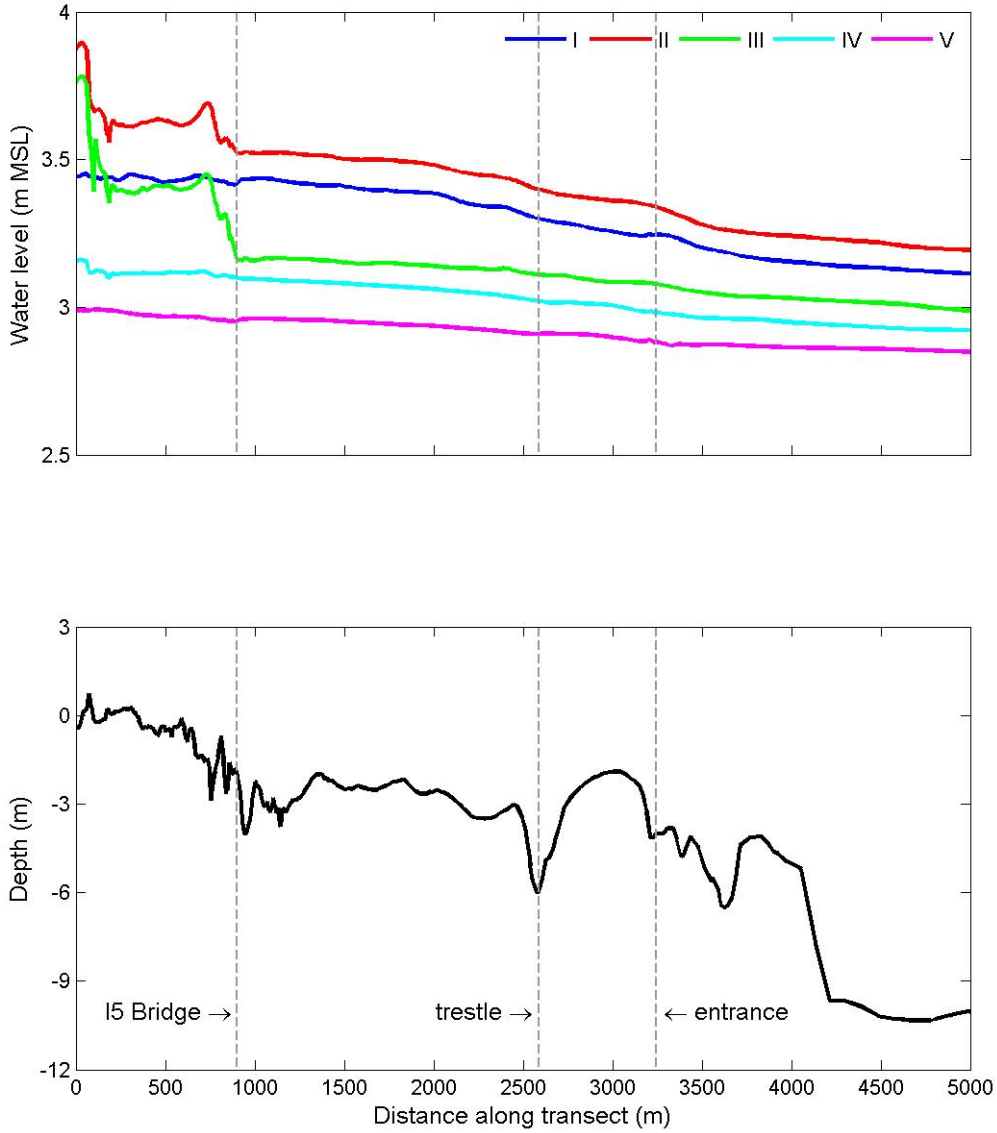

Figure 3.55. Maximum water level profile for the five extreme hydrologic events and bathymetry along the transect in Figure 3.25 for the Restoration Scenario B estuary. Events II and III show the steepest gradients in South Basin with Event III having the largest change overall. Water levels decrease gradually north of the I-5 bridge.

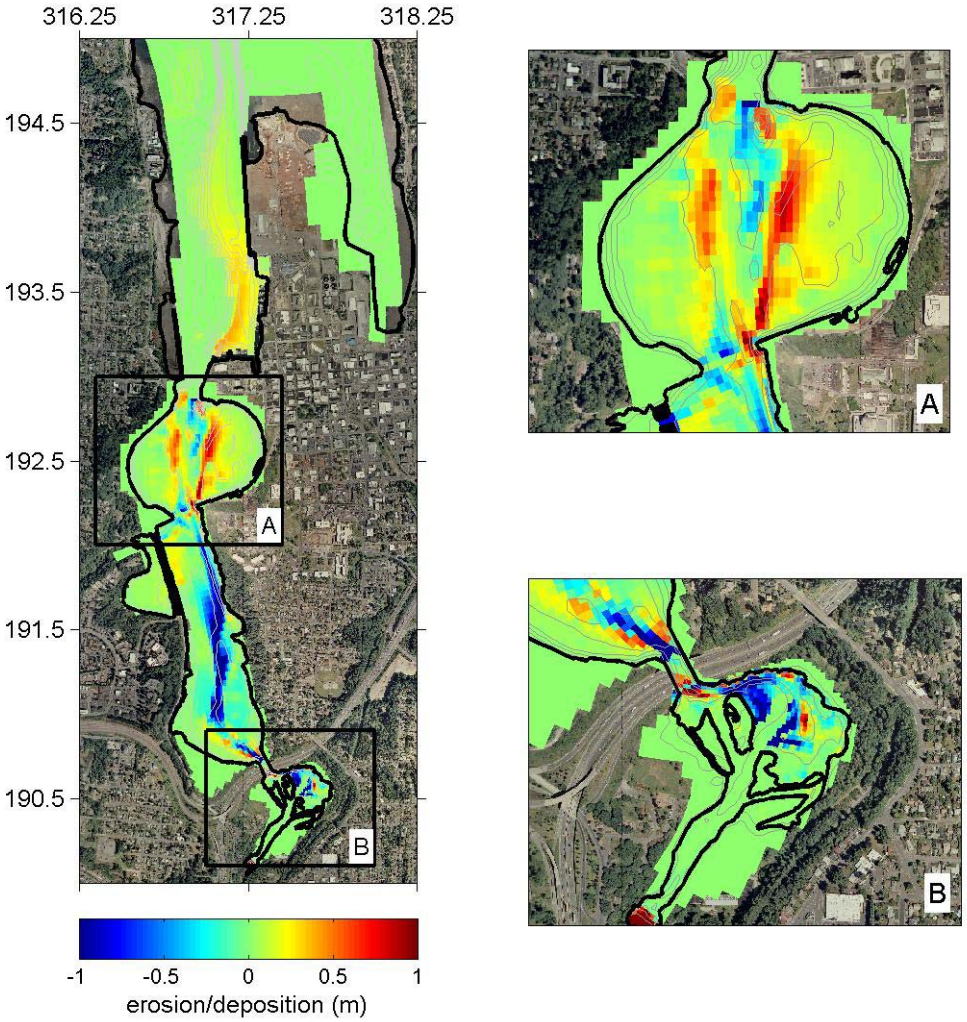

Figure 3.56. Erosion and deposition after the first post-dam year for the Restoration Scenario B estuary under lower erodibility conditions. The axes are in Washington State Plane South (km) and bathymetric contours in 1 m increments. Blues indicate erosion and reds show deposition.

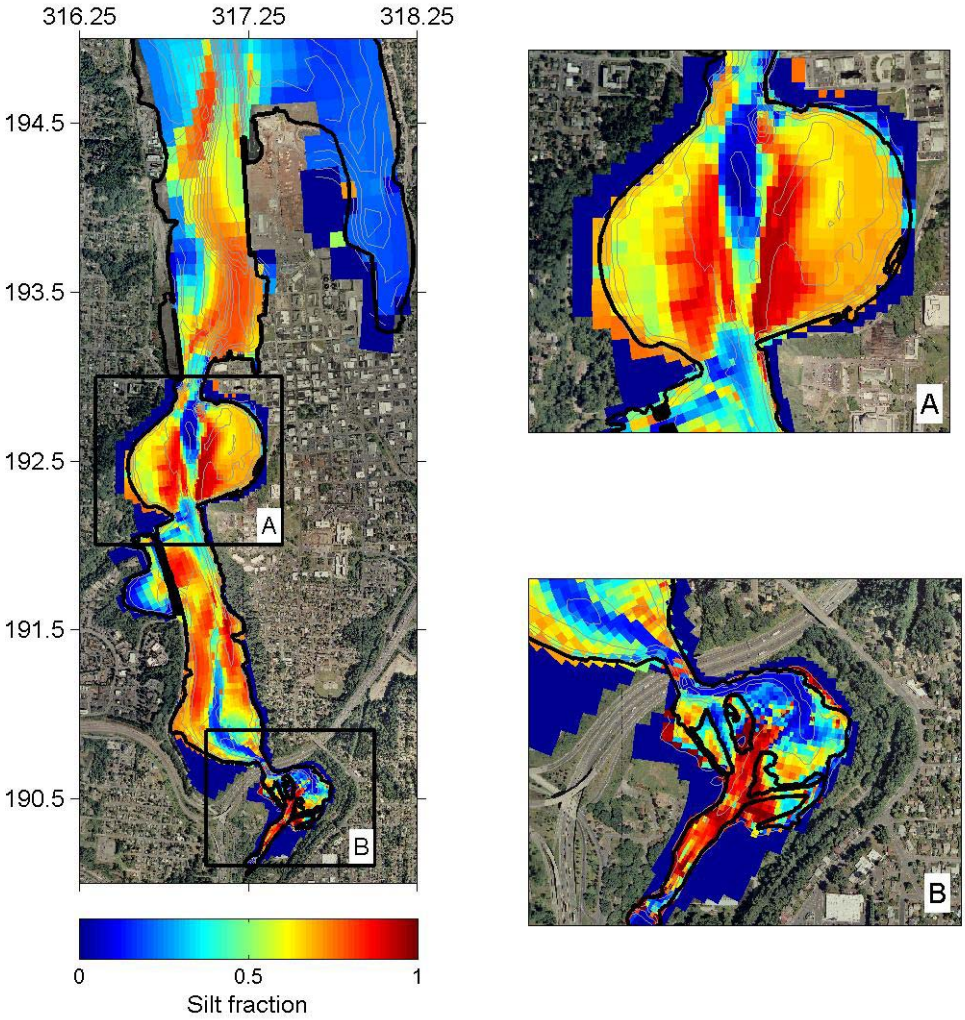

Figure 3.57. Silt fraction distribution after the first post-dam year for the Restoration Scenario B estuary under lower erodibility conditions. The axes are in Washington State Plane South (km) and bathymetric contours in 1 m increments. Blues indicate small and reds show large amounts of silt.

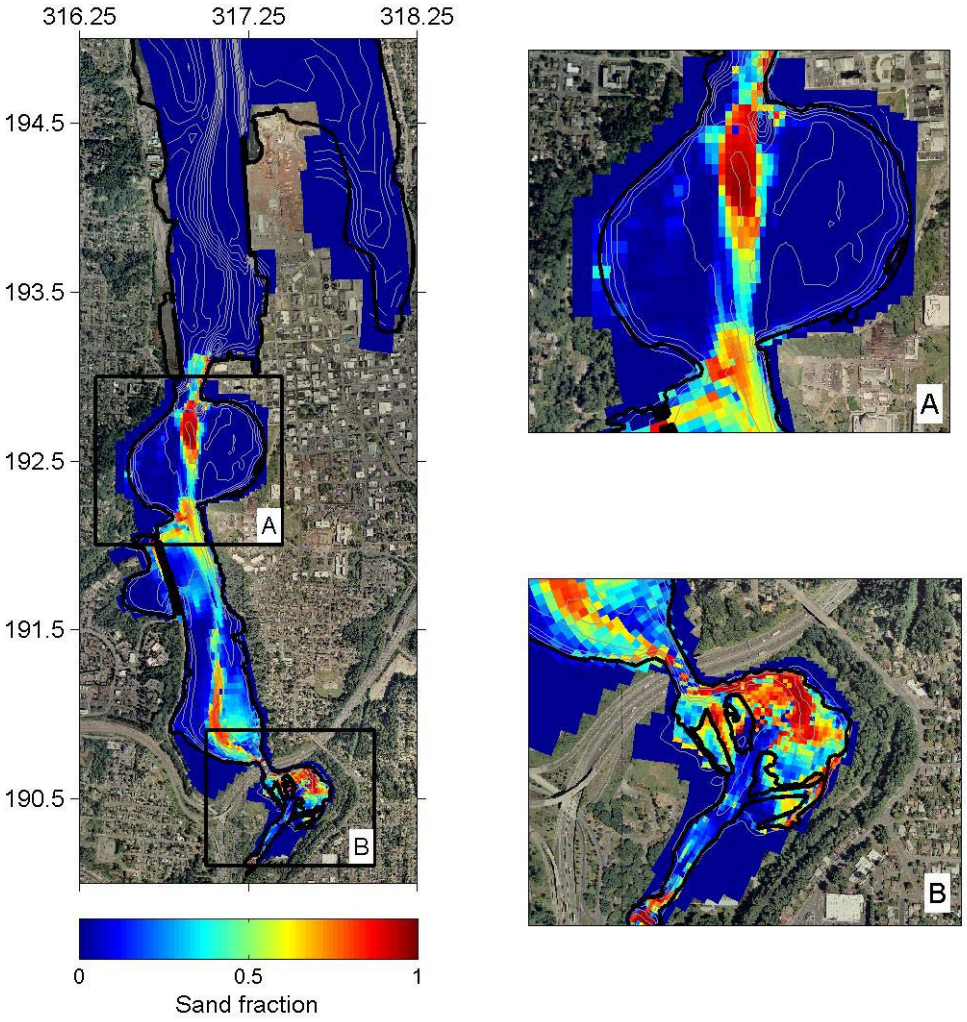

Figure 3.58. Sand fraction distribution after the first post-dam year for the Restoration Scenario B estuary under lower erodibility conditions. The axes are in Washington State Plane South (km) and bathymetric contours in 1 m increments. Blues indicate small and reds show large amounts of sand.

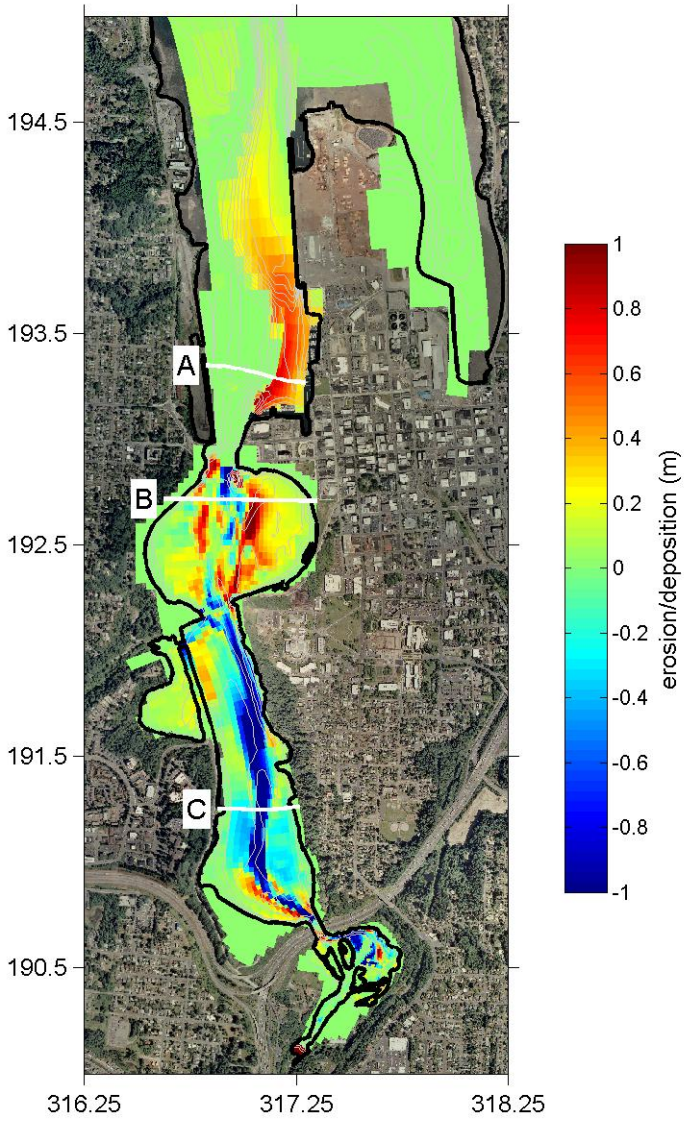

Figure 3.59. Erosion and deposition three years after dam removal for the Restoration Scenario B estuary under lower erodibility conditions. The axes are in Washington State Plane South (km) and bathymetric contours in 1 m increments. Blues indicate erosion and reds show deposition. Cross-estuary transect B will be examined in a subsequent plot.

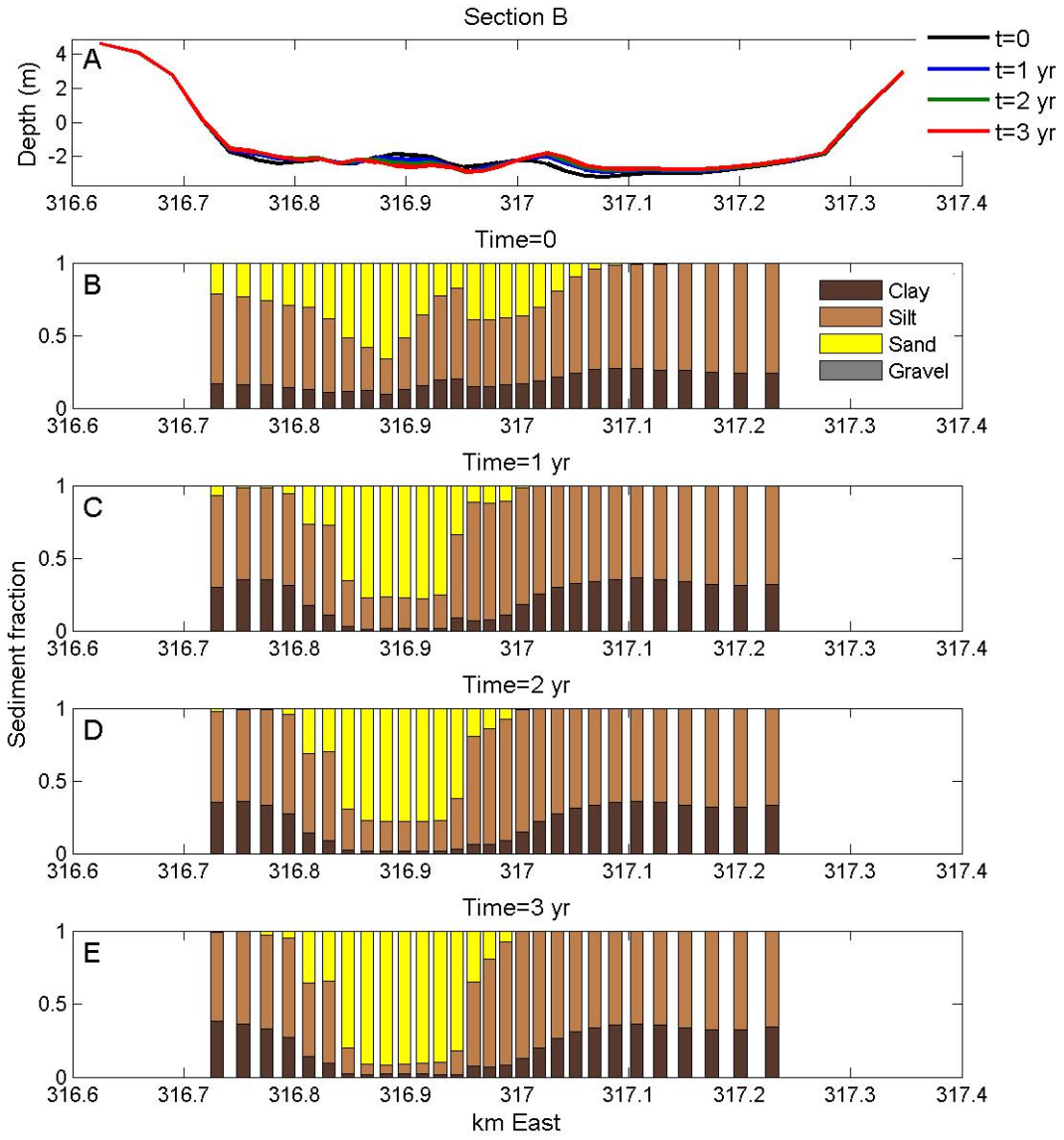

Figure 3.60. Cross-estuary transect Section B for the Restoration Scenario B estuary under lower erodibility conditions. Depth profiles show changes each year (Panel A). Surface sediment grain size fractions for the initial bed (B), first post-dam year (C), second post-dam year (D) and third post-dam year (E) show coarsening of the channel and fining of the flanks.

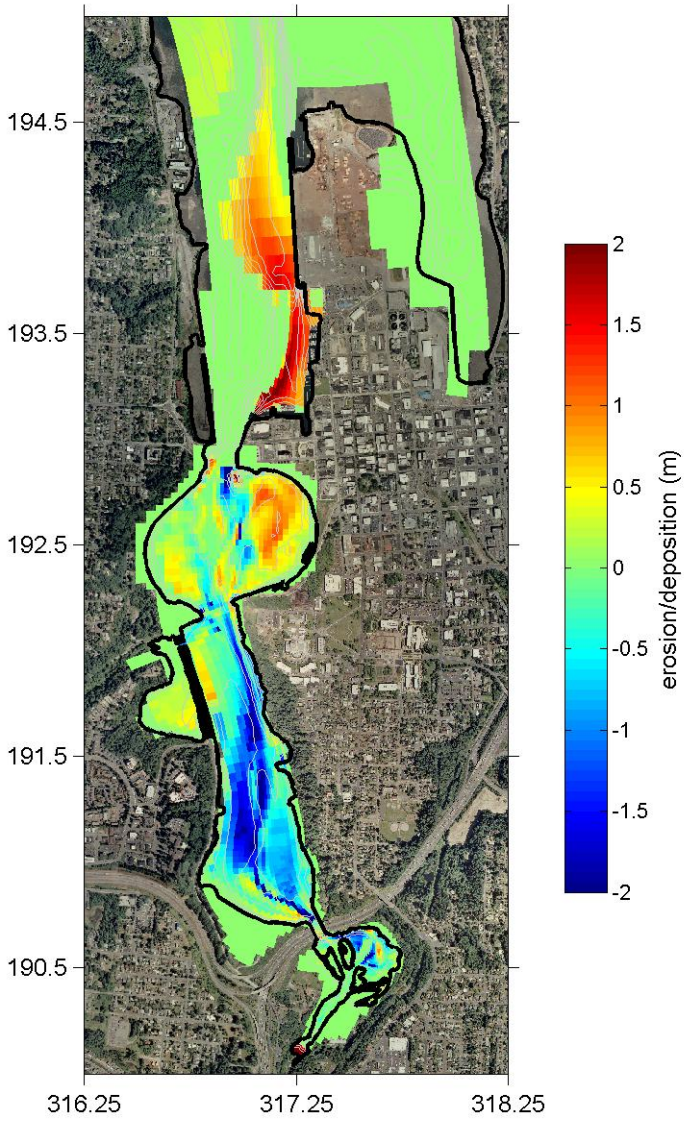

Figure 3.61. Erosion and deposition three years after dam removal for the Restoration Scenario B estuary under higher erodibility conditions. The axes are in Washington State Plane South (km) and bathymetric contours in 1 m increments. Blues indicate erosion and reds show deposition.

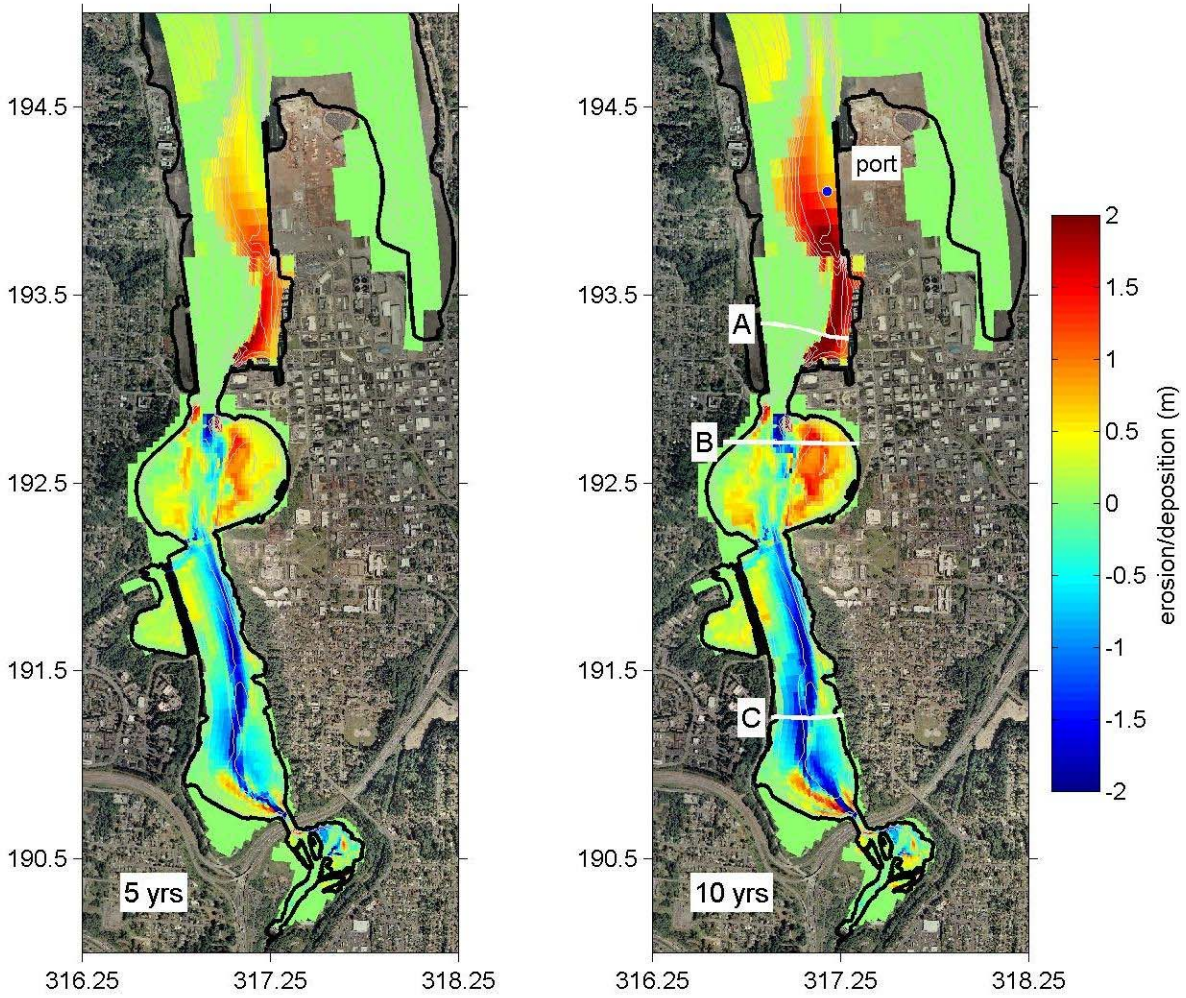

Figure 3.62. Erosion and deposition five and 10 years after dam removal for the Restoration Scenario B estuary under lower erodibility conditions with a lower density of mud. Blues indicate erosion and reds show deposition.

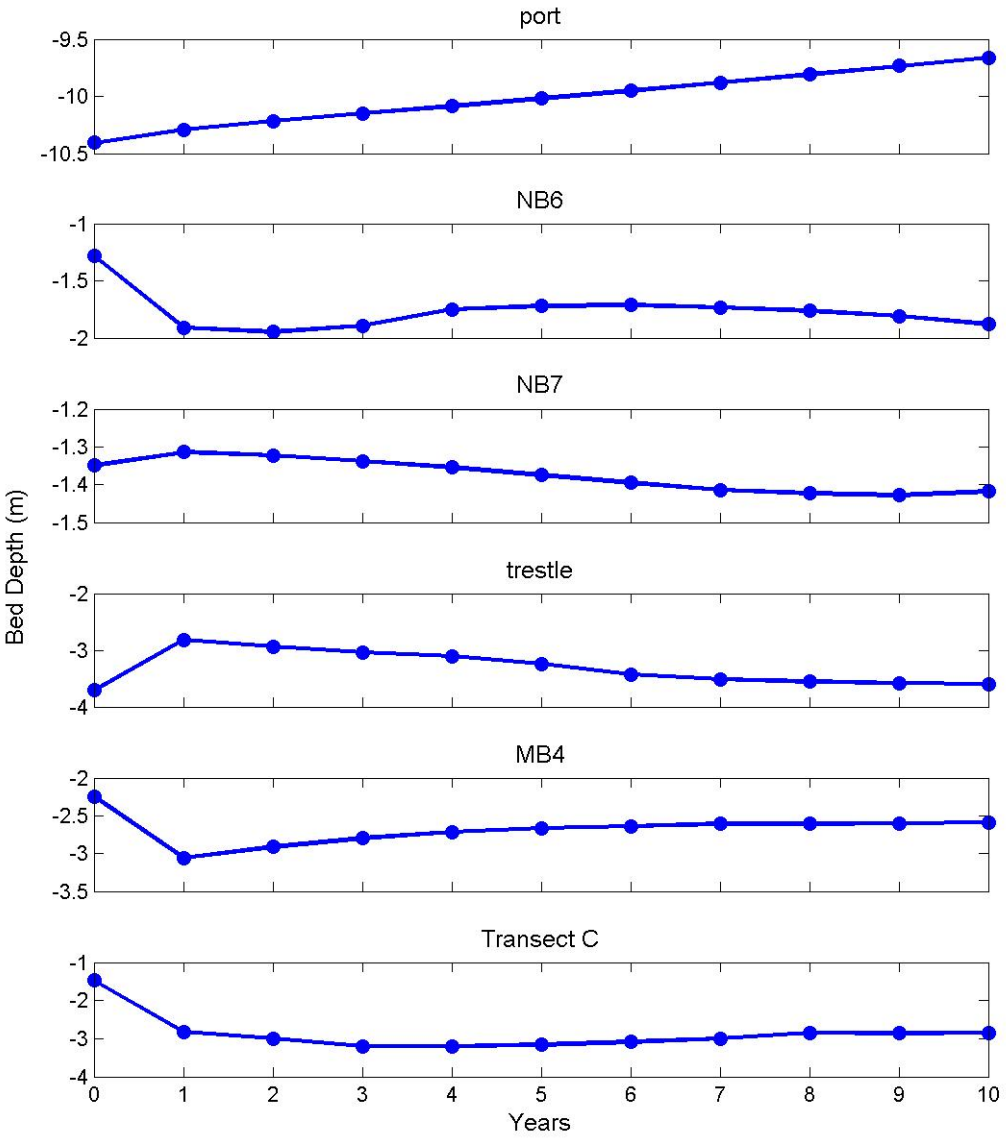

Figure 3.63. Bed depth at selected stations for the Restoration Scenario B estuary under lower erodibility conditions with a lower density of mud (scales vary by station). See Figures 3.27 and 3.41 for locations. The depth of the deepest point along Transect C is monitored in the final panel. With the exception of the port, most changes to the stations' bed depth occur within the first two to four years. The wider trestle shows a very small net change.

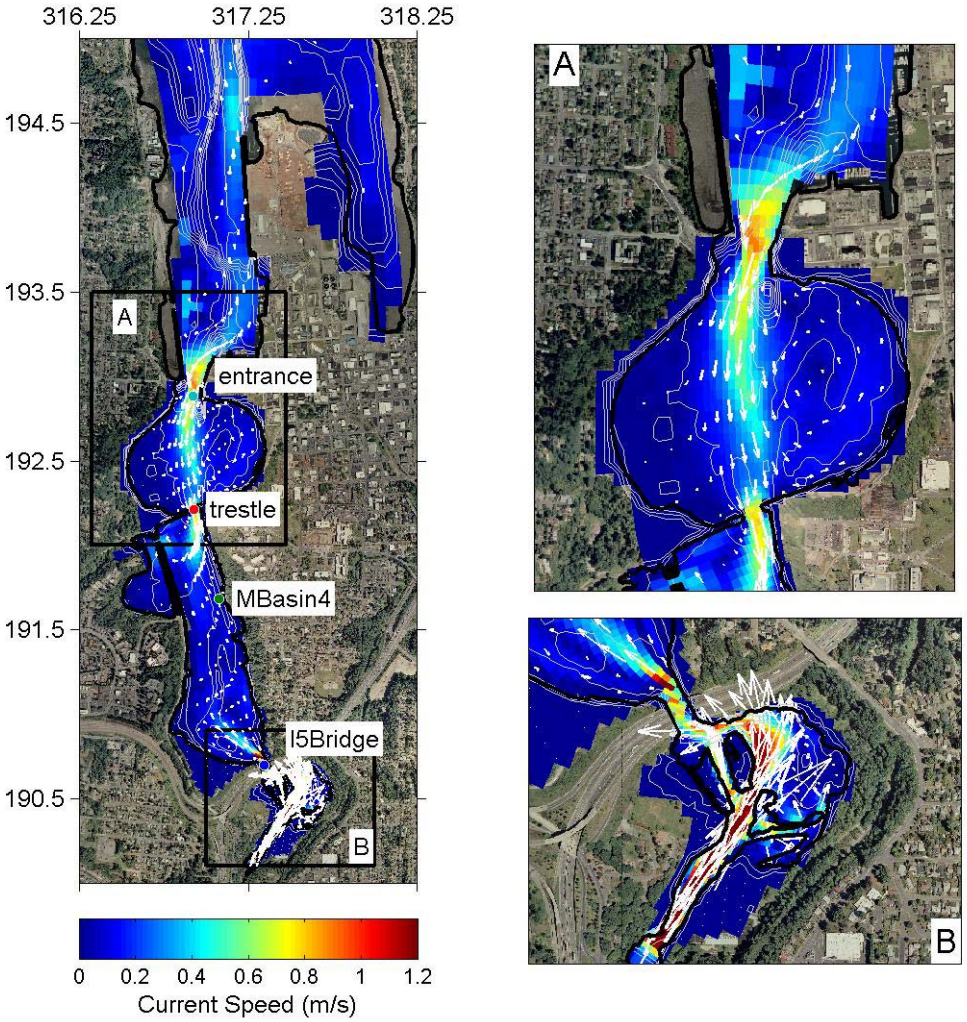

Figure 3.64. Maximum velocity magnitude and vectors during high river flow at flood tide for the Restoration Scenario C estuary. The axes are in Washington State Plane South (km) and bathymetric contours in 1 m increments. Blues indicate slow velocities and reds show the fastest speeds. The fastest currents are observed through the trestle and entrance and under the I-5 bridge. Speeds are slow throughout the estuary as the incoming tide encounters the outgoing river flow. South Basin shows chaotic circulation patterns from the tide-river interaction.

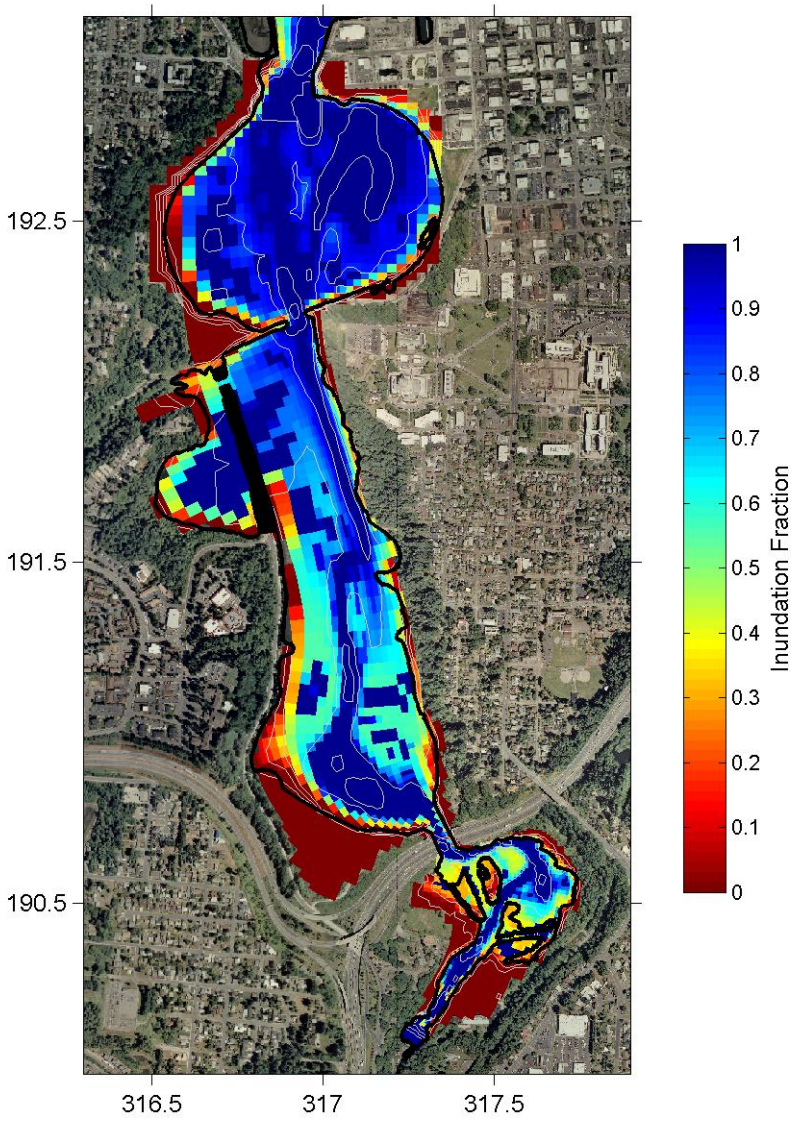

Figure 3.65. Annual mean inundation fraction for the Restoration Scenario C estuary. Blues indicate continuous submersion and reds show continuous exposure. The main channel, North Basin and part of Middle Basin appear to be underwater at least 80% of the year while elevations above 2 m are wet less than 50% of the time. Portions of the South Basin islands get submerged about 30 – 40% of the year.

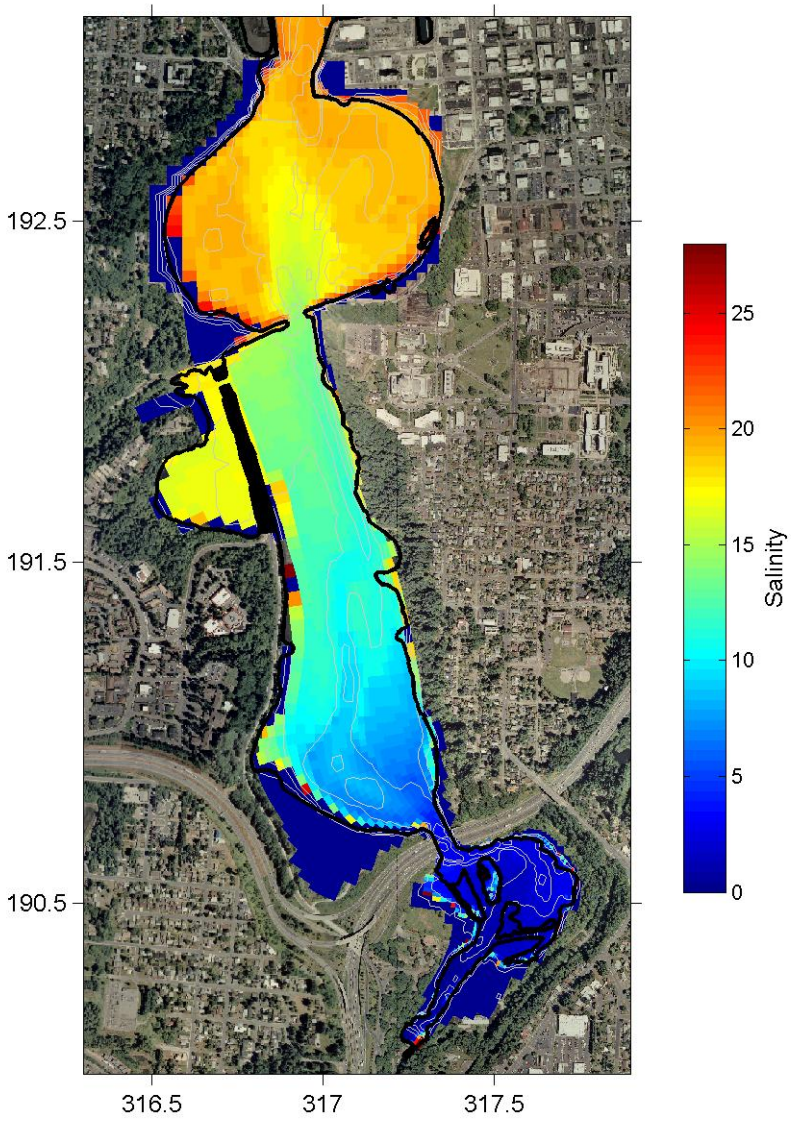

Figure 3.66. Annual mean near-bed salinity for the Restoration Scenario C estuary. Blues indicate freshwater and reds show the most saline water. A steady salinity gradient is observed from freshwater at the river mouth to approximately 15 ppt at the trestle. Percival Cove is saltier than Middle Basin, possibly due to the limited influx of freshwater into the cove from Middle Basin and the absence of Percival Creek in the model. North Basin shows an intrusion of 15 – 18 ppt water into a fairly uniform basin of 18 – 20 ppt brackish water.

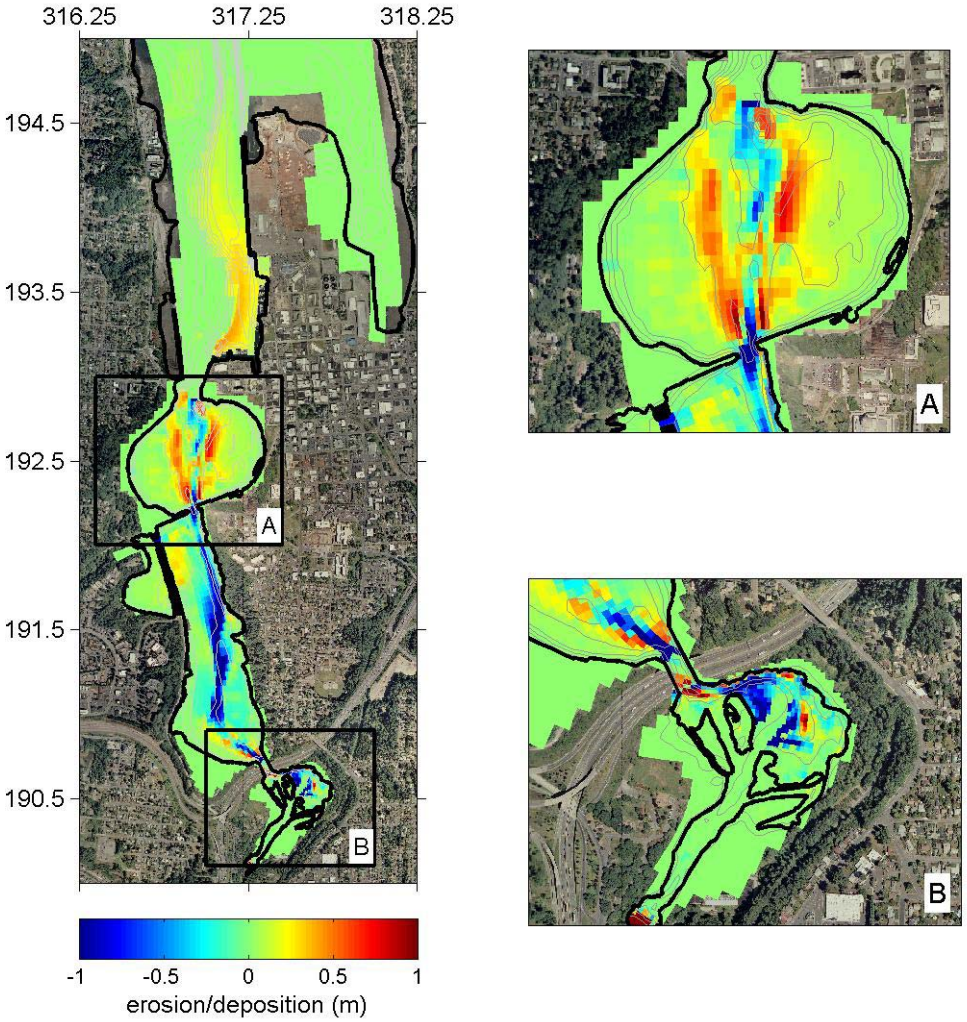

Figure 3.67. Erosion and deposition after the first post-dam year for the Restoration Scenario C estuary under lower erodibility conditions. The axes are in Washington State Plane South (km) and bathymetric contours in 1 m increments. Blues indicate erosion and reds show deposition.

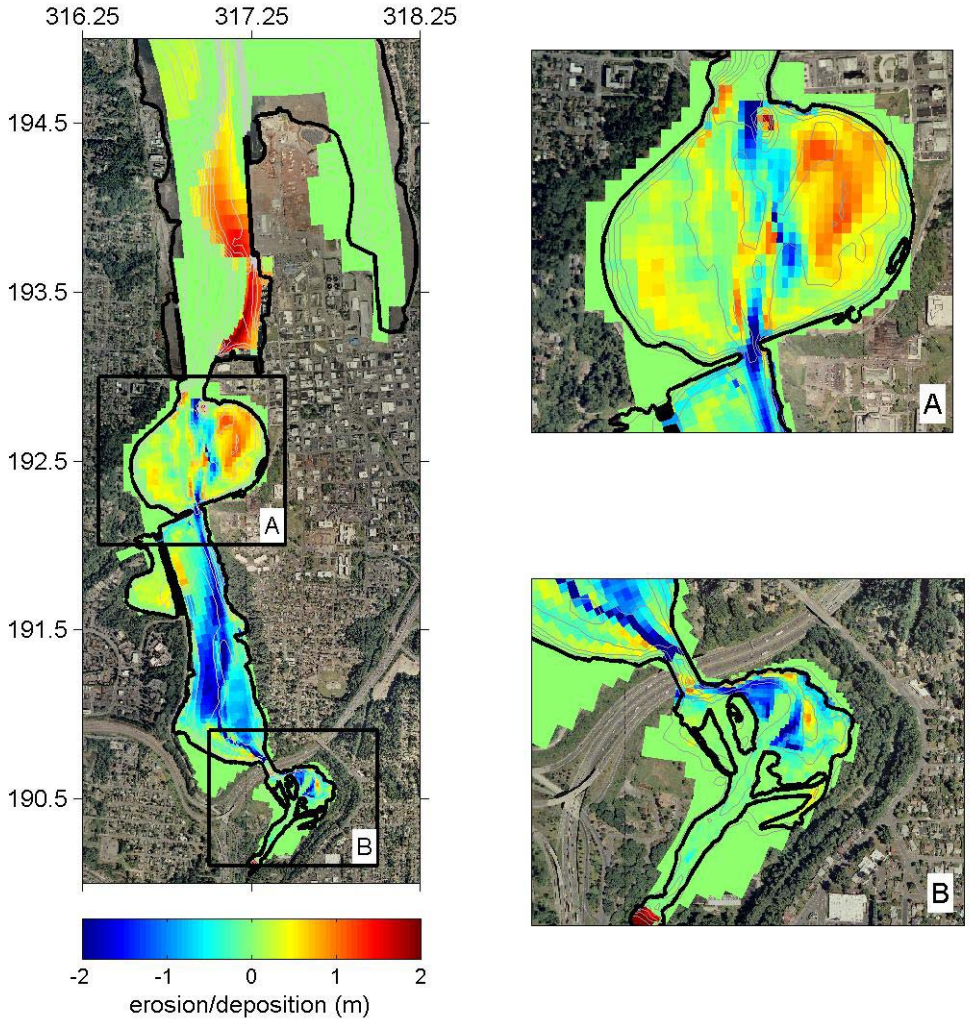

Figure 3.68. Erosion and deposition three years after dam removal for the Restoration Scenario C estuary under higher erodibility conditions. The axes are in Washington State Plane South (km) and bathymetric contours in 1 m increments. Blues indicate erosion and reds show deposition.

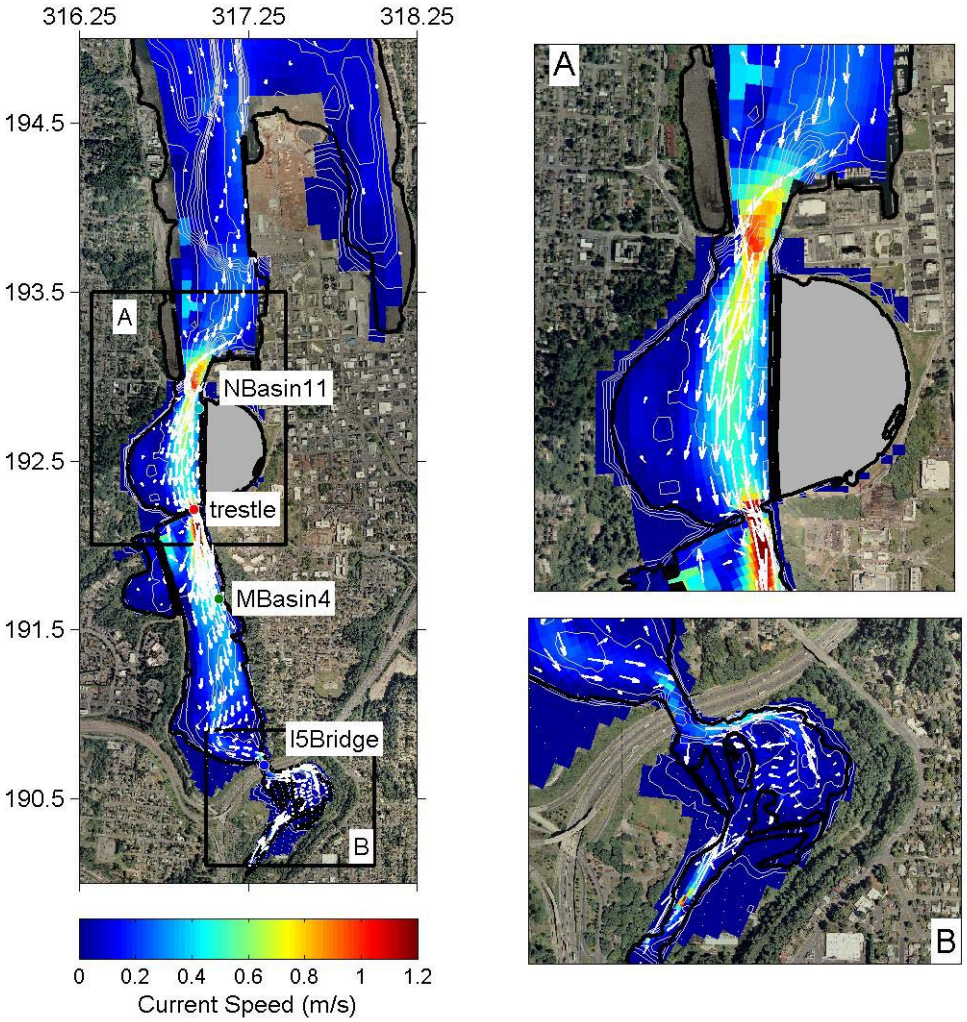

Figure 3.69. Maximum velocity magnitude and vectors during low river flow at flood tide for the Restoration Scenario D estuary. The axes are in Washington State Plane South (km) and bathymetric contours in 1 m increments. Blues indicate slow velocities and reds show the fastest speeds. The fastest currents are observed through the trestle and entrance while speeds decrease in Middle Basin. Speeds under the I-5 bridge are less than 0.5 m/s.

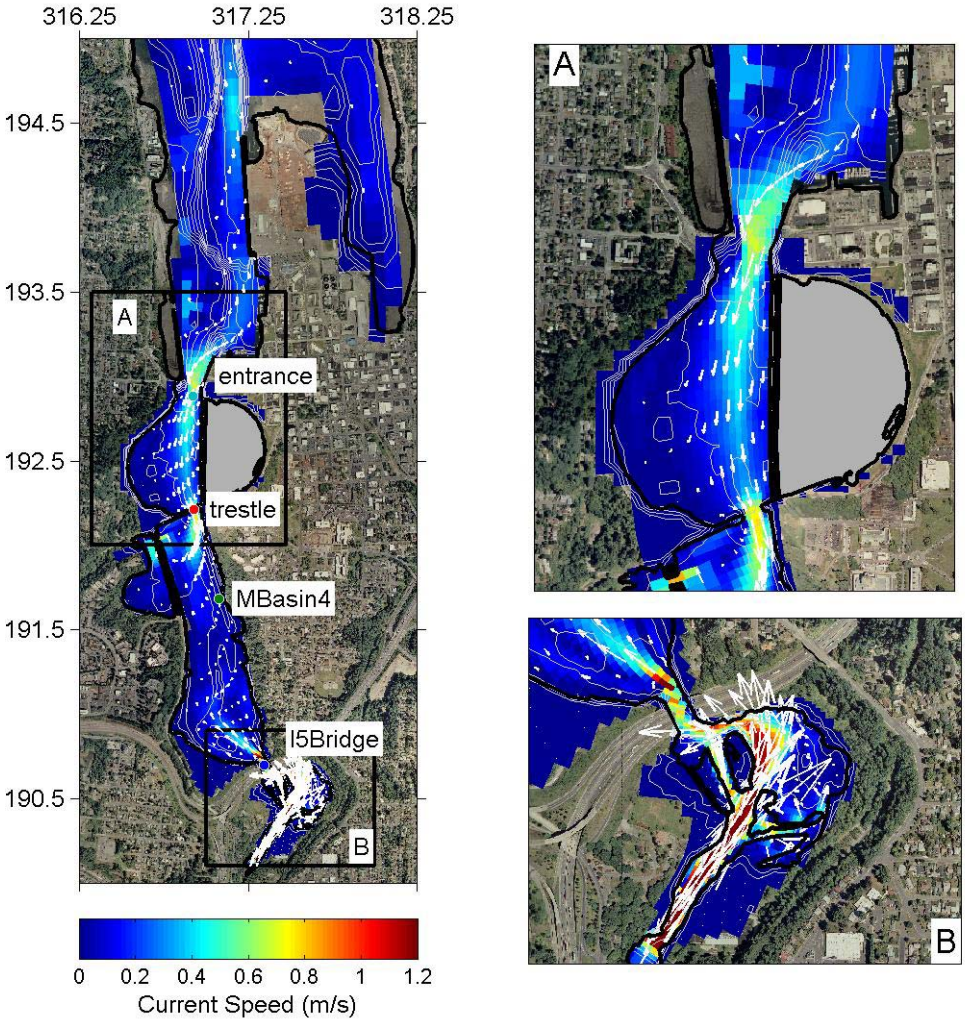

Figure 3.70. Maximum velocity magnitude and vectors during high river flow at flood tide for the Restoration Scenario D estuary. The axes are in Washington State Plane South (km) and bathymetric contours in 1 m increments. Blues indicate slow velocities and reds show the fastest speeds. The fastest currents are observed through the trestle and entrance and under the I-5 bridge. Speeds are slow throughout the estuary as the incoming tide encounters the outgoing river flow. South Basin shows chaotic circulation patterns from the tide-river interaction.

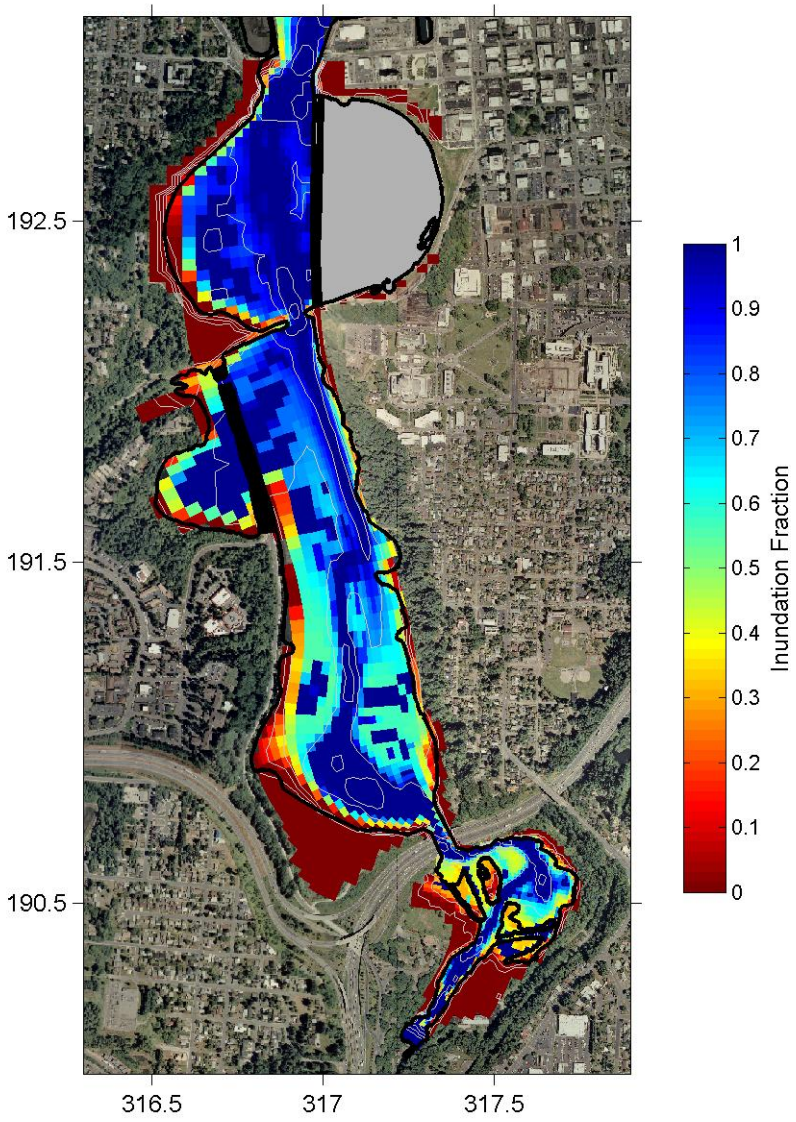

Figure 3.71. Annual mean inundation fraction for the Restoration Scenario D estuary. Blues indicate continuous submersion and reds show continuous exposure. The main channel, North Basin and part of Middle Basin appear to be underwater at least 80% of the year while elevations above 2 m are wet less than 50% of the time. Portions of the South Basin islands get submerged about 30 – 40% of the year.

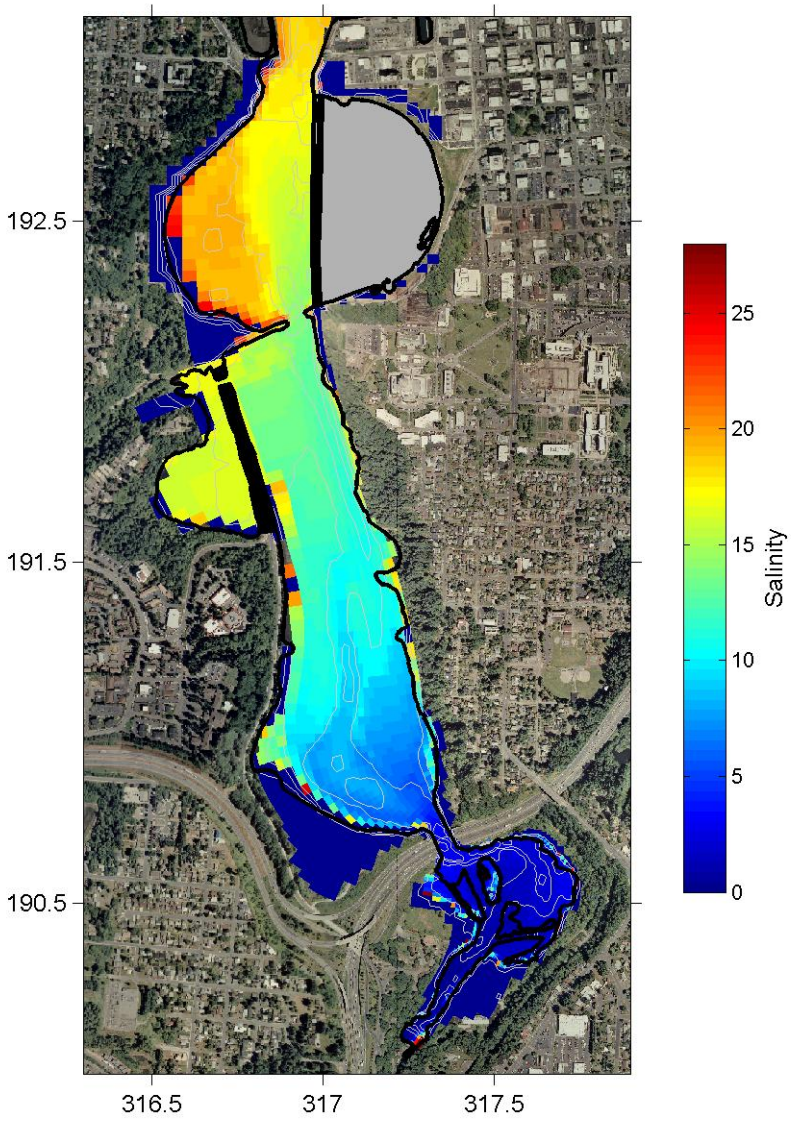

Figure 3.72. Annual mean near-bed salinity for the Restoration Scenario D estuary. Blues indicate freshwater and reds show the most saline water. A steady salinity gradient is observed from freshwater at the river mouth to approximately 15 ppt at the trestle. Percival Cove is saltier than Middle Basin, possibly due to the limited influx of freshwater into the cove from Middle Basin and the absence of Percival Creek in the model. North Basin shows an intrusion of 15 – 18 ppt water into a fairly uniform basin of 18 – 20 ppt brackish water.

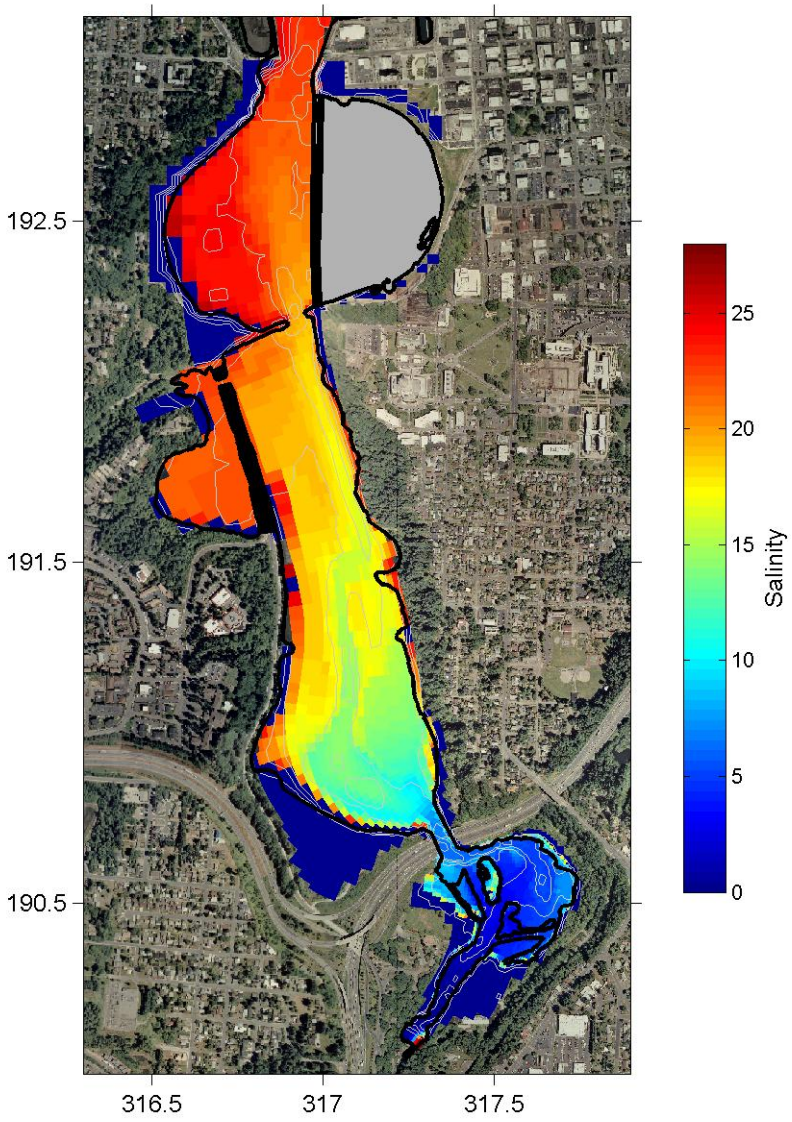

Figure 3.73. Dry season mean near-bed salinity for the Restoration Scenario D estuary. Blues indicate freshwater and reds show the most saline water. South Basin remains mostly fresh and Middle Basin contains water with salinities from 10 – 20 ppt. The main channel is fresher than the flanks in the center of the basin while salinities in Percival Cove and North Basin are almost uniformly above 20 ppt.

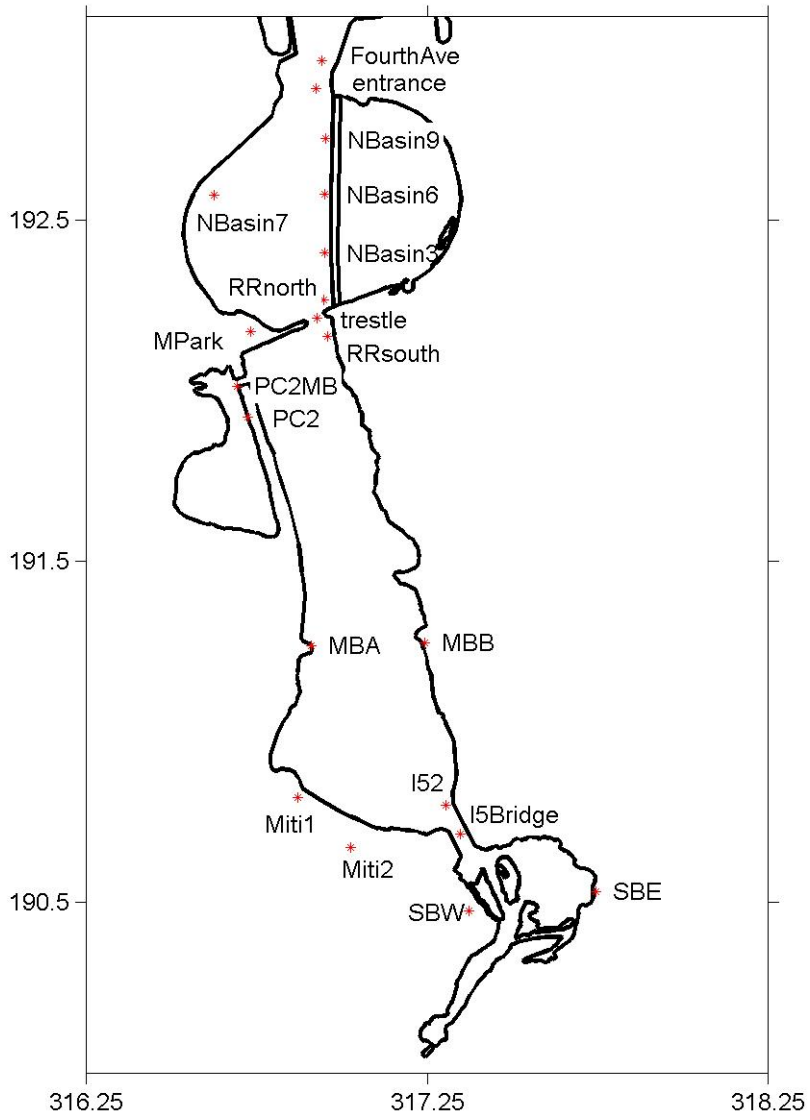

Figure 3.74. Observation stations used in Restoration Scenario D to record water levels and velocities during the five extreme hydrologic events. See tables in the text for maximum values.

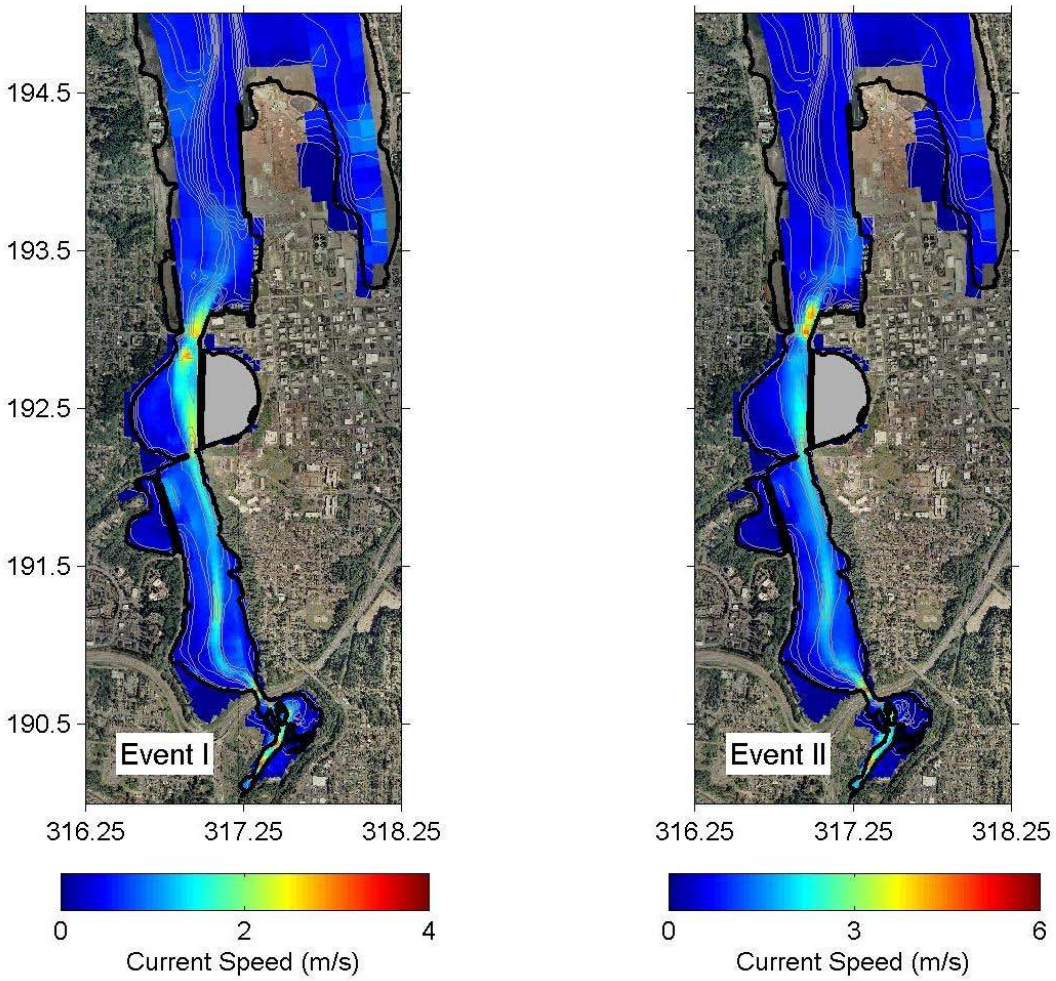

Figure 3.75. Maximum velocities for Events I and II in the Restoration Scenario D estuary. Blues are slower speeds and reds are faster (scales vary by event). Velocity magnitudes are largest immediately north of the estuary and under the I-5 bridge.

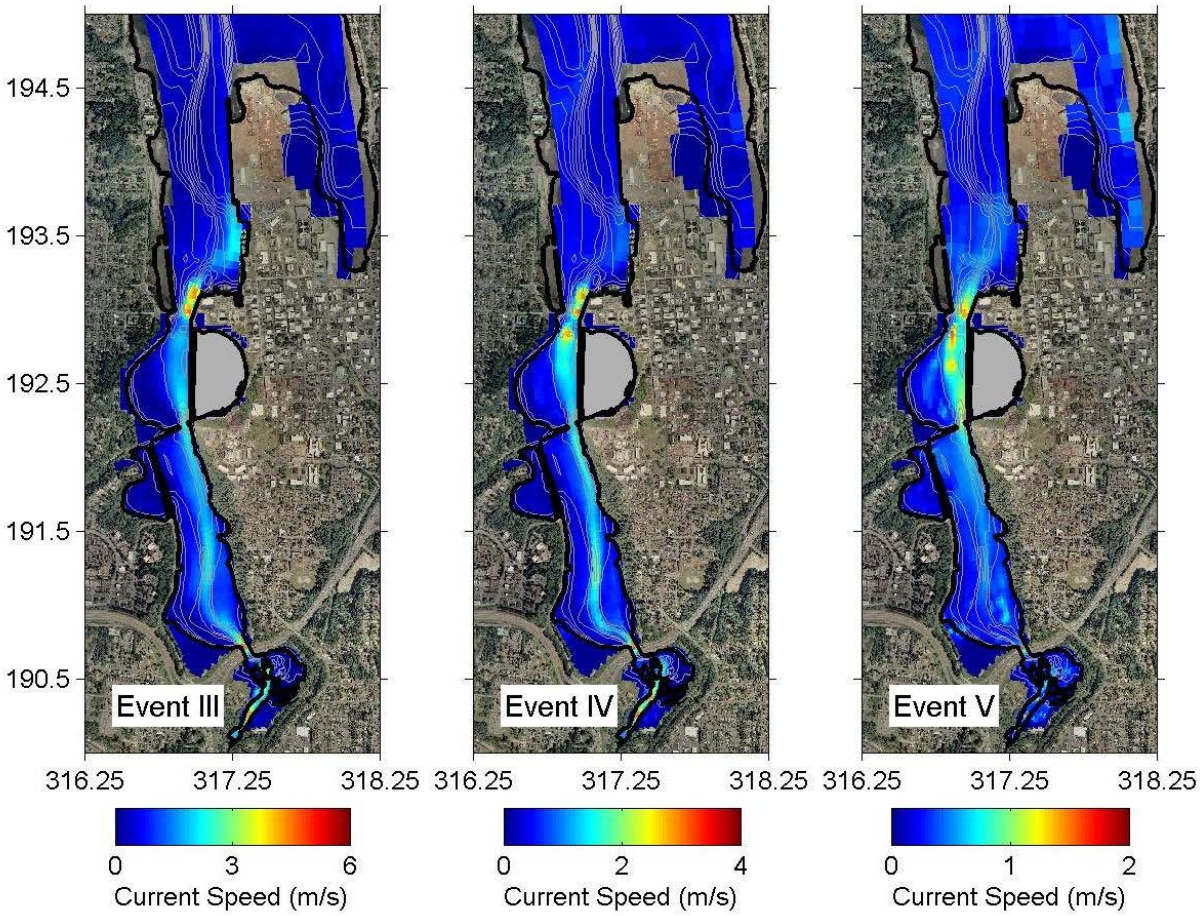

Figure 3.76. Maximum velocities for Events III, IV and V in the Restoration Scenario D estuary. Blues are slower speeds and reds are faster (scales vary by event). Velocity magnitudes are largest immediately north of the estuary and under the I-5 bridge.

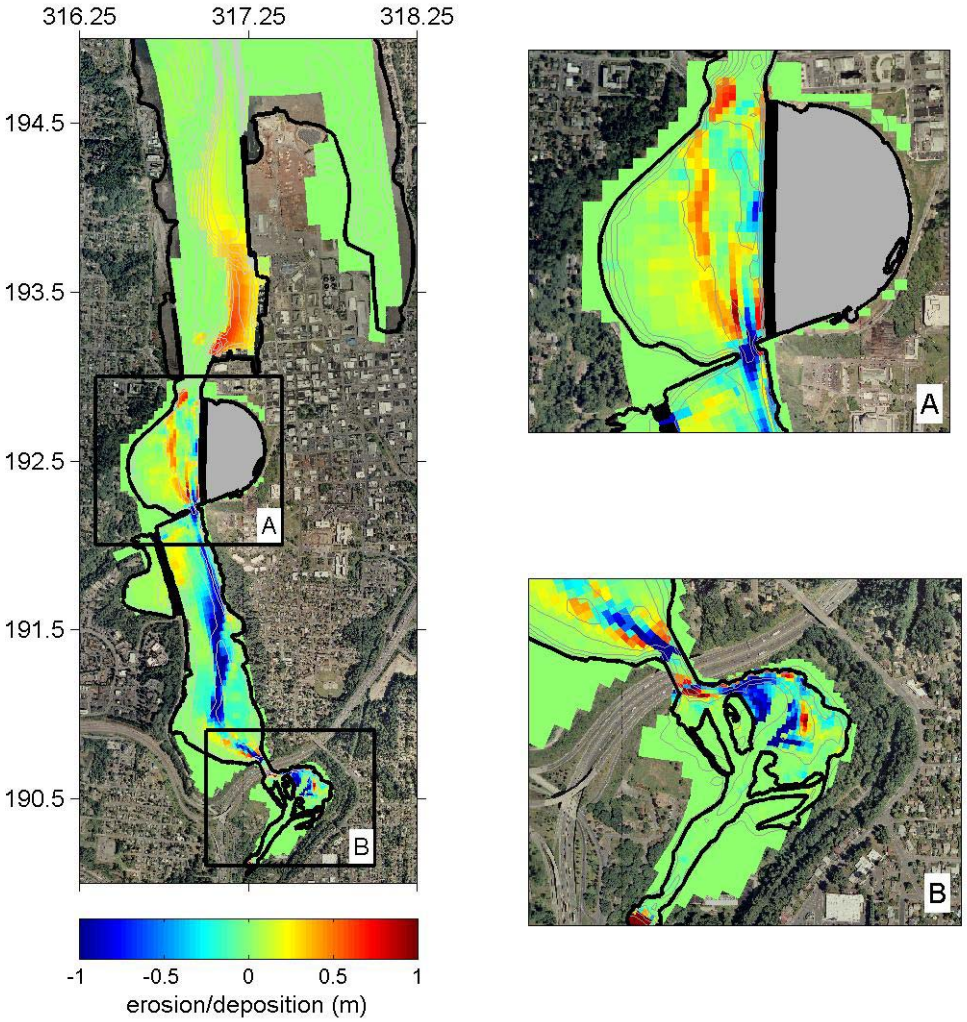

Figure 3.77. Erosion and deposition after the first post-dam year for the Restoration Scenario D estuary under lower erodibility conditions. The axes are in Washington State Plane South (km) and bathymetric contours in 1 m increments. Blues indicate erosion and reds show deposition.

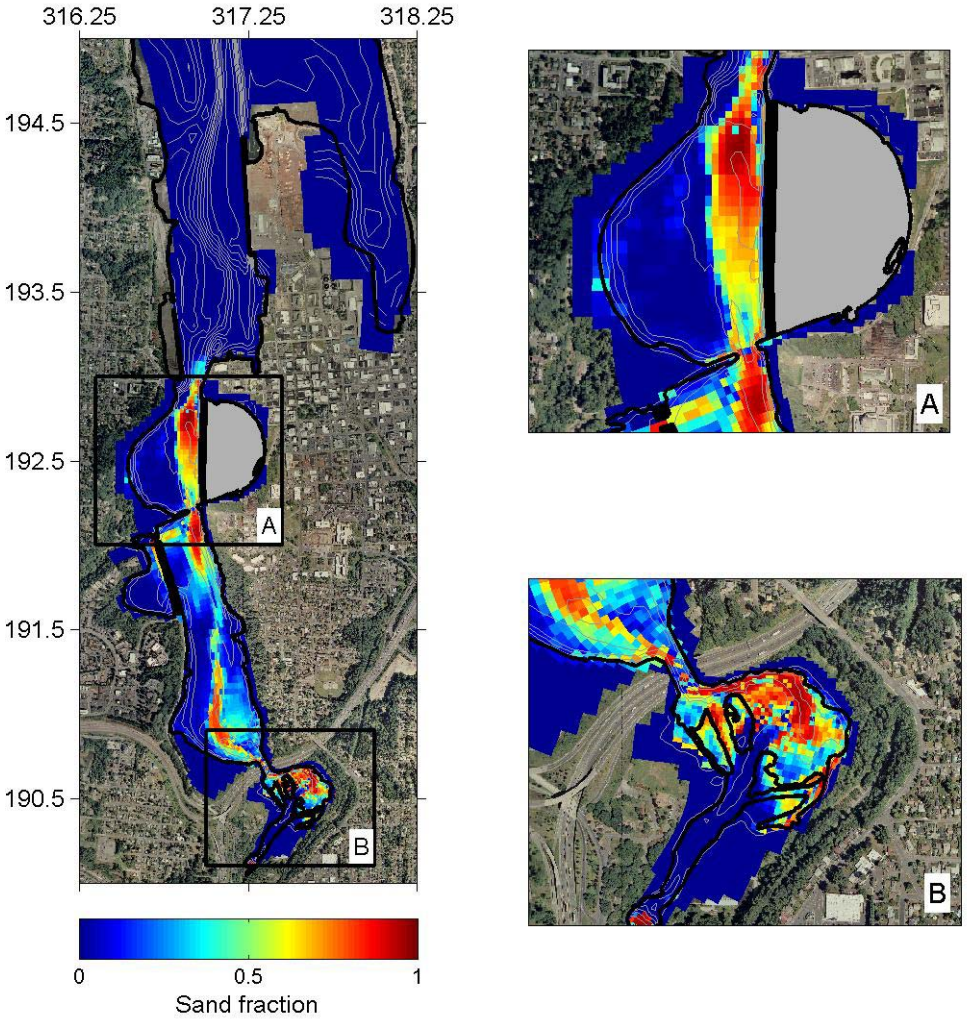

Figure 3.78. Sand fraction distribution after the first post-dam year for the Restoration Scenario D estuary under lower erodibility conditions. The axes are in Washington State Plane South (km) and bathymetric contours in 1 m increments. Blues indicate small and reds show large amounts of sand.

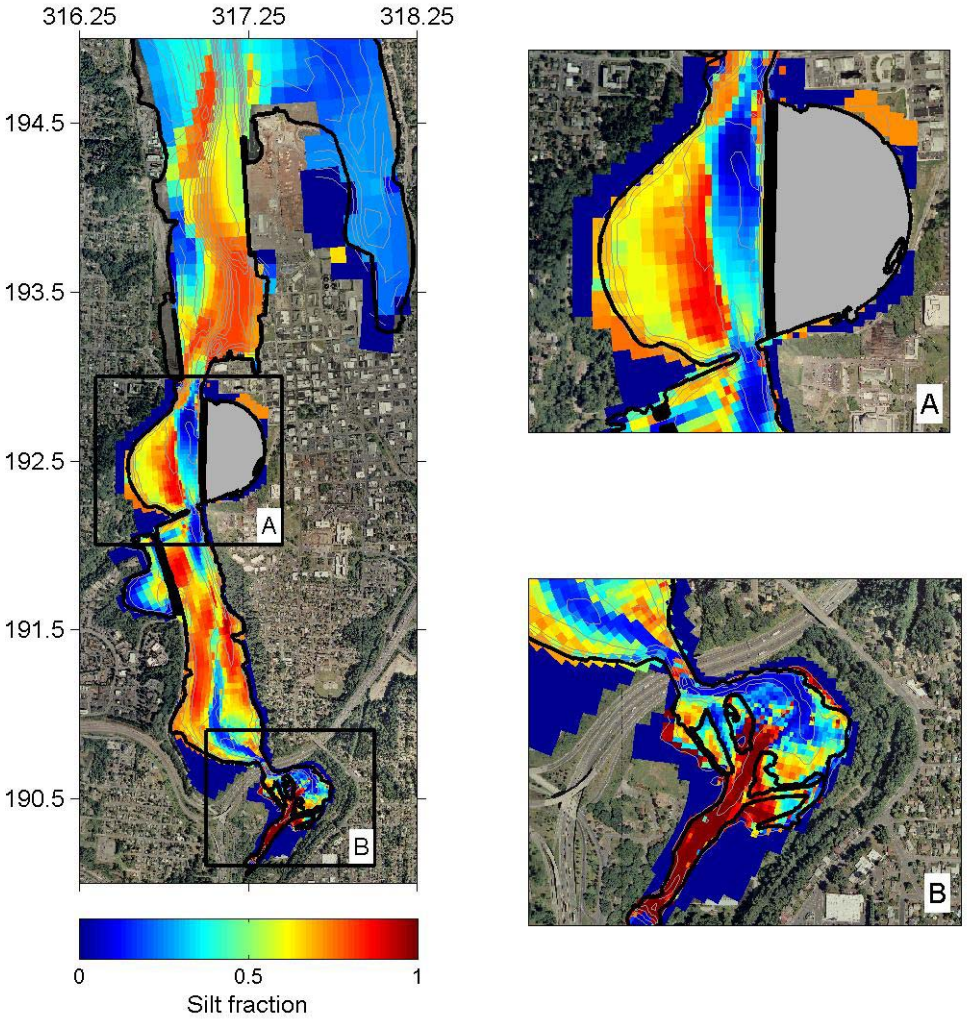

Figure 3.79. Silt fraction distribution after the first post-dam year for the Restoration Scenario D estuary under lower erodibility conditions. The axes are in Washington State Plane South (km) and bathymetric contours in 1 m increments. Blues indicate small and reds show large amounts of silt.

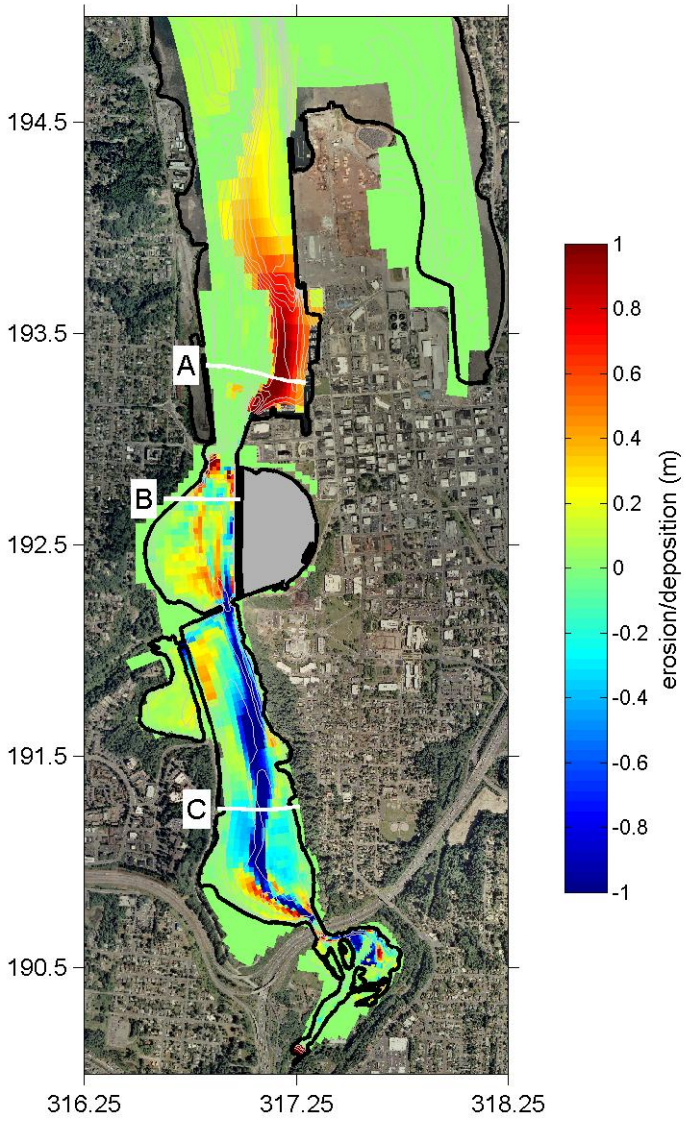

Figure 3.80. Erosion and deposition three years after dam removal for the Restoration Scenario D estuary under lower erodibility conditions. The axes are in Washington State Plane South (km) and bathymetric contours in 1 m increments. Blues indicate erosion and reds show deposition. Cross-estuary transect B will be examined in a subsequent plot.

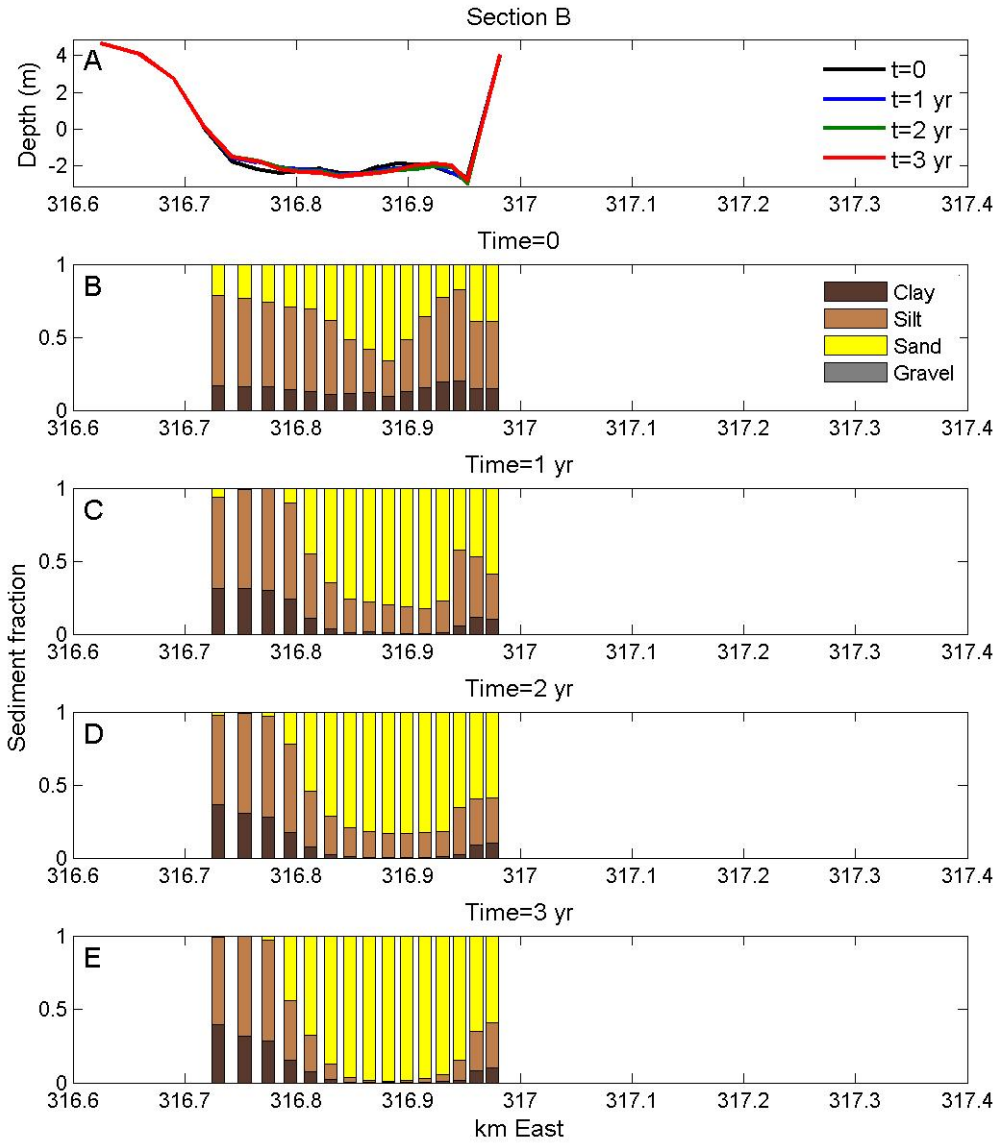

Figure 3.81. Cross-estuary transect Section B for the Restoration Scenario D estuary under lower erodibility conditions. Depth profiles show changes each year (Panel A). Surface sediment grain size fractions for the initial bed (B), first post-dam year (C), second post-dam year (D) and third post-dam year (E) show coarsening of the channel and fining of the flanks.

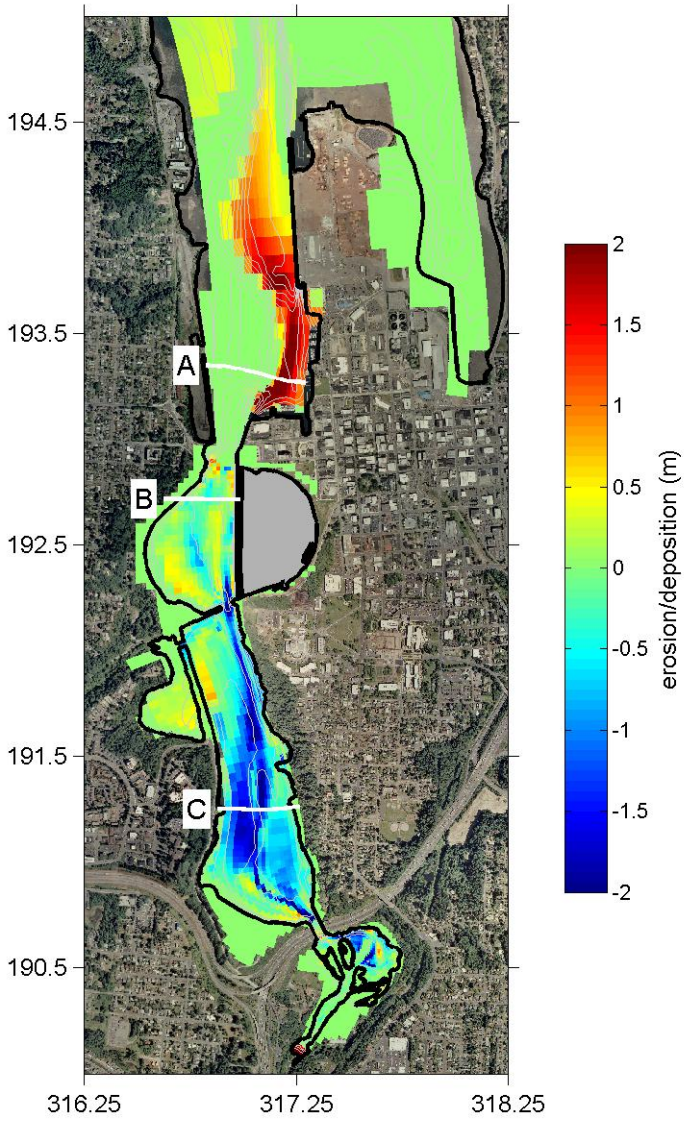

Figure 3.82. Erosion and deposition three years after dam removal for the Restoration Scenario D estuary under higher erodibility conditions. The axes are in Washington State Plane South (km) and bathymetric contours in 1 m increments. Blues indicate erosion and reds show deposition. Cross-estuary transects B and C will be examined in subsequent plots.

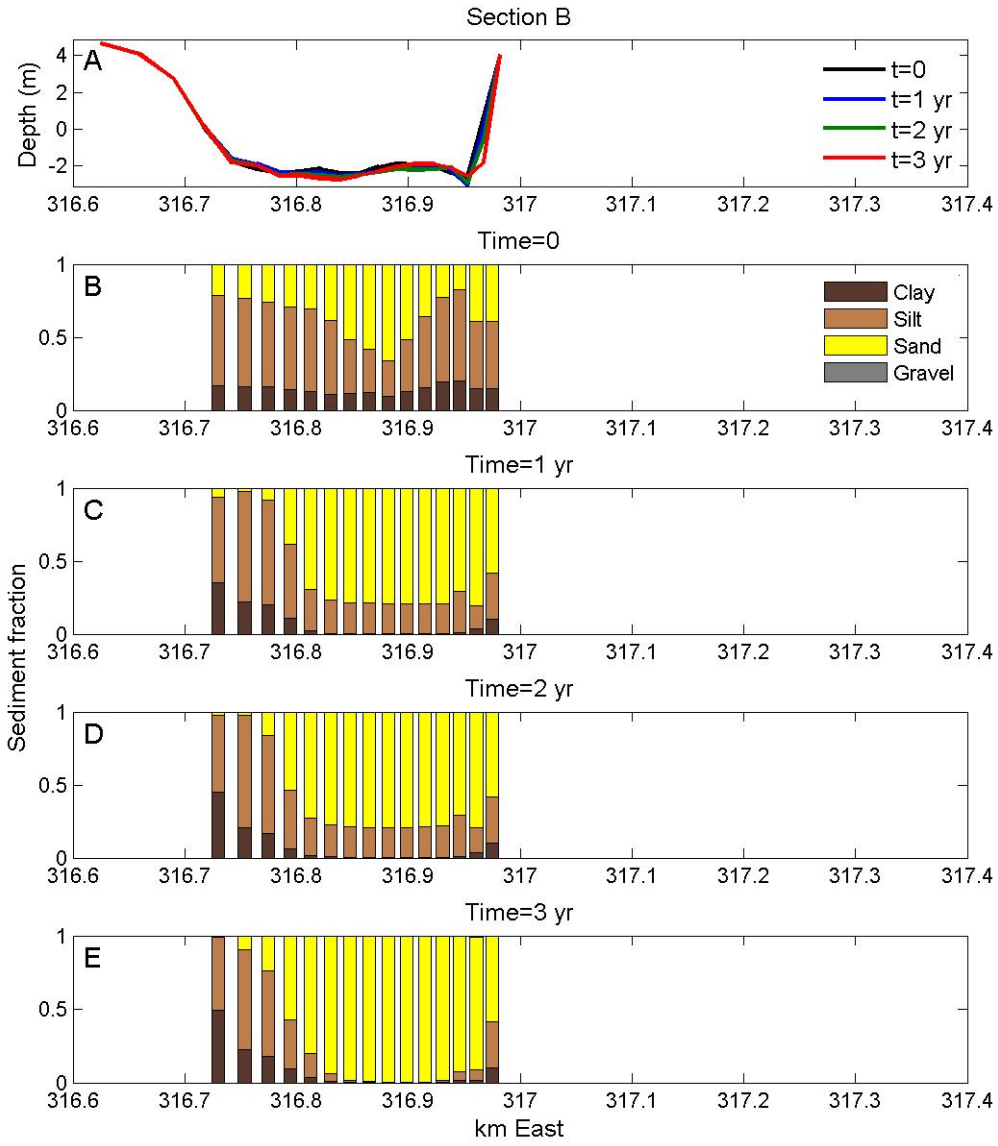

Figure 3.83. Cross-estuary transect Section B for the Restoration Scenario D estuary under higher erodibility conditions. Depth profiles show changes each year (Panel A). Surface sediment grain size fractions for the initial bed (B), first post-dam year (C), second post-dam year (D) and third post-dam year (E) show coarsening of the channel and fining of the flanks.

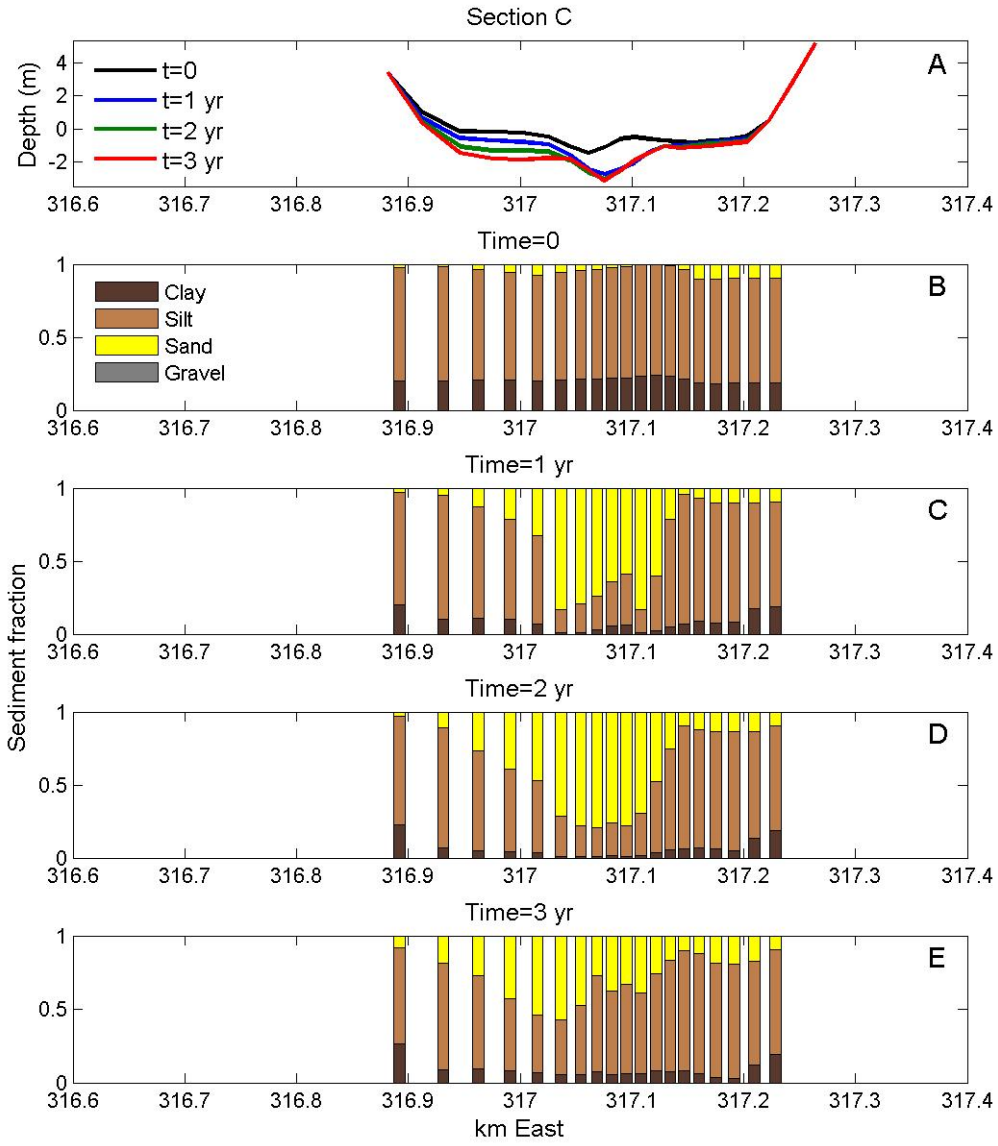

Figure 3.84. Cross-estuary transect Section C for the Restoration Scenario D estuary under higher erodibility conditions. Depth profiles show changes each year (Panel A). Surface sediment grain size fractions for the initial bed (B), first post-dam year (C), second post-dam year (D) and third post-dam year (E) show coarsening of the channel and fining of the flanks.

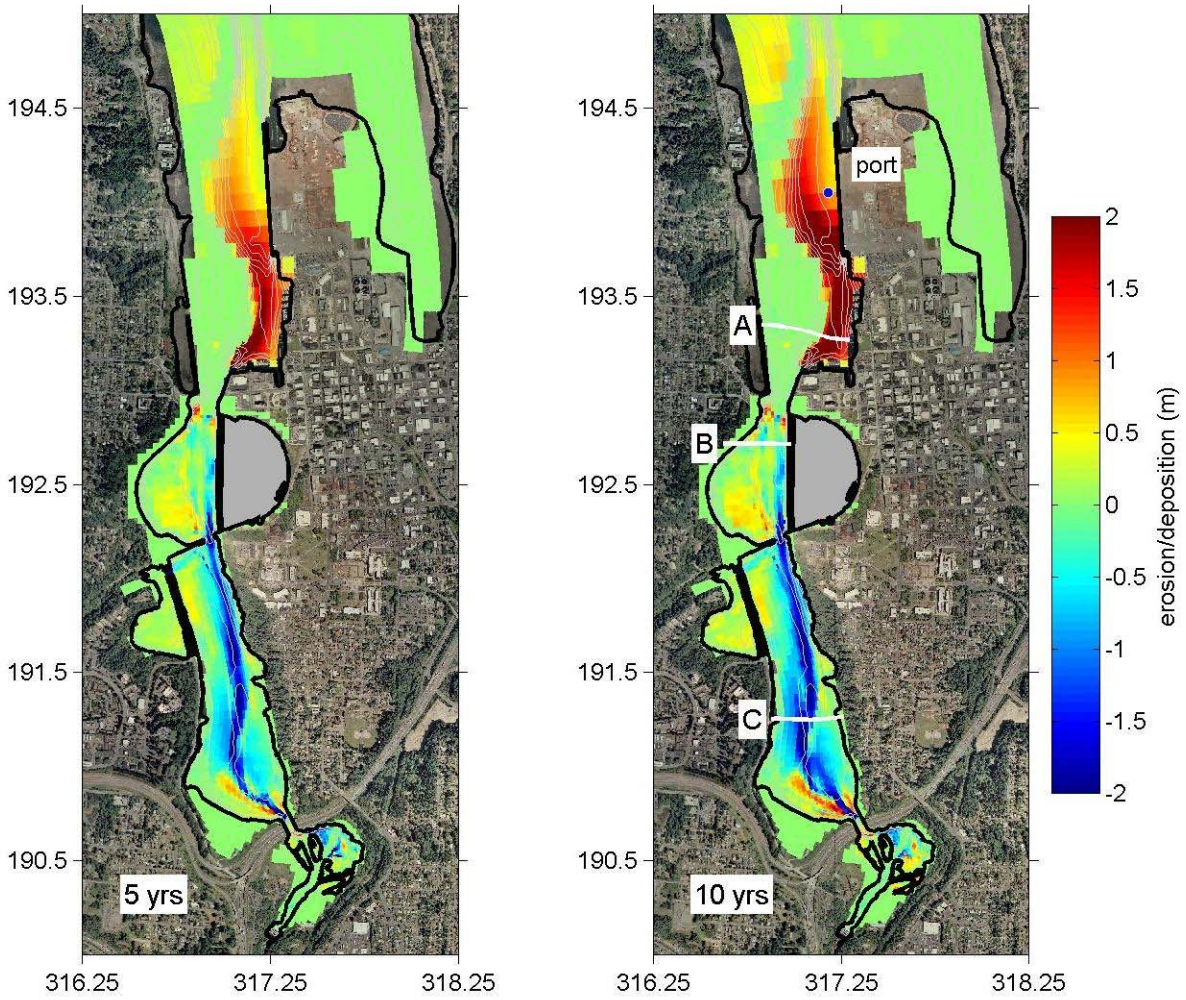

Figure 3.85. Erosion and deposition five and 10 years after dam removal for the Restoration Scenario D estuary under lower erodibility conditions with a lower density of mud. Blues indicate erosion and reds show deposition.

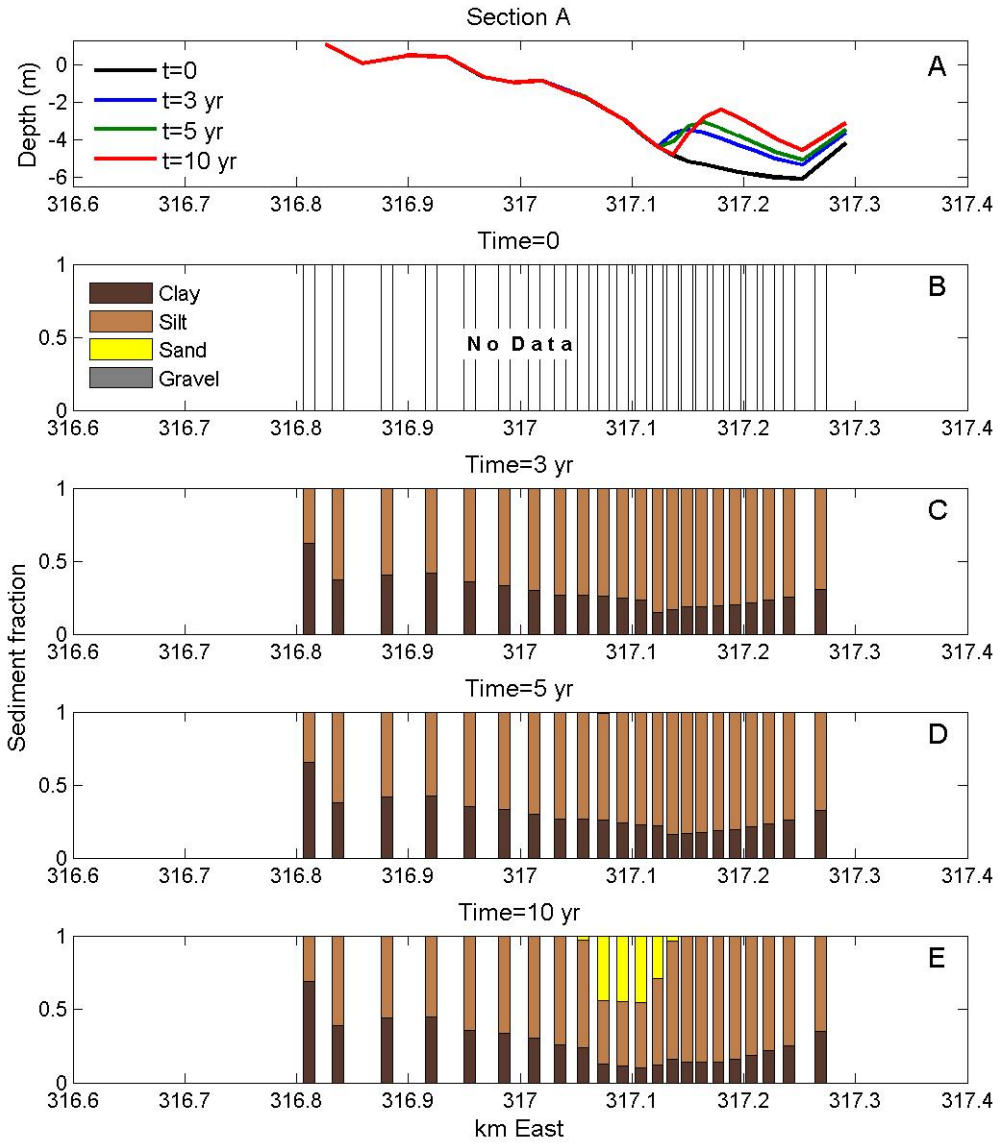

Figure 3.86. Cross-estuary transect Section A for the Restoration Scenario D estuary under lower erodibility conditions with a lower density of mud. Depth profiles show changes each year (Panel A). No initial surface sediment distribution was designed (B) but sediment grain size fractions for the third post-dam year (C), fifth post-dam year (D) and tenth post-dam year (E) show coarsening of the channel within a decade.

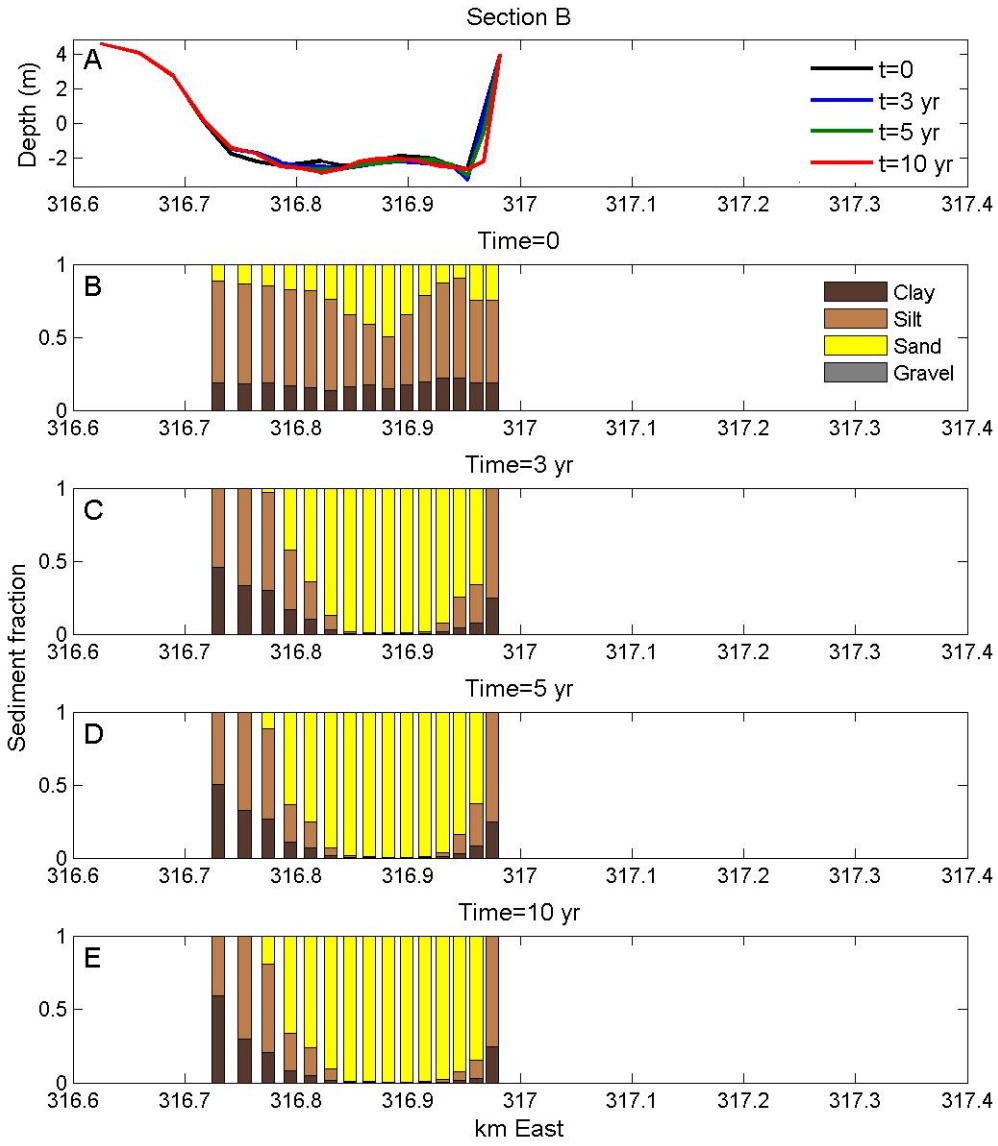

Figure 3.87. Cross-estuary transect Section B for the Restoration Scenario D estuary under lower erodibility conditions with a lower density of mud. Depth profiles show changes each year (Panel A). Surface sediment grain size fractions for the initial bed (B), third post-dam year (C), fifth post-dam year (D) and tenth post-dam year (E) show an initial coarsening of the channel and fining of the flanks.

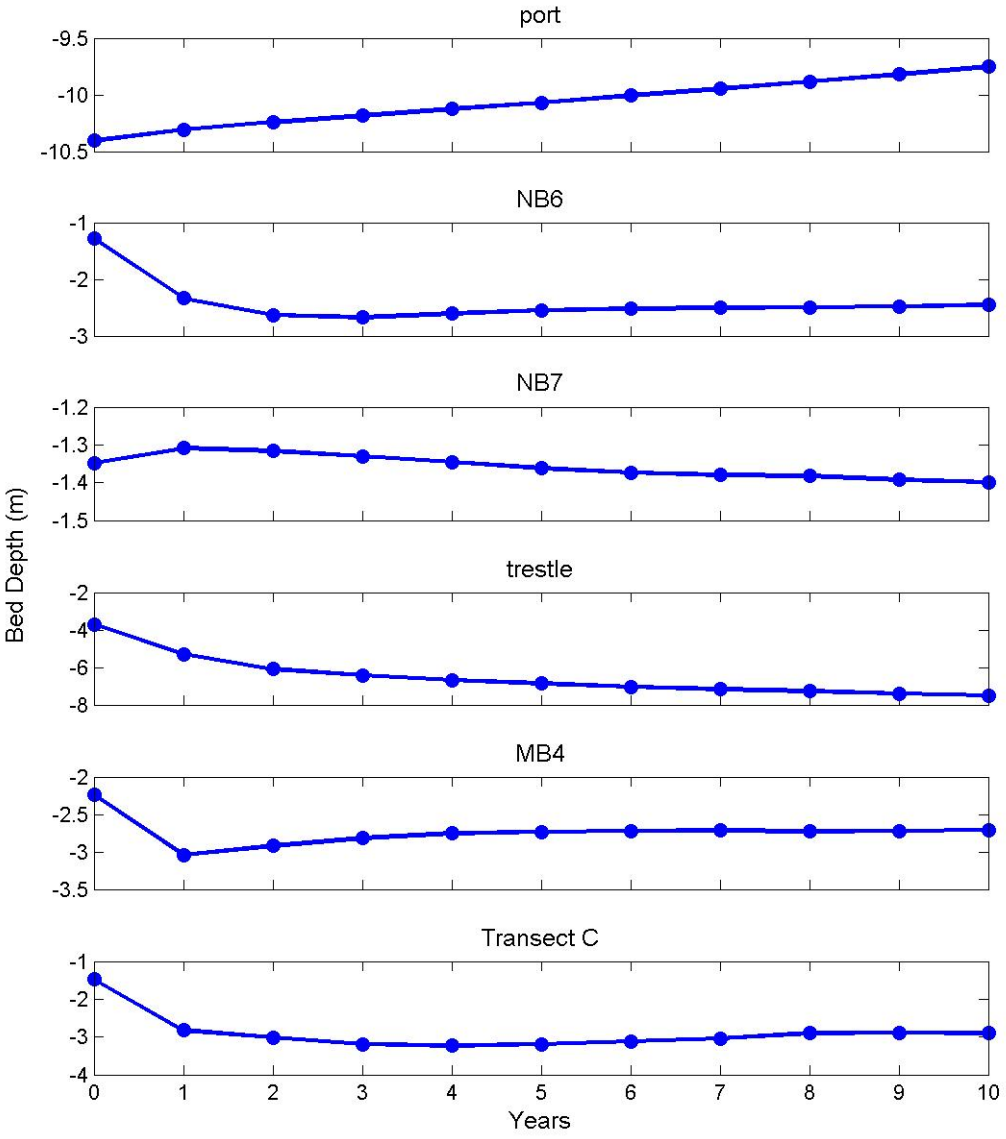

Figure 3.88. Bed depth at selected stations for the Restoration Scenario D estuary under lower erodibility conditions with a lower density of mud (scales vary by station). See Figures 3.27 and 3.41 for locations. The depth of the deepest point along Transect C is monitored in the final panel. With the exception of the port, most bed depth changes occur within the first two to four years. Central North Basin (NB6) shows more net erosion than in Restoration Scenarios A or B, possibly due to the presence of the dike.

CHAPTER 4

Discussion

The hydrodynamic and sediment transport modeling task of the DEFS was charged with answering a series of specific questions about the four alternative estuary restoration scenarios (Box 1.2). The approach to address the queries includes comparison of stimulation results between the predam and restored estuaries as well as comparison among the four restoration scenarios. Current restoration science suggests that the purpose of restoration is not necessarily to recreate a specific historic landscape but to attempt to restore a natural process. Comparisons with both the predam estuary morphology and the processes should help inform decision makers of the potential outcome of the proposed restoration scenarios. A subset of the model output was selected from each of the hydrodynamic/salinity and sediment transport/morphology simulations and has been discussed in this report. Given the inherent uncertainties involved with making predictions about possible future conditions, several limitations to interpreting the model results are identified. Suggestions to help reduce some of these uncertainties are enumerated at the end of this chapter.

Hydrodynamics and Salinity

The hydrodynamic results for the predam and four restored estuaries are similar enough to warrant a discussion simultaneously involving all five simulations. Localized differences related to the specific estuary design produce different results but several observations translate smoothly among the simulations, including velocity fields, inundation and salinity distribution.

In general, circulation patterns show more variation between the predam estuary and restored estuaries immediately after dam removal than among the four restored estuaries. The trestle area is the primary exception. The jet of water exiting the predam estuary is more widespread at comparable speeds of approximately 1 m/s than the jet from the restored estuaries. The outgoing current also does not turn east toward the marina in the predam environment, maybe due to poorly resolved bathymetry. Oppositely rotating

eddies form in North Basin during every flood tide for the predam estuary but only develop at low river flows for the restored estuaries. In North Basin, predam velocities are on average, consistently faster than in any of the restored estuaries. These differences likely result from the overall deeper estuary prior to dam construction as compared to the shallower estuary immediately after dam removal. Except for near the trestle, the restored estuaries have different constrictions than the predam estuary that affect the flow. At the trestle, velocities are slowest for Restoration Scenario B due to the wider opening between Middle and North Basins. The maximum velocity range at the trestle is 1 m/s (Restoration Scenario B) – 1.75 m/s (Restoration Scenarios A, C and D). At Percival Cove, Restoration Scenario C shows the slowest current speed, as a result of the expanded opening; the maximum velocity range is 0.4 m/s (Restoration Scenario C) – 0.7 m/s (Restoration Scenarios A, B and D). The freshwater impoundment in Restoration Scenario D has a negligible effect on velocities through the entrance or trestle as compared to the other scenarios. South of Percival Cove and the trestle region, velocities are similar among the four restored estuaries, with maximum speeds of approximately 1 m/s at the I-5 bridge. The presence of the modern islands in South Basin complicates the circulation patterns in the restored estuaries and, as such, the flow fields are substantially different between the predam and restored estuaries in this area. The overall similarity of circulation and velocity patterns among the restored estuaries indicate that the unique estuary shapes have only a minor impact on the hydrodynamics. Localized changes to the flow are observed where structures around the estuary have been modified.

The predam estuary and all four restored estuaries have a strong tidal influence with little to no difference in the amount of submerged or exposed intertidal flats among the four restoration scenarios. Inundation frequency is different between the predam estuary and the restored estuaries, as the predam estuary is deeper and the bed is inundated more of the time, especially in South Basin. The semi-diurnal tide controls the inundation, regardless of the shape of the restored estuary. Elevations higher than 2 m (MSL) are submerged less than 50% of the year while areas deeper than 4 m (MSL) are underwater at least 80% of the time. Because the shape of the tidal wave does not degrade between the entrance and the Deschutes River, water levels hardly differ among the restored estuary designs. At the peak of a high spring tide (2.1 m MSL), similar tidal inundations are observed for Restoration Scenarios A, B and D on the three-year evolved bathymetry (Figure 4.1). Portions of Tumwater Historical Park and the three islands in South Basin get submerged at this tidal height. As a major finding, however, the difference in hydrodynamics is minimal among the restoration scenarios and full tidal inundation can be expected to occur for a restored estuary.

The Deschutes River discharge influences the water circulation and salinities in the predam and restored estuaries. The intensity of the estuarine circulation differs between the predam and restored estuaries but still produces similar vertical and horizontal density gradients. Near-bed salinities in the predam estuary are 3 – 5 ppt saltier than any of the restored estuaries. The difference is likely related to the predam estuary being deeper than the restored estuaries, allowing larger volumes of marine water to enter the basin. The salinity is still altered by the river but the increased amount of high saline water dilutes the influence of the freshwater. Much smaller differences are seen in the near-bed salinity among the restoration scenarios and most are localized around the shape alterations of each particular estuary. For example, the annual average salinity in North Basin is

slightly less in Restoration Scenario B than in Restoration Scenario A or C due to the wider trestle opening. For Restoration Scenario D, North Basin salinity is the most spatially variable because of the freshwater impoundment modifying the circulation. The differences, while noticeable, do not create radically distinctive estuaries with the range for salinity remaining constant for the four restored estuaries. The annual mean salinity varies from 0 ppt at the river mouth to around 20 ppt in North Basin. A low river flow during the dry season results in a wider range from 0 ppt at the river mouth to above 25 ppt in North Basin. The seasonal variation in salinity as a result of varying river discharges may be important to the biological response of a restored estuary.

Extreme hydrologic events, simulated on three-year evolved bathymetry after the dam is removed for Restoration Scenarios A, B and D only, indicate that large flood events combined with extreme tidal oscillations generate faster velocities throughout the estuary. Event II has the highest velocities of the five events while Event V has the lowest. The current speed differences for Event II are negligible among the scenarios at the I-5 bridge and the Fourth Avenue Bridge, both of which will endure velocities of approximately 5 m/s (Figure 4.2). The wider trestle in Restoration Scenario B reduces the velocity magnitude by at least 0.5 m/s in the region around the trestle. At the Fourth Avenue Bridge outside of the estuary, current speeds for Restoration Scenario D are marginally slower than the other two scenarios, which could be related to the smaller volume of water that is exiting the estuary due to the freshwater impoundment.

The hydrodynamic/salinity results indicate a relatively similar estuary will develop regardless of which restoration scenario is pursued. Velocities at constricted points will be highest for Restoration Scenarios A and C, lowest for Restoration Scenario B and reside in the mid-range for Restoration Scenario D. Inundation for all of the estuaries is tidal-dominated with the river flow altering the water properties, such as salinity. Salinities are nearly constant among the restoration alternatives and will be fresher than those from the predam estuary until the morphology responds. Localized differences in maximum velocity magnitudes will be observed during extreme hydrologic events but the overall impact of the different scenario designs on the hydrodynamics is minor.

Sediment Transport and Morphology Change

Since 1951, when the dam was installed and created a lake environment, sediment transport has been in the form of river floods delivering varying amounts of sediment to the lake. Removal of the dam will restore tidal processes, resulting in significantly different sediment transport and morphological change. Comparing the results from the predam and restored estuary simulations shows a restored Deschutes Estuary would be similar to the predam estuary with comparable, although shallower, bathymetry.

The choice of two erodibility conditions produces a range for sediment flux through the estuary basins. Few discrepancies are observed among Restoration Scenarios A, B and C while Restoration Scenario D shows slightly different behavior resulting from the freshwater impoundment in eastern North Basin. For the lower erodibility condition, the amount of sediment exported in the first year after dam removal from South and Middle

Basins is nearly identical (Figure 4.3). The sediment flux through the entrance and into the port and marina region is approximately 25% larger for Restoration Scenario D than the other restoration scenarios. Nearly identical amounts of sediment pass beyond the port for all of the restoration scenarios, which means more sediment accumulates inside the port for Restoration Scenario D. The amount of sediment flux decreases by 45% of the previous year during the second year after dam removal for all of the basins in each of the restoration scenarios (Figure 4.4). In an indication that dynamic equilibrium is beginning to approach, approximately 55% of the first post-dam year sediment flux occurs during the third year after dam removal (Figure 4.5). The higher erodibility condition erodes more than twice the lower condition but shows a similar decreasing annual percentage. The trends for the higher erodibilities translate across all four restoration scenarios.

The effect of the erodibility conditions on morphological change is evident when the difference is taken between the three-year evolved bathymetries for Restoration Scenario A (Figure 4.6). Approximately 1.5 meters of additional sediment is eroded from Middle Basin under higher erodibility conditions than the lower conditions. Conversely, an additional 2 m of sediment is deposited outside of the estuary and less than 1 m of additional sediment accumulates in North Basin during the higher erodibility. The channel in Middle Basin erodes slightly more under lower erodibility conditions. The emerging spatial pattern is that Middle Basin erodes while North Basin and the region outside of the estuary accrete almost twice as much during higher erodibility conditions. The more intense morphological change could occur as larger amounts of bed sediment become suspended or remain in suspension, which creates a more turbid water column. As this sediment-laden water enters more quiescent areas (eastern North Basin) or deep regions (marina, port), the thresholds for erosion are no longer met and the sediment falls from suspension. The deposition difference between the erodibilities is similar in all of the restored estuaries, and therefore, the behavioral process for the estuaries is assumed to be the same. Tables of annual mean and maximum erosion/deposition and volume change by basin under the lower and higher erodibilities are presented for all four restoration scenarios in Appendix B.

Spatial variability of erodibility conditions within an estuary was not included in the simulations. A primary source of variability is the physical properties of the sediment, such as sediment grain size and water content (Postma, 1967). In addition, biological activity augments the effect from physical properties and can increase or decrease the erodibility depending on how organisms disturb the bed (Jumars and Nowell, 1984). While the physical properties of sediment typically vary across large spatial and temporal scales, the effect from biological activity has been observed to be localized and ephemeral (Wheatcroft and Butman, 1997). As a result, marine sediments with similar properties can respond differently because of a biological overprint. Hence, a variety of erodibilities could co-exist within a restored estuary, producing different results from those examined above. Given the constraints of the model and current state of knowledge, however, the range of model results from the two sets of simulated erodibility conditions can satisfy the needs of the Deschutes Estuary Feasibility Study.

Although the erosion/deposition pattern is similar among the restored estuaries, some localized differences are observed within North Basin and the marina. Restoration

Scenarios B, C and D are each compared to Restoration Scenario A, which is the least modified of the restored estuaries, by subtracting the three-year evolved bathymetries (Figure 4.7). The wider trestle opening in Restoration Scenario B allows an additional 0.5 to 1.5 m of erosion in North Basin while the area under the narrower trestle opening erodes at least 2 m more in Restoration Scenario A. The difference between Restoration Scenarios A and C is an almost imperceptible additional 0.5 m of erosion east of the wider Percival Cove bridge opening. Spatially, the largest difference is seen between Restoration Scenarios A and D. Depositional patterns in Restoration Scenario D are heavily influenced by the freshwater impoundment that reduces the area of North Basin by almost 50%. Consequently, an additional 0.5 to 1.5 m of sediment is exported from the estuary and accumulates in the marina. However, the erosion/deposition pattern in the restored estuaries is more sensitive to the erodibility conditions than the restored estuary designs.

The evolution of sediment grain size in the channels and on the flanks show recurring patterns across all four scenarios. Channels consistently coarsen as sand fractions increase and off-channel zones get finer with increasing percentages of silt and clay. The sediment grain size changes are sensitive to the erodibility conditions. Higher erodibility conditions cause more rapid coarsening of the channels and some spatial differences as compared to lower erodibility conditions. In general, the bed sediment distributions for Restoration Scenarios A, B and C converge to a nearly identical equilibrium. Clay content in the estuary is low, the silt and sand fractions are inverse distributions with silt on the flanks and sand in the channels, and gravel amounts are high in small localized areas. For example, central North Basin is sandy in the main channel and silty on the flats but the amount of sand appears to be controlled by the erodibility. The ease of winnowing the finer grain sizes from the sand is most likely the controlling process, i.e., higher erodibility will remove more silt and clay than lower erodibility conditions. Western North Basin in Restoration Scenario D shows marginally less silt and clay and higher sand fractions along the freshwater impoundment retaining wall. Overall, the degree of sandy channels and muddy flats is similar for the four estuaries and varies more with the erodibility than with the restored estuary design.

Port and Marina Sedimentation

The downstream positioning and deeper depths of the port and marina create a region where sediment accumulates after dam removal. Approximately 50% of the total deposition in the port and marina during three years occurs in the first post-dam year for both erodibility conditions in all four restoration scenarios. Uncertainty in the erodibility conditions for mud prevents an absolute value from being associated with each restored estuary design and the amount of accumulated sediment after three years varies more by erodibility than by scenario. For example, the deposited volume ranges from approximately 125,000 m^3 (Restoration Scenarios A, B and C) to 170,000 m^3 (Restoration Scenario D) under lower erodibility conditions (Figure 4.8). For the higher erodibility conditions, the volume more than doubles for Restoration Scenarios A, B and C to approximately 280,000 m^3 while Restoration Scenario D increases to 360,000 m^3.

Long-term Morphologic Change

The amount of sediment moving through the estuary basins varies each year after dam removal. The changes can be attributed to an initial response of the lake bed to new hydrodynamic forces – the tides and a free-flowing Deschutes River – followed by the new estuary bed adjusting towards a dynamic equilibrium. Each successive year of exposure to the new hydrodynamic forces reshapes the remnants of the lake environment. As seen in the bed levels at observation stations during 10 years of evolution, the majority of change occurs within two to four years. The volume change of the three basins and between the estuary entrance and northern edge of the port are calculated for the 10-year morphologic simulations (Figure 4.9). These simulations were conducted under lower erodibility conditions with a loose density of mud. Tables of annual mean and maximum erosion/deposition and volume change by basin are presented for Restoration Scenarios A, B and D in Appendix B. Several insights can be gleaned from the evolution of various parts of the estuary for the different restoration scenarios.

One of the first observations is the volume change in South and Middle Basin hardly varies for the restoration scenarios (Figure 4.9). Restoration Scenarios A and B also evolve nearly identically in North Basin and in the Port and Marina region, although slightly more erosion occurs in North Basin for Restoration Scenario B. North Basin in Restoration Scenario D shows a small net volume decrease of 1,500 m^3 while approximately 200,000 m^3 more sediment accumulates in the port and marina region.

The second observation is that the rate of change is different for each of the four areas. The port and marina region captures 100,000 to 150,000 m^3 of sediment in the first year and then approximately 35,000 to 40,000 m^3 annually after year five. North Basin accretes by almost 60,000 m^3 in the first year for Restoration Scenarios A and B before leveling to a fairly uniform annual accumulation of roughly 5,500 m^3 after year five. In Restoration Scenario D, however, North Basin accumulates 17,000 m^3 in the first year before an average erosion rate of 2,700 m^3/yr removes most of the sediment. The rate of change in Middle Basin is consistent for all three restoration scenarios with a severe erosion of 135,000 m^3 in the first year followed by a gradually decreasing pace, eventually reaching approximately 10,000 m^3/yr after year five. The rate of change in South Basin, which also shows constant behavior among the restoration scenarios, indicates an initial removal of 13,000 m^3 in the first year and an average annual accretion rate of less than 3,500 m^3 after year five.

Together, the two sets of observations suggest a restored estuary will have two phases of adjustment. The first phase will be one of rapid adjustment for the first three to five years after dam removal, regardless of the restoration scenario. Large amounts of sediment get removed from Middle Basin while North Basin accretes a sizeable portion of the liberated sediment (less is garnered in the North Basin of Restoration Scenario D). The port and marina region absorbs the majority of the sediment. Five years after dam removal and restored estuarine processes, rates of change have leveled slightly and the three estuarine basins appear to be a dynamic equilibrium. South Basin collects enough sediment after 10 years, 25,000 m^3, to produce a net volume change almost equal to the 13,000 m^3 initially lost. Middle Basin loses almost 250,000 m^3 of sediment during the same time frame. Erosion from Middle Basin is as steady as accretion in North Basin with the excess sediment passing downstream to the port and marina region. By the end

of a decade, North Basin in Restoration Scenarios A and B accretes more than 100,000 m^3 and the port and marina region accumulates 450,000 m^3. Under Restoration Scenario D, though, the port and marina collects 560,000 m^3 of sediment, a reminder of how the freshwater impoundment affects the estuary.

The erosion of Middle Basin contrasts sharply with the accretion in North Basin for Restoration Scenarios A and B. Yet, the possibility of opposite behaviors inside the restored estuary is within reasonable expectations. During the dammed phase of the estuary (1951 – present), the daily hydrodynamics are limited to river activity. The river discharges into a standing basin of water and the lake accumulates sediment until the available space is depleted, limiting further deposition. Additional sediment will bypass the first areas and begin accumulating in locations available downstream. The region between the water surface and the bed elevation becomes a repository for sediment but only if energy levels allow accumulation. Also known as the accommodation space, the volume decreases as sediment accumulates during quiescent periods and increases as sediment erodes during higher energy times (Woodroffe, 2002). Thus, the accommodation space of South Basin could be considered full and sediment is bypassing the basin to accumulate in Middle Basin. However, a dramatic shift occurs when tidal-dominated hydrodynamics return in a restored estuary, creating a substantially more energetic environment than the river-dominated lake. The broad, shallow flanks of Middle Basin can no longer maintain the quantities of sediment that have built up when subjected to the processes of a restored estuary. Conversely, North Basin, which is deeper and has large portions that remain submerged during low tide, provides the accommodation space for the sediment being removed upstream. The process is both redistributing sediment inside a restored estuary and conveying additional sediment from the Deschutes River. While estuaries in general are constantly in a state of flux as they respond to flood events, sea level change and tectonic activity (Davis, 1978; Cooper, 2002), readjustment after significant anthropogenic perturbations should be expected to occur.

The long-term volume change in South Basin also appears to behave paradoxically. The 13,000 m^3 of sediment initially lost increases the accommodation space. The next nine years of sedimentation is filling the newly available regions throughout the basin, which under the new tidal-dominated energy regime may be in previously unusable areas. Effectively, the accommodation space is larger and different parts of the basin can trap sediment in the South Basin of a restored estuary.

After 10 years of restored estuarine processes and morphologic change, the bathymetry of the restored estuaries evolves to be strikingly comparable to the bathymetry of the predam estuary (Figure 4.10). In North Basin, the bifurcated channel and shoal between the channels are very noticeable in the predam and Restoration Scenarios A and B estuaries but less evident in the Restoration Scenario D estuary. The depression in the northeastern quadrant of North Basin is deeper in the predam estuary compared to the Restoration Scenarios A and B estuaries. Although better defined and slightly deeper for the restored estuaries, the channel meandering through Middle Basin has a similar shape between the historic and simulated estuaries. The flanks of Middle Basin are shallower in the predam estuary by less than 0.5 m. South Basin is the most radically different between the predam and restored estuaries as the I-5 bridge constriction has

fundamentally altered this basin. However, South Basin evolves nearly identical bathymetry for each restored estuary. In general, though, the 10-year evolved bathymetry predicts a restored estuary with similar morphology to the predam estuary, especially through Middle Basin.

The evolved bathymetry allows some speculation about the hydrodynamic controls over the morphology. For example, the North Basin shoal could be a flood-tidal delta or a large braid bar. The likelihood that a flood-tidal delta forms is quite high if the estuary morphology is suspected to be tidally-dominated. However, large flood events could rework the bed sediment and cause more permanent changes by redirecting channel alignment. Further, the initial bathymetry, taken from modern Capitol Lake, could predispose the formation of the shoal, regardless of the hydrodynamics. Similar to spatial variability allowing multiple erodibilities to co-exist, the morphology is probably controlled by a combination of tidal and river forces. The interaction between the two forces could vary within the estuary, yielding perhaps a river-dominated South Basin, a transition zone in Middle Basin and a tidal-dominated North Basin. Any restored estuary could be expected to be an environment frequently in flux with constantly changing energy relationships.

Conclusion

The sediment transport/morphology simulations reveal that more variation is produced by uncertainties in the erodibility of mud than by the individual restoration scenarios. Despite these uncertainties, some consistent trends in the behavior of the restored estuary simulations include sandier channels, muddier flanks and gradually decreasing rates of volume change after the dam is removed. In general, Restoration Scenarios A, B, and C are negligibly different while Restoration Scenario D shows slightly more sediment being exported to the port and marina region. Long-term morphological simulations show the development of a restored estuary with similar bathymetry to the predam environment.

Limitations to Interpretation of the Results

Predictions of sediment transport in general, and specifically long-term predictions of mud transport and morphological change, contain many uncertainties. As explained in Chapter 2, several techniques were employed to limit or at least characterize these uncertainties and data shortcomings. Compromises made during model design and operation and limitations from field observations must be understood to retain confidence in the simulation results. The limitations that emerged can be divided into two source categories: 1) model design and operation and, 2) data input. A list enumerating the specifics in each category is below.

1) Model design and operation
    a. Use of the ‘morphological tide’ in sediment simulations – the benefits of coupling the complexity of the semi-diurnal tide with flood events has not been examined. Aligning discharges at particular stages of the tide to statistical significance could prove to be unachievable, however.

b. Selection of the number of sediment classes and sediment sizes – four sediment grain size classes were selected to characterize the sediment on the bed and in the river although the field data showed a wide range of sediment sizes in the lake. Specific sediment sizes were picked to represent each class but any number of other sizes within the sediment class could be purported to be as appropriate. Sensitivity of the final results to the number of size classes or the grain sizes chosen for each class was not explored though not believed to be large.
c. Depth of surface sediment mixing layer – for model stability, a value of 0.1 m was used as the depth of surface sediment mixed layer, which allows all sediment classes within that vertical zone to be active in sediment transport. In actuality, the surface sediment mixing depth may be smaller, resulting in different percentages of the sediment grain sizes remaining on the bed. While the trends in bed grain size evolution are probably accurate, the actual percentage of each class after several years may not be.
d. Averaging historical conditions – the Deschutes River hydrograph was deconstructed to reduce the high frequency noise of the data and produce representative climates ('salinity' and 'morphological' rivers). The river climatology assumes that future conditions will resemble those from the historical average. Another approach could have been to explore the effects of extreme conditions of flooding and drought on the morphological response.
e. Depth-averaged vs. 3-D simulations for sediment – the simplest hydrodynamic runs, without the additional calculations for sediment transport, required more than 200 hours of computational time to produce only one year of simulated time. To conduct long-term morphology runs would increase the computational time but the effect of estuarine circulation on sediment transport could be investigated. Given other uncertainties in the sediment transport calculations, the increase in model efficiency from employing a depth-averaged model seems justified.
f. Sensitivity of sediment transport to flocculation parameter – the selection of 10 ppt for maximum flocculation was based on scientific literature from the laboratory but laboratory results only marginally reflect *in situ* processes. Varying the flocculation parameter would not likely cause significant differences to the deposition patterns though some differences may result.
g. Bed roughness – bed roughness can vary spatially and depends on the size and distribution of small to medium scale bed morphology. Typically, bed roughness is a parameter that is adjusted to match model velocity with measured field data during the model calibration process. Since there was no model calibration for the restored estuary, the default bed roughness was selected. Numerous studies of estuarine hydrodynamics suggest that the default bed roughness values are acceptable and variation in roughness will have little effect on final morphodynamics.
h. Order of the wet-dry seasons and flood events within the wet season for the 'morphological river' – the river discharge time series input to the model leads with the wet season, causing the lake bed to be subjected to

large flood events first and then a long dry season. In addition, the flood events commence with the largest flow and each event is successively smaller. The effect that reordering the river flood events has on the resulting morphological response is unknown, though not believed to be large.

2) Data input
    a. Erodibility of the bed – a characteristic of the lakebed that could be measured in the field, erodibility of the lake sediment was not determined. Learning the spatial variability of this parameter would greatly improve the results by containing the range of erodibilities necessary to simulate. Another important factor for erodibility is biological feedback and, while presently not replicable in the model, biological effects are documented in scientific literature to have substantial influence on bed erodibility.
    b. Rating curve for Deschutes River – the rating curve applied to create the 'morphological river' was calculated in the 1970s during different usage of the watershed, including a larger intensity of logging. Urbanization, irrigation and other anthropogenic activities have affected the river sediment load in unknown ways. A modern rating curve would provide a better estimate of the present sediment load to the lake and possible future estuary.
    c. Surface sediment grain size information – Percival Cove, Budd Inlet and the upper reaches of South Basin were not sampled for surface sediment, causing large gaps in the initial sediment size distribution maps, such as no bed distributions outside of the modern lake. Higher density sampling in several areas of Middle Basin would also improve the initial sediment maps.
    d. Variation of sediment grain size with depth in the bed – a comprehensive coring effort would provide reliable information about the underlying stratigraphy, which could have large implications for erodibility of the sediment through time.
    e. Omission of Percival Creek – the lack of reliable data prevented placing a freshwater source into Percival Cove, affecting the salinity and flocculation in this area of the model.
    f. Wind and waves – simple wind and wave fields were developed to initialize the simulations. While wind data from the Olympia Airport are available, wave information from Budd Inlet was not available to set up the estuary. Stirring by the wind and waves may affect the density structure and turbidity of the water column as well as the net sediment transport.

Future considerations

The list of limitations identifies many areas for possible improvement to help reduce the uncertainties in the model predictions. Restrictions on resources and data will always be present but three topics warrant attention: developing a modern rating curve for the Deschutes River, gathering sediment grain size information in deficient regions and determining the erodibility of the bed. Each of these would have a noticeable impact on

reducing the uncertainty in the results. A new rating curve could change the amount of sediment entering the system and would more accurately reflect the present watershed conditions should a restoration be executed. Additional sediment grain size information, especially in South Basin, Percival Cove and outside the modern lake in Budd Inlet, would improve estimations related to the net transport of sediment in or out of a restored estuary.

Identifying the bed erodibility with field data would constrain the results that show more sensitivity to erosion conditions than restored estuary design. Because the factors that influence erodibility are numerous and cannot be reliably predicted, direct measurements are needed to characterize local erodibility for accurate predictions of sediment transport (Black et al., 2002). Several experimental apparatus have been designed to measure sediment erodibility. One such apparatus is a "Gust erosion chamber" (Gust and Muller, 1999; Thomsen and Gust, 2000). The device is comprised of a chamber, motor, pump and control unit. The chamber fits directly on the top of a sediment core tube, and uses a rotating plate to generate known and relatively spatially uniform stresses on the sediment surface. Using a "Gust Chamber" type device on newly collected cores in Capitol Lake would greatly reduce the uncertainty associated with characterizing the erodibility of the bed.

Another area of consideration is the condition of the lakebed between the current study and restoration, should the lake be returned to an estuary. The sediment transport/morphology simulations were conducted on lake bathymetry collected in 2004 and 2005. Given the volume of sediment entering the lake annually, the depth of the lake may change significantly in under a decade. Alternately, if a lakewide dredge occurs before the dam is removed, the initial bathymetry and sediment grain size distributions would be substantially different. Any large bathymetric change reduces the efficacy of the hydrodynamic and sediment transport modeling results and additional modeling would be prudent.

The development of the many different simulations for the Deschutes Estuary Feasibility Study offers a wide spectrum for future uses. As new questions emerge and management priorities shift, additional queries that have not yet been considered can be made. Local concerns about contaminant fate and pollution dispersion can be investigated, relying on the hydrodynamics and fine sediment transport portions of the existing model. An examination of water quality during various seasons or river flows could be conducted. Should speculation that climate change will affect the behavior of the Deschutes River, a new hydrograph can be developed and utilized. If the effects of sea level rise in the Deschutes Estuary and Budd Inlet provoke new interest, the model can be adjusted to simulate higher water levels. Any number of environmental and ecological investigations can be undertaken with additional data, improved modeling techniques and clearly formulated questions.

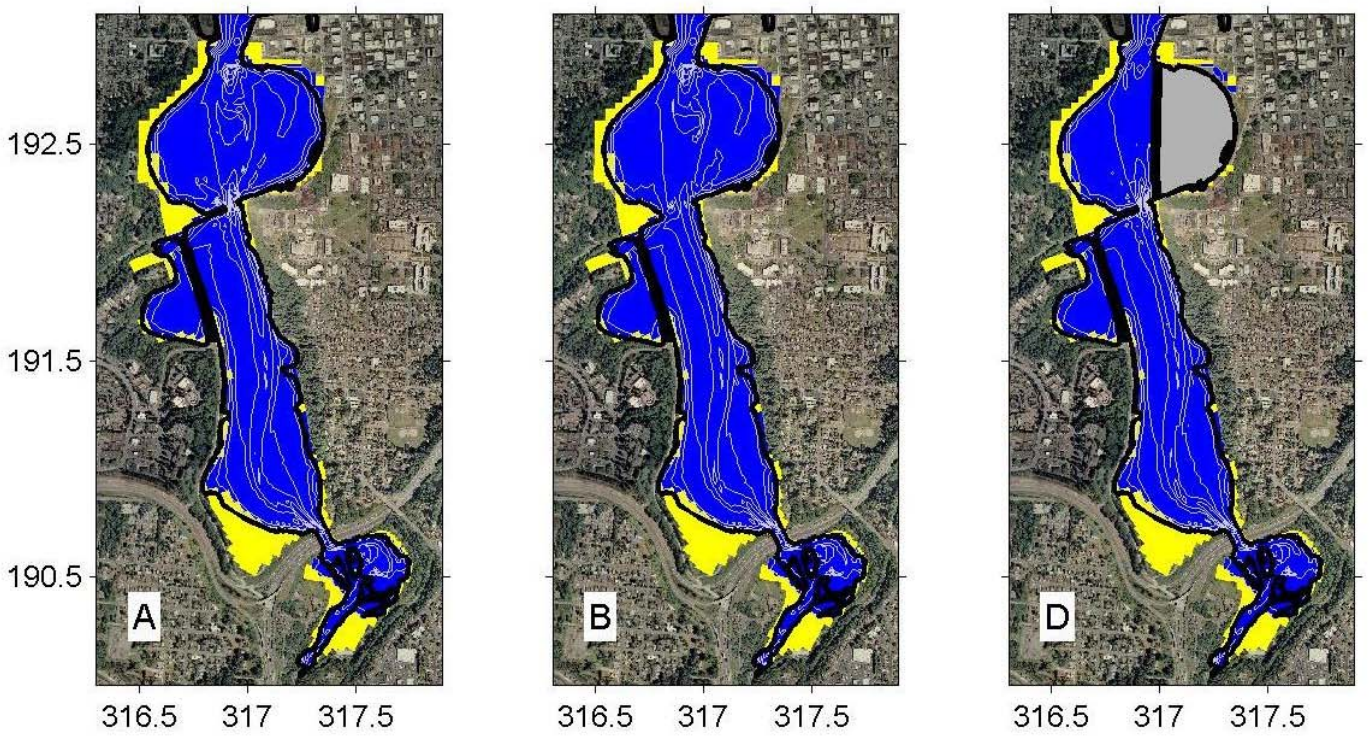

Figure 4.1. Areas of inundation at a 2.1 m high tide for three-year evolved bathymetry in the Restoration Scenarios A, B and D estuaries. Blue is submerged and yellow is not. The shape of the estuary does not appear to affect the inundation pattern.

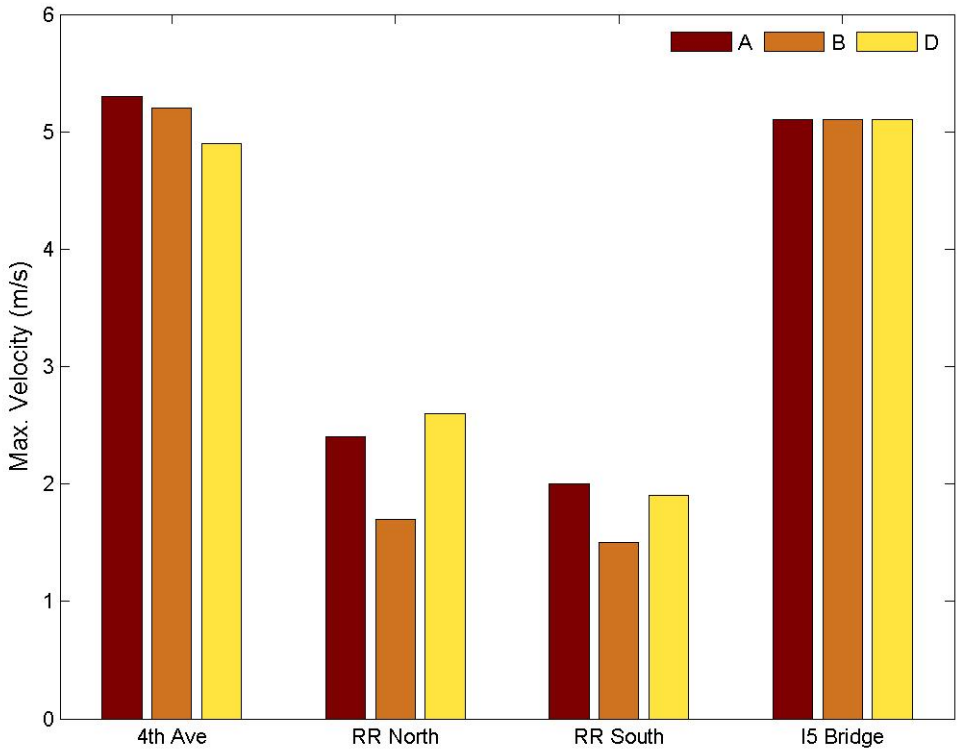

Figure 4.2. Maximum velocities observed during Event II at four observation stations. See Figure 3.27 for locations. The wider trestle in Restoration Scenario B decreases the current speed around the trestle.

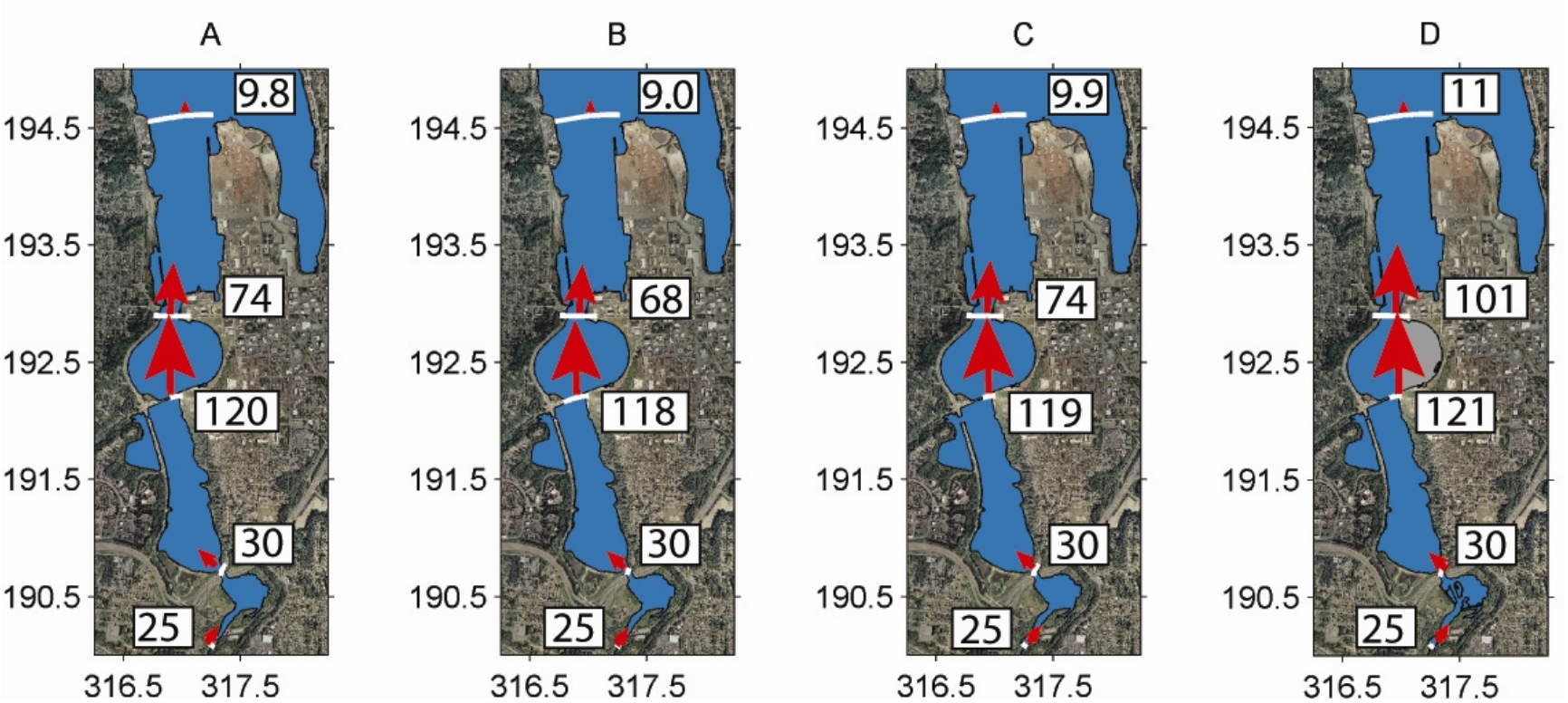

Figure 4.3. Sediment flux (x10^3 m^3) through cross-sections one year after dam removal for the four restoration scenarios under the lower erodibility condition. The initial bed response produces similar amounts of sediment flux from South and Middle Basins among the restoration scenarios. Restoration Scenario D shows a slightly larger flux from North Basin and into Budd Inlet. The design of the restored estuaries has an overall minimal effect on the sediment flux.

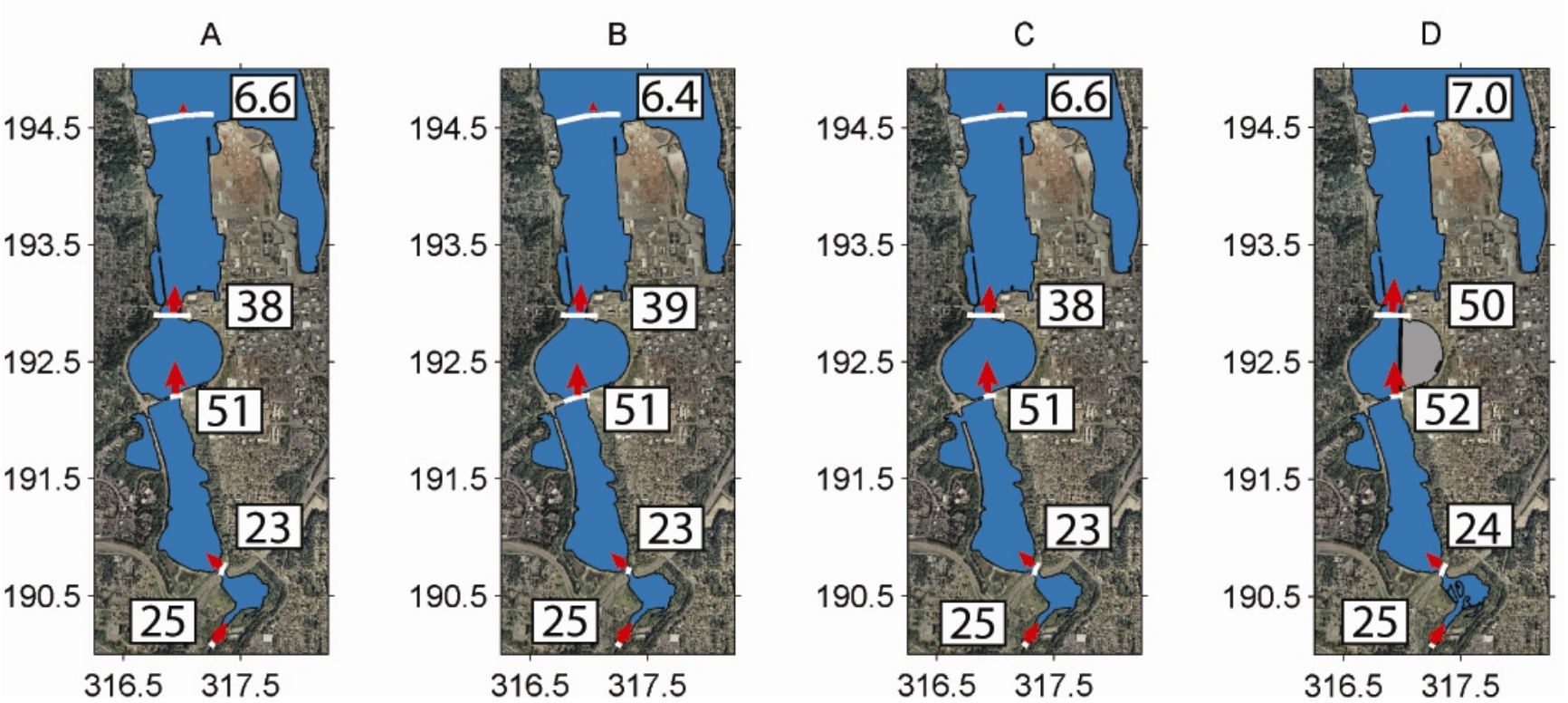

Figure 4.4. Sediment flux (x10^3 m^3) through cross-sections two years after dam removal for the four restoration scenarios under the lower erodibility condition. The initial bed response produces similar amounts of sediment flux from South and Middle Basins among the restoration scenarios. Restoration Scenario D shows a slightly larger flux from North Basin and into Budd Inlet. The amount of sediment passed through the cross-sections is approximately 45% less than during the first post-dam year. The design of the restored estuaries has an overall minimal effect on the sediment flux.

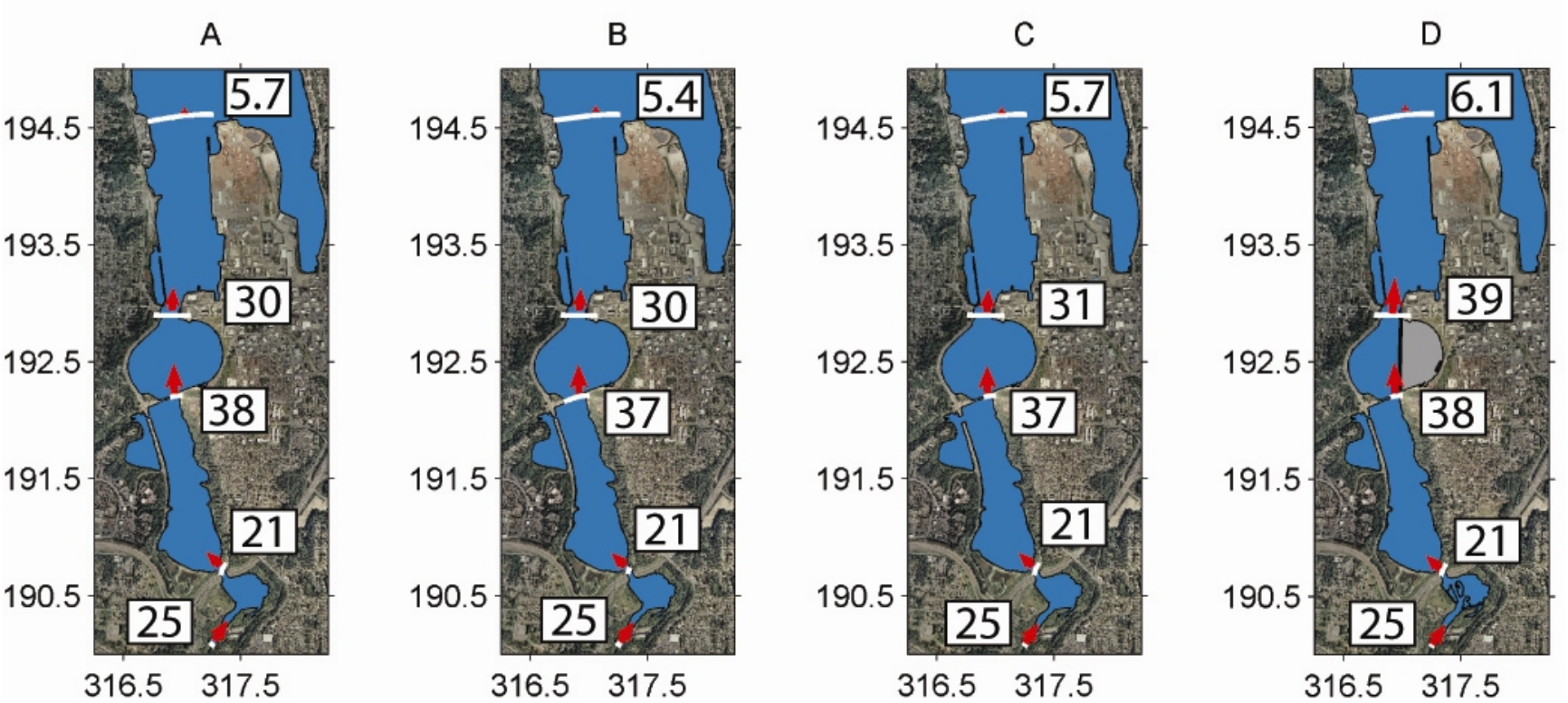

Figure 4.5. Sediment flux (x10^3 m^3) through cross-sections three years after dam removal for the four restoration scenarios under the lower erodibility condition. The initial bed response produces similar amounts of sediment flux from South and Middle Basins among the restoration scenarios. Restoration Scenario D shows a slightly larger flux from North Basin and into Budd Inlet. The amount of sediment passed through the cross-sections is 55% less than during the first post-dam year. The I-5 cross-section passes less sediment than that supplied by the Deschutes River, indicating accretion in South Basin. The design of the restored estuaries has an overall minimal effect on the sediment flux.

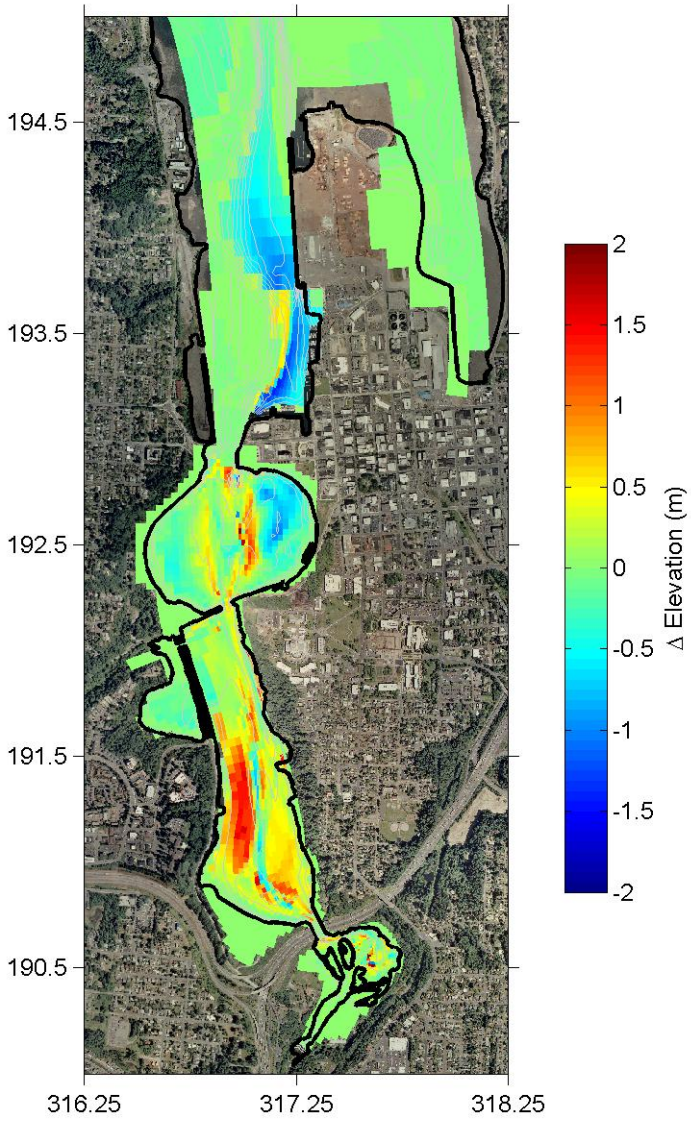

Figure 4.6. Difference between the final bathymetries of the lower and higher erodibilities after a three-year simulation in the Restoration Scenario A estuary. See Figures 3.28 and 3.37 for the lower and higher erodibility cumulative erosion/deposition, respectively. Red shows more erosion associated with the higher erodibility (or less deposition associated with the lower erodibility) and blue shows more deposition associated with the higher erodibility (or less erosion associated with the lower erodibility). Most of the deposition occurs within the estuary for the lower erodibility compared to in the port and marina for the higher erodibility.

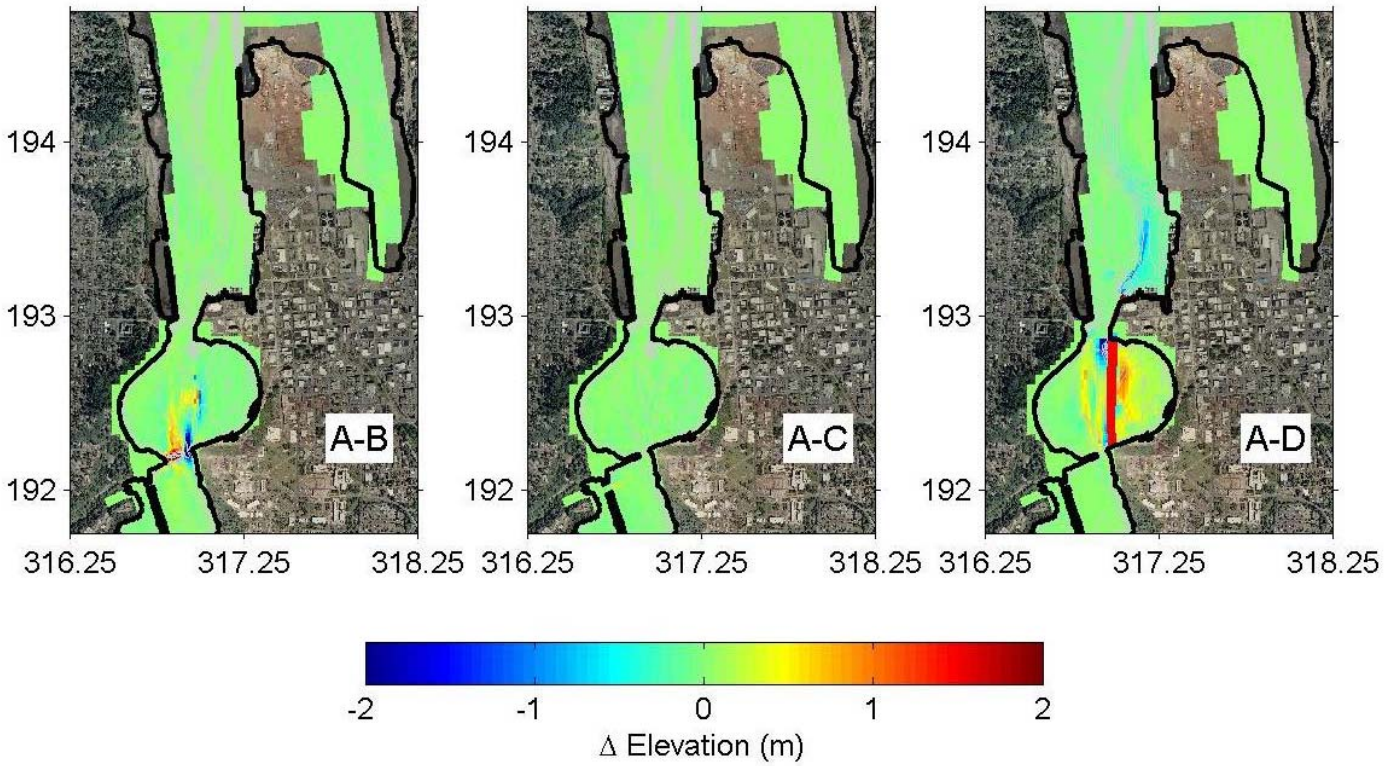

Figure 4.7. Difference between the three-year evolved bathymetry of the Restoration Scenario A estuary and each of the other three restored estuaries under the lower erodibility condition. Red indicates more deposition associated with Restoration Scenario A or more erosion associated with Restoration Scenarios B, C and D. Blue shows more erosion associated with Restoration Scenario A or more deposition associated with Restoration Scenarios B, C and D. The differences between Restoration Scenario A and Restoration Scenarios B and C are localized while the freshwater impoundment in Restoration Scenario D forces sediment to bypass the North Basin and deposit in the port and marina region instead of accumulating inside the basin as in Restoration Scenario A.

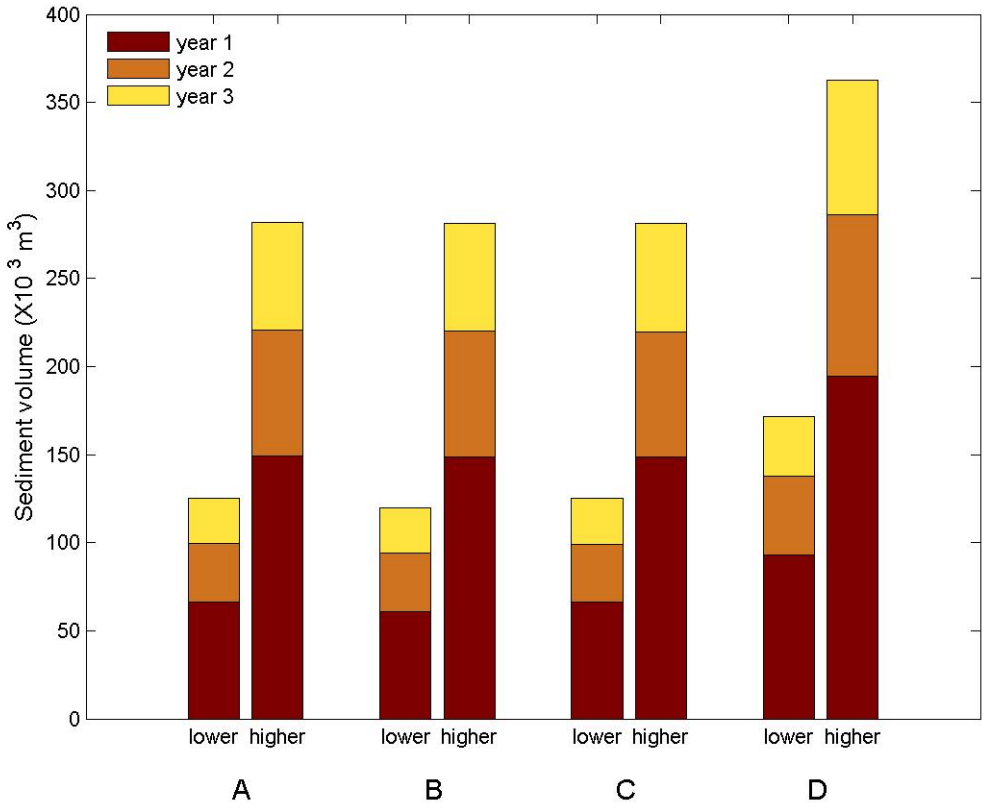

Figure 4.8. Ranges of sediment volume (x10^3 m^3) accumulated in the port and marina region during the first three years after dam removal for both erodibility conditions in the four restoration scenarios (A, B, C, D). Most of the change in volume occurs during the first year in all the restoration scenarios. Uncertainty in the erodibility provides a range of sediment volumes accumulated for each restored estuary design.

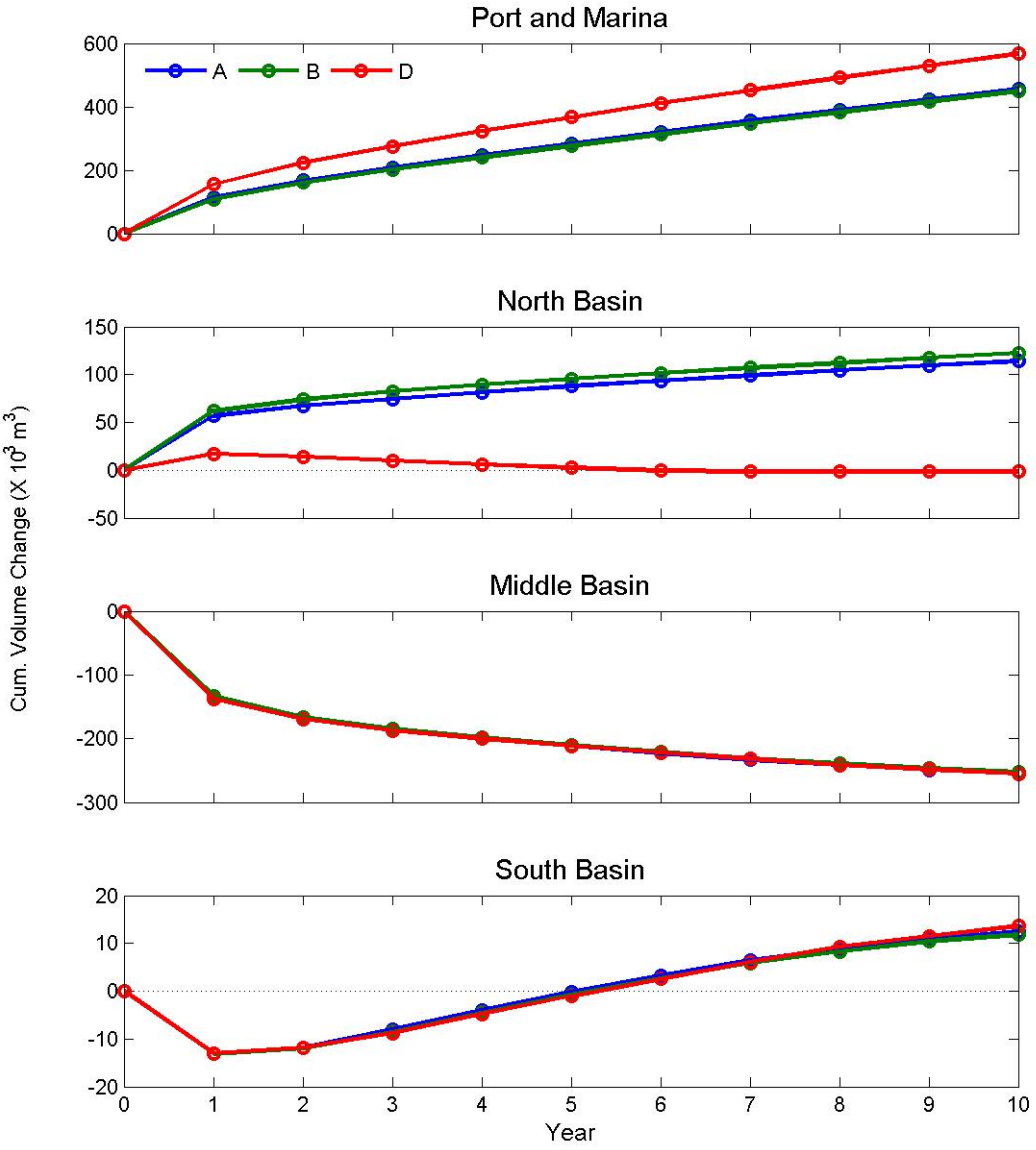

Figure 4.9. Cumulative volume change in four regions of a restored estuary for the 10-year morphological simulations under lower erodibility conditions with a looser density of mud. Restoration Scenario A is blue, Restoration Scenario B is green and Restoration Scenario D is red. Negative numbers indicate erosion and positive numbers indicate accretion in a basin. Minimal differences are observed among the scenarios in South and Middle Basins. The effect of the wider trestle opening (Restoration Scenario B) on the volume of North Basin is less than the freshwater impoundment (Restoration Scenario D). The sediment that would accumulate in eastern North Basin is likely deposited in the Port and Marina in Restoration Scenario D, which accounts for the larger volume change in the top panel.

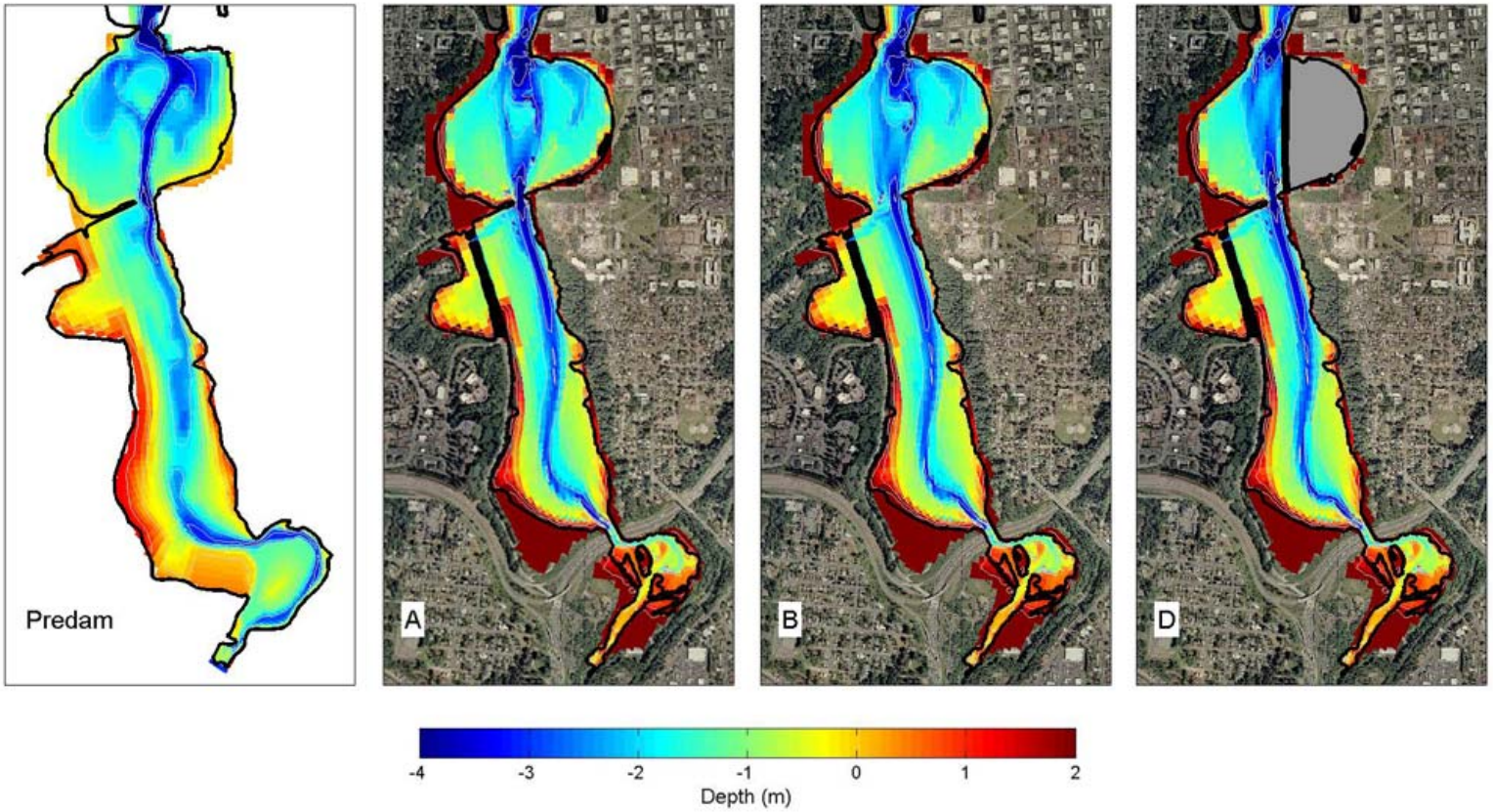

Figure 4.10. Initial predam bathymetry contrasted with the final bathymetry in the Restoration Scenarios A, B and D estuaries after 10 years of morphological simulations under lower erodibility conditions with a looser density of mud. In all three restored estuaries, a defined channel meanders from the I-5 bridge to the trestle. The bathymetry of North Basin is most affected by the different designs, with two channels in Restoration Scenario A, a broader and shallower set of channels in Restoration Scenario B and a slightly braided channel in Restoration Scenario D. Similar features to the predam bathymetry have evolved in the restored estuaries, particularly in Restoration Scenarios A and B. The bifurcated channel of comparable depths in North Basin indicates that a restored estuary similar to the predam environment may develop.

References

Amos, C. L., Feeney, T., Sutherland, T. F., Luternauer, J. L., 1997. The stability of fine-grained sediments from the Fraser River delta. *Estuarine, Coastal and Shelf Science.* Vol. 45, 507-524.

Andersen, T.J., 2001. Seasonal variation in erodibility of two temperate, microtidal mudflats. *Estuarine, Coastal and Shelf Science*. Vol. 53, 1-12.

Black, K. S., Tolhurst, T. J., Paterson, D. M., Hagerthey, S. E., 2002. Working with natural cohesive sediments. *Journal of Hydraulic Engineering*. Vol. 128, 2-8.

CLAMP Plan 2003 – 2013, 2002. Thurston Regional Planning Council.

CLAMP Technical Work Group, 2006. Deschutes Estuary Feasibility Study Restoration Criteria. 5 pp.

Cooper, J.A.G., 2002. The role of extreme floods in estuary-coastal behaviour: contrasts between river- and tide-dominated microtidal estuaries. *Sedimentary Geology*. Vol. 150, 123-137.

Dade, W.B., Nowell, A.R.M., Jumars, P.A., 1992. Predicting erosion resistance of muds. *Marine Geology*. Vol. 105, 285-297.

Davis, R.A. (Ed.), 1978. *Coastal Sedimentary Environments*. Springer-Verlag, New York, 413 pp.

de Deckere, E. M. G. T., Tolhurst, T. J., de Brouwer, J. F. C., 2001. Destabilization of cohesive intertidal sediments by infauna. *Estuarine, Coastal and Shelf Science*. Vol. 53, 665-669.

De Vriend H.J., Capobianco M., Latteux B., Chesher T., Stive M.J.F., 1993. Long-Term Modelling of Coastal Morphology: A Review, In: H.J. de Vriend (Ed.), Coastal Morphodynamics: Processes and Modelling. *Coastal Engineering*. Vol. 21, 225-269.

Einsele, G., Overbeck, R., Schwarz, H. U., Unsold, G., 1974. Mass physical properties, sliding and erodibility of experimentally deposited and differently consolidated clayey muds. *Sedimentology*. Vol. 21, 339-372.

Entranco 1984. Capitol Lake restoration analysis. Entranco Engineers. Bellevue, WA, 165 pp.

Eshleman, J., Ruggiero, P., Kinsley, E., Gelfenbaum, G., and George, D., 2006. Capitol Lake, Washington 2004 data summary. USGS Data Series report.

Garono, R.J., Thompson, E., Koehler, M., 2006. Deschutes River estuary restoration study: Biological conditions report. Earth Design Consultants, Inc. 138 pp.

Gelfenbaum, G., Roelvink, J.A., Meijs, M., Buijsman, M. and Ruggiero, P., 2003. Process-based morphological modeling of Grays Harbor inlet at decadal timescales. *Proceedings Coastal Sediments 03*. St. Petersburg, FL.

Grant, J., Gust, G., 1987. Prediction of coastal sediment stability from photopigment content of mats of purple sulphur bacteria. *Nature*. Vol. 330, 244-246.

Gust, G., Müller, V., 1999. Interfacial hydrodynamics and entrainment functions of currently used erosion devices. In: Burt, N. et al., (Eds.), *Cohesive Sediments*, 149-174.

Hill, P. S., 1998. Controls on floc size in the sea. *Oceanography*. Vol. 11, 13-18.

Hjulstrom, F., 1939. Transportation of detritus by moving water. In: Trask, P.D., (Ed.) *Recent Marine Sediments*, 5-31.

Jumars, P.A., Nowell, A.R.M., 1984. Effects of benthos on sediment transport: difficulties with functional grouping. *Continental Shelf Research*. Vol. 3, 115-130.

Latteux, B., 1995. Techniques for long-term morphological simulation under tidal action. *Marine Geology*. Vol. 126, 129-141.

Lelieveld, S.D., Pilditch, C.A., Green, M.O., 2003. Variation in sediment stability and relation to indicators of microbial abundance in the Okura Estuary, New Zealand. *Estuarine, Coastal and Shelf Science*. Vol. 57, 123-136.

Lesser G. R., Roelvink J. A., Van Kester, J. A. T. M., Stelling, G. S., Lakhan, V. 2004. Development and validation of a three-dimensional morphological model. *Coastal Engineering*. Vol. 51, 883-915.

Lesser, G., Kester, J., Roelvink, J.A., 2000. On-line sediment transport in Delft3D-Flow. Report Z3899, Delft Hydraulics, Delft, The Netherlands

Mih, W., Orsborn, J., 1974. Sediment removal and maintenance system for the upper basin of Capital Lake Olympia, Washington. Preliminary Report, Washington State University, Pullman, WA, 33 pp.

Paterson, D.M., Tolhurst, T.J., Kelly, J.A., Honeywill, C., de Deckere, E.M.G.T., Huet, V., Shayler, S.A., Black, K.S., de Brouwer, J., Davidson, I., 2000. Variations in sediment properties, Skeffling mudflat, Humber Estuary, UK. *Continental Shelf Research*. Vol. 20, 1373-1396.

Postma, H., 1967. Sediment transport and sedimentation in the estuarine environment. In: Lauff, G.H., (Ed.), *Estuaries*, 158-179.

Rhoads, D.C., Yingst, J.Y., Ullman, W.J., 1978. Seafloor stability in central Long Island sound. In: Wiley, M.L. (Ed.), *Estuarine Interactions*, 221-260.

Roelvink, J.A., 2006. Coastal morphodynamic evolution techniques. *Coastal Engineering*. Vol. 53, 277-287.

Stelling, G.S., Wiersma, A.K., Willemse, J.B.T.M., 1986. Practical Aspects of Accurate Tidal Computations. *Journal of Hydraulic Engineering*. Vol. 112, 802-817.

Stevens, A.W., Wheatcroft, R.A., Wiberg, P.L., In Press. Sediment erodibility along the western Adriatic margin, Italy. *Continental Shelf Research.*

Sutherland, J., Walstra, D. J. R., Chesher, T. J., van Rijn, L. C. and Southgate, H. N., 2004. Evaluation of coastal area modelling systems at an estuary mouth. *Coastal Engineering*. Vol. 51, 119-142.

Thomsen, L., Gust, G., 2000. Sediment erosion thresholds and characteristics of resuspended aggregates on the western European continental margin. *Deep-Sea Research I*. Vol. 47, 1881-1897.

URS Group, Inc. 2003. Capitol Lake floodplain analysis. 31 pp.

van Rijn, L., 1993. Principles of sediment transport in rivers, estuaries, and coastal seas. Aqua Publications, The Netherlands, 715 pp.

van Sickle, J. and Beschta, R. L., 1983. Supply-based models of suspended sediment transport in streams. *Water Resources Research*. Vol. 19, 768-778.

Walling, D. E., 1977. Assessing the accuracy of suspended sediment rating curves for a small basin. *Water Resources Research*. Vol. 13, 531-538.

Wheatcroft, R.W., Butman, C.A., 1997. Spatial and temporal variability in aggregated grain-size distributions, with implications for sediment dynamics. *Continental Shelf Research*. Vol. 17, 367-390.

Wilder and White, 1911. *Washington State Capitol Campus Master Plan*.

Woodroffe, C.D., 2002. *Coasts: form, process and evoloution*. Cambridge University Press, Cambridge, 623 pp.